# Object contrast determination based on peripheral vision under night-time driving conditions

**Kontrastbestimmung von Objekten bei peripherer Sicht unter nächtlichen Fahrbedingungen**

Dissertation von Katharina Schneider

August 2017

TECHNISCHE UNIVERSITÄT DARMSTADT

FACHGEBIET LICHTTECHNIK

# Object contrast determination based on peripheral vision under night-time driving conditions

Dem Fachbereich Elektrotechnik und Informationstechnik
der Technischen Universität Darmstadt

zur Erlangung des akademischen Grades eines
Doktors der Ingenieurswissenschaften
(Dr.- Ing.)
vorgelegte Dissertation

von
Katharina Schneider, M.Sc.
geb. am 20.01.1988
in Weinheim an der Bergstraße

| | |
|---|---|
| Referent: | Prof. Dr.-Ing. habil. Tran Quoc Khanh |
| Korreferent: | Prof. Dr. sc. nat. habil. Christoph Schierz |
| Tag der Einreichung: | 09.08.2017 |
| Tag der Prüfung: | 17.01.2018 |

D17

Darmstadt 2017

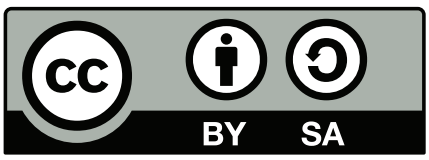

f

# Eidesstattliche Erklärung

**Erklärung laut §9 PromO**

Ich versichere hiermit, dass ich die die vorliegende Dissertation allein und nur unter Verwendung der angegebenen Literatur verfasst habe. Diese Arbeit hat bisher noch nicht zu Prüfungszwecken gedient.

Darmstadt, den 9. August 2017

_____

(Katharina Schneider)

*To my dad*

***Friedrich Adam Schneider***
**** 1960 † 2014***

*Cause you'll be in my heart*
*Yes, you'll be in my heart*
*From this day on*
*Now and forever more*
*You'll be in my heart*
*No matter what they say*
*You'll be here in my heart*
*Always*

# Acknowledgement

Die vorliegende Dissertation entstand im Rahmen meiner Tätigkeit als wissenschaftliche Mitarbeiterin am Fachgebiet Lichttechnik der Technischen Universität Darmstadt. Ich möchte mich bei allen bedanken, die zur Entstehung dieser Arbeit beigetragen haben. Besonderer Dank gebührt meinem Doktorvater, Herrn Professor Dr.-Ing.habil. Tran Quoc Khanh, der die Durchführung dieser Arbeit ermöglichte und mein fachliches Verständnis mit wertvollen Anregungen und Ratschlägen förderte.

Herrn Professor Dr.sc.nat.habil. Christoph Schierz danke ich für die Übernahme des Korreferats und für die konstruktive Zusammenarbeit mit dem Fachgebiet Lichttechnik.

Mein herzliches Dankeschön gilt meinen Kollegen am Fachgebiet Lichttechnik für die hervorragende Zusammenarbeit und anregende fachliche Diskussionen. Ganz besonders danke ich Nils Haferkemper, Jonas Kobbert, Daniel Englisch, Christoph Schiller und Peter Bodrogi.
Bei Frau Dorothe Drechsler möchte ich mich von ganzem Herzen für ihre Herzlichkeit und Wärme, für ihr Engagement und vor allem für ihre mentale Unterstützung bedanken.

Ich möchte mich ebenfalls bei meiner Korrekturlesern Anne Dörr, Michelle Baker, Pauline Elliott, Nils Haferkemper und Carsten Diem bedanken. Vielen Dank für Eure Hilfe.
Auch allen Probanden, die sich sowohl im Labor als auch meiner Feldstudie verschiedenen, anstrengenden Experimenten aussetzten, bin ich zu großem Dank verpflichtet.

Mein tiefster Dank gilt meiner Familie. Meinen Eltern danke ich sehr für ihre fortwährende Motivation. Dafür, dass sie immer hinter mir standen und mich bei jeder Entscheidung, die ich getroffen habe, unterstützt haben. Ich möchte mich ebenfalls bei meinen Freunden bedanken, die mich stets ermutigt und motiviert haben.

Ganz besonders möchte ich Herrn Alexander Kirchler dafür danken, dass er in den kritischen Phasen für mich da war. Danke dir für die aufmunternden Worte und die Geduld in der langen Zeit, aber vor allem, dass du immer an mich geglaubt hast.

# Abstract

Die Einführung der LED-Technologie in die Kfz-Scheinwerferentwicklung führte zu einem systematischen Fortschritt hinsichtlich der Verbesserung der Sichtbarkeit. Aktuelle LED-basierte Scheinwerfer bestehen aus einer bestimmten Anzahl horizontaler und vertikaler Segmente, mit denen eine räumlich fein aufgelöste Anpassung der Lichtverteilung möglich ist. Da jedes Pixel individuell angesteuert und gedimmt werden kann, führt dies zu einer wesentlich präziseren und adaptiven Lichtverteilung.

Ziel ist es, auf das plötzliche Erscheinen von Verkehrsteilnehmern (Fußgänger, Wildtiere oder Gegenverkehr) entsprechend reagieren zu können, indem einerseits die Lichtintensität der entsprechenden Pixel verringert wird, um eine mögliche Blendung zu vermeiden, andererseits, um das Licht gezielt in Richtung der vom Autofahrer wahrgenommenen „Objekte“ zu leiten. Dabei soll die Umgebung, die das Objekt umgibt, so ausgeleuchtet werden, dass eine maximale Sichtweite für den Fahrer ermöglicht wird.

Grundlage dieser Arbeit sind Untersuchungen, die sich mit der Detektion von Objekten im nächtlichen Straßenverkehr in Bezug auf die Kfz-Lichttechnik befassen. Dabei wird die Detektionsaufgabe des Autofahrers sowohl für das foveale als auch das periphere Sichtbarkeitsfeld des Fahrers betrachtet.
In einer ersten Untersuchung wird die Detektion von fovealen und extrafovealen visuellen Sehzeichen unter Laborbedingungen analysiert. Der experimentelle Aufbau und verschiedene Einflussgrößen werden vorgestellt und anschließend diskutiert. Um eine nächtliche Verkehrssituation möglichst realitätsnah simulieren zu können, wurden für die Untersuchungen zwei entsprechende Hintergrundleuchtdichten ($0{,}1\frac{cd}{m^2}$, $1{,}0\frac{cd}{m^2}$) ausgewählt. Die Ergebnisse werden als Wahrscheinlichkeitsprofil über die jeweiligen Exzentrizitäten dargestellt.

Darüber hinaus werden in einer Feldstudie zwei verschiedene Objektformen, die in Straßenverkehrssituationen auftreten können, ebenfalls unter verschiedenen Exzentrizitäten untersucht. Basierend auf den ermittelten Detektionsdistanzen der Objekte werden die Ergebnisse als Funktion des Kontrastes dargestellt.

In einem letzten Schritt werden Methoden zur Bestimmung und Auswertung des Objektkontrastes analysiert. Die Bewertung der Untersuchungen, die Ableitung von Empfehlungen für die praktische Anwendung sowie ein Ausblick auf weitere Untersuchungen werden gegeben.

The introduction of LED technologies into headlamp development has led to the systematic progress in headlamp design to improve visibility. Current LED light distributions consist of a specific number of horizontal and vertical segments, it tends to a spatially finely resolved adaptation of the light distribution, the so-called pixel light. This results in a much more precise light distribution, each segment can be individually controlled and dimmed. The aim of this technology is to be able to respond appropriately to the appearance of road users (pedestrians, wild animals or oncoming traffic), firstly by reducing the light intensity of the corresponding camera pixels in order to prevent glare and secondly to force it to the objects' direction. The environment surrounding the traffic area element shall be illuminated in such a way as to achieve maximum visibility.

The basis of this work is an investigation dealing with detection of objects in night-time traffic in relation to vehicle lighting technology. The present study examines the foveal and peripheral vision by means of detection. The intention is to obtain an insight into the cognitive abilities and different areas within the visual field for different visual conditions in night-time road traffic.
The first task consists in the detection of foveal or extrafoveal appearance of visual targets under laboratory conditions. An experimental setup developed for performing the detection experiments is introduced. Various influencing parameters are analysed and discussed in detail. In lighting technology, the respective required visual characteristics are determined by luminance or contrast. In order to be able to simulate a night-time traffic situation as effectively as possible, two background luminance levels ($0.1\ \frac{cd}{m^2}$, $1.0\ \frac{cd}{m^2}$) were selected for the investigations. The results are presented as probability profile over the respective eccentricity angles.

In addition, in a field study, two different target shapes that occur in road traffic situations are observed under different observation angles. Results for increment contrast functions based on the detection distances of the objects are presented.

In the final step methods to determine and evaluate the detection object contrast will be analysed. A critical examination of the investigations, a derivation of recommendations for practice as well as an outlook on further investigations are performed.

# Contents

# List of Figures

# List of Tables

# Chapter 1

# Introduction

In the past few decades the development in lighting technology has made major progress. New technologies in vehicle headlamps have a defined spectral and optimized light intensity distribution curve for the road geometry. Situational, geometrical or weather-related changes in driving scenarios (dry or wet road, road width, roads gradient, traffic density, distribution of the road users in the traffic area) lead to an irregular or limited illumination of the environment.
The luminous intensity distributions depend on the light sources luminance distribution and the optic's shape of the headlamp system. Current national and international standards for exterior automotive lighting (ECE- and SAE-standards) are based on results that arose during the period between 1950 to 1975 using the illuminance and partially the luminance as decisive photometric parameters. At that time the investigations were mainly carried out with young participants. Although driving situations like intersections, roundabouts or curves are very common traffic situations, the technical considerations for new product development did not contain much knowledge about the peripheral viewing conditions.

Currently, lighting technology has been based in particular on the measurement of lighting conditions related to foveal information reception. For this purpose data from a wide range of experiments are available, both in the threshold and supra-threshold range. The quantitative knowledge of peripheral visual properties is sparse, especially with regard to headlamp designs. Previous investigations have either been carried out with simple visual tasks or have been performed in point-to-point measurements to determine specific perceptual properties. The description of peripheral visual properties in the context of ordinary visual tasks therefore requires even more extensive investigations in practical requirements, such as the technical production of visual information. On the other hand, the investigations should not deviate from the existing knowledge thus allowing interpretation of the results to be linked to the known knowledge.

## 1.1 Motivation

Against this background, the present work examines the visual perception of foveal and extrafoveal visual signs both under laboratory conditions and in a field study under real conditions. Thus, both homogeneous and temporally altered background luminances are analysed. The ability to detect and localize visual stimuli have great significance for practical information presentation. Basic questions are "is a signal present?" and "where is it with regard to your own position?" Therefore, the first

task is the determination of the stimulus presence. Along with the detection the eye also computes the stimulus position automatically. This becomes clear in a subsequent precise movement of the fixation.
This work will have three essential parts. An overview of the structure including investigated parameters, methods and research objectives is illustrated in Figure 1.1. All three parts have their own research questions and pursue the goal to investigate the effect of different luminous intensity distributions in front of the vehicle provided with LED headlamps using a target detection paradigm and contrast-based modelling.

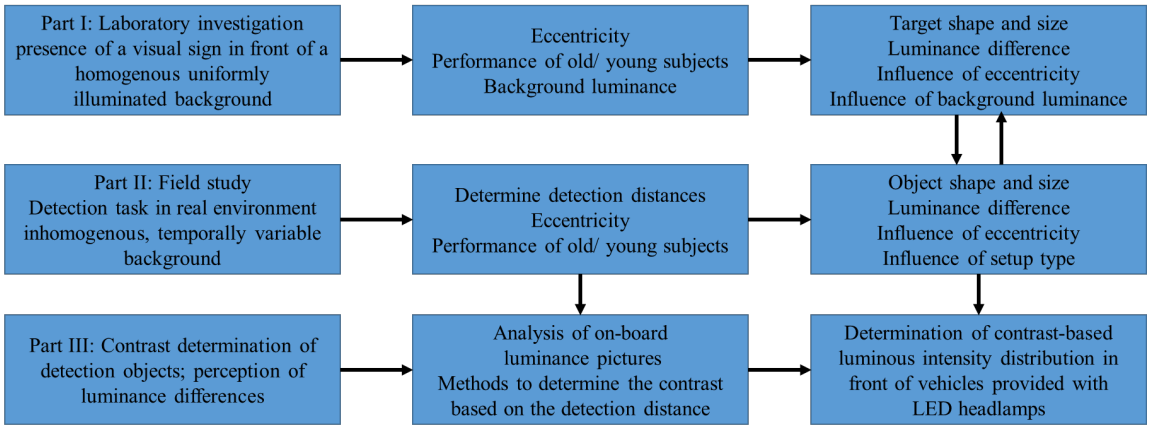


**Figure 1.1: Thesis structure. Investigated parameters, methods and research objectives are illustrated.**

As can be seen from Figure 1.1, both homogeneous and inhomogeneous, and also temporally altering background luminance distributions will be analysed. Fundamentally, it is essential to know the limits of the required visual characteristics, in lighting technology this is ensured as a function of luminance and contrast. This thesis presents the task of measuring binocular properties in the threshold and suprathreshold range from simple to difficult requirements:

- Determine the presence of a visual sign in front of a homogeneous, uniformly illuminated background (laboratory conditions). This will be investigated in Chapter 5.
- Detection in a real environment, the contrast with the environment is temporally variable and inhomogeneous (field study). This will be investigated in Chapter 6.
- Determination of the visually relevant contrast value from the luminous intensity distribution measured in front of the test vehicle provided by its LED headlamps. This will be described in Chapter 7.

The latter case corresponds to the most common situation in vehicle lighting practice. In this case, for appropriate modelling, a visually relevant contrast value is to be determined from more or less noisy spatially resolved luminance images of the object and its background.

The first part of the experiment deals with the detection of visual targets at luminance levels as on night-time road lighting ($0.1\frac{cd}{m^2}$to $1.0\frac{cd}{m^2}$) under laboratory conditions. The results of the experiments show a probability profile over the off-axis angle for each contrast.

The attention of the human being to visual stimuli is concentrated in a more or less narrow area around the visual axis. Objects can be perceived in this area deliberately and make it possible to adapt actions accordingly. In the road traffic, danger mainly occurs to road users when obstacles appear suddenly from the side. Since the distance to the obstacles is very low, short reaction times are necessary, that are actuated due to a certain reflex to avoid a collision. In order to be able to react in a timely and controlled manner, a large visibility field is fundamentally important. This means that the conspicuousness of the visual object must be large, so that it can also be perceived under a large eccentricity apart from the visual axis. Uncontrolled and thus endangering reactions of a car driver can occur even if objects are difficult or too late to be perceived.
Still the task of a front lighting system is to transfer light onto the road and also the roadside areas to ensure safe viewing conditions for the driver. With the partial high beam function, it is possible to illuminate the drivers own lane even if there is some oncoming traffic. These problems will be analysed in the second part of this thesis. A field study setup with real detection objects is provided. In this case the object is integrated into an environment with constantly changing parameters, meaning, the subjects have to connect direction information across time and space to observe the object's mean direction and speed.

If the luminance contrast of the detection object on and alongside the road is high enough in order to achieve 99.0% detection probability for a sufficient distance, a safe visibility condition is highly guaranteed. This distance needs to be longer than the stopping distance (at a given vehicle speed) in order to avoid an accident. To enhance the lighting conditions for safe detection, headlamp systems have been improved (glare free high beam) by adopting new technologies.
The third part is concerned with the contrast perception in night-time traffic situations. A particularly important point for the design of the luminous intensity distribution related to the detection distance is the influence of the area ahead of the vehicle (3.0 to 12.0 m). According to classical stray light theory, a bright front area would have a negative effect on the threshold contrast. In addition, the position of the object has an influence on the threshold contrast. In order to design luminous intensity in angular direction of relevant objects, on-board luminance images are analysed. The necessary amount of luminous intensity in direction of the object can be calculated from the level of object luminance contrast on a certain background luminance distribution. In this work factors influencing this contrast value for safe object detection will be examined.
The models calculating the detection distance, that were determined in earlier investigations, are based exclusively on foveal observation. However, this is rarely the case for applications in real road traffic. Furthermore, the equations for the calculation of the contrast threshold towards foveal vision were obtained under photopic

conditions. This includes answering the question of the impact of the background luminance on the predicted relationship, which has not been taken into account yet. Different already existing methods for determining the contrast based on luminance images are introduced and then compared with the own results.

With the introduction of the white light emitting diodes (LED) at the beginning of the $21^{st}$ century as light source for headlamp systems, new concepts for intelligent and adaptive lighting systems were implemented. The state of the art in front lighting systems are ADB (adaptive driving beam) modules using LED pixels instead of mechanical actuators [42]. For the development of new ADB systems different technologies (e.g. LED-pixel, LCD with LED illumination, MEMS with both laser and LED illumination) are used to increase the number of pixels up to 2 million [43]. At the points where an oncoming or preceding vehicle is detected by the camera, the light intensities are dimmed or switched off for every angle segment dynamically in relation to a level below the glare limit.

The main light distribution is designed by high-resolution LED pixel light sources. Actual headlamp systems consist of 84 discretely constructed LEDs, all of which can be controlled individually and achieve an angular resolution of 1.0° [42]. With three rows and a maximum of thirty columns, an LED precision raster module was developed for the first time [44]. With this increased resolution, it is possible to adapt the system to the particular traffic situation and thus to fade out required areas. With a resolution increased by a factor of 3.5 compared to the previous model, the faded out regions can be minimized, that is, the driver receives a safety gain through an increased use of the high beam, which results in a larger illuminated area.
The increased number of pixels in each headlight increases the illuminated area and can be fully configured without the use of a mechanical actuator. Since the sensors within the vehicle have increased in number and quality, a new control concept has been created with the software program Matlab Simulink [45]. The control units receive their information via the camera and navigation system of the vehicle. Within these control units, the individual desired light distributions are calculated a hundred times per second for both the left and the right [44]. One advantage of the new system is, on the one hand, the easy integration into existing vehicle electronics and, on the other hand, the implementation of new optimized light functions [42].

In order to compare and evaluate these technologies, criteria such as illuminance and resolution need to be analysed. The first important parameter is the achievable contrast ratio of the module, which is limited by the contrast ratio of the light source matrix and its optics. Secondly, the angular range (for example only partial high beam or full bending light) is another key parameter for the design. Subsequent, the contrast (luminance level) needs to exceed the legal requirements and must be related to an eccentricity range (definition of the vertical and horizontal cut-off line). If the pixel light source has a contrast ratio of less than 200:1 it is challenging to build a useful ADB-module [43].
These technological improvements are currently enhanced by social changes. In

the past 20 years, urbanisation has been taken place on all continents, as there is a constant growth of metropolises with more than 10 million inhabitants in continents like North and South America, Asia and parts of Europe. Associated with those effects is a strong traffic compression, so that visual improvement for night drive situations in road traffic becomes more important. At the same time, there is a demographic change resulting in an aging society, which can especially be seen from industrial nations. This leads to the question of how the deficit of vision faculty should be registered related to age and how it could have an impact on the development of future light systems.

## 1.2 Outline

Several foveal investigations in mesopic range have been performed in photometrical studies already. Both the threshold and the over-threshold range were examined. In contrast to previous studies the aim of this work is to make a statement about the peripheral behavior of the human eye. At the same time, the perception characteristics in the periphery are analysed in relation to a night-time situation in road traffic. Both homogeneous and heterogeneous backgrounds with constantly changing luminances are observed in the investigations.

In Chapter 2 the fundamentals for the visual information processes regarding to object detection as well as the challenges of the night-time driving task will be described. Based on the findings, the description and selection of suitable methods for determining detection at the 99% perception threshold as well as a context-based description of suitable psychophysical methods follow.

Chapter 3 provides an overview of the current state of the art and regularities that must be taken into account when implementing new headlamp systems. In addition, accident statistics are consulted.

In Chapter 4 a literature analysis of the most important detection (and object recognition) threshold results arising from earlier investigantions will be evaluated in order to define consequences and guidelines for the future ADB headlamp light distributions.

Chapter 5 describes the experimental setup developed for performing the detection experiments in the laboratory. The basic components as well as the critical points during their selection are illuminated. In addition, the selected test method, the procedure for carrying out the examinations and the selected participant groups are discussed. The results are analysed and the various influencing parameters are discussed in detail.

In Chapter 6, two different target shapes that occur in road traffic situations are observed in a field study under different eccentricities. Two measurement methods, static and dynamic, are developed for determining the detection distance. Results for increment contrast functions based on detection distances are analysed. The

results are compared with earlier research studies from Chapter 4 and discussed based on the individual influencing parameters.

In Chapter 7 several methods to determine and evaluate the contrast of detection objects will be analysed. Recommendations for contrast determination will be given.

Chapter 8 the results of the laboratory and field investigations are compared to each other. Therefore, the single parameters influencing the detection task are analysed in detail to make a prediction about possible trends.

Chapter 9 describes the determination of a contrast-based light distribution in front of a vehicle that is provided with LED pixel headlamps.

Chapter 10 summarizes the main findings of the present work in short form. A critical examination of the investigations, a derivation of recommendations for practice as well as an outlook on further investigations are performed.

# Chapter 2

# Fundamentals

This chapter describes the lighting and human eye physiology basics, which are helpful for the understanding of further work and the reasons for the decisions made. Furthermore, the processes that are important for the detection of a visual object are presented.

## 2.1 Visual system

Vision is only possible when light is present. Light is electromagnetic energy, which as a whole forms an electromagnetic spectrum. This electromagnetic energy is generated by electrical charges, which spreads in wave form. The electromagnetic spectrum is described by wavelengths, which can be subdivided from extremely short-wave gamma rays ($10^{-12}$ m) to long-wave rays ($10^{4}$ m) [2]. The range of the visible light lies in a wavelength range between 380 nm and 780 nm, whereby short-wavelength lengths appear as blue, medium wavelengths as green and yellow and long wavelengths appear orange and red.
The human visual system is an essential part of the information reception of the environment. Human vision is a complex process that depends on many aspects. Any change in environment luminance or colour, in the size and distance of the visual target or visual conditions due to external influences, results in a change in perception.
The adaptation level also plays an important role in the visual process. Depending on the region, different receptors are addressed which process the stimulus. Adaptation is controlled by switching processes on the retina [46]. While in scotopic vision (night vision) the rods take over the visual function, in the photopic area (day vision) the cones and their subsequent processing stages are responsible for the perception of brightness [47] compare Chapter 2.1.2.
Conditions under which the human eye perceives a visual target have a considerable influence on the visual process. In this case, peripheral vision, which locates certain visual objects, must be distinguished from foveal vision, which is responsible for recognizing an object. The difficulty in the localization of a vision target is to determine a structure of the visual object related to its usually heterogeneous background at a specific time. The visual object must therefore clearly differ from its background in order to be able to be perceived [48].

### 2.1.1 Anatomy of the human eye

The visual system consists of the two eyes, the afferent visual pathway (optic nerve, chiasma opticum, tractus optici, corpora geniculata lateralia) and the virtual cortex in the occipital region of the brain [1]. In addition, the cortical areas of association, in which more complex perceptions arise, also belong to the visual system, but seeing as such is a performance of the brain. The human eye is one of the important organs of the human being and the imaging component of the brain. It is the optical system that enables humans to produce optical images and thus to perceive information about its visual environment with all forms and features of objects. The schematic structure of the human eye is shown in Figure 2.1.

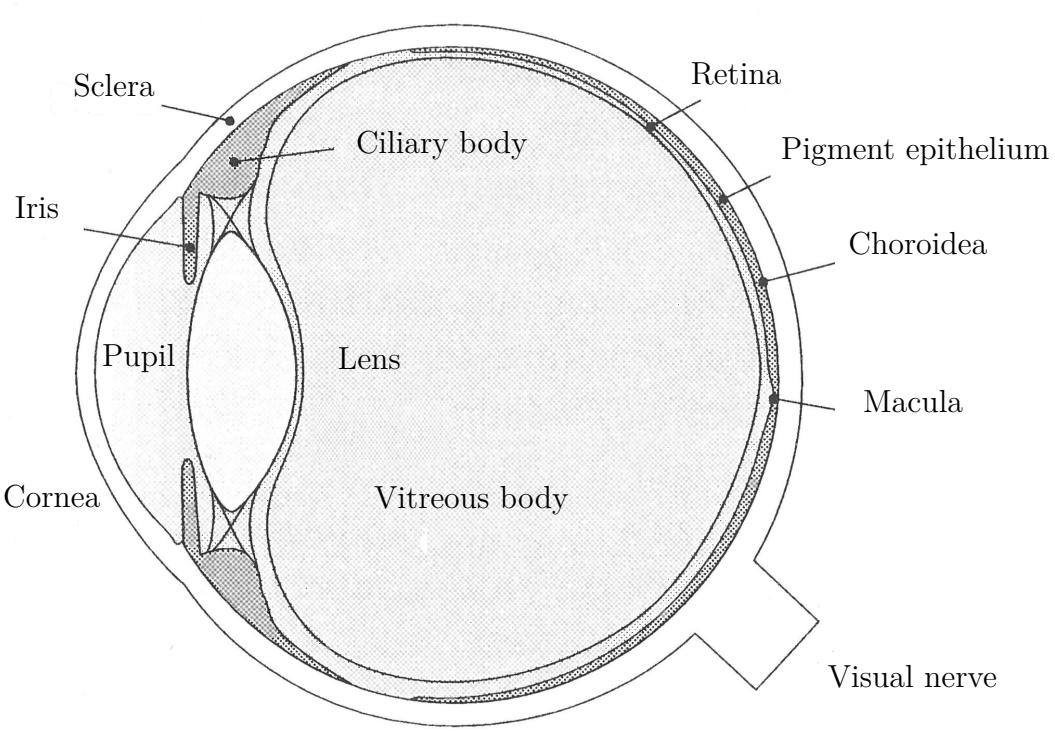


Figure 2.1: Structure of the human eye (horizontal section) according to [1]. An object is imaged under the visual angle $\theta$ as image via the optical apparatus of the eye on the retina. The electromagnetic radiation on the optical path passes through the cornea, the aqueous humor, the eye lens, the vitreous body, and the retina's nerve tissue. Finally, it is absorbed by the receptors of the retina and converted into electrical signals.

The light reflected from the environment enters the eye through the pupil and is focused by the cornea and the lens. A sharp image of the viewed object is then generated on the retina, on which the photoreceptors are placed. In the photoreceptors, which are referred to as rods and cones, visual pigments are present, which are altered by the light incidence and thus trigger electrical signals. A further neuronal processing, that is, the signals from the receptors pass through the connected nerve cells and are transferred to the brain via the optic nerve. The actual visual process thus takes place in two transformation steps. First, there is a transformation of the

incident light, that is reflected by an object, into an image on the retina. In a second step, the image produced on the retina is converted into an electrical signal, which can be processed in the brain [2].

### 2.1.2 Receptor distribution

The task of the photoreceptors, which are elements of the receptive fields on the visual cortex of the human eye, is to convert a light stimulus into an electrical signal and thus to transfer the information to the brain. As illustrated in Figure 2.2 the electrical signal is pre-processed by interconnections in the nerve cells of the retina. This means that the arising images on the retina must pass through all other layers of the retina before they are converted into electrical signals in the receptors. The information is transferred to the bipolar cells from the receptors, from which the ganglion cells move within the retinal nerve endings (axons) to the papilla, before leaving the eye via the optic nerve. In addition, horizontal cells and amacrine cells provide cross-linking within the retina.

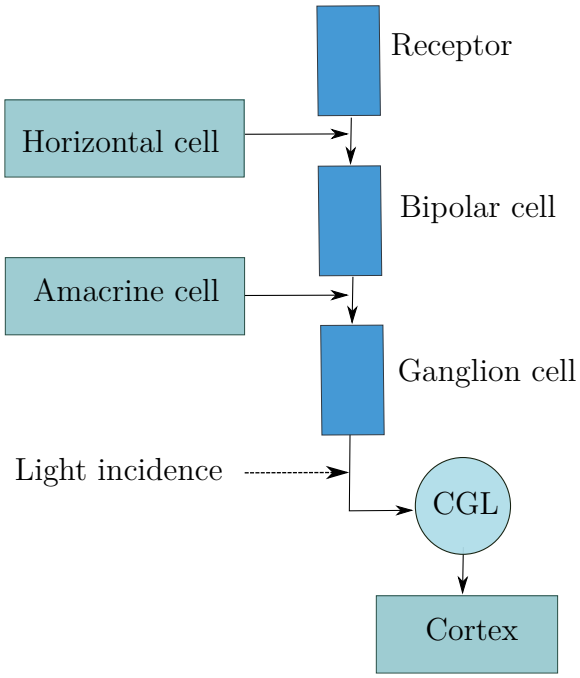


Figure 2.2: Neuronal chain of the visual path (cone system, simplified schematic representation). The cone system consists of 4 neurons that are connected in series: receptor (cone), bipolar cell, ganglion cell and the CGL (corpus geniculatum lateral). Within the retina, horizontal cells and amacrine cells provide cross-linking. [2] [1].

In the final ganglion cell layer, the signal components are subdivided by different features such as color, contrast or movement. The individual information is further processed on the visual cortex, i.e. it is matched with already known information stored in the memory. This reconciliation with already acquired experiences leads to a conscious perception or recognition of visual targets.

If the ambient brightness changes around the eye, it is able to adapt to the darkness in the shortest possible time. In this case, the visual system becomes more and more sensitive in the dark, which is referred to as dark adapation.
Distributed throughout the entire retina are the photoreceptors, the so-called rods and cones. As already mentioned, the light impacting the receptors triggers electrical signals because it is absorbed by the visual pigments of the receptors. The human eye possesses approximately $5 \cdot 10^6$ cones and $120 \cdot 10^6$ rods, which are arranged in a different distribution on the retina. The distribution of the receptors is shown in Figure 2.3. The functionality of the central region of the retina is described in more detail below.
The Fovea Centralis (also called Macula or yellow spot) is located on the optical axis (0.0°). It is a small area on which cones are closely connected with nerve fibers are located. The nerve-bracts and blood-vessels are thereby crowded to the edge of the fovea. The result is a depression with a diameter of about 3.0° to 5.0°, where light scattering is the lowest on the entire retina. The so-called blind spot (Papilla n. optici), in which no receptors are present, is located at an angle of 15.0°. In the peripheral retina the visual acuity decreases starting from the Fovea Centralis with an increasing observation angle to the visual axis. This can be explained by the receptor distribution on the retina. As it is illustrated in Figure 2.3 the concentration of the cones decreases continuously with increasing peripheral angle.

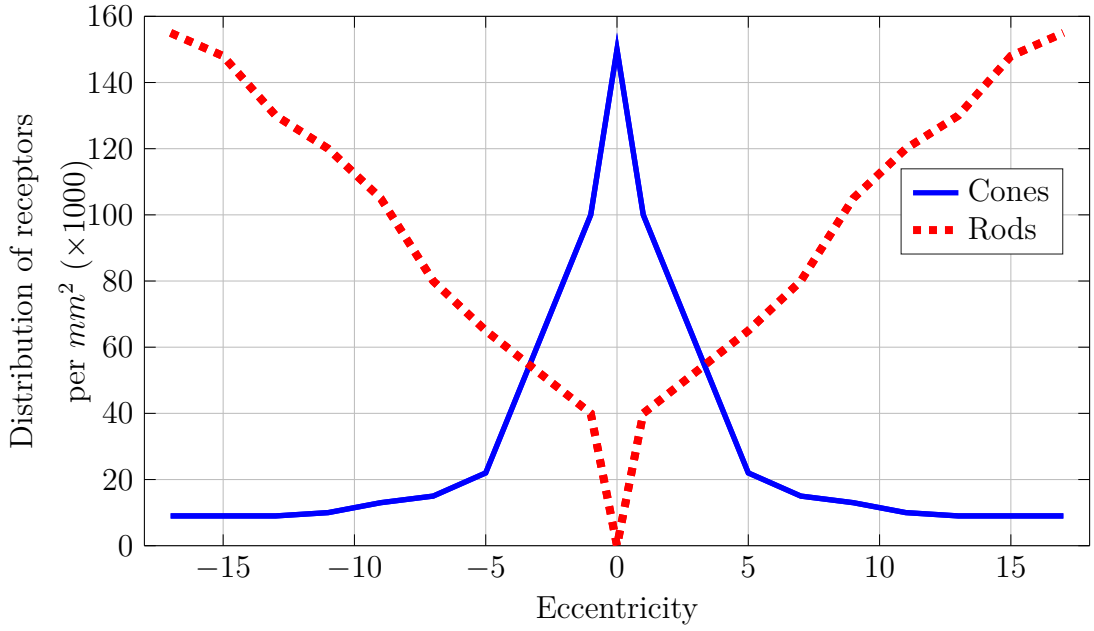


Figure 2.3: Receptor distribution in the retina by Osterberg [3]. Cones illustrated as solid line, rods marked as dashed line.

Nevertheless, most cones are found outside the Fovea Centralis. Only one percent (50,000) of the 5 million cones can be found outside of the Fovea Centralis [2]. In addition, the diameter of the cones increases towards the periphery, which means that the connection of many cones and rods is bundled into a ganglion cell. While in the fovea one cone receptor is directly linked to a ganglion cell, in the

periphery several thousand receptors behave as on unit and are connected with a single ganglion cell.
As Figure 2.3 shows, there are no rods within the Fovea Centralis, outside the density increases continuously and reaches a maximum at about 20.0° on both sides of the optical axis. Subsequently, the density of the rods ($1.5 \cdot 10^5 mm^2$) decreases again to one-third with increasing peripheral angle.
On the one hand, the interconnection of several thousand receivers in the periphery leads to a summation of the incident light energy and thus to a sensitivity increase. The human being can therefore make a statement about whether a light stimulus is present or not, since better reaction to changes in the light stimuli caused by the arrangement of the receptors is possible (phasic behaviour) [49]. On the other hand, in the fovea, longer-lasting light stimuli are signaled better (tonic behaviour).

**Dark adaptation.** The ability of the visual system to adapt to a wide range of ambient brightness is called light or dark adaptation. Figure 2.4 shows the temporal profiles of the dark adaptation of the cones and rods. The ordinate represents the luminance difference $\Delta L$ between an object and its environment that is barely perceptible. The adaptation is divided into two areas, the cones and rods adaptation. The current adaptation state of the receptors is determined over the duration of 25 minutes related to the luminance variation the environment.

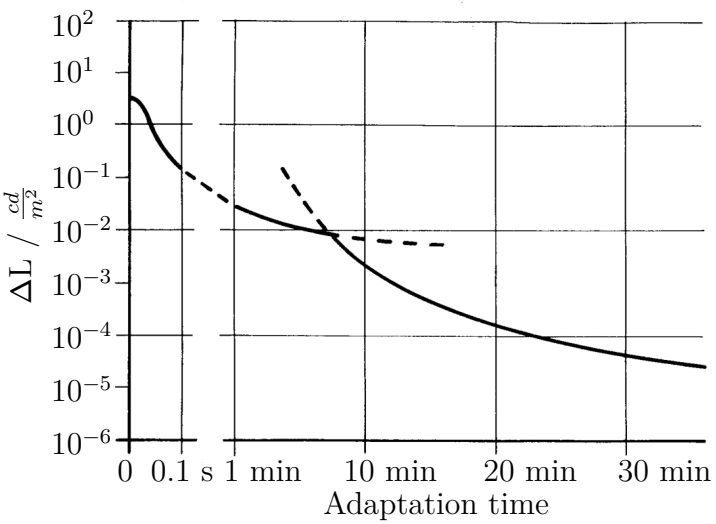


Figure 2.4: Dark adaptation process. The adaptation is divided into two areas, the cones (left curve) and the rods (right curve) adaptation [2].

In the first minutes the adjustment is dominated by the cones. After a time period of approximately 7 to 8 minutes the cones reach their sensitivity threshold and do no longer contribute the adaptation process. This is the case at a background luminance of approximately $0.001 \frac{cd}{m^2}$. The rods reach their maximum sensitivity asymptotically at about $10^{-6} \frac{cd}{m^2}$. While the entire dark adaptation is completed after approximately 30 to 60 minutes (scotopic adaptation), for the light adaptation, only a few seconds (up to one minute) are required.

**Conversion of light energy into electrical energy.** A transformation from the light energy into the form of electrical energy occurs within the rods and cones on the retina. A photoreceptor can be subdivided into an external and internal segment as it can be seen in Figure 2.5.

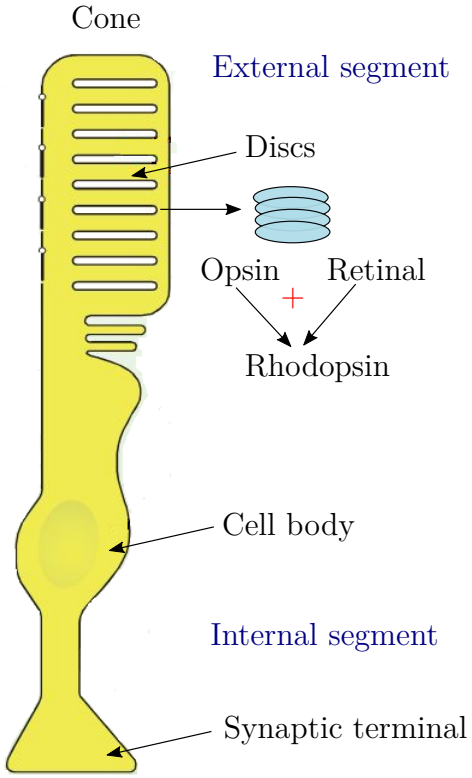


Figure 2.5: Schematic structure of a photoreceptor (cone) that consists of two parts: A long protein called opsin, and a smaller fraction called retinal. If these two parts are linked together, the visual pigment is able to absorb light.

On each outer segment of the receptors millions of molecules of the visual pigment (Rhodopsin) are located. These molecules, in turn, consist of two parts: A long protein called Opsin, and a smaller fraction called Retinal [2]. If these two parts are linked together, the visual pigment is able to absorb light. If a photon (light quantum) is recorded, an isomerization occurs, means the Retinal changes its form. A chemical chain reaction is triggered by this change in shape. The shape change of a single Retinal leads to a release of millions of molecules which leads to an activation of the receptor. The properties of human perception, such as dark adaptation, are also influenced by visual pigments of the receptors. During day vision (photopic vision), the cones are active, which have a high sensitivity and thus can also recognize color details. On the other hand, the rods on the retina are occupied by the case of low brightness (scotopic vision).

### 2.1.3 Retinal processing of the visual stimulus

The process of seeing can be described as follows. A certain stimulus is applied on the photosensors. This results in a sensor potential drop. A light stimulus produces

an action potential in the ganglion cells. Now a certain area on the retina (a so-called receptive field) is stimulated, which has an inhibiting or exciting effect on the frequency of the action potential. The receptive fields are arranged concentrically and form two parts: the centre and the periphery. The receptive fields of the two areas react in opposite directions. If the centre is addressed by a stimulus, the action potential frequency increases, if the periphery is exposed, the action potential is inhibited accordingly.
The various areas in which the entire visual field is divided have different characteristics and can receive information accordingly. Based on this temporal as well as spatial information structure, a decision is made how perceptible the object is. Based on the knowledge of the semantics and syntax of the current situation, the human brain forms a pattern preference that allows to take information from the environment in the appropriate situation [50]. Semantics here means the meaning or designation of signs, syntax represents the connection of a character set and the connection of individual characters. The more syntax is available, the more information the human brain already knows, the more information can be processed faster. The sensitivity of the peripheral visual field to changes in stimulus is based on a evolutionary adaptation [48]. While this sensitivity was used as a warning of possible dangers earlier, it has an important protective function with regard to road traffic now.

## 2.2 Detection of visual targets

In this work a distinction is made between the two terms of detection and identification. Since these two concepts deal with situations in night traffic, the salience, that is, the form of the stimulus may be considered. The salience of an object or person is the state or quality by which it differs relative to its neighbours. Salience is very important for subsequent experiments because it describes the difference between an object and the surrounding background. Before participating in an experiment, the subjects were concerned about what they should particularly pay attention to, i.e. the experiment is performed by the respective situation and also the interpretation of the test person. With every new requirement, which is provided on the subject, the salience is also changed: “A figure that I can’t recognize correctly any more, is less salient for an identification, but for a detection more salient, since I’m still able to perform the latter” [48]. This concept of salience is essential for the understanding of this work: Salience is the strength of the perceived context differences between a target and its background.

**Participant’s attention.** Care must also be taken to the participant’s attention. In order to simulate a real course on the road, the attention of the subject is an important influence factor. The participants must concentrate on something to be attentive and neglect other aspects at the same time.
The human brain processes and selects information permanently in order to optimally adapt the behaviour to the respective situation. If this selection is based on the visual system of the subject, this means that not all of the visual information can be processed, but the human directs his attention to something specific.

In literature reference is made here to different definitions of attention, since the term attention is used for some areas of interest [48] [51]. In this work a total of three types of attention are differentiated: spatial attention, feature-based attention, and object-based attention. As a headlamp illuminates a certain region, the spatial attention also moves to a certain location of the visual field. While in the case of feature-based attention, an object is weighted only on the basis of one feature, the object is weighted more heavily in comparison to other objects in object-based attention.

**Reflection coefficient.** According to Blackwell for a positive contrast approximately the same behaviour of the threshold contrast is applied as for negative contrasts [37]. Non-luminous objects viewed against the road surface usually have a negative contrast (compare Figure 2.6), since the horizontal illuminance is higher than the vertical. Therefore objects appear in the night street lighting as silhouettes. Van Bommel found out that the luminances on road surfaces of $0.5\frac{cd}{m^2}$ and $1.0\frac{cd}{m^2}$ with two vertical illuminances respectively, define the areas of the diffuse reflection coefficient [52]. The reflection coefficient specifies if an object can be detected or is invisible due to low contrast.

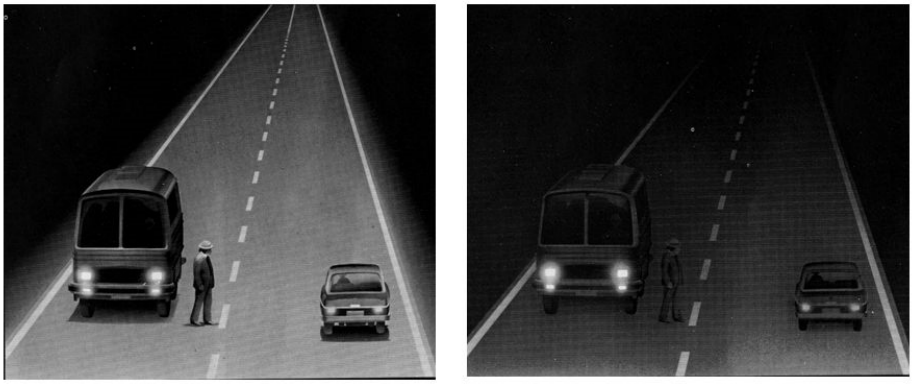

Figure 2.6: Night-time traffic situation in relation to the contrast function according to [4]. Left: negative contrast; right: no contrast.

## 2.2.1 Visual information processing

The night-time road traffic is predominantly in the mesopic range ($0.1\frac{cd}{m^2}$to $5.0\frac{cd}{m^2}$). A complete dark adaptation is rarely experienced by a driver, since almost always light sources are present in the field of vision. A road traffic scenario can be subdivided into many individual processes, that all influence one another in different ways. In addition to the task of driving, the driver uses his visual system to record the entire traffic area to be able to react to the situation accordingly.
While the driver follows the road in foveal direction, possible signal signs on the edge of the road are perceived only based on their luminance difference to the background or distinctive shape structure as illustrated in Figure 2.7 [50]. In order to identify a object, the driver needs to perceive the target foveally.
Within the mesopic range, the spectral sensitivity of the visual system changes with the adaptation level and retinal eccentricity [50] [53].

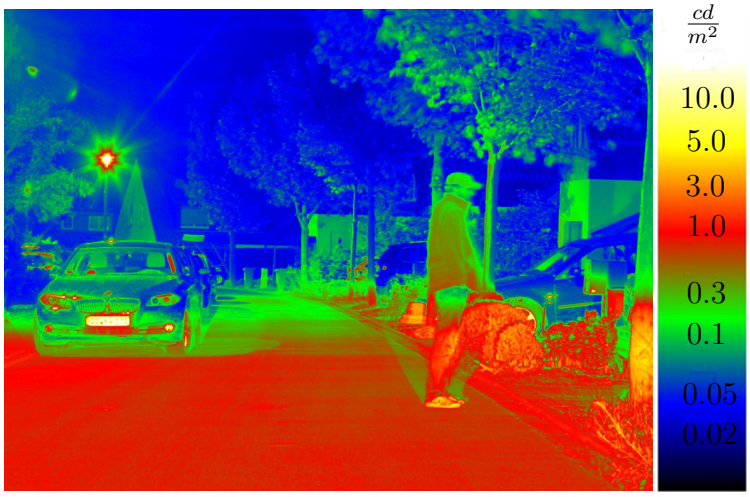


Figure 2.7: Luminance picture of illuminated road in the city. Human being (male, height 1.85 m) stands alongside the road and is perceived on the basis of its luminance difference to the background or distinctive shape structure.

In a typical night drive situation, the driver has to sweep for obstacles with a typical gaze behaviour. Visual processes, such as searching, reading or inspecting depend on visual perception. During a fixation period through outer visual conditions the area of perception is not expanded over the entire visual field, it is constrained to a sort of extended central lobe [54]. This lobe is defined as visibility field. Using it for scanning the environment in as far as it determines fleetness, certainty or reacting upon visual stimuli, the visibility field merges with the peripheral threshold contrast. Inditsky [55] evaluated the visibility field in a model, using the knowledge of the peripheral threshold contrast as a function of the eccentricity.
While scanning its environment the human brain incepts saccadic eye movements searching for noticable objects (compare Chapter 2.2.2). To identify an object, the fixation must be keeping up (e.g. to identify a traffic sign). Since the structure of a traffic scene is complex, there are several factors that influence the detection of an object. The factors that affect the detection behaviour are:

- The size and shape of the object
- The chromaticity of the object
- The object's position and its movement in the visibility field of the driver
- The luminance level and distribution in front of the vehicle

The individual factors will be covered in more detail below.

### 2.2.2 Peripheral vision

In the central visibility field objects can be identified, while the peripheral visibility field is used to perceive objects and their localization. If the human eye takes a stimulus in the periphery, it is brought to the Fovea Centralis for a clear identification [50]. The Fovea Centralis can only occupy 1.5° around the visual axis which

corresponds to a circle with a diameter of 1.0 cm at viewing distance of 40.0 cm. The entire visual procedure is divided into three parts: First, a peripheral detection of an object occurs, followed by a saccade and a fixation [50] [5].

To make a statement about what kind of object is involved, it must be depicted in the Fovea Centralis. The Fovea Centralis is indicated as the place of the sharpest sight on the retina. The eye constantly carries out very small movements. In order to capture objects in the whole visual field the rest of the retina has been provided with other preferred features which allow to quickly detect rapidly moving objects, i.e. possible dangerous obstacles. A movement of the object in the peripheral visual field provokes a jerky movement (reflective saccade). In order to be able to track the object, the eye makes slow follow-up movements. During the actual identification, the image of the visual object is held for 150.0 ms (reading) to 500.0 ms during the search of an object [48].
Extrafoveal perception is also important for the perception of large complex scenes (e.g. crossroads). Fundamental information like large contrast gradients along the object contours, motion, etc. need to be detected. Several interdependencies have an influence on the mapping of the visual space and perception of transient happenings. Besides the extrafoveal perception the performance of realistic visual objects is of importance. This can be explained by the fact that the decrease of visual capability starting from the fovea is not abrupt but gradual, so that stimuli of sufficient intensity can still be perceived up to large eccentricities in periphery.
The whole procedure can be expressed on the basis of a control circuit for information acquisition processing, that is illustrated in Figure 2.8. The question is to

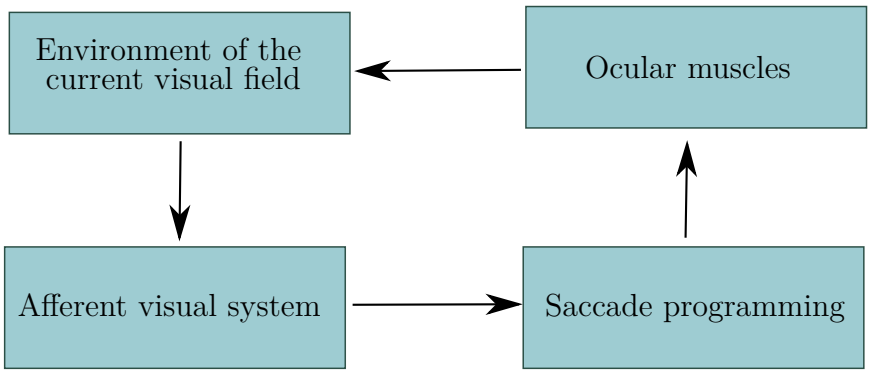


Figure 2.8: Control circuit for information acquisition processing. The visual impression of the current environment is transported to the brain via the afferent visual system. In the brain area that is responsible for the saccade programming, the next saccade target is selected and the next saccade aim point is calculated to reach the next point. Appropriate neural signals are sent to the brain stem, which move the outer eye muscles in motion and the eyes to the new aim point [1].

what extent the significance of this functional classification (foveal and extrafoveal perception) on the retina for road traffic is. As a rule, it is assumed that objects which are relevant to the driver are not randomly located at their fixation point, but appear at some point in the paracentric or peripheral visual field. The peripheral vision function must perceive the object. The gaze movement, which is responsible for

the resolution of the viewing application, must signal whether the object is relevant or not. If this is the case, a gaze movement is performed which transports the object to the fovea to receive more object details. A vehicle driver therefore continually uses this functional antagonism between the fovea and periphery to transfer objects, which are relevant, for an exact analysis in the retina centre. A safe participation in road traffic is only possible if both components of the visual perception are intact. The visual impression of the current environment is transported to the brain via the afferent visual system. In the brain area that is responsible for the saccade programming the next saccade target is selected and the next saccade aim point is calculated to reach the next point of interest. Appropriate neural signals are sent to the brain stem, which move the outer eye muscles in motion and the eyes to the new aim point.
Real field studies with monitoring eye tracking devices have shown that the gaze behaviour is also dependent on the traffic situation [56] [21].

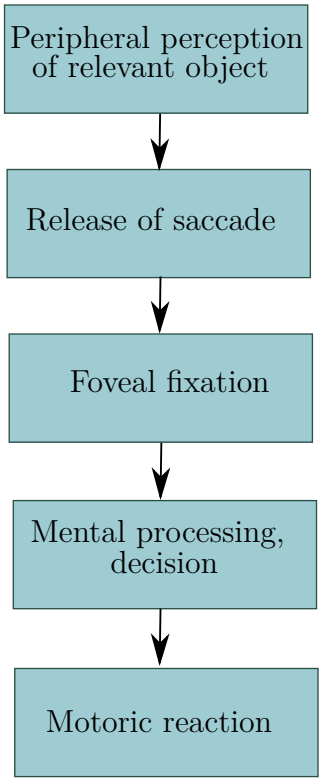


Figure 2.9: Object appears at some point in the paracentric or peripheral visual field. After releasing saccades the object is fixated in the fovea. The information is processed and followed by a motoric reaction of the driver (e.g. a braking action) [1].

Much more gaze movements have to be carried out in a city traffic situation in order to be able to capture all relevant objects compared to driving on a rural road. In this case, the saccades are restricted to a relatively small central visual angle area in which the roadway section far away from the driver is located. The position of the points of view depends also on the course of the roadway. In a right bend, the target points on the right edge of the road are piled up, in a left bend the target points are on the left, i.e. in direction of the bend [5].
Moreover, it has been shown that the strategy by which the driver triggers the gaze behaviour is influenced by his experience. While a new driver is still relatively undirected and aimless gazing, an experienced driver has already learned to unconsciously direct his points of view to the places where the occurrence of dangerous objects is to be expected in an increased degree [56]. The driver's vision strategy therefore aims to capture a maximum of relevant information with as few as possible eye movements. A maximum of three saccades per second can be performed as a larger number is not possible due to the required processing time [57]. An illustration of the procedure is shown in Figure 2.9.
It has been shown that the predominant number of saccades is in an eccentricity range up to a maximum of 10.0°. Saccades with larger amplitude are rarely triggered. If peripherally located objects greater than 10.0° need to be detected, the driver takes a head turn to support. It often also leads to a combination of saccades and head rotations in order to keep the partial movements of both com-

ponents as low as possible. The triggering of saccades and head rotations and thus the selection of the fixation points is usually unconscious [58].

### 2.2.3 Perception and reaction in traffic

In all situations in which the driver does not expect a certain event, e.g. if a pedestrian unexpectedly appears out of a concealed area, a saccade movement is required, which results in a reaction time delay. The reaction of the driver during an emergency braking can be divided into the following time sections [33]:

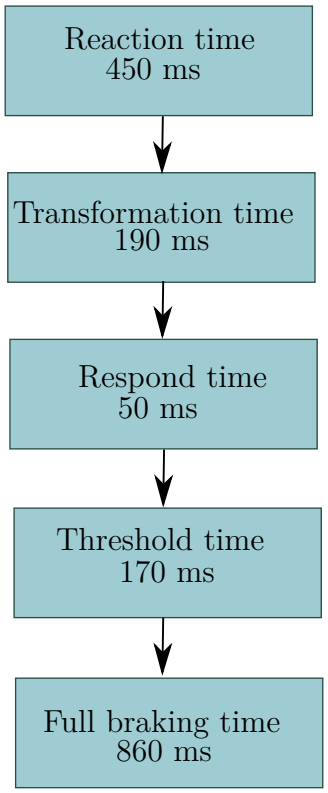


Figure 2.10: Singe time periods of driver's reaction during an emergency braking according to [1].

1. Reaction time: From the beginning of the object fixation to the muscular reaction. The basic duration includes the time for foveal processing of the stimulus, recognition of the situation and decision about the subsequent reaction (450.0 ms).

2. Transformation time: From the beginning of the muscular reaction to the brake pedal contact (190.0 ms).

3. Respond time: From the beginning of the brake pedal contact to the braking action (50.0 ms).

4. Threshold time: From the beginning of the braking action to the block- or regulation drawing (170.0 ms).

5. Full braking time: From the beginning of the blocking track drawing to the vehicle stopping. The full braking time depends on the vehicle speed, quality of the brakes and road surface.

The temporal sequence of a deceleration can thus be divided into two parts, the psychophysical times and technical times. However, the values are only applicable to a limited extent in practice since the reaction time measurements are usually performed in known situations [33]. Adding up all given guideline values (1. to 5.) results in a loss of time of 860.0 ms.
The gaze movement time, on the other hand, is composed of the saccade latency, saccade duration and saccadic suppression. For the road traffic, smaller values of saccade amplitudes from 5.0 to 10.0° are particularly relevant. If one adds the gaze movement time to the loss of time, the resulting times are considerably longer than 1.0 s (compare Table 2.1). This makes it clear that whenever the perception of a driving object is necessary, or if the attention of the driver is required, a deceleration time of more than 1.0 s is to be expected.

| Saccade amplitude / ° | 5.0 | 10.0 | 15.0 | 20.0 |
|---|---|---|---|---|
| Latency | 378 s | 406 s | 435 s | 464 s |
| Duration | 128 s | 153 s | 178 s | 203 s |
| Saccadic supression | 50 s | 50 s | 50 s | 50 s |
| Gaze movement | 556 s | 609 s | 663 s | 717 s |
| Total reaction time | 1416 s | 1469 s | 1523 s | 1577 s |

Table 2.1: Total reaction time including gaze movement and increased attention level according to [1] [33].

## 2.3 Contrast definition

In the mesopic region the perceptual conditions are changed. While the visual acuity of an emmetropic eye is approximately 1.0 at daytime, the visual acuity decreases to 0.5 at night-time. The contrast sensitivity and colour vision are also reduced. Recognizing an object at a night's drive in time is essential for an accident prevention. The difficulties in night-time traffic situations are to recognize not illuminated or not self-illuminating road users. In headlamp standards the distribution of the headlamps' illuminances are indicated. Neither the luminous flux nor the illuminance can be perceived by the human eye directly. The photometrically equivalent to the perceived "brightness" is the luminance.
To give an example, the illuminance on a white sheet of paper that is printed with a black number "one" is the same at all positions. Even so the black number will be perceived as "darker". A statement about whether an object can be perceived or not can be expressed by the luminance contrast.
The so called Weber contrast is defined as follows:

$$K_W = \frac{L_O - L_U}{L_U} \tag{2.1}$$

where $L_U$ describes the background luminance and $L_O$ the object luminance. This definition is suitable for proportional small objects in a large environment [5]. One differentiates the positive contrast ($L_O > L_U$) and the negative contrast ($L_O < L_U$). Furthermore, there is a contrast definition according to Michelson

$$K_M = \frac{L_O - L_U}{L_O + L_U} \tag{2.2}$$

which is also indicated as modulation. This definition is used if a clear distinction between the object and the background luminance is not possible. It is defined as ratio of amplitude to mean value of the luminance distribution. Another contrast definition is used for characterisation of optical displays:

$$K = \frac{L_2}{L_1} \tag{2.3}$$

with $L_1 > L_2$ ($L_1$, $L_2$ object or background luminance). In the following course of this work, the Weber contrast definition will be used only.

In contrast to stationary street lighting in the case of headlight illumination, objects almost always appear in positive contrast. As presented in Figure 2.11, the luminance difference of an object compared to its surroundings decreases with increasing distance to the vehicle.

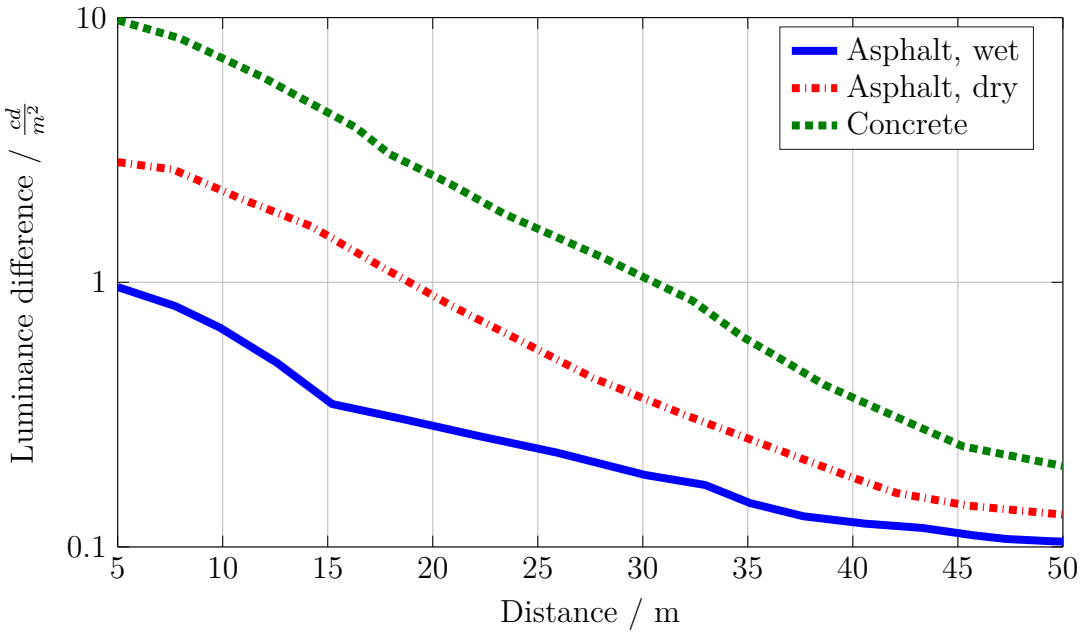


Figure 2.11: Luminance difference of different road surfaces in front of the vehicle as a function of the distance, halogen headlamps, low beam [5].

Starting from the illuminance that is directed to the object related to its reflectance, the object luminance and thus the contrast of the object to its background can be computed.

### 2.3.1 Visibility Level

The visibility level VL is defined as ratio of object contrast and threshold contrast. If the existing contrast $K$ is larger than the threshold contrast $K_{\text{thresh}}$, the object is visible. A visibility level of VL= 1.0 corresponds to the perception probability of 50.0% and perception criterion "visual object just seen". The visibility level is defined as follows [59]:

$$VL = \frac{K}{K_{\text{thresh}}} = \frac{\frac{\Delta L}{L_u}}{\frac{\Delta L_{\text{thresh}}}{L_u}} \tag{2.4}$$

The visibility level is based on the model of Adrian [13] and is the most common theoretical model used to assess road lighting quality. It is proposed as an improvement of previous methods and a quality index in road lighting design, that serves to assess automotive lighting performance. Unlike illuminance levels, the VL also provides the psychophysical aspect, means a link between lighting design and a real driving task. It can also be applied to actual visual performance on the road.

The reference performance of the VL is the detection of a small uniform target in front of a uniform background and also a field factor, that is dependent on the task of the driver. A case of visibility level model application for a standard night traffic scenario would be, to consider, how well a small target on the road can be detected by a driver at a certain distance.

The main condition is aligned in terms of driving safety: the lighting needs to be optimized according to a visual task which is critical for a possible hazard (for example a collision). Nontheless, in literature the VL index is often deprecated [60]. A standard target is more difficult to detect than most obstacles on the road. Conducting experiments with small uniform square targets neglects the importance of more realistic targets such as pedestrians which differ in terms of shape, size, reflection, complexity and texture.
Moreover, the vehicle's headlamp lighting is not taken into account. In conclusion "small target visibility" (STV) is not clearly measurable and also difficult to verify in the field. Therefore the definition of a threshold of the VL is also complicated since its relevance to real driving situations is limited. In American standard [61] the VL is proposed as a quality assessment index, but not in European standard [62]. Still, the VL is subject to a number of weaknesses with regards to the driving task and the not realistic shape of the reference target.

### 2.3.2 Influence of age

In the course of life, every human is increasingly restricted by the functionality of the visual system in all areas through the progression of life years. Physiologically a compaction of the optical media is developed, especially in the lens of the eye, which leads to a reduction in mesopic vision and an increase in the sensitivity to glare.
The most important parameter for the evaluation of vision is visual acuity. Once the light enters the eye, it is focused by the cornea and the lens. The cornea has a decisive influence on the eye optics with 75.0% of the refractive power [63]. The remaining 25.0% refractive power is determined by the lens, which, unlike the cornea, is not rigid but can be adjusted in its shape in order to adapt to stimuli at different distances. In order to focus an object, the optical power in the human eye is automatically increased. This process is called accommodation and describes the curvature of the lens caused by the contraction of the ciliary muscles at the front of the eye.

While observing an object the focus of the human eye adjusts continuously, it accommodates. Hence it is possible to focus to both near located and far-away located objects, whereas it is not feasible to focus near and far-away objects at the same time [2]. Nevertheless, the accommodation is also limited: the so-called near point denotes the distance below which the lens can no longer accommodate.
With increasing age of a person the distance of the near point is raising significantly, one speaks of middle aged vision (presbyopia). This can be explained by the hardening of the crystalline lens, that occurs with increasing age which in turn affects

the accommodation. Whereas the near point of a twenty-year-old is approximately 10.0 cm, it increases for a sixty-year-old to in 100.0 cm [48]. While presbyopia is unproblematic in young life years, the ability to accommodate decreases for all persons of 45 years and above rapidly.
Other symptoms that can appear over the course of the human life span are senile miosis and cataract. In adolescence the crystalline lens is exceedingly transparent. With increasing age this transparency decreases especially for light with a short wavelength [51]. The lens of a twenty-year-old absorbs 10 times less light than the lens of an eighty-year old, this means that the more light is absorbed, the less light is transmitted and leads to a loss of important information in vision. With an advanced age the crystalline lens becomes clouded (opacification) and additionally effects like increment lenticular scattering can occur which results in a cataract. The weightiness of the cataract is dependent on size and position of the opacity on the lens and therefore a personalised disadvantage.

In the peripheral retina the visual acuity declines beginning with the fovea with increasing eccentricity to the visual axis. This can also be expounded by the distribution of the receptors in the retina (compare Figure 2.3). On one hand, within the fovea the rod density increases with a high gradient, on the other hand, the density of the cones decreases. For an eccentricity of $\theta = 4.5°$ the rods are about twice as many as cones in place. For $\theta = 10.0°$ the rods are thirteen the amount of cones. Visual acuity is dependent on the distribution of the cones in the retina. While the number of the cones remains virtually constant during the human life span, certain receptors lose any of their functionality, as the spacing and regularities of the receptor structure is reduced. This can be explained by the fact that the number of cells in the retina's ganglion cell layer decreases [64].

## 2.4 Psychophysics

In this work the perception of the human eye will be analysed. Since it is not possible to objectively measure the ability of a subject and thus his sensitivity to a stimulus, the results have to be obtained by visual observation task of test subjects. Therefore, methods based on psychophysics are used, this means a physically measurable stimulus is compared with the individual sensitivity of the participant.

### 2.4.1 Psychometric function

By a binary evaluation of a stimuli, for example, a "yes" and "no" evaluation, a relative frequency is obtained for each intensity. Illustrating those intensities, the data typically have a S-shaped, monotonically increasing behaviour (compare Figure 2.12). Using the psychometric function, a psychophysical link between the intensity and relative frequency of the positive evaluation can be assumed. Each point on the function can be interpreted as a response probability with respect to the intensity [65]. The normal distribution, as well as the logistical or Weibull function, are in most cases suitable as an approximation to the psychophysical behaviour [66].

Ideally, the subject can differentiate precisely between perceived and not perceived stimuli, as in this case, the function's gradient is as large as possible.

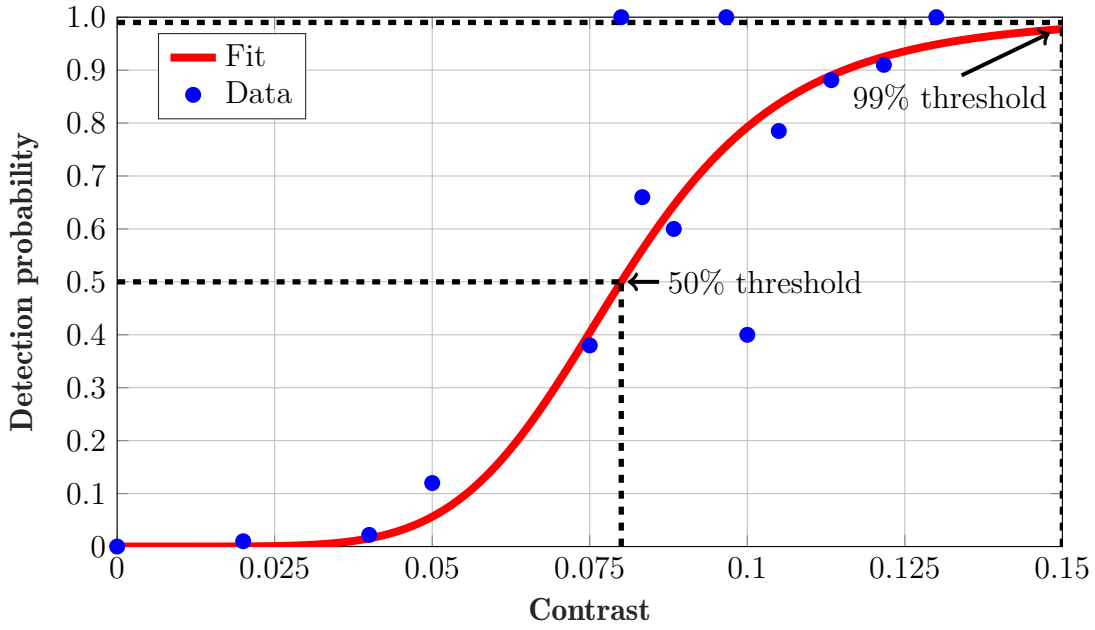


Figure 2.12: Detection probability related to contrast, fitted S-shaped psychometric function (solid line) to data points (blue), 50% as well as 99% detection probabilities are marked with dashed lines.

It is always possible that a subject responses with an incorrect evaluation. An incorrect evaluation is taken into account with a failure rate $\gamma$ and expresses the amount of wrong answers. Thus, it represents a limitation factor of the function. The psychometric function can be expressed as follows:

$$F(x) = \gamma + (1 - \gamma - \lambda) \cdot \frac{1}{1 + \left(\frac{x}{\alpha}\right)^{-\beta}} \tag{2.5}$$

with

- $\gamma$, failure rate
- $\lambda$, probability rate
- $\frac{1}{1+\left(\frac{x}{\alpha}\right)^{-\beta}}$, logistic function, $\alpha$ corresponds to the 50% threshold, $\beta$ is proportional to the gradient
- $x$, intensity, in this investigation $x = K$, $x = \Delta L$

Based on the gradient of the psychometric function it can be seen to what extent an increase in detection probability can be achieved with increasing contrast. The threshold of the psychometric function is denoted at 50% and describes the point at which bright and dark are perceived as equivalent.

### 2.4.2 Determination of the threshold contrast

There are several methods to determine the just noticeable difference and subsequently, the psychometric function. It is important to note that biological systems are variable in their responses, that is to say, a participant possibly can make a mistake. Adaptive methods are particularly efficient, since they adapt the stimulus of each test run to the result of the previous test run.
The contrast sensitivity is determined by means of the threshold contrast. In Table 2.2 adaptive methods that can be used for the determination of the threshold contrast are presented.
In the following, the methods mentioned in Table 2.2 will be explained in more detail.

- **Method of average error.** The participant has to adjust a variable stimulus so that it is just perceived (absolute threshold) repeatedly or coincides with a predetermined standard stimulus (difference threshold). From the participant's responses, the mean value and difference threshold are calculated. The difference between mean and difference threshold is called constant error.

- **Limits method.** A stimulus series is presented in which the reactivity is alternately increased or decreased. For example, a stimulus is increased in intensity in small steps until the stimulus is perceived. Then the stimuli presentation is continued with an above-threshold stimulus, which is lowered until the threshold is reached. With this method as many as possible series of stimuli have to be carried out, until at the end the mean value is assumed as an estimate for the threshold value.

- **Method of constant stimuli.** A further method for threshold determination is the so-called method of constant stimuli. In this method, previously defined stimuli are presented randomly one after the other. Since each stimulus is repeated n-times, the proportion of the "yes" responses (object perceived) can be calculated as a probability. Subsequent, the psychometric function is determined from these data points.

As already mentioned, adaptive methods are particularly suitable to determine the psychometric function, since the sensitivity of the subject increases with the stimulus level. In this work the method of constant stimuli was used for contrast determination in the laboratory investigations.

In Figure 2.13 a flow diagram that describes the determination of the psychometric function is illustrated. To determine the threshold value, a whole series of stimuli is presented as a data set. Additionally, for each experiment, the factor of the participant's response is taken into account, this means that the stimulus needs to be changed constantly.
The threshold value is determined as follows:
During a test run, a systematic variation of the stimulus intensity (contrast change) occurrs in many intermediate steps. Therefore the contrast levels are randomized. The participant's answers are recorded by pressing a button on a input device (yes/

| Method | Presentation | Task | Order | Criteria |
|---|---|---|---|---|
| Method of average error | Objects should be indistinguishable | Participant adjusts equal luminance | - | Contrast sensitivity difference is expressed by the adjustment error |
| Limits method | Objects have variable contrast | Threshold is adjusted with up/ down method | From seen to not seen and conversely | Mean value of all measurements |
| Method of contstant stimuli | Objects with different discrete contrast values | Decision, if seen or not | randomized | frequency distribution by 50% detection probability |

Table 2.2: Test methods for threshold contrast determination for interval scaled and normally distributed variables according to [34].

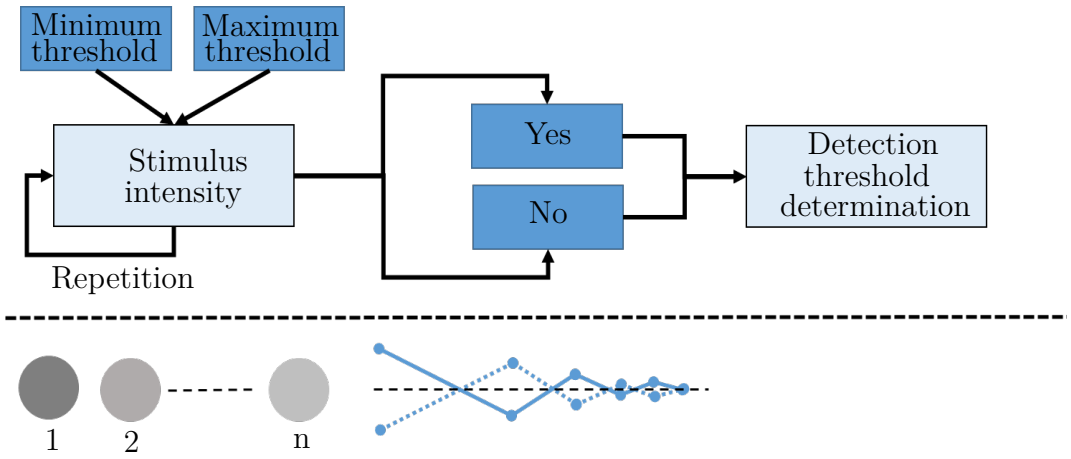


Figure 2.13: Determination of the detection threshold. Repeated target presentation at different intensities; Individual minimum and maximum thresholds are set for two luminance levels. Thus each subject receives the same boundary conditions.

no answer), whether the stimulus was seen or not. If the participant is not sure of his answer, he does not press any button. In this case the perceived threshold is below the threshold value. This does not mean that the difference is invisible or imperceptible, but the detection probability decreases ($< 50\%$). Depending on how the participant reacts to the stimulus, the intensity of the subsequent stimuli is automatically adjusted. The stimulus is thus adapted individually to the sensitivity of the subject and set to a fixed value at the beginning. The individual threshold values were determined at the end of the adaptation time.
In order to determine the perception thresholds from the respective contrast stimuli, the responses given by the subject were fed into a psychometric function. From this function the absolute threshold contrast is calculated. In case of yes /no experiments, the threshold is usually set to a probability of 50% (of the "yes" responses). In this investigation the 99% detection probability was determined and is also de-

fined as threshold value in the further course of this work.

### 2.4.3 Automatic Staircase

Classical psychophysical methods have the disadvantage that, depending on the design, they lose a considerable amount of time that is used to examine stimuli intensities away from the threshold. Adaptive Staircase processes stand out due to their simplicity and flexibility. The stimuli are varied by an algorithm depending on the previous response of the test person. This results in a temporal advantage in determination of the threshold as the detection object intensities are dynamically adapted. The Staircase method approaches the suspected threshold very quickly and thus uses the maximum amount of information from each stimulus presentation [67]. Therefore, most of the presented stimuli are very close to the threshold. The required time for a threshold determination can thus be greatly shortened.

In Figure 2.14 an example for the course of the threshold determination by means of one test iteration is presented. On the left hand side the initial values of the upper ($S_O$, solid line) and lower ($S_U$, dashed line) Staircase response are indicated: If the object is not perceived the intensity is increased (+), if the object is perceived the intensity is reduced (-).

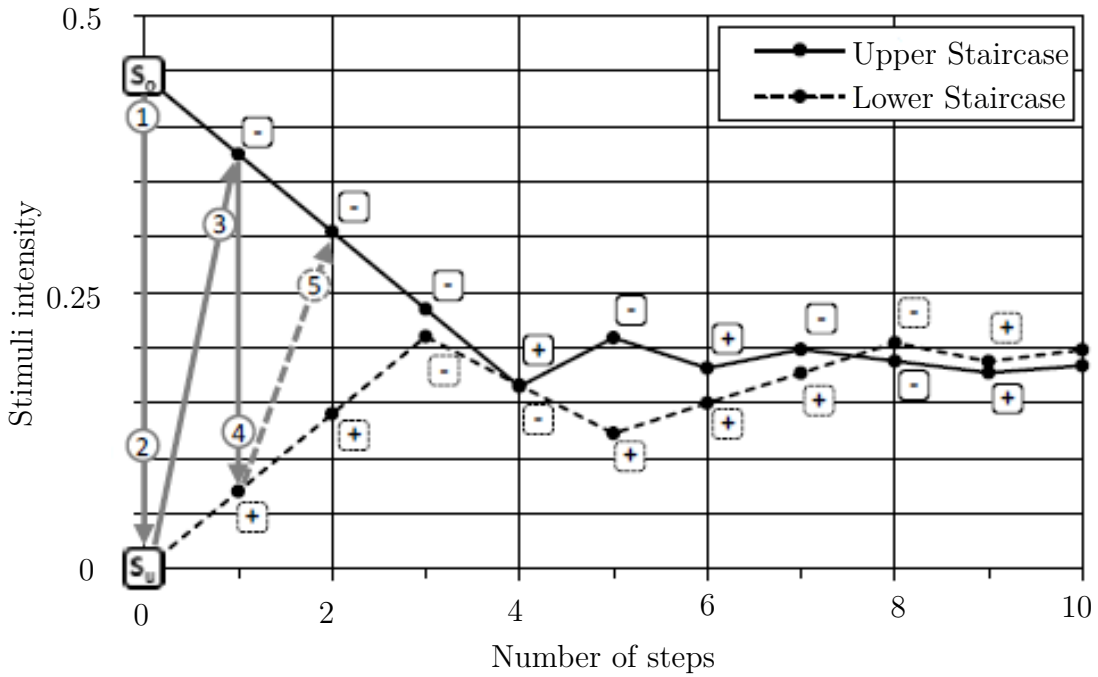


Figure 2.14: Schematic representation of the double Staircase according to [6] [7]. Initial values of the upper ($S_O$, solid line) and lower ($S_U$, dashed line) Staircase response: if the object is not perceived the intensity is increased (+), if the object is perceived, the intensity is reduced (-). $S_O$: start value.

The initial values $S_O$ and $S_U$ of the two staircase procedures are determined individually for each participant in a rough determination of the threshold [7] [6]. For this purpose, the intensity of the detection object is increased by the participant

based on the maximum representable contrast of the object from 0% in steps of 10%, until the object can be safely detected for the first time. Based on this value, the initial values can be set flexibly. According to preliminary tests $S_O$ was set to 99% and $S_U$ to 5% of this contrast.
A detailed description of the adaptive methods is omitted here. A more detailed description of the Automatic Staircase method used in this work can be found in [6].

## 2.5 Statistics

An experiment is a procedure which proves cause and effect correlations. Participants are tested under various conditions for several test runs. Thereby, independent variables and their effect on dependent variables are recorded. The boundary conditions are kept constant during the experiment, so that differences in dependent variables are exclusively reliant on the systematic change in independent variables. The statistical analysis of the variables is based on several criteria to construe the results. For an evaluation the following factors should be analysed [35]:

- Significance of measured mean value differences
- Uncertainty/ confidence range of the measured mean value
- Interrelationships between independent variables
- Reproducibility (reliability)

### 2.5.1 Analysis of variance

A common method for evaluating experiments is the so-called analysis of variance (ANOVA) . It is a method to analyse whether the values of dependent variables in different sample groups are significant or whether differences can only be explained by random errors [35]. Differences between the measured values are divided into two parts: a systematic analysis of variance part due to influences of the independent variable, and an unsystematic part, which is created by coincidence. Both sizes are set in relation with each other. The result is the so-called F-value. If the F-value is sufficient large, it can be assumed that differences between individual groups are not due to random fluctuations respectively.
In this case the result is significant and is given with a value $p < 0.05$. Furthermore, for any possible composite of independent variables an interaction for significance can be quantified and tested. Interaction describes the factors influencing each other with regard to their effect on dependent variables.
One must distinguish between an analysis of variance with only one independent variable (one-factor analysis of variance) and one with multiple independent variables. In order to perform an analysis of variance, certain requirements must be fulfilled.
In addition to a normal distribution of the data, a one-factor or two-factor analysis of variance must also ensure variance homogeneity over all samples (the variances of the individual samples must be the same [68]). Overall, this test method can

be understood as a decomposition of the total variance. An advantage of using analysis of variance is that it is very robust against infringements of assumptions. For the following investigations, the requirements were proven and deviations were considered to be sufficiently small.

### 2.5.2 Significance tests

Table 2.3 provides an overview of possible test procedures that can be applied to interval scaled and normal distributed variables. There are a number of methods that can describe the relationship between two variables.

| Number of samples | Dependence | Test |
|---|---|---|
| 2 | Independent | t-test |
| 2 | Dependent | t-test for dependent samples |
| $> 2$ | Independent | One-factor variance analysis |
| $> 2$ | Dependent | One-factor variance analysis with repeated measurements |
| $> 2$ | Independent | Two-factor variance analysis |
| $> 2$ | Dependent | Two-factor variance analysis with repeated measurements |

Table 2.3: Test procedures for interval scaled and normally distributed variables according to [35].

A variance analysis with repeated measurements considers that more than two dependent variables are related to one another [35]. If two or more samples exist, the samples can be compared in pairs, but with a small sample number, this becomes problematic. Therefore, a global test is used to prove all samples. In this work, a two-factor variance analysis is used as global test. If this test provides a significant result, the samples are compared in pairs to determine possible significances. Using those methods clear distinctions must be made between individual definitions:

- Detection: Is the luminance difference or contrast of an object just noticeable?
- Simple identification: Is an object perceivable based on a specific attribute?
- Complex identification: Is an object perceivable based on all attributes?

A detailed description of the different statistical methods can be found in [35] or [68].

# Chapter 3

# State of the art

The following chapter provides an overview of the current state of the art and regulations that must be taken into account when implementing new headlamp systems. In addition, accident statistics are consulted to underline the importance of the topic.

## 3.1 Accident statistics

For better understanding the safety aspect of the road network in Germany, a brief overview of the current accident statistics is provided. Two-thirds of the accidents in road traffic occur at night-time outside urban areas and mostly under unfavorable weather conditions without any street lighting. 80% of the fatal accidents with pedestrians happen in the dark. Since there are not many pedestrians out at night-time the accident risk can classified as significantly high. Additionally it should be noted, that approximately 85% of the pedestrians wear dark clothes with a small reflection coefficient [69]. From CIE No.191 [69] it can be inferred:

"A pedestrian wearing grey clothing seen against the road surface (black/grey) has achromatic contrast whereas a pedestrian with coloured clothing has chromatic contrast. Also, coloured traffic signs have chromatic contrast against the surrounding scene due to the selective reflectance of the coloured markings at different wavelengths."

A total of 2.5 million traffic accidents occurred in Germany in 2015, with 2.2 million accidents involving no personal injury. In the remaining 0.3 million casualties, 1% (3,459) of the accidents were fatal, in 22% (68,706) the road users were badly hurt and 76% (233,494) of the cases were only slightly injured [70]. Of the total of 3,459 fatal accidents, 1,024 people aged 65 or more were concerned. Furthermore 1,181 of the fatal accidents took place at night or at dusk. A significant improvement could be achieved, as in 1991 about 11,300 people were killed [71]. Of the 0.3 million accidents involving personal injuries, about 3097 people were involved in an accident with animals on the road, 2228 of the animals involved in the accident were wild animals [8] (compare Figure 3.1). Overall, a total of 651 accidents with objects on the road were recorded.

Since in this work the influence of the age is also considered, age-related accident statistics are also of interest. The percentage of people aged 65 and over as a whole is growing steadily, from 15.5% to 21.0% in the last 20 years [9].
At the end of 2014, a total of 17.1 million people aged 65 years and older lived

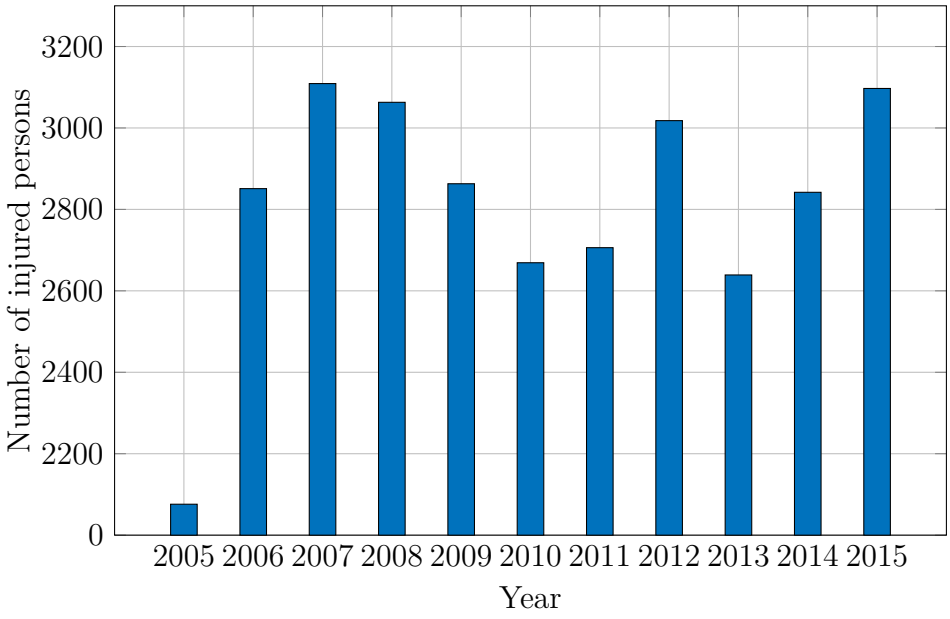


Figure 3.1: Number of injured persons in accidents caused by wild animals on the road (in Germany) according to [8].

in Germany. In 2015, 73,338 elderly people were involved in accidents involving personal injuries, which was 12.9% of all accidents. As a result, seniors have a distinctly minor part of accidents compared to their part of the population, which can be explained by their reduced attendance in traffic as vehicle drivers. Seniors are more active these days than former generations and are more likely to use a vehicle, but overall, their average driven distances per year is still significantly lower compared to younger age groups [9]. The group of seniors is a very inhomogeneous age group, as far as their perception, visual performance and health are concerned. In particular, the deterioration of the visual faculty and reduction of the reactivity with increasing age are important influence factors. The availability of older people, especially older women, is also significantly lower than the amount of male seniors [9]. The type, duration and frequency of the participation in road traffic of older male drivers differs significantly from younger age groups and thus have an impact on the accident behaviour.

In 2015 a total of 48,690 people aged 65 or more had accidents in road traffic, 35,267 seniors were slightly injured (increase of 2.4%) and 12,399 were badly injured (increase of 1.7%) [9]. This resulted in an accident increase of 2.3% compared to the previous year.
Complex situations in road traffic are more difficult to cope for older participants than for younger age groups. For example, “off-road driving” was the most common cause of accidents of 467,81 vehicle drivers involved in personal injuries (17.7%). It was followed by “turning, reversing and starting” corresponding to 16.5%. Thus, the accident causes point to age-related limitations of visual perception.
As illustrated in Figure 3.2 a total of 46,781 accidents involving personal injury occurred to drivers who were at least 65 years old, 36,916 were accused of misconduct

in road traffic. For old pedestrians the most frequent accident was “wrong behaviour when crossing the road”(80.8% ). In over half of the cases (66.4%) it was “crossing of the road, without paying attention to vehicle traffic”. Further casualties had a significantly lower importance [9].

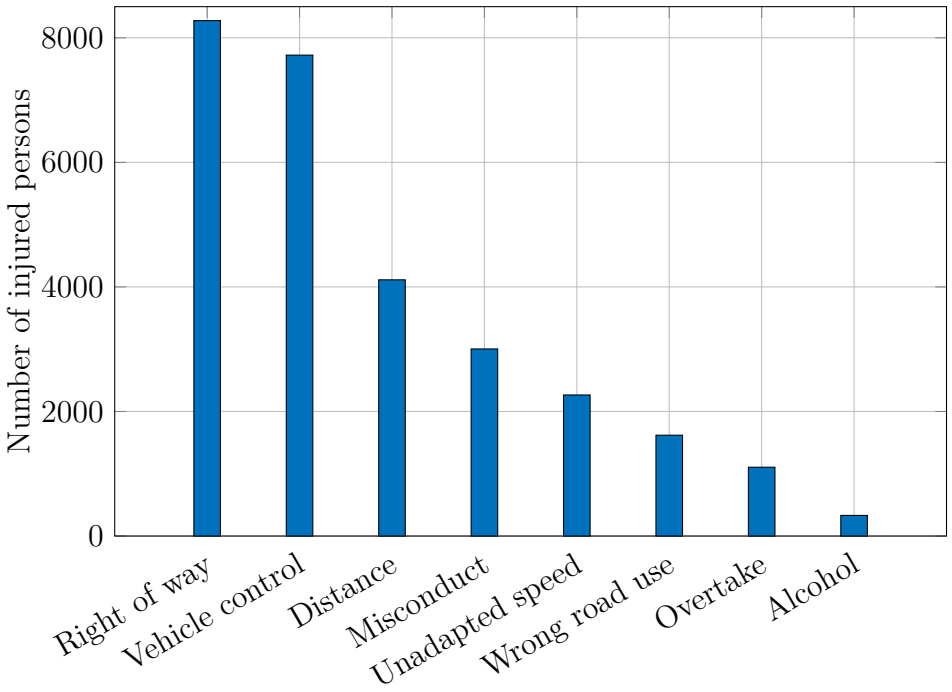


Figure 3.2: Misconduct of seniors at the age of 65 years and older as vehicle driver according to [9].

For the reasons outlined above, it is definitely necessary to performe both age-based examinations and investigations, which examine the perception of an object, in more detail.

## 3.2 Development trends of frontlighting headlamps

From the above-described aspects, two vehicle and lighting-technical requirements can be summarized:

- **Detection.** First, the headlamp system should be realized with a homogenous luminous intensity distribution to reach the maximum achievable visibility distance. On the one hand, the lateral driving area and driving environment must be considered, since road markings, traffic signs and possible objects need to be recognized. This has the consequence that the subjective feeling of the driver's safety is also increased. In order to achieve large detection distances, it is desirable to keep the contrast as large as possible, i.e. along the road axis, as much light as possible should be projected onto large distances. For the light sources of the headlamp system this means that both high luminous flux and optimized optics of the headlamps are necessary.

- **Glare.** Second, the glare of oncoming traffic or traffic ahead should be prevented or minimized. Therefore, the luminous intensity distribution of the headlights as well as the entire operating system of the headlights should be designed in such a way that the illuminance at the eye produced by oncoming or preceding traffic do not exceed the regulations' maximum permissible value.

Depending on configuration, a visibility distance of 50.0 m to 85.0 m can be achieved using the low beam function. Using low beam is a kind of compromise, since it must be able to provide a maximum visual range to the driver ahead of the vehicle. At the same time oncoming traffic or other road useres should not be glared. Therefore, the corresponding ECE (Economic Commission for Europe) regulations define the upper limits of illuminance [10]. Since the nineties, new lighting systems have been continually developed, which allow a higher visibility and still reduce glare. The development of present and future headlamp systems for visual improvement is characterized by the following three technological developments [72]:

- Development of light source technology
- Development of adaptive lighting
- Development of the assistance light system

In Table 3.1 the lighting properties of current headlamp light sources with different spectral distributions are illustrated.

| Lamp type | Luminous flux / lm | Maximum luminance / $\frac{Mcd}{m^2}$ | Luminous efficacy / lm/W | Color temperature / K |
|---|---|---|---|---|
| Halogen (H7) | 1100 | 30 | 25 | 3200 |
| Xenon (D2S) | 3200 | 90 | 90 | 4300 |
| LED (cold white) | 1000 | 75-90 | 75 | 4300 to 4600 |

Table 3.1: Lighting properties of current headlamp light sources according to [36].

### 3.2.1 ECE standards

National and international standards require that automotive vehicles use lighting systems at night, in order to improve the visibility of the road environment [62] [61]. ECE regulations are constantly adapted to the technical development of luminaires and lamps. Today's possibilities for adapting the light distribution to the traffic situation are also taken into account by updating standards.
Amendments or revisions are prepared in the technical bodies of the Groupe de Travail "Bruxelles 1952" (GTB) and submitted to the decision-maker Groupe de Rapporteur Eclairage (GRE). Subsequently, the submission is delivered to the Working Party 29 (WP.29) of the ECE, where it is ultimately adopted [73]. The rules for the registration of vehicles and components are binding for ECE member countries, which acceded the agreement (since 1958).
Figure 3.3 shows the photometrically requirements for headlamps in accordance with

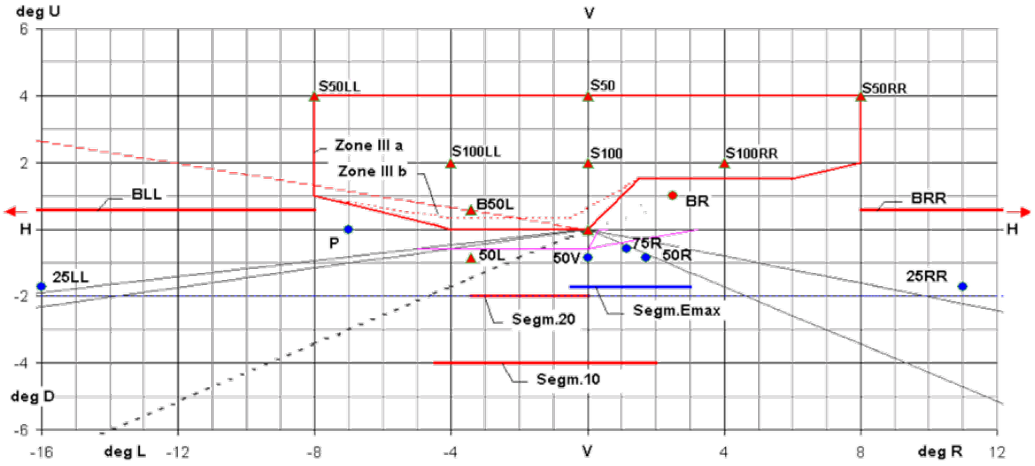


Figure 3.3: Photometrically requirements for headlamps in accordance with the European approval area (low beam) [10]. The measuring points are marked into the perspective image of the road. V-V: Vertical line through the vanishing point; H-H: Horizontal line through the vanishing point; B50L: Point of view of an observer in the opposite vehicle, 50 m away on the left side of the road; 75R: Point on the right side of the road, 75 meters away from the spotlight.

the European approval area (low beam). The measuring points are marked into the perspective image of the road. According to the regulations the headlamps' light distribution must be designed in such a way that the road is illuminated with certain minimum and maximum values. These systems need to provide enough visibility to the drivers, in order to perform their driving task in a safe way, independent of the current situation.
The small measured angular range will only be sufficient for a smaller percentage of traffic situations (i.e. only straight roads), a larger angular range will allow more complex situations (curves, marking of pedestrians close to the road). From earlier studies can be noted that the illuminance is not a good predictor for detection distance [34] [74], but it is used in the legislation to give minimal values for the detection distance (ECE No.20 [10]), ECE No.98 [75]).

### 3.2.2 Adaptive high beam systems

Adaptive front-lighting systems are subject to the Economic Commission for Europe (ECE) in a total of 62 countries, both European and others [31]. In ECE regulation No. 123, reference is made to ADB systems. According to [31] an ADB system is defined as follows:

"Adaptive front lighting system means a lighting device, providing beams with differing characteristics for automatic adaptation to varying conditions of use of the dipped-beam (passing beam) and, if it applies, the main-beam (driving-beam) with a minimum functional content..."

Considering the drivers point of view the ADB system should fulfill several re-

quirements. Beginning with a sufficient illumination of the horizontal and also vertical visual field of the driver, the ADB system is supposed to minimize glare towards oncoming and preceding traffic simultaneously. Hence, both the horizontal and vertical angular resolution are defined to be as fine as possible. In addition the homogeneity of the luminous intensity distribution must be ensured.
The requirements to technical parameters that also need to comply regularities are summarized as follows:
In the region with pixels turned on, the maximum illuminance (according to 25 m distance) is expected to be $E_{max} = 120.0\ lx$ (SAE limit), whereas the illuminance has to be $E_{max} = 0.5\ lx$ in the region with pixels switched off [31]. The state between the on and off (sharp horizontal and vertical cut-off lines) should be realized as a steep gradient. Thereby, the vertical range is supposed to lie within $H = -2.0° - 6.0°$ and horizontal range $H = \pm 8.0° - 12.0°$. Those values were determined from [43] in real traffic situations (Germany).

## 3.3 Research hypothesis

The aim of every headlamp system is to illuminate the driver's visual field so that all important information can be obtained considering the limits of the light output of the headlamp system to ensure safety. The following situation should be assumed: A person drives on a country road at night-time. An object, for example a wild animal, which frequently occurs in road traffic, appears from roadside in a certain distance (compare Figure 3.4). Hence, the question is asked with which probability the driver is able to detect the object. Therefore, the object detection probability is investigated as a function of the eccentricity, which is related to a reference point (the area ahead of the vehicle).
A luminance range from $0.001\frac{cd}{m^2}$ up to $5.0\frac{cd}{m^2}$ (corresponding to the area ahead of the vehicle, using low beam) is considered, with the upper luminance value depending on the object chromaticity and eccentricity. In this area, the visibility changes with the luminance level and thus also with the contrast of a corresponding object.

The aim is to increase the driver's safety. The question to be answered is, if there is an approach to perceive an object earlier and consequently to increase the response time of the driver to avoid an accident.
Thus, the purpose of this study is to contribute improvements in ADB light distributions from detection performance perspective. To increase the object's detection probability the luminance of the detection object must also be increased (compared to its background). The luminance level and luminance distribution in front of the vehicle are changing constantly. The second parameter is the object itself. Beginning with the chromaticity, shape and size of the object, both, its position in the visual field and its movement are an issue.

For static laboratory tests with real headlamp luminous intensity distributions it needs to be proved whether the mean luminance of the foveal area (2.0°) or the mean luminance of the visual field is decisively for the detection distance calculation (for the adaptation). In addition, the question has to be clarified, whether the

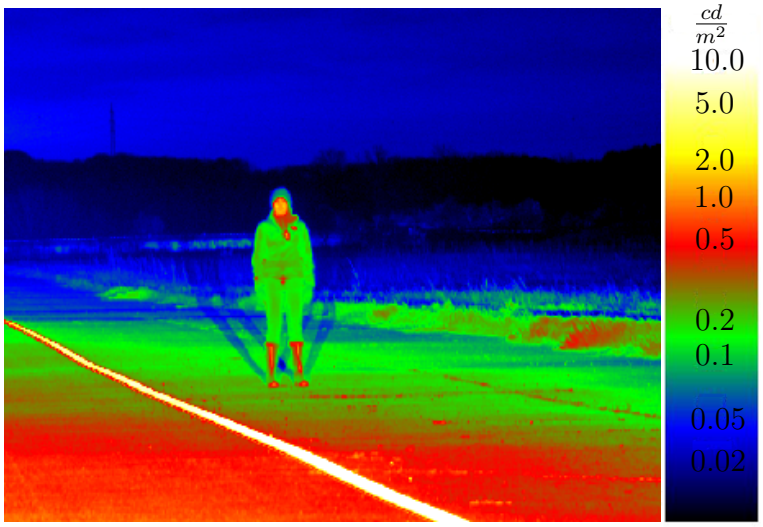


Figure 3.4: Luminance picture of human being on side of the road (female, height 1.76 m, completely dressed in black clothes, reflection coefficient < 5%). Person is perceived based on its luminance difference to the background or distinctive shape structure.

brightness impression is influenced by a specific luminance distribution.
It is known from literature, that many of the factors influencing the threshold contrast are known already. However, almost all results were obtained under laboratory conditions. The validation of data under night-time conditions in road traffic is still unknown for many influencing factors.

A particularly important point for the design of motor vehicle light distributions is the influence of the area ahead of the vehicle (3.0 to 12.0 m) on the detection distance. A bright area ahead of the vehicle would effect the threshold contrast negatively (according to scattered light theory). In addition to area in front of the vehicle, the position of the detection objects have also an influence on the detection distance. The investigations presented for the determination of the detection distance considered foveal observation exclusively. In real road traffic this case does not occur very often.
For complex detection objects, such as pedestrians and animals, the critical question to be answered is how to define the object size to be able to detect it. More important is, which attribute of the detection object is significant for a detection. One could, for example, ask which part of the pedestrian's body leads to a detection. In addition, the theoretical calculations of the required resolution for a certain object contrast were mostly performed only for laboratory conditions. To what extent these results can be used or transferred to real road traffic applications has not been tested yet.
In the following, the parameters which will be investigated in this work are summarized:

- Visual perception of objects in night-time traffic situations (mesopic range).
- Influence of object's shape

- Influence of object's size
- Influence of participant's age
- Influence of driving mode (static (laboratory conditions) or dynamic (field study in realistic traffic conditions including a driving task))
- Boundary values of the required visual characteristics depending on luminance or contrast
- A statement about how the perception changes with increasing contrast
- Probability with which the object is detected, depending on the object's position (eccentricity) and contrast compared to its background

# Chapter 4

# Previous findings in literature

In Chapter 2 the foundations for the construction of the visual system as well as the challenges of perception in the mesopic area of vision were described. In the following, a brief overview of studies carried out with regard to target detection for vehicle driving applications will be given. The findings will be integrated into the context of this thesis.

## 4.1 Luminance difference threshold model of W. Adrian

In 1946 Blackwell published investigations on the threshold luminance contrast that is essential for 50% detection probability of a visual target on a homogenous background under static viewing conditions in laboratory [37]. Based on Blackwell´s results Adrian recalculated the threshold contrast for a 99.93% probability [13]. Adrian´s model describing the visibility of objects in addition of some more experimental data laid the foundations for the visual performance model of the CIE (Commission Internationale De L'Eclairage) [59].

Adrian developed a model to describe the visibility of an object [13]. The model computes the target contrast and apparent size, contrast polarity (positive or negative, background (adaptation) luminance, observer's age, possible disability glare and observation time.
The term contrast sensitivity is used to describe visual perceptions. In past studies, the contrast perception and therefore also the contrast sensitivity were often examined. The contrast perception is dependent on the luminance of the environment ($L_u$). Adrian's model [13] considered the ability to detect a small target (uniform square, 18.0 cm $\times$ 18.0 cm) that was placed on the road at a defined distance ahead (86.0 m) as a quality index of the lighting installation. Starting from psychophysical data, with this model the detection threshold $\Delta L_{\text{thresh}}$ of a reference target for a given lighting installation can be determined for laboratory applications.

In his investigations Adrian also considered the visibility level (VL) which is another important aspect according to driving task. The VL is defined as the ratio between the actual contrast $K$, the difference $\Delta L$ between the target and its background and the detection threshold $\Delta L_{\text{thresh}}$. A visibility level of 6 means that the target's luminance contrast is six times the contrast that is needed for the detection of an object for a standard observer under laboratory conditions.
For road lighting applications Adrian approached a defined VL threshold for the visual detection task while driving which led to a reference illumination level for road

light engineering [18]. He proposed VL values in a range between 4 and 30 (compare Chapter 4.1.3.5). Subsequently, the individual parameters of Adrian's model will be described in more detail.

### 4.1.1 Law of perception according to Berek

In 1943 Berek developed the so-called law of perception of light stimuli [11]. Visual targets were presented with a positive contrast in front of a defined background luminance under laboratory conditions. The function determined by Berek is essentially based on the measurements of Knoll [76], Siedentopf [77], Schönwald [78], Arndt [79] and Schuhmacher [80]. This law contains three basic variables: the inner field luminance $B_i$, relative luminance $\Delta B = B_i - B_u$ and contrast $\frac{B_i - B_u}{B_u}$ (compare Figure 4.1).

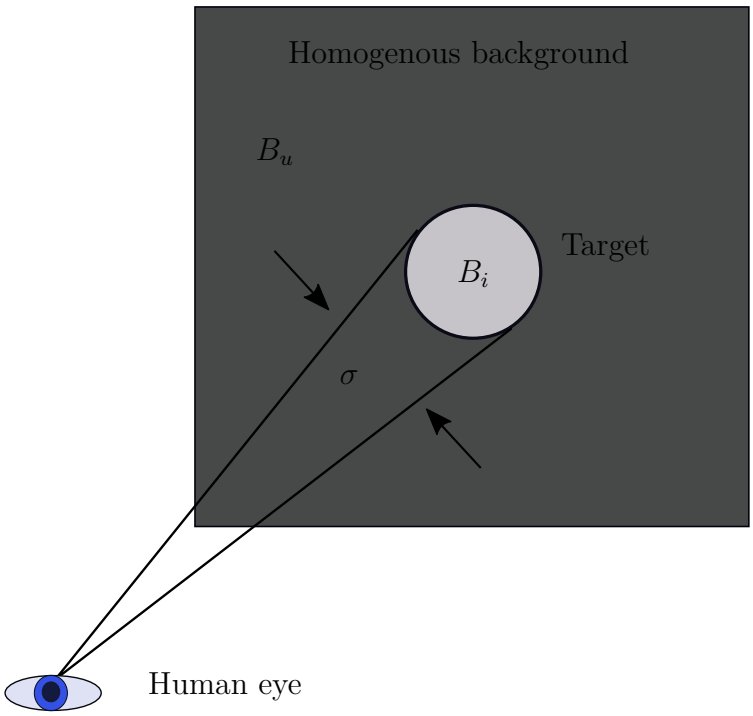


Figure 4.1: Experimental arrangement for determining the perception of light stimuli according to [11]. $B_u$: Background luminance; $B_i$: Inner field luminance; $\sigma$: Visual angle.

For marginal cases, Berek defined the relative luminance in relation to the visual angle $\sigma$ as follows:

$$\log\left(B_i - B_u\right)_{\sigma \to 0} = x + z \log\left(\sigma\right) \tag{4.1}$$

$$\left(B_i - B_u\right)_{\sigma \to \infty} = B \tag{4.2}$$

For very small visual angles, the correlation between $\log(B_i - B_u)$ and $\log(\sigma)$ is linear, while $\log(B_i - B_u)$ approaches a limit for large angles [11] . Assuming a

constant background luminance $B_u$, the parameters x, z and B can also be assumed to be constant. In this case, Equations 4.1 and 4.2 can be described as:

$$(B_i - B_u)_{\sigma \to 0} = \phi(B_u) \cdot \sigma^{z(B_u)} \tag{4.3}$$

$$(B_i - B_u)_{\sigma \to \infty} = B(B_u) \tag{4.4}$$

Furthermore, Berek assumed that the dependence of the relative luminance $B_i - B_u$ on the visual angle can be represented by an overlap of the two limiting cases. This interaction can be made additive (first case) or interacted (second case). The following equations are obtained:
First case:

$$B_i - B_u = \phi \cdot \sigma^z + B \tag{4.5}$$

Second case:

$$B_i - B_u = (\sqrt{\phi \cdot \sigma^z} + \sqrt{B})^2 \tag{4.6}$$

For both limiting cases the mean error was calculated. Among the observations of Knoll [76] a mean error $m$ using a measurement of $\log(B_i - B_u)$ was determined for a luminance value of $10^{-8} \frac{cd}{m^2}$. For Equation 4.5 the mean error resulted in $m = \pm 0.099$, using Equation 4.6 the mean error resulted in $m = \pm 0.052$. Compared with Equation 4.5, the same results were almost twice as high as the mean error of Equation 4.6. This proportion behaved similar for other luminance values [11]. Therefore Berek stated Equation 4.5 as less appropriate.
From Equation 4.6 it is evident that Berek worked out two characteristic variables in his model. $\phi$ describes the characteristic luminous flux function and B the characteristic luminance function. If the condition $B_i > B_u$ is used, the law applies in the range of all background luminances for the relative luminous flux. Setting $z = -2$ according to Ricco's law [11] one obtains:

$$(B_i - B_u) \cdot \sigma^2 = (\sqrt{\phi} + \sigma \cdot \sqrt{B})^2 \tag{4.7}$$

From Equation 4.7 it can be seen that $\phi$ has the dimension of an illuminance and $B$ the dimension of a luminance. Therefore, the characteristic luminance function is defined as follows:

$$\sqrt{B} = Q \cdot B_u^q \tag{4.8}$$

The dependency of the luminous flux function $\phi$ on the background luminance proved to be more complicated. The transition from scotopic vision to photopic vision is suggesting that there is an interaction of the two laws, one of which is due to the effect of the rods (first term) and the other to the influence of the cones (second term). The characteristic luminous flux $\sqrt{\phi}$ can be expressed as follows:

$$\sqrt{\phi} = \log(C) \cdot B_u^q + P \cdot B_u^p \tag{4.9}$$

with

$$\begin{aligned} C = 1.0479 \pm 0.0002; \qquad & c = 0.00208 \pm 0.0001 \\ P = 0.5 \pm 0.07; \qquad & p = 0.52 \pm 0.03 \\ Q = 0.0058 \pm 0.002; \qquad & q = 0.412 \pm 0.006 \end{aligned} \tag{4.10}$$

where the values of the coefficients and exponents for the luminance B are in $\frac{cd}{m^2}$ and for the observation $\sigma$ in angular minutes [11].
For very small viewing angles $\sigma$, the size $\sigma \cdot \sqrt{B}$ next to $\sqrt{\phi}$ is negligible in Equation 4.7. Ricco's law applies for the relative luminous flux:

$$(B_i - B_u) \cdot \sigma^2 = \phi \tag{4.11}$$

This is true for Ricco's limiting angle [11]:

$$\bar{\sigma} = \varepsilon \cdot \sqrt{\frac{\phi}{B}} \tag{4.12}$$

Berek assumed this as limit of $\sigma$ for which $\sigma \cdot \sqrt{B}$ is equal to the fraction $\varepsilon$ of $\sqrt{\phi}$. For large vision angles $\sigma$, Equation 4.7 merges into Weber-Fechner law:

$$B_i - B_{u_{(\bar{\sigma} \to \sigma)}} = B \tag{4.13}$$

Assuming $\sqrt{\sigma} \leq \varepsilon \cdot \sigma \cdot \sqrt{B}$, Berek determined the corresponding limiting angle for this range:

$$\sigma = \frac{\bar{\sigma}}{\varepsilon^2} \tag{4.14}$$

Thus, the Weber-Fechner law is more applicable: the smaller the visual angle is, the greater the background luminance is.

### 4.1.2 Contrast threshold experiments of Blackwell

In 1946, the American researcher Blackwell, also conducted studies in contrast sensitivity. The aim of his research was the determination of the threshold contrast of a normal human observer under experimental conditions [37]. In his investigations, visual targets were also presented with a positive contrast in front of a defined background luminance. Stimuli were projected randomly onto a observation screen (one experiment session contained 320 stimuli presentations). Nine observers performed the experiment at the same time, sitting at the rear of an observation room sitting on chairs that were mounted either on the floor or on a balcony (two levels). The participants were young women, aged 19 to 26 years, whose visual acuity in each eye and in both eyes was approximately 20 without refractive correction. [37].

Overall, five contrasts were selected on the basis of previous observations (0.24, 0.37, 0.55, 0.75, 1.0). A fixation point was located in the centre of the observation

surface. The stimuli were projected in one of eight positions on the circumference around the fixation point (3.0° radius). The presentation time of the targets was 6.0 seconds and the size of the visual target varied from $0.06 - 2.0°$. The participants responded by rotating a recording switch to the position where they assumed the appearance of the target. The luminance region to be analysed was in a range from $3 \cdot 10^{-4} \frac{cd}{m^2}$to $3 \cdot 10^{2} \frac{cd}{m^2}$. Blackwell determined the 50% detection probability threshold using the Urban method [37]. To achieve a detection probability of 90% Blackwell defined to multiply the 50% threshold by a factor of 1.62 [37]. According to Blackwell, in order to get from 50% frequency to 100% detection probability, a factor of 2 to 2.4 would be necessary [12].

### 4.1.3 Model for visibility of objects

The model of Adrian allows the calculation of the luminance difference threshold $\Delta L$ for various sizes of targets as a function of the background luminance [13]. It was created in 1961 and modified on several occasions (until 1989), for instance to incorporate the influence of observation time and age of subjects [12] [81].
The principle of his investigations is presented in Figure 4.2. In a predefined environment a circular target was located with a positive contrast (object size $\alpha$) [82]. The targets were exclusively achromatic targets. One after the other, visual stimuli were presented to the subjects foveally.

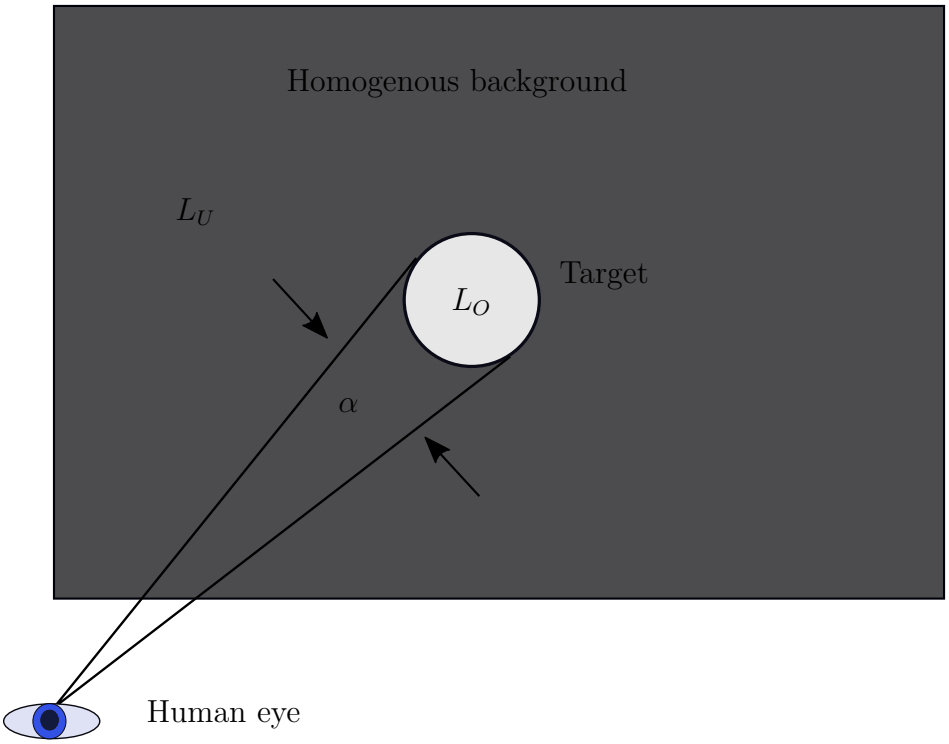


Figure 4.2: Experimental arrangement for determining the detection probability according to [12]. $L_U$: Background luminance; $L_O$: Object luminance; $\alpha$: Observation angle.

The participants had the task to locate a focus point in the middle of the visual

field permanently. In this case, the presentation time of the target was unlimited for the observer.

The aim of this investigation was also to analyse of the perception of a visual sign as a function of the background luminance. With his function Adrian describes the difference threshold $\Delta L = L_O - L_U$ and thus all parameters that have an influence on it. Equation 4.15 describes the final version of his model:

$$\Delta L_{thresh} = k \cdot \left( \frac{\nu\phi}{\alpha} + \nu L \right)^2 \cdot \frac{a(\alpha \cdot L_u) + t}{t} \cdot F_{CP} \cdot AF \tag{4.15}$$

- $k$, factor for the detection probability
- $\nu\phi$**,** $\nu L$, luminous flux or luminance function of Ricco's/ Weber's law
- $\alpha$, target size in angular minute
- $a(\alpha \cdot L_u)$, Blondel-Rey constant
- $t$, presentation time in seconds
- $F_{CP}$, factor for positive/ negative contrast calculation
- $AF$, age factor

In the following, individual components of Adrian's model will be discussed.

#### 4.1.3.1 Luminous flux or luminance function $\phi$,$L$

The background luminance plays an important role for the determination of the differential threshold $\Delta L$ [12]. The behaviour of $\Delta L$ as a function of the observation angle is shown in Figure 4.3 and is based on the data of Blackwell [37]. The curve progression can be divided into two areas. For small angles of observation Ricco's law is applied, here the curve is almost linearly declining. In this range, the multiplication of illuminance and illuminated area on the retina is almost constant. Ricco's law describes the process of visual perception. Several receptors are connected neuronic and can be seen as a receptive unit. This applies to the foveal as well as to the extrafoveal region [83]. The Ricco area is left at the moment the threshold value is reached. It says that, irrespective of the spatial arrangement of the receptors on the retina, only the light quantity has an influence which is actually absorbed by the receptors. This means that the threshold luminance, independent of its temporal or spatial spread, leads to a stimulus perception. For observation angles which are larger than 1.0°, the behaviour follows Weber's law [84].

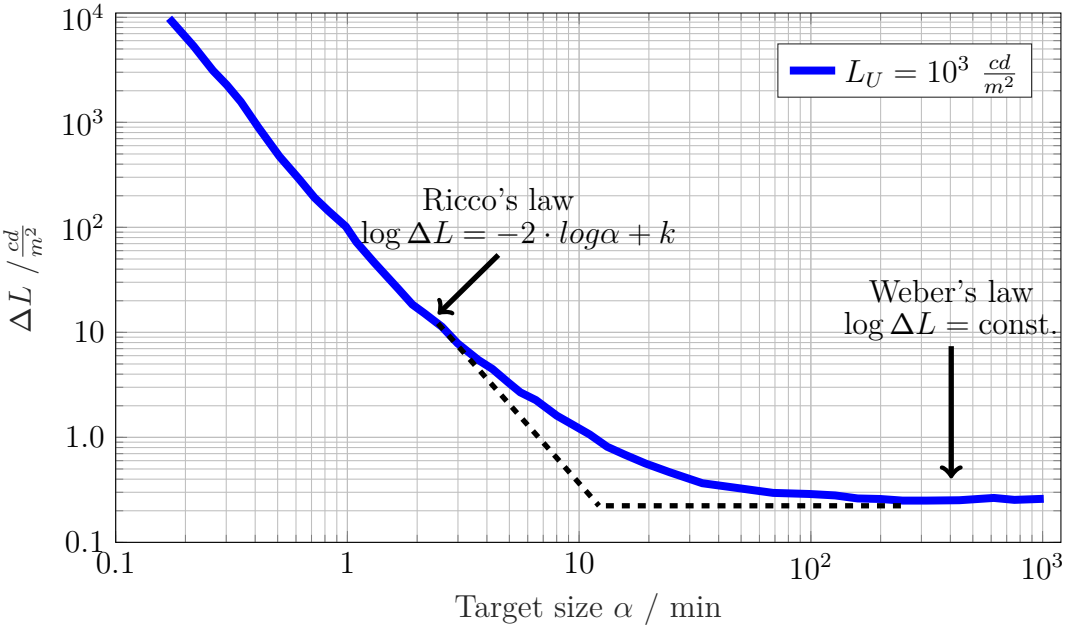


**Figure 4.3: Luminance threshold $\Delta L$ as a function of the observation angle $\alpha$ at a background luminance $L_U = 10^3 \frac{cd}{m^2}$. For small angles of observation Ricco's law is applied, for large angles Weber's law [13].**

The perceptional threshold is then only dependent on the luminance of the visual object, whereas the observation angle has no significant influence any more. According to Adrian [12] the behaviour of the function can be described as follows:

$$\text{Ricco:} \quad \log \Delta L = z \cdot \log \alpha + k, \quad \alpha \to 0 \tag{4.16}$$

$$\text{Weber:} \quad \log \Delta L = \text{constant}, \quad \alpha \to \infty \tag{4.17}$$

With the inverse of the logarithm of the two equations (with $x = \log_a(y) \Leftrightarrow y = a^x$) and the transmission to the luminous flux and luminance function, Equations 4.16 and 4.17 can be interpreted as follows:

$$\Delta L = \phi(L_u) \cdot \alpha^z \tag{4.18}$$

$$\Delta L = L(L_u) \tag{4.19}$$

Subsequently, a geometric summation of the two functions according to Berek was carried out (compare Chapter 4.1.1).

$$\Delta L = \left( \sqrt{\phi \cdot \alpha^z} + \sqrt{L} \right)^2 \tag{4.20}$$

with $z = -2$

$$\Delta L = \left( \frac{\sqrt{\phi}}{\alpha} + \sqrt{L} \right)^2 \tag{4.21}$$

A slow increase in background luminance shows a continuous increase in contrast sensitivity. Adrian distinguishes a transition area between a certain and uncertain perception. Therefore, in a simplified manner, Equation 4.15 can be represented as follows:

$$\frac{\Delta L}{\frac{cd}{m^2}} = k \cdot \left( \frac{\sqrt{\phi}}{\alpha} + \sqrt{L} \right)^2 \tag{4.22}$$

In order to compare his findings with the models of Berek and Blackwell, Adrian ascertained a total of three analytical functions for three luminance ranges (based on [37], p. 640, Table VII):

- $L_u \geq 2.59 \frac{cd}{m^2}$

$$\sqrt{\phi} = -0.059 + 0.343 \cdot \log\left(L_U\right) \tag{4.23}$$

$$\sqrt{L} = -1.382 + 0.643 \cdot \log\left(L_U\right) - 0.00475 \cdot \left(\log\left(L_U\right)\right)^2 \tag{4.24}$$

- $L_u \leq 4.18 \cdot 10^{-3} \frac{cd}{m^2}$

$$\sqrt{\phi} = 0.028 + 0.173 \cdot \log\left(L_U\right) \tag{4.25}$$

$$\sqrt{L} = -0.891 + 0.5275 \cdot \log\left(L_U\right) + 0.0227 \cdot \left(\log\left(L_U\right)\right)^2 \tag{4.26}$$

- $4.18 \cdot 10^{-3} \frac{cd}{m^2} < L_U < 2.59 \frac{cd}{m^2}$

$$\sqrt{\phi} = -0.072 + 0.3372 \cdot \log\left(L_U\right) + 0.0866 \cdot \left(\log\left(L_U\right)\right)^2 \tag{4.27}$$

$$\sqrt{L} = -1.256 + 0.319 \cdot \log\left(L_U\right) \tag{4.28}$$

Table 4.1 shows the respective values for the luminous flux or luminance function of the three models. It can be noted that there is an increase by a factor of 2 between the models of Berek and Blackwell in the luminance range $0.1 \frac{cd}{m^2}$ to $1.0 \frac{cd}{m^2}$. This can be traced to the receptor distribution on the retina, since a transition from cones to rods occurs in this area.

#### 4.1.3.2 Detection probability factor $k$

Adrian chose the method of adjustment, means the test stimulus is raised from sub-threshold values until it can be perceived. In contrast to many previous studies he investigated the nearly one hundred percent detection probability (99.93%). While he was able to directly compare his results to Berek, he had to perform calculations

| | Berek | | Blackwell | | Adrian | |
|---|---|---|---|---|---|---|
| $L_u$ | $\sqrt{\phi}$ | $\sqrt{L}$ | $\sqrt{\phi}$ | $\sqrt{L}$ | $\sqrt{\phi}$ | $\sqrt{L}$ |
| $10^{-5}\ \frac{cd}{m^2}$ | 0.161 | $0.114 \cdot 10^{-2}$ | 0.146 | $0.11 \cdot 10^{-2}$ | 0.837 | 2.961 |
| $10^{-4}\ \frac{cd}{m^2}$ | 0.371 | $0.293 \cdot 10^{-2}$ | 0.217 | $0.231 \cdot 10^{-2}$ | 0.664 | 2.638 |
| $10^{-3}\ \frac{cd}{m^2}$ | 0.587 | $0.758 \cdot 10^{-2}$ | 0.323 | $0.539 \cdot 10^{-2}$ | 0.491 | 2.269 |
| $10^{-2}\ \frac{cd}{m^2}$ | 0.822 | 0.019 | 0.399 | 0.013 | 0.400 | 1.894 |
| $0.1\ \frac{cd}{m^2}$ | 1.120 | 0.050 | 0.476 | 0.023 | 0.323 | 1.575 |
| $1.0\ \frac{cd}{m^2}$ | 1.620 | 0.174 | 0.848 | 0.055 | 0.072 | 1.256 |
| $10.0\ \frac{cd}{m^2}$ | 2.790 | 0.337 | 1.920 | 0.163 | 0.351 | 0.937 |

Table 4.1: Comparison of the three models regarding the luminous flux and luminance functions according to [11] [37].

for a comparison with Blackwell's data. In his experiments Blackwell applied the forced choice method, meaning, he analysed the fifty percent detection probability of the subjects. His results complied with a mean value which corresponded to the cumulative frequency [37].

By reproducing the results of Blackwell, Adrian developed a function which corresponds to a multiplication by a factor of 3.1 (see Table 4.2). The derived data from Blackwell show a clear salient point between $0.001\frac{cd}{m^2}$ and $0.1\frac{cd}{m^2}$ of the background luminance. This phenomenon is caused by the transition from cones to rods on the retina. This is subordinated in the Berek function. The already mentioned deviation of the measurement points from Berek's curve finds their explanation, as the measured values lie exactly on the Blackwell function.
In his investigation Adrian compared his findings with the results of Aulhorn [28]. Since Aulhorn examined only three subjects (one subject was 55 years old) under mononcular vision. Adrian assumed a higher $\Delta L$ for monocular observations (by 1.64) and also for advanced age (by factor 1.59). This resulted in a difference factor of 2.6 ($1.66 \cdot 1.59$), whereby Adrian also considered two younger participants, that required lower threshold values, which resulted in a final difference factor of 2.4. Therefore the so-called probability factor $k$ corresponds to a 50% probability for $k = 1$ and a 99% probability for $k = 2.6$ (comparison to Aulhorn) in Adrian's final model. Table 4.2 shows of the probability factor for the detection of an object for the results of Adrian. In order to guarantee a better comparison, the factor was determined for the models of Berek and Blackwell as well.

| Author | Probability factor | Detection probability |
|---|---|---|
| Berek | k=1.0 | 99 % |
| Blackwell | k=1.0 | 50 % |
| Blackwell | k=3.1 | 99 % |
| Adrian | k=1.0 | 50 % |
| Adrian | k=2.4 | 99 % |

Table 4.2: Probability factor for 50% or 99% detection probability of an object. Comparison of Adrian [13], Blackwell [37] and Berek [11].

#### 4.1.3.3 Presentation time $\frac{a(\alpha \cdot L_u)}{t}$

In his investigations Adrian analysed a presentation time of 2.0 s or unlimited [13]. He described the influence of the presentation time of the target as follows:

$$\frac{a(\alpha \cdot L_u) + t}{t} \tag{4.29}$$

If the target size is lower than 60.0' the presentation time could be calculated as follows:

$$a(\alpha \cdot L_u) = \frac{\left(a(\alpha)^2 \cdot a(L_u)^2\right)^{0.5}}{2.1} \tag{4.30}$$

where

$$a(\alpha) = 0.36 - 0.0973 \cdot \frac{(log(\alpha) + 0.523)^2}{(log(\alpha) + 0.523)^2 - 2.513 \cdot (log(\alpha) + 0.523) + 2.7895} \tag{4.31}$$

and

$$a(L_u) = 0.355 - 0.1217 \cdot \frac{(log(L_u) + 6)^2}{(log\,(L_u) + 6)^2 - 10.4 \cdot (log\,(L_u) + 6) + 52.28} \tag{4.32}$$

As mentioned above this is valid for an observation time of 2.0 s or unlimited. For shorter presentation times $\Delta L$ needs to be increased to ensure a target detection. As it can be seen from Table 4.3 for a shorter observation time the essential $\Delta L$ to perceive an object is considerable higher.

| $t$ [s] | $\frac{a(\alpha \cdot L_u)+t}{t}$ |
|---|---|
| 2.0 | 1.0 |
| 0.35 | 1.03 |
| 0.1 | 1.1 |
| 0.01 | 1.18 |

Table 4.3: Presentation times $t$ for a target with $a = 60.0'$, using a background luminance of $L_u = 1.0\frac{cd}{m^2}$.

#### 4.1.3.4 Age factor $AF$

Ocular transmittance decreases with increasing age [85]. Therefore the necessary $\Delta L$ is significantly higher for older people. Based on findings of Mortensen-Blackwell [86] Adrian defined an equation to describe the contrast as function of the aging process. The luminance difference $\Delta L_{\text{age}}$ of a human that is older than 23 years can be described as follows:

$$\Delta L_{\text{age}} = \Delta L_{23} \cdot AF \tag{4.33}$$

where $AF$ indicates the age factor that can be determined for two age groups:

$$AF = \frac{(\text{Age} - 19.0)^2}{2160.0} + 0.99, \quad 23 < \text{Age} < 64 \tag{4.34}$$

$$AF = \frac{(\text{Age} - 56.6)^2}{116.3} + 1.43, \quad 64 < \text{Age} < 75 \tag{4.35}$$

The increase of the luminance threshold with growing age is also included into the age factor. For the calculation of the luminance threshold of older participants Equation 4.22 must be be multiplied by $AF$, since it is only valid for young observers with an average age of 23 years ($AF_{23} = 1.0$).

#### 4.1.3.5 Visibility Level VL

The Visibility Level VL describes the relation between the object contrast and threshold that is essential to perceive the object with nearly 100% under laboratory conditions. According to the lighting design of headlamps or road lighting, visual information that is obtained from the driver in a night-time road traffic situation can be measured by the VL. This fact is directly linked to an increased safety, which rises with an elevated visibility level. The VL, based on the CIE report 19.2 [59], was defined as follows:

$$VL = \frac{\Delta L}{\Delta L_{\text{thresh}}} = \frac{L_O - L_U}{L_O - L_{U,\text{thresh}}} \tag{4.36}$$

For practical applications a multiple of the luminance difference is needed dependent on the visual task [13]. The essential visibility level for different tasks can be described as a function of the adaptation luminance and the required visual acuity of the human eye. As VL levels for secure safe traffic conditions Adrian ascertained values between 10 and 20 under street lighting illumination [87].

### 4.1.4 Field factor

The results that were presented so far are valid for laboratory observation conditions. For night-time driving a “field factor” that accounts for unexpectedness and reduced fixation time of the target, applies [88]. The best way to describe vision for driving applications are visual functions such as luminance contrast sensitivity, perception of object shapes and also their temporal dependencies. According to Adrian the quality of roadway lighting can be expressed by the amount of visual information that can be obtained from the visual system.
Earlier studies revealed, considering the fixation time and location in the visual field while driving, that a human can fixate a single point for 0.2 s in average only for luminance levels around $2.0\frac{cd}{m^2}$ [82] [89]. Lossagk suggested a field factor of 4.6, leading to ten times $\Delta L$, which he applied to analyse thresholds according to visual task demands [89]. To include the unexpectedness and a reduced fixtaion time he

assumed a field factor of 10.

Based on driving experiment results by Dunbar [90] (using a 30.0 cm× 30.0 cm gray square as detection object) and de Boer [91], Adrian found appropriate luminance levels. In a field study, de Boer analysed an object with the size 20.0 cm× 20.0 cm in a distance of 69.0 m to the observer. The object size was chosen according to an obstacle that most drives can just perceive. Hence, Adrian suggested that the ratio of the background to target luminance did not decrease considerably below $\Delta L = 1.76$ for a background luminance of $1.0\frac{cd}{m^2}$ [88]. Based on the results of de Boer he found the luminance threshold to be $\Delta L = 0.43$, which is also valid for practical conditions. According to Adrian an observer (25 years of age) would require a luminance threshold value of $\Delta L = 0.08$ for a background luminance of $L_u = 0.08\frac{cd}{m^2}$ to detect an object with a probability of 99.93% [13].

### 4.1.5 Comparison of Adrian, Berek and Blackwell

In summary, it can be stated that the analytical presentation of Blackwell's results describes the basic connection of the analysed visual function more accurately and more securely than the approach of Berek.
The newly developed function of Adrian is composed of five components, is subdivided into three specific luminance ranges and considers two self-sufficient luminance and luminous flux functions. With these values, the threshold difference of different object sizes (for positive and negative contrasts) can be obtained easily. The model is applied for binocular, free viewing observations under laboratory conditions.

## 4.2 Previous laboratory research

**Detection probability according to H. Fleck.** Fleck performed experimental measurements of threshold contrasts as a function of eccentricity (peripheral threshold contrasts) [50]. From his findings he developed a model for forecasting off-axis threshold contrast functions on different visual conditions based on spatial frequency filters. His investigations were divided into two parts. In a first step he analysed the detection of a single target, i.e. perception of target presence in front of a homogenous background. In a second step he considered the discrimination of a target for the same test conditions.
The experiments were performed under binocular observation, using an adaptation luminance of nearly $20.0\frac{cd}{m^2}$ and a presentation time of 300.0 ms [53].
The participant fixated a marking in the middle row of a CRT-screen at a distance of 41.0 cm, the targets appeared every 6.0 s at the fixation point (foveal) or peripheral up to 30.0°. The appearance positions of the targets were separated by distances of 2.0°. The targets were the letters "O" and "D" (angular size of 18' by 36') or a rectangle (angular size of 27' by 48'). During a test run the targets took four different constant contrasts (0.05, 0.11, 0.2, 0.23) [50]. Since Fleck used the method of constant stimuli the participant answered "present" or "not present" in case of the detection task by using a simple keyboard. In the discrimination experiments the answers were "O" or "D", respectively.

In summary he peformed 500 test sessions each involving 180 target presentations. As illustrated in Figure 4.4 he determined the probability profiles of the detection as a function of the eccentricty.

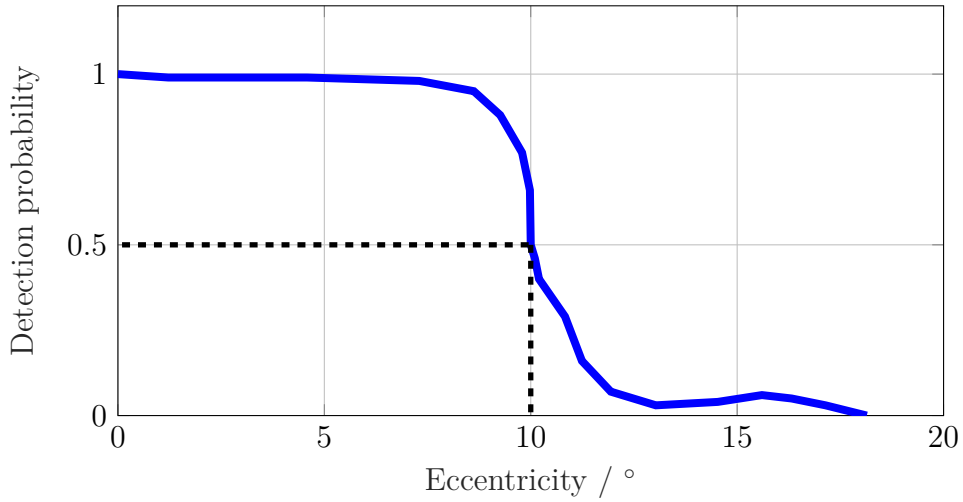


Figure 4.4: Detection probability of the letters "O" (18') as a function of the eccentricity (for a fixed target contrast) according to [14].

His experimental data showed that the complexity of the foveal task leads to an increase in threshold contrast for peripheral detection task (depending on the eccentricity). He found out that the higher the visual contrast was, the greater the overall effective visibility field was. According to Fleck the relative standard deviation, which is dependent on the threshold contrast, remains independent of the eccentricity for the detection task. In addition the decrease in peripheral detection performance with increasing observation angle strongly depends on the adaptation level. The peripheral detection is also reduced for luminances in the mesopic range [50].

**Approach for hemispheric objects according to J. Lecocq.** Lecocq developed a new approach to determine the VL for applications on dry as well as on wet road surfaces [60]. This model was based on the model of Adrian [13]. In contrast to Adrian he replaced the plane circular target by hemispheric targets. The simulated curve of targets faced down the road towards the observer. The advantage of this procedure was, that Lecocq was able to take the luminance distribution over the target surface into account. Therefore his calculations were more complex but closer to real situations in road traffic. According to Lecocq, "hemispherical multifaceted targets relate better to real, complex objects encoutered on the road surface". In his investigations he found out that a uniform road surface luminance provided a good background for an object detection, since a dry road surface results in a strong increase of luminace uniformity [60].
For a wet road surface, the luminance becomes more various because of bright patches and specular reflections on the surface which results in a complicated detection task for the driver. If an object lies outside the illuminated area, where less

specular reflection is, the visibility of targets is not ensured any more. Lecocq's approach to increase the visibility was, first, to either increase the size or number of lamps and second, to increase the number of lighting positions.
Lecocq also examined the influence of the reflection coefficient $\rho$ of the target. An increase of $\rho$ from 0.2 to 0.5 was considered to compare planar and hemispheric targets directly. The plane targets gave a misleading indication of the visibility whereas for hemispheric targets he concluded that miminum values of VL are suffcient to indicate a deficit in visibility, so that objects may not be detected.

**Disadvantages of visibility level computation according to R. Brémont**
Brémont [15] performed several experiments regarding the VL based on the model of Adrian [13]. According to Brémont the driving task is not regarded in Adrian's model. Therefore the focus of Brémonts investigations was placed on the driving task while detecting objects. His first experiment was conducted in laboratory. The participant's task was to detect a uniform square target for different contrasts and eccentricities. In the second part of the experiment the participant's additional task was to detect the same targets while tracking a black square in a circuit with an input device [15]. During the second experiment part the contrasts were set to the individual detection threshold of each subject. As background luminance $L_U$=0.65$\frac{cd}{m^2}$ was chosen. The gaze behaviour was controlled by an eye tracking system. The evaluation was performed by using a two-factorial variance analysis.
Both investigated parameters had a negative influence on the object detection. Possible hazards can appear, if the driver is confronted by a complex task. The tracking task resulted in a decrease in detection performance from 84.2% to 67.5% ($p = 0.001$).

In a second experiment in laboratory Brémont analysed three more conditions. The first test condition was in similar circumstances and tasks as in the prior experiment: detecting an uniform square in front of an homogenous background. In the second test condition the same targets were presented, but the background was replaced by a photograph of an urban night-time scene in Paris (compare Figure 4.5).

The detection object was located on road surface. In the third test condition the detection objects were integrated into a background scenario that consisted of video sequences of the same urban road in Paris. Using the videos sequences Brémont simulated a typical driving situation at night-time (especially motion of road users). The analysis showed that test conditions with an inhomogenous background had a great impact on the detection behaviour of the participants. The detection performance decreased from 99.0% (first condition) to 81.0% for a photograph generated background down to 37.0% for a background that contained a video sequence.
Detection performance here describes the interaction of individual parameters combined with the detection task, such as the additional tracking task, the change of the background luminance or driving task, that have an influence on the participant's detection behaviour.

Since many scientific works considered the so-called "field factor" Brémont implemented another study including several parameters that were not discussed by

Figure 4.5: Picture of a urban road scene in Paris as background (test condition 2) according to [15]. The participant's task was to detect a grey square (located on lower half of the picture, right hand side).

Adrian. As it can be seen in Figure 4.6, in a field study (1.2 km closed road circuit in France), the detection performance of participants for uniform square objects was analysed regarding the participant's position in the test vehicle (as driver or passenger). The task was to detect a square on the test track as soon as possible (under road lighting), in the first part as driver, in the second part as passenger in the test vehicle.

Figure 4.6: Field study on a 1.2 km closed road circuit (CETE Rouen, France) according to [15]. The participant's task was to detect the grey square on the test track (in front of the test vehicle).

Brémont adapted the mean detection distance to the visibility level. He recognized that a unique adadptation luminance for all targets is better than the local background luminance [16]. Based on his results he suggested to use the highest contrast among the four edges of the square rather then the mean contrast.

**Detection distance of targets on a driving simulator according to R. Brémont** In another investigation Brémont simulated a driving experiment that was conducted in a virtual night-time rural highway [16]. The aim of this study was to implement a simplified version of the VL for automotive lighting design. As detection objects more familiar targets were compared to a reference grey card (road sign, pedestrian, vehicle). The objects were presented as grey uniform shapes and with a more realistic inhomogenous structure (compare Figure 4.7). By using a driving simulator it was also possible to analyse the time-varying apparent size of targets. Furthermore, it was Brémont's objective to identify a relation between the lighting recommendations and road safety.
The experiment was carried out in a driving simulator in a laboratory environment. The participants were confronted with a virtual highway environment at night-time that was only illuminated by the vehicle's headlamps and without any other traffic participants (visual field was covered 37.0° horizontally and 30.0° vertically). The distance from the subject to the simulator screen was 3.0 m. The participant's task was to detect various objects while driving and to indicate the presence of every object by pressing a button on the steering wheel. The detection distance was recorded and then compared to the VL (calculated from the size and contrast of the object).

Luminance measurements of the displayed computer graphic images were conducted by using a imaging photometer with a 980 × 980 pixel resolution. Recordings of the environment were evaluted every 10.0 m at a distance from 20.0 m to 150.0 m to the detection object. In total, 90 luminance pictures were analysed.

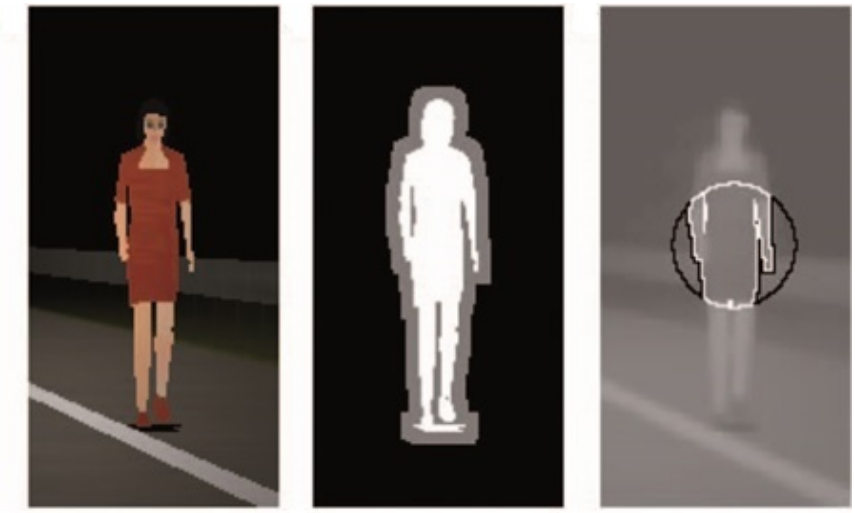

Figure 4.7: Evaluation of the luminance measurement according to [16]. Figure left: textured pedestrian (woman, red dress). Figure middle: corresponding mask of the pedestrian (white for the object shape). Figure right: foveal region from which data are extracted in the luminance picture (pixels within the white contours belong to object luminance, pixels within the black contours to the background luminance) according to [17].

The background luminance was determined based on the model of Moon and Spencer [17]. This model considers non-uniform surroundings. As it can be seen in

Figure 4.7 the background was defined within the region covered by foveal vision. A disc approximately 1.58 cm diameter was centred in the middle of the target. The pixels that were located within that region, excluding target pixels, were selected as background pixels. The background luminance $L_u$ was then determined as mean of the luminance values. On the other hand the object luminance was calculated as average luminance of the object's pixels (one pixel had a diameter of 1.56 mm). Brémont used the values from the luminance pictures for calculating the VL based on Adrian's model. He computed the VL of every object for every distance. For the computation he assumed a 35-year-old observer (mean age of the participants in his experiment) and a presentation time of 0.2 s. For comparison with the own results of this thesis, selected distances are shown in Table 4.4.

| Object | Distance / m | Size/ min | $L_O/\frac{cd}{m^2}$ | $SD/\ \%$ | $L_u/\frac{cd}{m^2}$ | $K$ | VL |
|---|---|---|---|---|---|---|---|
| Uniform square | 80.0 | 9.8 | 7.97 | 25 | 1.41 | 4.64 | 57.0 |
| | 90.0 | 8.9 | 4.13 | 31 | 0.83 | 3.96 | 34.6 |
| | 100.0 | 7.2 | 1.99 | 25 | 0.47 | 3.23 | 15.3 |
| Pedestrian (uniform) | 80.0 | 32.5 | 2.82 | 30 | 0.18 | 13.97 | 200.0 |
| | 90.0 | 29.2 | 1.60 | 32 | 0.08 | 18.16 | 141.4 |
| | 100.0 | 26.0 | 0.87 | 34 | 0.04 | 18.50 | 81.9 |
| Pedestrian (textured) | 80.0 | 32.5 | 1.79 | 64 | 0.17 | 9.54 | 128.4 |
| | 90.0 | 29.2 | 1.02 | 50 | 0.08 | 10.56 | 85.4 |
| | 100.0 | 25.9 | 0.56 | 53 | 0.04 | 12.11 | 51.5 |

Table 4.4: Calculated parameters from the luminance pictures [16]. The luminance variation inside a target is described with the luminance standard deviation SD with respect to the mean luminance.

The derived detection distances are presented in Table 4.5. As anticipated by the author, the reference object (uniform square) was more difficult to detect than most tested object shapes. The experimental object detection distance of the most visible object (the uniform vehicle) was only 40.0% higher than that of the reference target [16].

| Object | Reference (uniform square) | Pedestrian | Pedestrian (uniform) |
|---|---|---|---|
| EDD | 106.0 | 124.0 | 128.0 |
| CCD | 115.0 | 129.0 | 124.0 |
| VL | 9.0 | 6.0 | 9.0 |

Table 4.5: (Experimental) Mean object detection distance EDD in m, computed detection distance (CCD) in m and visibilty level (VL) of all participants accordiung to [16]. The individual reaction time was taking into account.

As a last result it can be noted that the objects were more visible if they were uniform compared to those with inhomogenous structures. Brémont assumed the

high reflectance of the uniform targets as the main reason for these findings, as it makes them more conspicuous than the textured targets.

**Effect on participants task to object detection according to A. Mayeur.** The purpose of this investigation was to evaluate how a tracking task affects target detection in mesopic range for different eccentricities [18]. The experiment was divided into three parts. In the first experiment individual detection thresholds of participants were measured in peripheral vision. Mayeur analysed eccentricities up to 7.0°, that included any point on the driver‘s lane more than 15.0 m ahead of the vehicle (1.5°, 4.0° and 7.0°). He specified a fixation point at the center on the road surface. A fixation target, that consisted of a black square ($L_U$ =0.1$\frac{cd}{m^2}$) was projected at 0.25° in a distance of 2.0 m. The presentation time of the detection objects was 150.0 ms and they appeared randomly at different eccentricies with different contrasts in a time period of 3.0 s [18]. The evaluated parameters were the eccentricity (1.5°: proximity of the fovea, 4.0°: parafoveal region and 7.0°: perifovea) and contrast $K$ (0.0, 0.1, 0.21, 0.33, 0.41, 0.6). Overall 180 stimuli (10 presentations $\times$ 3 eccentricities $\times$ 6 contrasts) were presented to each subject.
In the second part of the experiment the participant's task apart was to track a target. A tracking object was moved along a circuit with two crank handles and had to be held within the circle [18]. The contrast was defined for each participant individually to its detection threshold. In a third part the first task (steering a peripheral target) was repeated adding the tracking task, using prior determined individual contrast values. Here, the aim was to assess the participant's performance considering an additional influence factor that simulated the driving task in real road traffic applications. Overall thirty-nine participants with an average age of 35.5 years conducted the experiment. All of them were naive to the purpose of the experiment. On average the detection rate decreased from 57.2% to 44.4% for an eccentricity of 1.5° and to 30.7% for 4.0° and 7.0°. Based on the results of all three parts the participants' individual detection contrasts were calculated (two-factorial variance analysis). A significance could be established for the eccentricity ($F = 124.73$, $p = 0.0$), whereas an interaction between the two analysed factors existed. In the last evaluation step the effect of detection task on peripheral objects (single-task) was compared with the third part's data (double-task). The results are presented in Figure 4.8.

The average detection performance decreased from 84.2% to 67.5%. The performance for 7.0° showed a significant difference compared to smaller eccentricities. As a result it can be noted that a target detection rate of 70.0% could be established in peripheral detection conditions. The results showed that the difficulty of target detection increases with an additional task. Mayeur came to the conclusion that the model of Adrian is limited, since it is based on single task experiments under laboratory conditions. According to Mayeur detection of a small standard target is more difficult than of real obstacles. Furthermore, the detection of a square target neglects the importance of real objects like pedestrians or wild animals [18].

**Target detection according to A. Mayeur.** The purpose of Mayeur's study was to evaluate the impact of a complex background and apparent motion on target

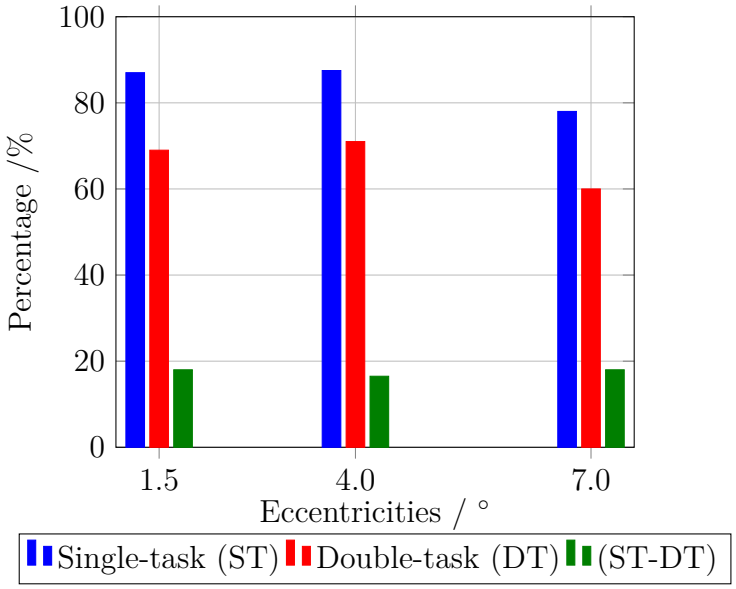


**Figure 4.8: Percentage of correct detection for the peripheral detection task. Contrast values at the individual detection threshold (IDT) according to [18].** 1.5°: **mean IDT =0.29,** 4.0°: **,mean IDT =0.397,** 7.0°: **mean IDT =0.487. The data were extracted for the single task, the double task and for both.**

detection performance for three luminance contrasts [19]. In his experiment the participants had to detect standard square targets varying in terms of contrast under three conditions: a uniform background, real images of traffic scenarios, and video sequences. As luminance levels, relevant values for night-time road applications were chosen. The images and video sequences were also selected in relation to a driving task. The experiment took place in laboratory. The subjects sat in an ergonomic adjustable seat. The participant's answers (targets' onset) were documented by a foot pedal. The subject's task was to detect square targets with various contrasts (0.0, 0.3, 1.2 and 4.8) and eccentricities on a homogenous background (compare Figure 4.9). The targets and the background images were displayed on a screen by a video-projector (1.5 m × 2.0 m). The background luminance was below $1.5\frac{cd}{m^2}$ (consistent with road lighting in practice). The gaze behaviour of the participants was controlled with an eye-tracking system. Like in [18], a black square fixation target appeared for 230.0 ms at different eccentricities on the projection surface. An example of a detection square at 7.0° is presented in Figure 4.9. In the first part of the investigation reference data for each participant were collected to be able to compare with the laboratory data.

In the second part the target detection performance was determined by replacing the homogenous background by photographs of night-time traffic scenarios. The same luminance contrasts were used in both experiments to determine the impact of a complex background on the detection task. In the third part the background was modeled by a video sequence that illustrated the same traffic scenario as on the photograph. While searching for targets in a "road scenario", the participants were asked to simulate the vehicle direction with a steering wheel. The simulated vehicle followed two-lane streets at about $50.0\frac{km}{h}$.

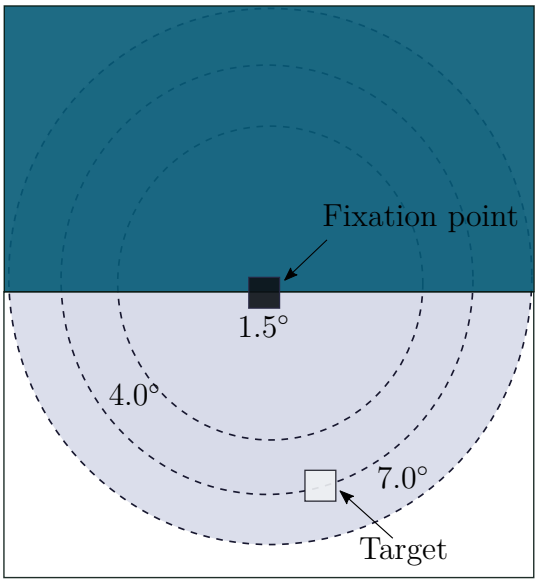


**Figure 4.9: Schematic of the projection surface for a stimulus at an eccentricity of 4.0° according to [19].**

The aim of this simulation was to suspend the participant in a situation that is more comparable to real driving tasks. As result can be noted, that there was no effect of steering the wheel on video which resulted in no influence in detection performance [19]. The approach of the third experiment was to find out if there is an impact of a dynamic background in comparison to a static background on the detection task.
The target position was randomly chosen, but was always located on a homogeneous spot on the road surface to ensure uniformity. Moreover, targets did not appear during turnings or crossings in the video sequence. In the third part, the targets did not move, since the background was changing continuously. Subsequent, the luminance on each image was determined by using the photometric calibration of the display device.
Overall twenty-eight participants with a mean of 39.9 years of age performed the experiment. Table 4.6 illustrates the influence of the individual parameters on the detection performance. Within the statistical analysis the eccentricity was included as covariance. For the detection performance analysis Mayeur clustered the influence factors of all participants into subject factors, contrast and condition as within-subject factors. He set the statistical significance level to $p < 0.05$.
The results showed that both the apparent motion and also spatial context had a negative impact on the peripheral target detection performance [19]. The mean detection rate decreased from 99.0% to 81.0% for the first part and to 37.0% for the second as well as the third part. According to Mayeur, the investigated contrast values that were determined under laboratory conditions may lead to poor performance if one additional context variable appears. Therefore, according to road lighting design the model based on laboratory data is definitely insufficient.

| Factor | $\chi^2$ | p-value |
|---|---|---|
| Experiment part | 208.9 | 0.0 |
| Contrast | 43.89 | 0.0 |
| Eccentricity object | 3.3 | 0.069 |
| Age | 1.77 | 0.184 |
| Experiment part and contrast | 14.13 | 0.007 |
| Experiment part and eccentricity | 6.67 | 0.036 |
| Contrast and eccentricity | 17.71 | 0.0 |

Table 4.6: Comparison of the influence factors for the detection performance according to [19].

## 4.3 Previous field study research

**Detection distance based on heamplamp light distributions according to J. de Boer.** De Boer and Morass investigated the influence of luminous intensity of two different headlamp types in object direction (sealed beam lamps, halogen) [20]. In the analysis of the visual range or detection distance they defined the following parameters as a decisive for the detection [20]:

- Luminous intensity of the headlamps in object direction $I_{obj}$
- Luminous intensity of the glare source $I_B$
- Longitudinal distance from the test vehicle to the glare source $x$
- Lateral distance from the test vehicle to the glare source $y$
- Mutual position of the test vehicle and the glare source $P(x,y)$
- Detection object (size, reflection coefficient)
- Weather conditions
- Speed of the vehicles

Entering those parameters into an equation De Boer and Morass defined a function to describe the visual range V of a participant as follows:

$$V = V(I_{obj}, I_B, P(x,y)) \tag{4.37}$$

De Boer and Morass implemented quasi-stationary experiments, means participants sitting in a test vehicle drove through a test track (straight road, 6.4 m road width) and passed several stationary glare sources which represented oncoming traffic. The test vehicle was driven at a speed of $60.0\frac{km}{h}$. In every test run, detection distances of five detection objects that were arranged in a distance of 60.0 m to each other were determined. The detection objects were grey cards covered with grey woolen, mounted at a height of 40.0 cm (size 28.0 cm $\times$ 28.0 cm) with a reflection coefficient of $\rho = 0.08$.

They also investigated the influence of the grey card's position on the dectection distance. The grey cards were located on the left hand side (distance $d = 4.5$ m to the drivers position), the right hand side (distance $d = 1.35$ m to the drivers position) and in the middle of the road (distance $d = 1.35$ m to the drivers position). Figure 4.10 shows the results of detection distances by means of an isocandela diagram of the headlamps (low beam) [20].The perspective image of the street viewed from the right headlamp side is also indicated. On the left hand side is an additional scale, which corresponds with the distance from the headlamp to the observers eye of the or the detection object. In Table 4.7 the corresponding visual ranges V related to $I_{obj}$ and $P(x,y)$ are presented.

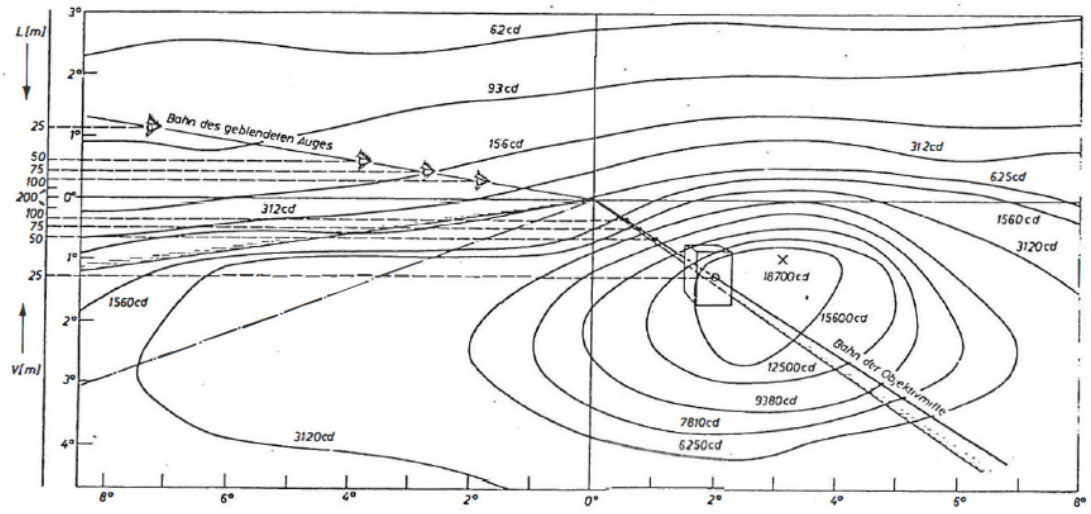


Figure 4.10: Isocandela diagram of the headlamps (low beam) [20]. The perspective image of the street viewed from the right headlamp side is also indicated. On the left hand side is an additional scale, which corresponds with the distance from the headlamp to the observers eye or the detection object.

| $P(x,y)$ / m | Distance $x$ / m | $I_{obj}$ / cd | | | |
|---|---|---|---|---|---|
| | | 1000 | 3000 | 10000 | 25000 |
| Left $y = -1.95$ | 90.0 | 37.0 | 49.0 | 67.0 | 81.0 |
| | 60.0 | 31.0 | 47.0 | 65.0 | 79.0 |
| Middle $y = -1.35$ | 90.0 | 31.0 | 57.0 | 88.0 | 102.0 |
| | 60.0 | 34.0 | 56.0 | 87.0 | 101.0 |
| Right $y = 4.55$ | 90.0 | 36.0 | 62.0 | 94.0 | 120.0 |
| | 60.0 | 35.0 | 62.0 | 94.0 | 120.0 |
| Right $y = 7.5$ | 90.0 | 45 | 68.0 | 95.0 | 113.0 |
| | 60.0 | 44.0 | 67.0 | 94.0 | 112.0 |

Table 4.7: Determined visual range V related to different headlamp luminous intensities in object direction $I_{obj}$ and the mutual position of the test vehicle and the glare source $P(x,y)$ (left, middle, right) according to [20].

In this case the luminous intensity of the glare source $I_B$ is set to zero.

Figure 4.11 illustrates the calculated visual ranges V as a function of the distance L between the test vehicle and the detection object.

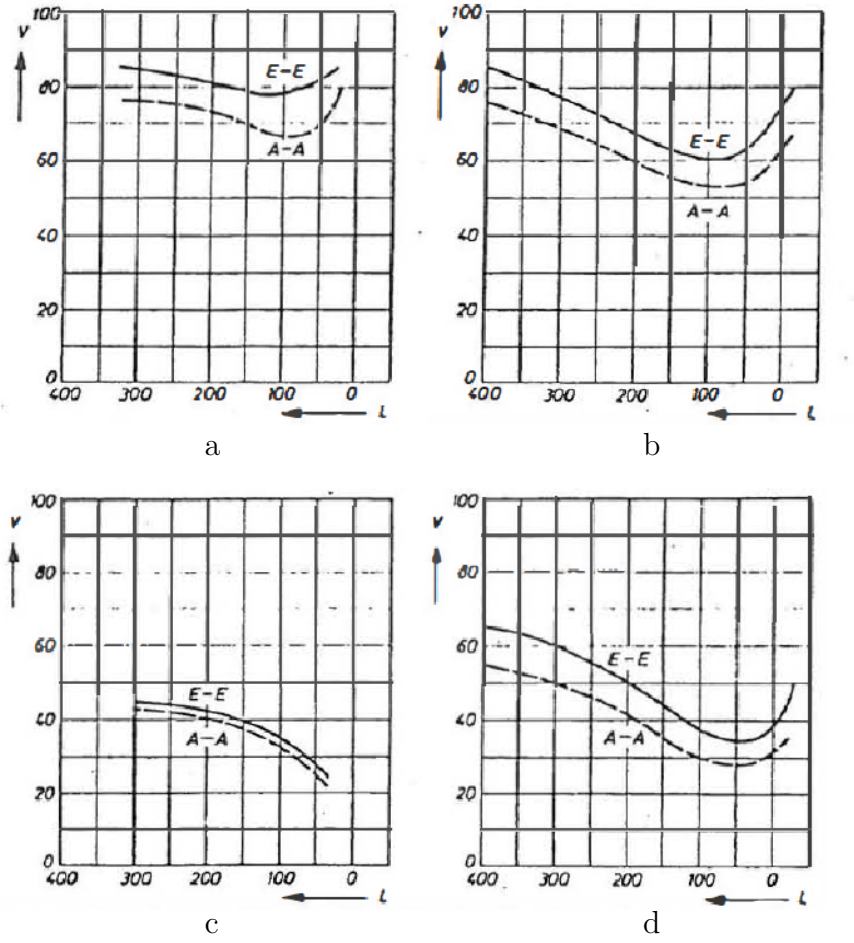


Figure 4.11: Determined visual range V as a function of the distance L between the test vehicle and the object according to [20]. a: Right hand side, halogen; b: Right hand side, sealed beam lamps; c: Left hand side, halogen; d: Left hand side, sealed beam lamps.

The results show that the detection distance is dependent on the glare intensity, illuminance level, size and position of the detection object related to the glare source. It can be recorded that the detection distance rises with increasing illuminance in object's direction. De Boer and Morass concluded that a prediction of detection distance is only possible if it is based on the illuminance.

**Detection distance investigations according to J. Damasky.** Based on the model of Blackwell, Damasky carried out investigations in the laboratory as well as in field studies [21]. Under laboratory conditions he conducted investigations for a subdivided adaptation field. As illustrated in Figure 4.12 he screened road scenario pictures onto a projection surface, whereas the background luminance within the simulated road was homogeneous. He used two projectors to picture the background and the detection targets separately. The detection objects' luminance could be adjusted in a range from $0.001\frac{cd}{m^2}$ to $75.0\frac{cd}{m^2}$, since the subject's task was to increase the contrast of the detection target by varying the lamp voltage until it could be

perceived.

Figure 4.12: White target represents dummy on the roadside. Projection surface for a divided adaptation field according to [21]. Two projectors were used to picture the background and detection targets separately. The triangle represents the roadway.

For the background luminance under laboratory conditions, he chose a homogeneous luminance level that corresponded to a point on road surface at a distance of 35.0 m (low beam condition). Therefore the background luminance was less than $0.01\frac{cd}{m^2}$. As detection objects, Damasky used squares and rod-shaped objects. Those were presented with both a positive and a negative contrast. As illustrated in Figure 4.13 and Figure 4.14, Damasky's results show that the contrast sensitivity is dependent on the average road luminance. He assumed the average luminance on the road surface as adaptation luminance.

In a second part he compared his results obtained in laboratory with a validation field test. He performed field experiments in two different environments to obtain 95% detection and identification object luminance data. He used a test vehicle with a special measurement setup (self-constructed head-up display) in which objects could be displayed in the visual field of the driver. The detection objects were generated by a CRT display mounted on top of the test vehicle and projected into the driver's visual field by an optical combiner (composed of a lens and mirror). In Table 4.8 the detection targets that were projected into the visual field of the participants are presented. The detection objects appeared at different positions that are typical for real traffic scenarios (traffic signs, pedestrians). The detection objects were human dummies (diameter 2.06°), square-shaped traffic signs (diameter 0.65°) and rear lights (diameter 0.16°). Some of the objects appeared in different chromaticities (grey, red, yellow, blue), e.g. the rear lights were always presented in red.
First, he carried out investigations on a closed area (straight road, 1.2 km length, runway of the airport Griesheim, Germany). The second environment was a test track in real night-time traffic space. Overall seven participants conducted the experiments (26-33 years of age).

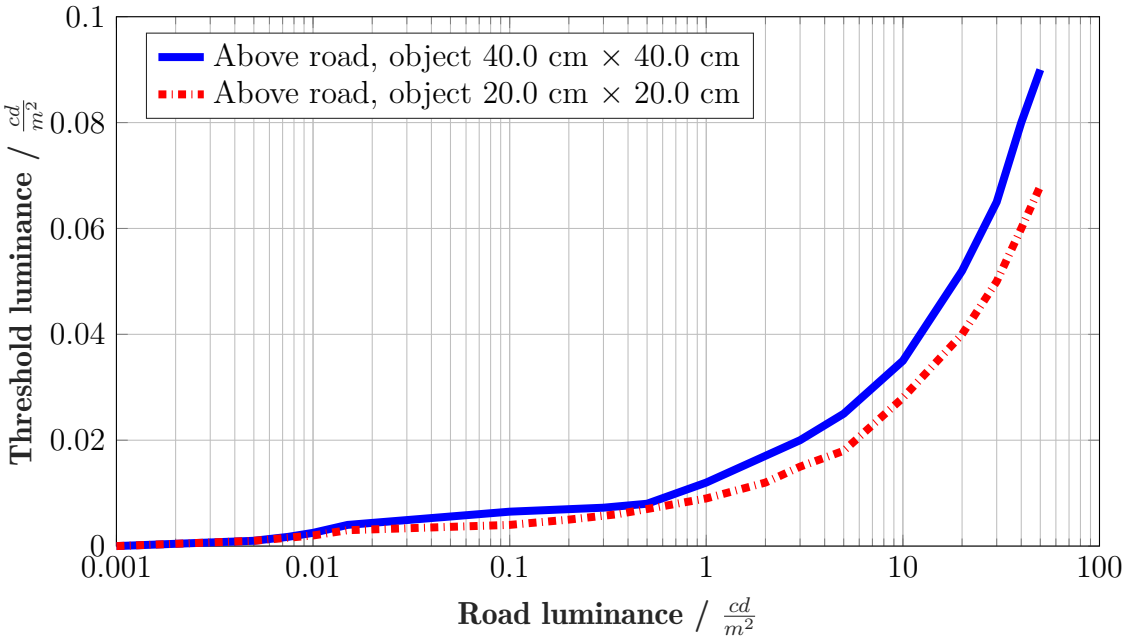


Figure 4.13: Threshold luminance for a detection target above the road for a divided adaptation field; positive object contrast for an assumed observation distance of 50.0 m according to [21].

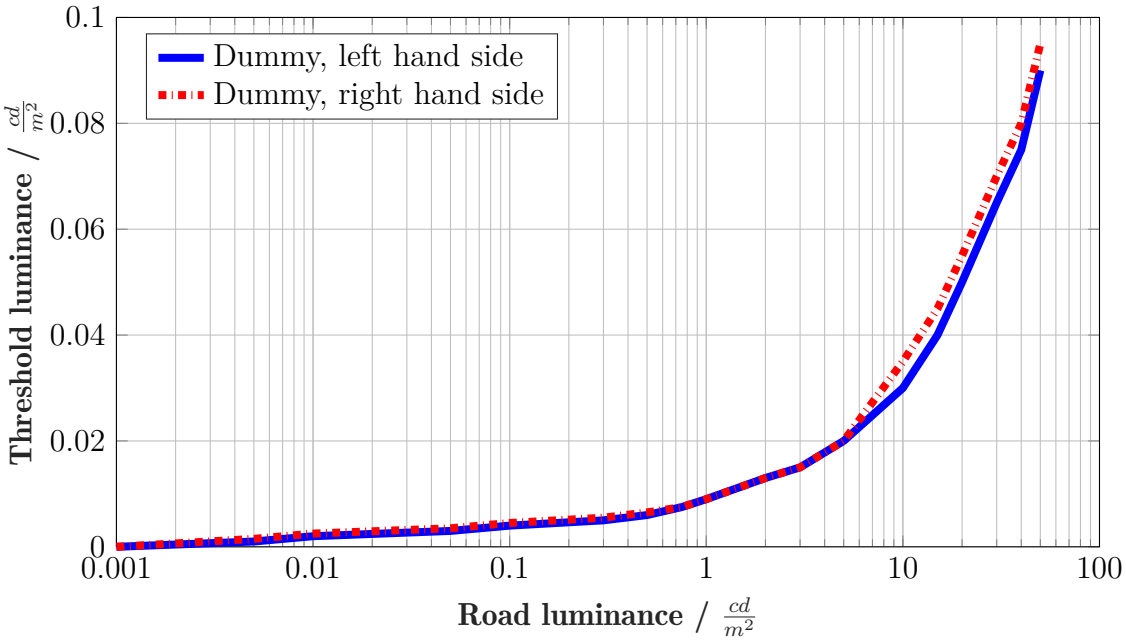


Figure 4.14: Threshold luminance for a human dummy in positive object contrast for an assumed observation distance of 50.0 m according to [21].

In the first part the participant's task was to drive along the runway (luminance ahead of the vehicle ranged between $0.02\frac{cd}{m^2}$ and $0.09\frac{cd}{m^2}$) and to detect or identify objects [21]. Damasky analysed the following factors: object type (vertical and

horizontal eccentricity, size, shape), vehicle velocity (static or dynamic), object chromaticity (red, blue, yellow, grey), knowing or unknowing participant (knowledge of targets' appearance position) and visual task (detection, identification or identification of object chromaticity) [21]. The results of Damasky are compared with the own results in Chapter 7.

| Detection object | Horizontal position/ ° | Vertical position/ ° | Object size / ° | size / $cm^2$ |
|---|---|---|---|---|
| Traffic sign right | 3.57 | 1.80 | 0.65 | 40.0 × 40.0 |
| Traffic sign left | -5.50 | 1.80 | 0.65 | 40.0 × 40.0 |
| Traffic sign overhead | 0.21 | 6.95 | 0.65 | 40.0 × 40.0 |
| Object on runway | 0.00 | 2.00 | 0.65 | 40.0 × 40.0 |
| Traffic sign right | -0.30 | -0.46 | 0.16 | 10.0 × 10.0 |
| Dummy left | -3.50 | -1.37 | 2.06 | 175.0 × 40.0 |
| Dummy right | 1.20 | 1.37 | 2.06 | 175.0 × 40.0 |

Table 4.8: Objects used in both field studies (closed areas and real traffic scenario) according to [21].

**Visibility effects of road lighting according to Y. Akashi.** Akashi performed a field study to analyse visual performance according to the driving task [92]. The participants drove through a test track (lighted street) performing a decision making task. They had to indentify the direction of moving targets that were located next to the road. The speed of the moving target was $10.0\frac{km}{h}$. The participants were instructed to drive along on a test track with a speed of $32.0\frac{km}{h}$, to follow the fixation target and to respond if the target moved toward or away from the street by braking or accelerating the test vehicle at the moment of decision.
The setup included sequentially activated targets and a fixation target, that was a life-sized picture of a deer mounted on a ladder construction (1.2 m height). The other targets consisted of five square flip-dot discs (14×14 array, edge length 20.0 cm × 20.0 cm) that were placed next to each other since the central target was positioned 8.0° to the right of the fixation target. Every time when the wheels passed a infrared sensor across the road pavement on the test track, one of the flip-dot discs was activated, simulating a movement towards or away from the participant. In this investigation the parameters to be studied were the targets' movement direction and the lighting condition. As light sources a ceramic halide light source and a high-pressure sodium light source were compared. The experiment was conducted under day and night-time conditions.

In his evaluation Akashi compared the accelerating and braking reaction times of the participants for three lighting conditions (ceramic metal halide (CMH) high and low, high-pressure sodium (HPS)). In average the accelerating reaction times were between 0.96 s and 1.2 s, whereas the braking reaction times resulted between 0.86 s and 0.92 s. In total, the response times were shorter under a metal halid light source than under a high-pressure sodium system. The results showed that the braking response as well as the acceleration response times decreased monotonically with an increasing unified luminance. The task performance in his experiment

was the same at an unified luminance and changed for luminance values below $0.6\frac{cd}{m^2}$. Therefore Akashi suggested to use luminance as suitable variable to characterise light levels for different light sources with respect to a complex visual task [92].

**Peripheral visual performance according to J. Bullough.** Bullough performed a static field study analysing peripheral visual performance for various headlamp conditions (halogen, HID and advanced forward-lighting systems (AFS)) [93]. Detection targets with different size were located at various positions along the edges of left-turn and right-turn bends. The aim of this study was to make a prediction of peripheral visibility under arbitrary beam patterns as function of target characteristics. The targets consisted of (20.0 cm × 20.0 cm) square arrays of white flip dots and have already been used in [92]. It was also possible to change the size of the target by switching off some of the flip dots, so that two more target shapes could be analysed (7 (10.0 cm × 10.0 cm)×7 array and L-shaped array). The subject's task was to search for targets and to respond to every target onset, that were presented randomly with a 2.0 s or 4.0 s delay for different headlamp conditions, two bend directions and different target sizes. Every subject performed 3 trials for each target under twelve conditions (3 headlamps× 2 target sizes× 2 bend sides). As result can be noted that reaction times to large targets were shorter than to small targets. In addition, the most peripheral targets detection resulted in the longest reaction times. The target size, target position as well as the headlamp condition had an significant influence on the reaction time [93]. Furthermore, the impact of an increasing headlamp intensity in specific regions in the beam pattern improved visual detection while passing left-hand and right-hand bends.

**Threshold VLs for detection of pedestrians at night-time according to K. Ising.** Ising [94] introduced a modified visibility model of Adrian [13] containing the CIE general disability glare equation [95]. He also considered factors influencing the detection performance like the participants' age or target reflectance.
The participant's task was to detect various objects located on the left and right hand side of a rural road while driving in a test vehicle with a speed of $40.0\frac{km}{h}$. The participants were divided into two groups. Fifty percent of the participants were clarified about the experiment ("initiated"), the other half was not informed (" naive"). The distances between the test vehicle and detection object were recorded. The detection objects were divided into large (rectangle, 183.0 cm × 30.0 cm) and medium objects (rectangle, 76.0 cm × 30.0 cm) and had reflection coefficients of 0.06, 0.12 and 0.25. The objects were analysed for low beam, high beam and a modified high beam headlamp system.

Ising conducted photometric measurements to determine average visibility levels (using Adrian's model). He assumed the target and background luminance measurements to be evenly spaced along the height of the objects. As a result twelve contrast levels were computed for large objects and eight for mid-sized ones. Caused by the inhomogenous distribution of the headlamps and heterogeneous background the contrast level of each target was distributed in a wide range. Hence, Ising divided the targets into sub-targets (large objects into three parts (37.0 cm height),

mid-sized targets into two parts (25.0 cm height)) and recalculated the contrast and the VL.

As it can be seen in Figure 4.15 considerably higher visibility levels were determined for older participants. While the position and also the size of the target did not have a significant influence on the VL, the objects with 6.0% reflectance exhibited a higher VL compared to objects with 25.0% reflectance. The average difference in visibility level was 3.1. Higher visibility levels were calculated under

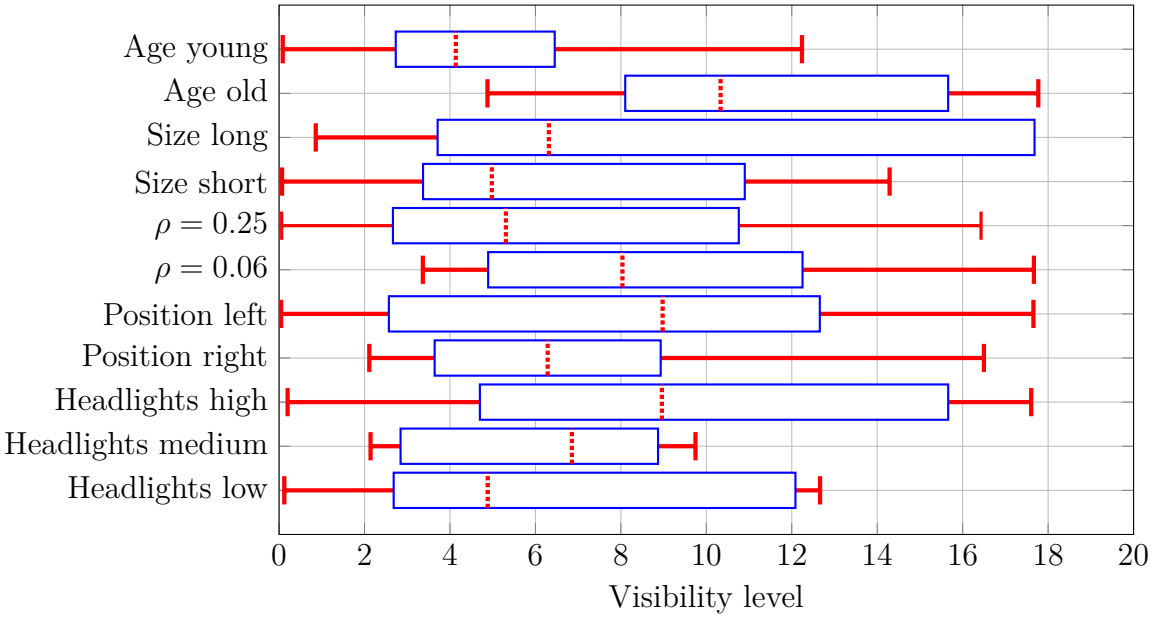


**Figure 4.15: Influence factors of the visibility level on initiated participants according to [22], illustrating median, upper and lower quartiles and full range.**

high beam than under low beam lighting. The effect of the age on the VL was highest for high beam illumination compared to modified high beam and low beam. According to Ising, the relation between participants age and headlight illumination also plays an important role. For example a naive participant of 65 years of age will require a VL in a range of 49.9 to 88.5 to detect an object [94]. Based on Ising's results it can be noted that average threshold visibility levels amounted to values from 0.1 to 18.0 for initiated participants and from 14.0 to 89.0 for naive participants [94]. The presented visibility levels were based on average detection distances of all participants, so the individual detection performances were not taken into account.
The wide variation of the values leads to the conclusion that the driving task under night-time illumination has significant influence on the detection. According to Ising redefining the target size variable could be another limitation factor, since subdividing the objects into other means of characterizing target size would lead to different results. The approach to subdivide the objects can be advantageous as multiple contrasts can be determined to describe the behaviour along object's surface. For example, the clothes of a pedestrian for instance vary in colour and reflectance continously.

**Visibility levels at target detection according to K. Ising.** The aim of Ising's second study was also to determine the VL distribution for a detection task while driving a vehicle [22]. For the VL determination the target and background luminance at various positions were measured. He used a modifyied model of Adrian that included more recent findings involving glare sources. As an example, the detection probability results for uninitiated participants are shown in Figure 4.16. Ising used a log-normal distribution function to fit the data. He concluded that Adrian's model provides a good foundation for visibility level determination but has several limitations and requires a modification to implement important influence factors.

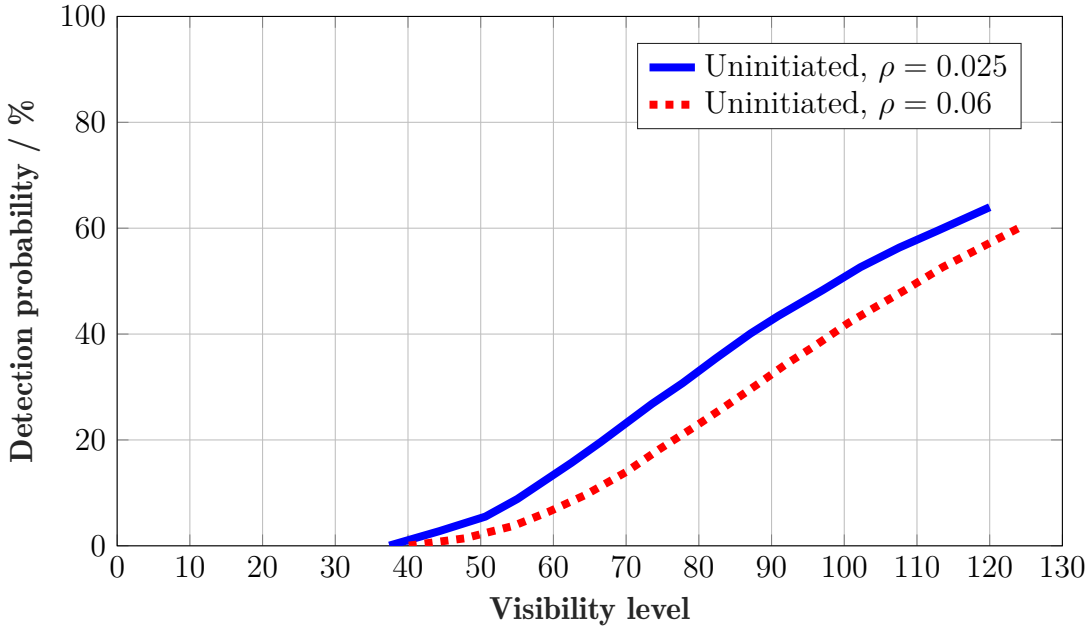


Figure 4.16: Detection probability distribution in % related to the visibility level for uninitiated participants according to [22]. Data were calculated from 6.0% and 25.0% reflective targets.

According to Ising the Adrian model did not cover factors like different headlamp types or reflection of the targets [22]. To minimize these above-mentioned effects, in his experiment only young participants and low beam headlamps were considered. The luminance was determined for five distances to the detection object (30.0 m, 46.0 m, 61.0 m, 91.0 m, 122.0 m). For each distance the object luminance was measured at three heights for mid-size objects and at five heights for larger objects. The background luminance was determined below and above the targets, as well as at three or five heights along both sides of the target [94].

Ising assumed the object detection to be navigated by the highest contrast area on the target surface and the maximum VL at each distance between the test vehicle and target. The highest VL at each object position was chosen to represent the participants' visual performance, if the participants were initiated (compare Figure 4.16). Caused by the inhomogenous illumination of the headlamps and

heterogeneous background the contrast level of each target had a large variation. Hence, Ising divided the targets into sub-targets (large objects into three parts, mid-sized targets into two parts) and recalculated the contrast and the VL.

**Visibility level computation according to R. Brémont.** Brémont performed a field study, comparing six different methods for the visibility level determination [96]. He focused into two main aspects: the first question was how to define the background and adaptation luminance so that one can get the best correlation between the detection distance and VL. Second, he computed the VL at the moment of object detection instead of using a conventional angular size. For his investigation Brémont used the same test setup as in [15] on a 1.2 km closed road circuit (CETE Rouen, France).

For the VL evaluation of the photometric measurements he used a photometer to compute the object contrast. The measurements were derived in a distance of 30.0 m to the object (in a height of 1.2 m above the road surface) [96]. Overall five measurement points were taken for each object location (one on the square surface and one at each edge of the square (left, top, right, bottom)). Illuminance measurements were carried out as well. The headlights were not taken into account. Subsequent the VL was determined by using the model of Adrian (presentation time of 0.2 s, 10' angular size, for a 25-year-old participant). He analysed three different methods while he changed the background luminance to compare the VL values.
In the first approach he used the pavement luminance, in the second the mean luminance surrounding the object (mean of the four measurement points: bottom, left, top and right). In the third approach he used the luminance that led to the highest contrast between the object and its background. In additon, he considered another two methods for setting the adaptation luminance. Using the first method he calculated the detection threshold using the background luminance as reference. The second method included an estimation of the adaptation luminance as the mean background luminance over all detection targets that were anlysed in the study (in total 16). Based on the result of the average background luminance the adapation luminance was fixed to unique value ($L_a = 0.4\frac{cd}{m^2}$).
The VL had a strong dependence on the measurement method. The deviations between the methods ranged between 58.0% up to 71.0% [96]. Based on his results Brémont recommended method six as most suitable for this application. In this case the background luminance with highest object contrast was chosen and the adapation luminance was fixed to unique value (representing the road surface luminance).

In a next step he compared the visibility level capacities to predict the detection distance. The comparison was performed by evaluating the relation between the two parameters linearly and non-linearly. First a linear relation between the VL and the detection of a target was assumed, whereas the detection distance was taken as an index of driving performance [96]. Using the "mean of four points" measurement method for the background luminance, the adaptation luminance was set to a unique luminance value for the whole road section. Although these results included a four points computation of the background luminance for VL computations, the

linear hypothesis was not strongly supported by the determined data. Furthermore, a nonlinear increasing relation was tested and the method using the highest object contrast was chosen (fixed adapation luminance, method six). Therefore no definite statement regarding the method selection could be made.
As the detection distance is not only dependent on photometric parameters, it is not possible to completely express detection performance of the participants by VL. This can be explained by several reasons. The detection distance was underestimated in this investigation, since the reaction times of visual detection and participants response (pushing a button) were not taken into account. The speed of the test vehicle was also not considered. The luminance measurements were performed with just one geometry (30.0 m distance to the object, 1.2 m height) [16]. It must be considered that the geometry varies with the distance to the target. Thus, it can be stated that the background luminance measurements did not correspond to the background luminance at the detection moment. This assumption can be supported by the significance analysis of the individual methods.

**Effect of the driving activity according to A. Mayeur.** In this investigation the same test setup as in [15] was used. The focus of Mayeurs study was to analyse the effect of driving activity on peripheral target detection [23]. He conducted a close-circuit field study and evaluated the effect of driving activity comparing the driver towards passenger status at the same time. The main independent variables were the participant's status and visibility level on detection targets. Mayeur put the hypothesis that passengers have better performances than drivers since passenger's workload is smaller than driver's workload (single detection task).
Thirty-four participants (average age 36 years) performed the experiment and were divided into two subgroups A and B (group A: started as passenger in the first part, as driver in second part; group B: started as driver in the first part, as passenger in second part). As visual targets sixteen grey squares (20.0 cm $\times$ 20.0 cm) were placed on the test track in order to receive relevant luminance contrast values (compare Figure 4.17).

The test track was a straight road (length of 450.0 m, width of 8.0 m) including a road lighting installation. The measurements were performed in a distance of 30.0 m and an observation height of 1.2 m to the detection object (corresponding eccentricity of 2.29°). The VL as well as contrast were computed based on Adrian's model (for a subjects with 23 years of age). As it can be seen in Figure 4.17 sixteen contrast values from 0.016 to 0.608 and a VL from 0.2 to 16.9 were calculated [23]. The results suggest that the passengers' performances were higher than drivers' performances. The results between drivers and passengers were significant, but the effect on the detection distance was comparatively small. Since the experiment's only task was to detect an object while driving, Mayeur assumed that it can be traced to low complexity of the task.
The results showed that the driving activity, even with a marginal demand on information processing, has a negative influence to the driver and should be included in future road visibility indexes. Mayeur expected the difference between driver and passenger status to be more significant for a more complex environment [23].

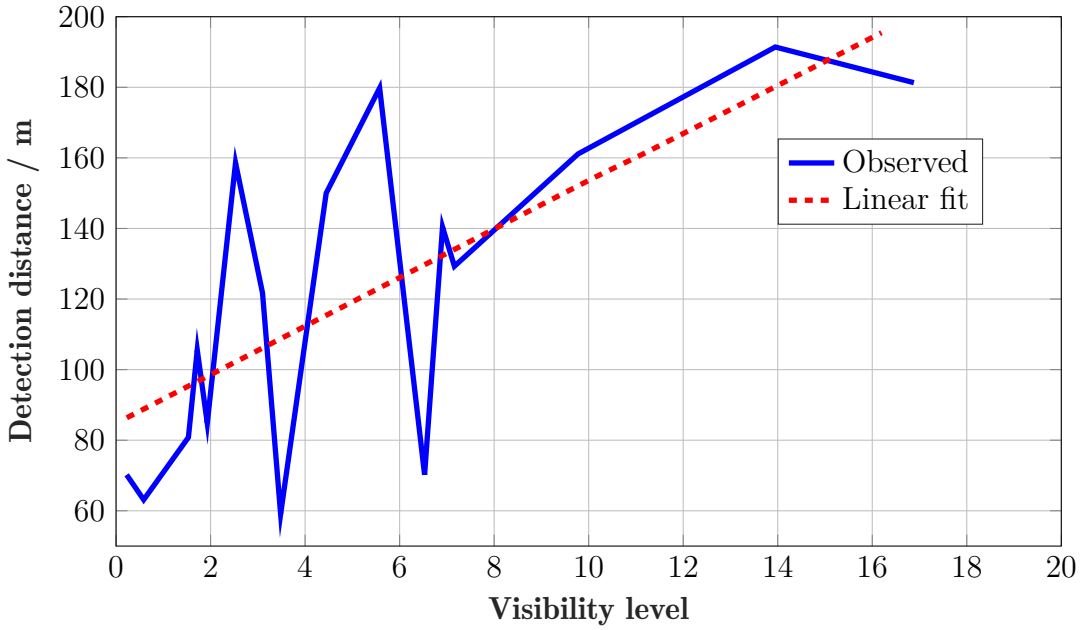


Figure 4.17: Mean detection distance according to the visibility level VL from [23]. Sixteen grey squares (20.0 cm × 20.0 cm) were placed on the test track in order to receive relevant luminance contrast values. The measurements were performed in a distance of 30.0 m and and an observation height of 1.2 m to the detection object.

**Detection distance determination according to R. Gibbons.** In a field study Gibbons determined the detection distances of pedestrians and small objects, that were located on and also along the roadway, at five adaption levels under three light conditions (two LED and high-pressure sodium (HPS)) in roadway scenarios [97]. Luminance levels of both the detection object and surrounding background were established. The test vehicles (1999 Ford Explorer, 2000 Ford Explorer) were equipped with high-intensity discharge headlamps (Bi-Xenon) and only used with low beam. The data were recorded by GPS as well as video recorders and luminance cameras, which were included into the test vehicles. The investigated parameters were: effect of age, overhead lighting, vehicle speed, visual angle and object's position related to the detection distance.
Gibbons divided the in total 36 participants in two equal age groups: younger drivers (25-30 years of age) and older drivers (60 years of age and older). The adaptation luminance was the luminance, viewed from inside the test vehicle, for a given combination of overhead lighting level and two road surfaces [97]. It varied in a range from 0.11 to $0.54\frac{cd}{m^2}$ for concrete and 0.07 to $0.35\frac{cd}{m^2}$ for asphalt. The test vehicles were driven at a speed of $56.0\frac{km}{h}$ and $80.0\frac{km}{h}$, the offsets of the pedestrian to the roadway (from driver's head position) were at 3.0 m (left), 7.7 m (left), 8.9 m (right), 21.0 m (right), based on a fixed theoretical detection distance of 83.0 m. This detection distance was based on a 1.0° downward viewing angle with a vehicle height of 1.45 m [97]. The pedestrians were located in an illuminated section of the road (vertical illuminance was measured on pedestrians face). The participants were instructed to say "person" or "pedestrian" when they first saw the detection object. Every subject completed the test trial 12 times for each lighting type (in

total 3×24 trials).
With increasing adaptation luminances the detection distances rised. The second influence factor was the partcipants' age. The mean detection distance of older partcipants was considerably shorter compared to young participants. This can be attributed to the visual acuity that decreases with growing age (all participants were tested with the Snellen visual acuity test). With rising offset of the object to the roadway, the spectral effects became more significant, but this effect was not consistent for all eccentrities. Starting from an adaptation luminance of $0.07\frac{cd}{m^2}$ the detection distance decreased with an increasing eccentricity [97]. At higher adaptation luminances the relation between the object's position and detection distance varied more, so no tendency could be noticed. The results of this investigation did not reveal a spectral effect of street lighting on mesopic visibility in periphery. Overall, the results for the detection differences among the luminance levels were equivalent to Adrian's model ("At the lowest adaptation luminance ($0.1\frac{cd}{m^2}$), mean detection distance was only about 10.0 m shorter than at higher adaptation levels, likely because a dark-adapted eye is more contrast sensitive.") [13] [81].

**Detection of roadside targets according to I. Reagan.** Reagan conducted a field experiment on a public, rural, unlit and two-lane road in which twenty participants from 30 to 48 years of age were asked to search a set of 60 targets. Reagan's intention was to gain further informations about the benefits of adaptive headlights to visual performance [98]. The participants completed the target detection trials three times, first with adaptive high-intensity discharge headlamps, second with high-intensity discharge headlamps and third with halogen headlights. While driving through the test track the driver's task was to search for targets and to push a button on the steering wheel to indicate target's appearance.
The aim of this investigation was to evaluate differences in drivers' detection performance of targets that were located alongside the road as a function of conventional or adaptive headlights. The investigated parameters were: three different headlight types (halogen, HID and adaptive HID), target reflection coefficient (0.1 and 0.38), targets' location (inside or outside of a bend, beside the road (left or right)) and type of bend (straight, gradual bend or sharp bend). The test vehicle's speed ($48.3\frac{km}{h}$) was recorded at the moment of driver's response. The "visibility distance" for each target was developed as distance between the target and point where the target could be seen first. The speed and vehicle's position data were collected using a combination of inertial and GPS navigation system.

The low-reflectance targets (20.32 cm × 30.48 cm size) and adaptive HID headlights had signifcantly larger detection ratios compared to halogen and HID headlights. The average visibility distance of targets that were located inside the bends was 64.4 m. The participants detected high-reflectance targets in average 3.0 m sooner using adaptive HID headlamps compared to halogen system.
The results showed that adaptive HID headlamps improved drivers' detection performance for targets with low reflection coefficient. This headlight system enabled an earlier detection of roadside targets compared to halogen headlamps. The strongest effects were associated for low-reflectance targets on the inside of bends [98]. Ac-

cording to Reagan the relation between peripheral and foveal vision might be one explanation which could be the differential benefit for targets with small reflection coefficient. To detect or identify a small object on roadside foveal vision is required. With growing darkness the receptors lose their sensitivity which results in a decreased ability of many visual functions.

In 2017 Reagan performed another experiment analysing targets on roadside related to headlamp systems [99]. The aim of this study was to evaluate whether target detection was affected by three headlight systems, that were already used in [98], using high beam. The same test environment and detection targets as in [98] were used. The results showed that detection performance was similar for all headlamp systems. It was established that drivers detected low reflectance targets on straight road sections in a larger distances driving with halogen high beam compared to adaptive HID high beam headlights. For targets that were located on the inside of bends the adaptive HID highbeams was advantageous with regard to the detection performance. In contrast to his results in [98] better detection results were performed using halogen headlamps compared to HID and adaptive HID systems under low beam conditions.
Comparing the average detection distances from the two studies indicated, longer mean target detection distances for participants driving with high beams arised uniformly, which results in visibility benefits for systems that optimize proper high beam use [99].

## 4.4 Contrast determination

There are several methods to determine the contrast of a detection object related to its background. Mostly the contrast can be calculated from the so-called detection distance meaning the distance between the detection object and its observer. In the following paragraph certain methods for determination of the detection distance of an object will be introduced.

### 4.4.1 Detection distance

The distance that can be measured from the observer's position to the detection object is to be understood as detection distance. In this case, one has to distinguish between "just detected" and "securely recognized", since both options provide different detection distances.
In literature, detection distance is not clearly defined in terms of the quality characteristics of motor vehicle lighting. One can find synonyms like visibility [5], visual range [39], driver's visibility [20], visual distance [24], perceptibility [50] or recognition distance [38].
Determining the detection distance of a headlamp system is an important safety-relevant quality feature. A high detection distance allows the driver to react to occurring obstacles, e.g. pedestrians crossing the road. Especially at night-time, accidents are characterized by serious consequences. In the case of accidents involving severely injured persons, the proportion of night accidents is 36.5% in average,

in accidents with deaths even 47.0% [71] [8].
Many factors affect the detection performance, e.g. attention, tiredness, visual performance, visual object (size, shape, position) but also general conditions such as weather, road surface and light conditions. Considering all parameters it can be noted that the visual performance and headlamp light distribution are most essential for the detection of an object [38].
Visual performance enables the driver to perceive and recognize his environment. In this context, especially the headlamp light distribution has a major effect on threshold contrast. At best the headlamp system should be able to illuminate the road, as well as possible obstacles in traffic area, and thus precisely produce the contrasts that are necessary for object detection. For an exact prediction of the detection distance for a specific headlamp system, all influencing parameters must be considered. In the following, existing methods for the determination of the detection distance are presented. The results from the literature review are divided into two groups. First, models that are based on threshold contrast investigations in the laboratory are presented, second, methods used in real field studies are considered.

### 4.4.2 Contrast models

**Illuminance model according to S. Völker.** A common method for contrast determination is the so-called illuminance model [34]. Using this model the headlamp light distribution, which is usually simulated or measured by means of a vertical screen set up 25.0 m forward of the headlamp (ECE-measuring screen), is converted into a street display. In the resulting image (an example can be found in Figure 4.18), intersections of certain iso-lux lines with road markings (e.g. right road edge) can be found. These intersections define the range, which is often used in the sense of visibility distance.

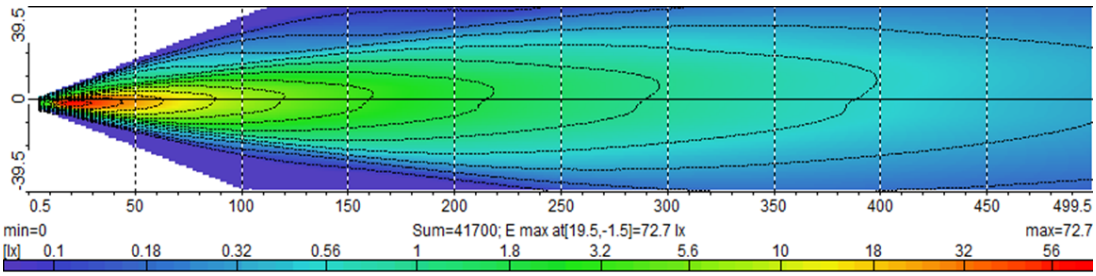


Figure 4.18: Determination of the detection distance using isolux lines of a headlamp light distribution. Standard high beam 3.0 lx line in a distance of 160.0 m (birds view perspective).

The model does not take into account the visual object's nature and luminance distribution surrounding it. Thus, two essential quantities influencing the threshold contrast are neglected. According to Völker a prediction of object detectability with this model is not possible. This is also confirmed by his investigations [34].

**Luminance difference measurements according to M. Eckert.** Based on Adrian's model [13] [82], Eckert developed a model to calculate the detection distance, which can be used for the reconstruction of traffic accidents [5]. His investigations focused on vehicle involving pedestrian confrontation scenarios. In Eckert's model a pedestrian is considered as a critical visual object. Therefore, according to Eckert the following approach applies:

$$\Delta L > \Delta L_{\text{thresh}} \tag{4.38}$$

$\Delta L$ describes the existing luminance difference between the object and its environment, while $\Delta L_{\text{thresh}}$ is the threshold luminance level that is essential to detect an object with specific size within a surrounding background luminance. Eckert determines the luminance difference $\Delta L$ of a pedestrian as follows: In a first step the luminance values from 11 up to 13 measurement points on the pedestrian's surface and also 11 to 13 points on pedestrian's environment are determined (compare Figure 4.19).

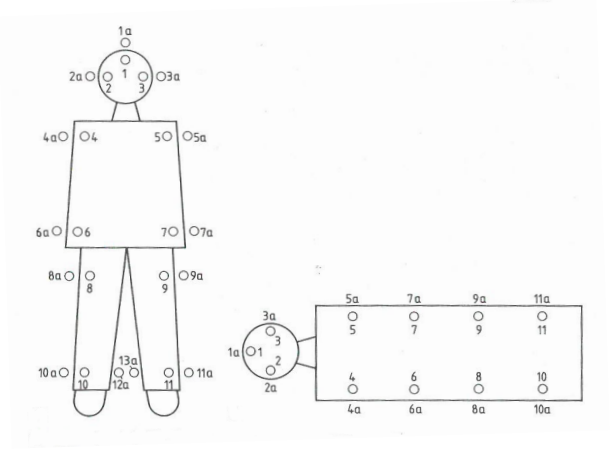


Figure 4.19: Measurement points for luminance analysis of a pedestrian from [5]. Luminance values from 11 up to 13 measurement points on pedestrian's surface and also 11 to 13 points along pedestrian's outline are determined.

The measurement points are located close to the transition from the silhouette of the object to its background. Subsequent, $\Delta L$ can be calculated by means of the luminance points. $\Delta L$ is only relevant for detectability, if it extends at least over a visual angle of 0.5°, which covers at least two of the provided measuring point pairs [5]. Eckert determined the threshold luminance $\Delta L_{\text{thresh}}$ according to Adrian's model [13]. He used a modified version of Equation 4.15:

$$\frac{\Delta L}{\frac{cd}{m^2}} = k \cdot \left( \frac{\sqrt{\phi}}{\alpha} + \sqrt{L} \right)^2 \cdot F \tag{4.39}$$

with

- $k$, factor for the detection probability; $p = 1.0$ corresponds to 50% detec-

tion probability, $p = 3.1$ corresponds to 100.0% detection probability; recommended for road traffic

- $\sqrt{\phi}$, $\sqrt{L}$, luminous flux or luminance function according to Ricco's/ Weber's law [37]
- $\alpha$, observation angle of the detection object in angular minute
- $F$, practice factor; $F = 10.0$ considers difference between laboratory and field investigations [5]

$\sqrt{\phi}$ and $\sqrt{L}$ are derived from Blackwell data [37] and describe the relation between the threshold and background luminance. For the luminance range between $0.004\frac{cd}{m^2}$ and $0.6\frac{cd}{m^2}$, $\sqrt{\phi}$ and $\sqrt{L}$ can be calculated using Equations 4.27 or 4.28. The values of $\sqrt{\phi}$ and $\sqrt{L}$ can be found in Table 4.1.
The detection distance can be determined by equaling $\Delta L$ to $\Delta L_{\text{thresh}}$:

$$\Delta L = \Delta L_{\text{thresh}} \tag{4.40}$$

Transposing Equation 4.39 applies to:

$$\alpha = \frac{\sqrt{\phi}}{\sqrt{\frac{\Delta L}{k \cdot F}} - \sqrt{L}} \tag{4.41}$$

The detection distance $d$ results from the observation angle $\alpha$ and the dimensions $m$ of the detection object:

$$d = \frac{m}{\tan(\alpha)} \tag{4.42}$$

**Visibility level determination according to S. Kokoschka and D. Gall.** Kokoschka and Gall developed another model for the detection distance determination [24]. Since it is also based on the data of Blackwell [37], it is similar to Eckert's model [5] and considers foveal perception in the same manner. This model is based on the precalculation of threshold contrast. The threshold contrast is then defined as a function of the object size and background luminance and is compared to the actual contrast.
The detection object VL was calculated for a headlamp system at different distances. If VL reached a defined limit, the driving visibility distance was achieved.
The visual field in night time driving situations is characterized by an inhomogenous background luminance distribution. To adapt their model to real conditions in night time traffic, Kokoschka and Gall extended the model of the observer situation (vehicle driver) by the following factors:

- The detection object edges are evaluated to be relevant.
- The environment that is directly adjacent to the detection object is assumed to be contrast relevant.

- The average contrast of the object's edges is determined out of the integral parts of the object edges.
- The adaptation luminance is defined by the background luminance.

The detection object luminance is influenced by several external factors. According to [24] the luminance that is seen by vehicle's driver $L_o$ can be expressed as follows:

$$L_o = L_{\text{nat}} \cdot e^{-\sigma_e \cdot x} + L_{\text{hl}} \cdot e^{-\sigma_e \cdot x} + L_{\text{sky}} \cdot \left(1 - e^{-\sigma_e \cdot x}\right) + L_{\text{stray}} \tag{4.43}$$

with

- $L_{\text{nat}}$, luminance at the detection object's position, generated by natural lighting
- $L_{\text{hl}}$, luminance at the detection object's position, generated by headlamps
- $L_{\text{sky}}$, average luminance of the sky; in homogeneously covered sky identical with luminance of horizon
- $L_{\text{stray}}$, scattering luminance, generated from headlights on line of sight to the observer
- $\sigma_e$, weakening index of the atmosphere
- $x$, distance between observer and detection object

Equivalent to the luminance of the detection object the luminance of the environment $L_u$ can be calculated:

$$L_u = L_{\text{nat,u}} \cdot e^{-\sigma_e \cdot x} + L_{\text{hl,u}} \cdot e^{-\sigma_e \cdot x} + L_{\text{sky,u}} \cdot \left(1 - e^{-\sigma_e \cdot x}\right) + L_{\text{stray,u}} \tag{4.44}$$

with

- $L_{\text{nat,u}}$, luminance of the detection object's background, generated by natural lighting
- $L_{\text{hl,u}}$, luminance of the detection object's background, generated by headlamps
- $L_{\text{sky,u}}$, average luminance of the sky; in homogeneously covered sky identical with luminance of horizon
- $L_{\text{stray,u}}$, scattering luminance, generated from headlights on line of sight to the observer
- $\sigma_e$, weakening index of the atmosphere
- $x$, distance between observer and detection object

The surrounding area includes all elements, that are not part of the detection object. Hence, those elements represent the largest part of the driver's visual field. The environment includes the road and adjacent ground, as well as the sky. In [24] the determination of the detection distance is also described. The determination process is divided into eight process steps:

1. **Calculation of stray light luminance of vehicle headlamps.**
2. **Calculation of detection object luminance** $L_o$ according to Equation 4.43.
3. **Calculation of background luminance** $L_u$ according to Equation 4.44.
4. **Calculation of detection object contrast** $K$**.** An edge contrast is calculated for each adjacent edge of the detection object and its background. From the all partial contrasts an average edge contrast can be determined as follows:

$$K = \sum_i \frac{K_i}{n}, \qquad K_i = \left| \frac{L_{o_i} - L_{u_i}}{L_{u_i} + L_{\text{stray}}} \right|, \quad i = 1...n \tag{4.45}$$

5. **Calculation of adaptation luminance** $L_a$. The reflected light from detection object into environment produces a stray light veil through scattering on the retina. Firstly, the scattered light leads to a reduction of detection object contrast, secondly, an increase in retina excitation is apparent, which is comparable to an increase of the average background luminance. Those effects in the eye emerge according to the stray light theory of Holladay [100] by the so-called equivalent veiling luminance, which simulates stray light veil on the retina by means of background luminance. The adaptation luminance $L_a$ can be expressed as follows:

$$L_a = 0.926 \cdot L_u + L_{\text{stray}} \tag{4.46}$$

6. **Calculation of detection object size** $s$**.**
7. **Calculation of visibility level VL.** The visibility level is defined as follows:

$$VL = \frac{K}{K_{\text{thresh}}} \tag{4.47}$$

with calculated mean edge contrast of visual object $K$ and calculated threshold contrast $K_{\text{thresh}}$ for the perceptual criterion "just seen". In [101] a description of the theoretical threshold contrast is given, which is based on Blackwell data [37]. It is determined as follows:

$$K_{\text{theory}} = k_{min} \cdot f_1 \cdot f_2 \tag{4.48}$$

with $f_1 = 1 + \left(\frac{L_a}{c_1}\right)^{c_2}$, $f_2 = 1 + \frac{\alpha_0}{\alpha}$ and $\alpha_0 = c_3 + c_4 \cdot \left(1 - \frac{1}{1 + \frac{L_a}{c_5} c_6}\right)$, whereas $\alpha$ describes the observation angle. The values of the constants are:

$c_{min} = 0.00275$, $c_1 = 0.185$, $c_2 = 0.484$, $c_3 = 7.5$, $c_4 = 133$, $c_5 = 0.00075$, $c_6 = 0.383$. The practical threshold contrast differs from the theoretical one in two aspects: the practice factor $F$ and threshold increase factor $TSF$ that describes the threshold contrast difference between a homogneous and inhomogenous environment.
More difficult, practical conditions at higher perceptual levels can be taken into account by a multiplication factor or practice factor $F$. The size of this factor depends on the particular visual task and is estimated for individual cases. Typical practice multiplication factors in daylight conditions are in the range from 10 to 20 [101]. For visual tasks at night, the practical factor $F$ assumes values from 50 to 100. Therefore $K_{thresh}$ can be calculated as follows:

$$K_{thresh} = TSF \cdot F \cdot K_{\text{theory}} \tag{4.49}$$

with $TSF = \frac{1}{4} \cdot \frac{\left(1+\frac{L_u}{L_a}\right)^2}{\frac{L_u}{L_a}}$ and $F$ dependent on the respective perception criterion.

8. **Calculation of detection distance.** For calculating the existing contrast, Kokoschka and Gall assumed the mean edge contrast. Therefore the contrast can be described as follows:

$$K_e = \frac{\sum_i \gamma_i \cdot \left|\frac{L_o - L_u}{L_u + L_{\text{stray}}}\right|}{\sum_i \gamma_i} \tag{4.50}$$

with solid angle element $\gamma_i$ of edge i. A boundary value for VL is then defined for the detection distance calculation. The observation angle $\alpha$ is expressed as follows:

$$\alpha = \frac{\alpha_0}{\sqrt{\frac{K_E}{K_{min}} \cdot \frac{1}{f_1} \cdot \frac{1}{VL \cdot TSF \cdot F} - 1}} \tag{4.51}$$

Hence the detection distance results in:

$$d = \frac{s}{\tan \alpha} \tag{4.52}$$

An example of Kokoschka's model is illustrated in Figure 4.20. The solid line shows the calculated threshold contrast for every possible distance. On this basis the mean edge contrast of a detection object is calculated (dashed line). The ratio of edge and threshold contrast is the visibility level. As already mentioned the detection distance is defined with a boundary value (here: VL = 1.0 in a distance of approximately 83.0 m).

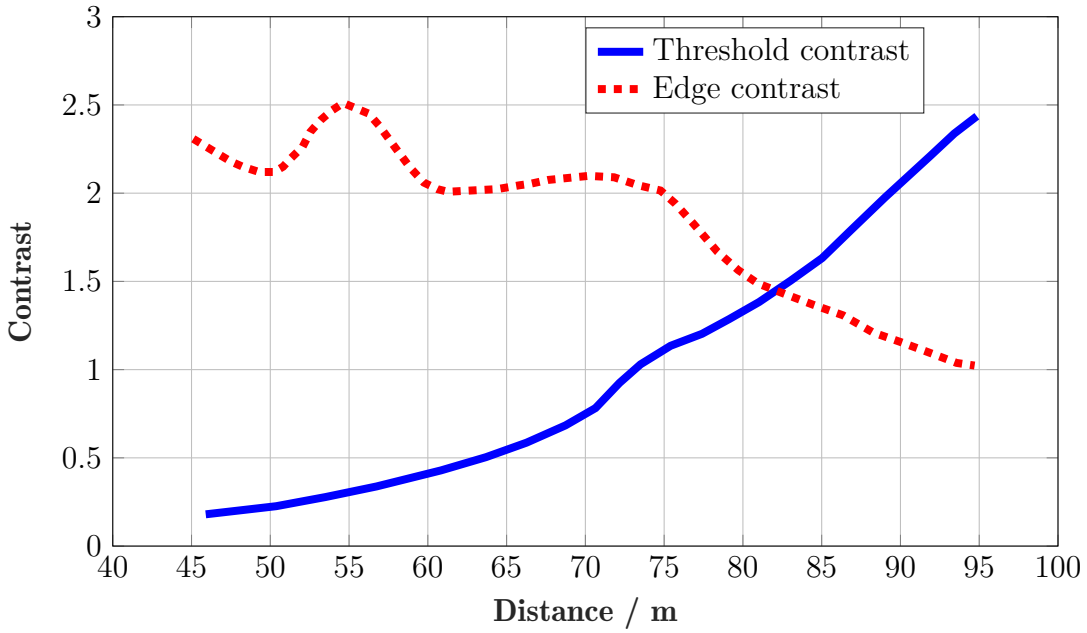


Figure 4.20: Comparison of the threshold and edge contrast according to distance; solid line shows the calculated threshold contrast for every possible distance. On this basis the mean edge contrast of a visual target is calculated (dashed line) [24].

The main difference between the two models (Eckert and Kokoschka) is that Kokoschka calculated the threshold contrast instead of the threshold luminance. There is also a difference in the manner of contrast determination with regard to factors encountered in practice. Kokoschka and Galls' model was validated for a headlamp distribution. The main focus of their investigations was to determine the detection distance in road traffic under fog conditions. Validation was therefore limited by the fog conditions situation and did not address the influence of different light distributions.

**Contrast determination according to D. Kliebisch and S. Völker.** Kliebisch and Völker compared in total eight measurement methods to determine the contrast of a grey card (size 30.0 cm × 30.0 cm, $\rho = 0.046$) related to its background (straight street, no additional outdoor lighting) [34]. In a first step, they specified the object's and environment's area. In a second step they divided the background in convenient parts corresponding to the edges of the grey card. They defined detection distances related to the threshold contrast for every contrast configuration. As a result they suggested the following influence parameters to define the grey card contrast:

- Shade of the grey card
- Maximum of all edge contrasts
- Object contrast related to top edge, left edge and right edge

They concluded that detection distance determination is basically possible using the threshold contrast. Kliebisch and Völker also considered other parameters that

influenced the contrast. They defined the factor "uniformity" to describe the luminance behaviour on object's surface. Uniformity was defined as relation between minimum $L_{min}$ and average luminance $L_{av}$ on the object's surface [38]:

$$u = \frac{L_{min}}{L_{av}} \tag{4.53}$$

This assumption can be critical for some measurements. The minimum luminance on object's surface corresponds to a minimum luminance value that is measured by the luminance camera. This means, the minimum value is conform to just one single pixel value, which makes measurements potentially susceptible to distort under certain conditions.
Another approach to define uniformity is to divide the detection object's surface into a square with a size of $3 \times 3$ pixels and calculate the average luminance of each square [34]. The overall minimum luminance of the average square luminances indicates the minimum object luminance:

$$L_{min} = \min(L_{av,sq_1},...,L_{av,sq_x}) \quad \rightarrow x = 1,..,n \tag{4.54}$$

Another procedure to describe luminance is the background luminance computation. Therefore, Kliebisch and Völker superimposed a circular cursor with a size of 1.0° and 2.0° surrounding the detection object: for one thing, at a distance where the object had not been recognized yet and for another thing at the detection distance. The average luminance of the cursor's surface was then assumed as background luminance.
A third opportunity was to calculate the average luminance of the whole luminance picture. They conducted a linear regression to show the dependence of uniformity, background luminance and threshold contrast on detection distance. As it can be seen from Table 4.9 the threshold contrast ($\beta = 0.888$) has the most influence on detection distance.

| Factor | Regression coefficient $\beta$ | p-value |
|---|---|---|
| Uniformity | -0.202 | 0.007 |
| Contrast | 0.888 | 0.274 |
| Background luminance | 0.121 | 0.003 |

Table 4.9: Results of the multiple regression. Dependence of the uniformity, the background luminance and the threshold contrast on the detection distance [38].

In a second experiment in 2005 Kliebisch and Völker figured out to what extent the perspective and position of the cut-off line effects the detection distance [25]. They determined the detection distance for one light distribution only. For their investigations they used the same test setup as in [74]. Based on the findings of the investigation they concluded that the position of the cut-off line had a strong influence on detection distance. In addition, the position of the observer (perspective) had no effect on the detection distance. As result can be noted that small differences in luminance distribution lead to differences in detection distances.

**Detection distance requirements according to J. Locher and S. Völker.** Locher and Völker [39] investigated in detection distance with regard to vehicle headlamps. In their study they evaluated luminance contrasts using image-resolving luminance measuring devices. They considered detection distances of real visual objects, like a pedestrian, deer or rabbit (realized with dummies). The research goal was to find out which parameters affect detection distance regarding to headlamps. Therefore, Locher and Völker analysed the luminous flux, illuminance, luminance, homogeneity of illumination, areas with high luminance amounts ahead of the vehicle and headlamp construction.
The experiments were carried out in a light tunnel at the company Hella KG in Lippstadt, Germany. During the test implementation the participants sat behind a constructed headlamp system, while detection objects, that were mounted on skateboards, randomly approaching towards the participants at a constant speed. The participant's task was to indicate "sure identification" of the object by pressing a button. For the experiment nine heterogeneous headlamp systems were considered (six halogen headlamps, three xenon headlamp systems).

Table 4.10 shows the results of the variance analysis for comparison of the influence factors on detection distance. Here, the term "luminance" describes the integral of the luminance along the visual axis, where the lower limit of the luminance is significantly lower than the near field area [39]. The upper luminance limit was bounded by the length of the light tunnel. The F-value represents the ratio of the mean squared errors. The proportion of variance defines the respective ratio of the overall variance $\sigma$. In this case the luminance captures 41.0% of the overall variance, which results in the highest influence of all six influence (combination) parameters.

| Factor | Proportion of variance | F-value |
|---|---|---|
| Luminance | 41.0% | 706.6 |
| Headlamp system | 3.4% | 107.6 |
| Detection object | 1.5% | 8.7 |
| Homogeneity and luminance | 1.8% | 59.9 |
| Detection object and luminance | 2.8% | 17.9 |
| Headlamp system and luminance | 8.0% | 137.8 |

Table 4.10: Comparison of influence factors on detection distance (using a two-factor variance analysis) according to [39]. The F-value represents the ratio of the mean squared errors. The coefficient of variation defines ratio of the variance $\sigma$.

The results of the study show that the headlamps' luminous flux correlate with the detection distance substantially [39]. In total, the xenon headlamp systems did not have advantage over the halogen systems, but they were able to produce a comparable higher luminous flux which resulted in higher luminance values in several areas in front of the vehicle. Furthermore, they found out that the luminance is the decisive element according to object detection distances.
Table 4.10 also illustrates that the illuminance homogeneity (integral) as well as the luminance integral of the area ahead of the vehicle had very little influence on the

detection distance. From the received luminance distributions Locher and Völker derived a luminance parameter with high predictive capabilities for detection [39]. The determined luminance values that are essential for detection within a range, have not been considered for the evaluation and construction for headlamp systems yet.

By using luminance cameras it was possible to document a whole scene and to collect more than two million luminance data points. The luminance values were determined alongside the optical axis, where the detection objects approached. In addition, the participants were asked at which character they were able to recognize the human, the deer or the rabbit. According to the participants the rabbit was detected based on his upper body (head and ears). Hence, the average luminance of the rabbit's upper body was chosen as object luminance and the area around the rabbit's torso as background luminance.
Overall the detection of the rabbit resulted in lower detection distances compared to a grey card. This can be traced to the more complex shape of the rabbit that need to be perceived. The grey card can be clearly recognized on the four edges. Therefore, according to Locher and Völker the detection of objects with sharp outlines seems to be easier [39].
The luminance areas of the deer shape that were analysed are decisive for the detection. In this case those areas were the legs of the deer. Hence, a definition of the object contrast was complex, as the in total four object contrasts (corresponding to the four legs of the deer) exhibit a large number of variations for calculating a contrast.

For these reasons, Locher and Völker decided to analyse only one version of the contrast determination. They considered the average luminance of all four legs as object contrast. The background luminance was defined as the region surrounding the deer's legs that follow the fall off of the legs. As well as the evaluation of the rabbit the detection distance was lower compared to the distance of a grey card caused by the complex shape structure. For one thing, another point could be an incorrect definition of the object or background luminance, for another thing possible factors influencing the detection could not have been considered.
For both object shapes, for the rabbit as well as the deer, the threshold contrast had a major influence. Hence, an evaluation of the luminance pictures was considered reasonable.
As a third object shape a human being (dummy) was chosen. The dummy's clothes were changed to represent a light and darkly dressed pedestrian. The relevant luminance areas of the dark-clothed pedestrian were the hands. Thus, Locher and Völker considered the average luminance of both hands. The higher hand contrast was set as object contrast. Again, the area surrounding the hands was chosen as background luminance. Compared to the dark-clothed pedestrian the appreciable feature of the bright dressed pedestrian were the legs. A comparison of the detection distances showed that the pedestrian dressed in bright clothes had significantly higher detection distance compared to a grey card.
From their results it can be concluded, that the luminances beyond the cut-off-line,

that are responsable for detection distances even in the near field area, play an essential role. Overall, the "real" detection objects could be detected in distances from about 55.0 m range under poor and about 100.0 m for good visbility conditions.

**Luminance picture evaluation according to D. Kliebisch.** Kliebisch [74] conducted another investigation regarding the detection distance in terms of vehicle headlamps. To ensure a better comparison to earlier studies, he also used a grey card as detection object [39] [24]. The experiments were also carried out in the light tunnel at the company Hella KG in Lippstadt that has already been used in [39]. The test track was on middle of the right roadway (within the tunnel). On a train that was running on rails, a grey card (size 30.0 cm $\times$ 30.0 cm, $\rho = 0.049$) could be moved toward or away from the participants (compare Figure 4.21). Different headlamp systems that were mounted on a barrel construction and arbitrarily exchangeable were used.

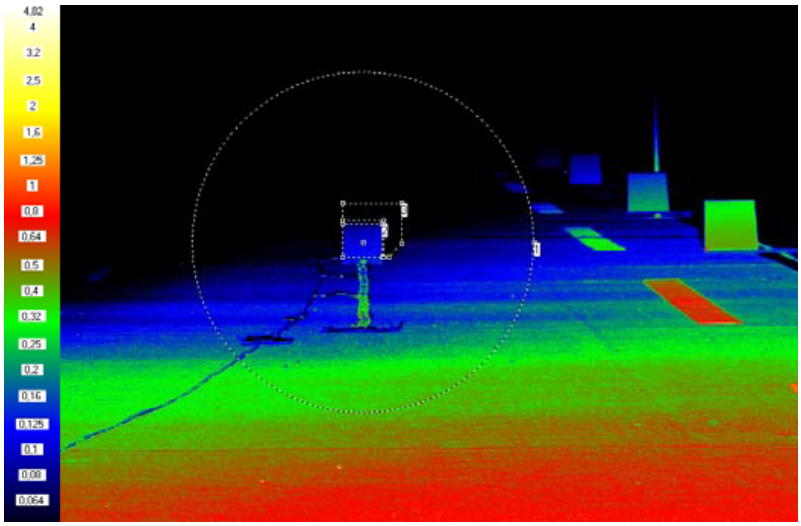


Figure 4.21: Different positions of grey cards (size 30.0 cm $\times$ 30.0 cm, $\rho = 0.049$) on the test track (luminance picture), located in the middle of the right roadway; distance between the grey cards: 5.0 m [25].

The aim of this study was to develop a model to describe the detection distance determination for different headlamp types (six halogen headlamps, three xenon headlamp systems). In total, luminance pictures of nine different headlamp systems, to determine the grey card contrast related to its background, were evaluated. First, suitable regions were set in the luminance image in order to determine object and background luminance. The object luminance was defined as mean object luminance, whereas the background luminance was determined as mean luminance of the immediate background. As background, a region surrounding the grey card, which included the upper dark part, was chosen. As presented in Figure 4.21 as third region, a 2.0° cursor surrounding the object, was selected. The mean luminance corresponded to the background luminance.
In a second step, the existing luminance difference $\Delta L$ as well as the contrast $K$ were calculated for each distance. From the apparent object size and background

luminance, the threshold luminance difference $\Delta L_{\text{thresh}}$ could be calculated with the model of Adrian or Kokoschka, depending on the distance to the object. For each distance the threshold contrast was determined and compared to the corresponding real threshold contrast. For a detection of an object the existing contrast needed to be larger than the threshold contrast. With Kliebisch´s model it was possible to predict the detection distance of a grey card that was presented foveally with a mean deviation of 3.0 m. As the limiting criterion for object detection Kliebisch indicated an average contrast limit of $K_l = 2.83$ [74].

**Uniform detection characteristic according to W. Kosmatka** Kosmatka developed a model in which only the object luminance is decisive for the object detection [102]. Accordingly, the required object luminance was calculated for a particular direction. This luminance was then transferred into illuminance and thus into the luminous intensity of the headlights. Whether this model delivers reliable predictions has not been validated.

**Visibility and recognition distances according to J. Kobbert.** Kobbert performed a field study to compare different headlamp systems (LED, combination of laser booster and LED) in relation to object detection and recognition rates [26]. The subject's task was to drive through a test track (straight road, 1.2 km length, runway of the airport Griesheim, Germany) with a speed of $60.0\frac{km}{h}$ while detecting dummies (180.0 cm × 30.0 cm, $\rho = 0.05$, compare Figure 4.22, left hand side) simulating pedestrians at, in total, five positions along the road the road.

Figure 4.22: Detection objects were placed at different position along the test track. Left side: human dummy (180.0 cm×35.0 cm, $\rho = 0.05$), right side: square combination (Square: 40.0 cm× 40.0 cm, small square: 25.0 cm× 25.0 cm, $\rho = 0.05$) [26].

In a second experiment, a combination of a large and small square was used as detection object (square: 40.0 cm × 40.0 cm, small square: 25.0 cm × 25.0 cm, $\rho = 0.05$; compare Figure 4.22, right hand side). In this case the participants had to tell which direction the smaller square indicated (left, right, bottom, up).
In a third part the participant had to remain at a fixed position in the test vehicle

while the detection object (darked clothed pedestrian, square combination) moved towards the test vehicle. The task was also to detect or identify the detection objects. The detection distances were recorded with a differential GPS and illuminances on the objects' surface were determined. Two age groups, a young group (24 subjects from 25 to 30 years of age) and old group (6 subjects from 55 to 65 years of age) performed the experiments.

Table 4.11 shows the 50% and 95% detection probabilities as well as the 50% and 95% recognition probabilities that were determined for the dynamic test setup.

| Headlamp function | 50% detection probability | 95% detection probability |
|---|---|---|
| LED, passing beam | 48.2 m | 26.4 m |
| LED, driving beam | 110.2 m | 70.0 m |
| LED and laser booster | 168.8 m | 132.3 m |
| | 50% recognition probability | 95% recognition probability |
| LED, passing beam | 14.2 m | 0.0 m |
| LED, driving beam | 69.2 m | 25.3 m |
| LED and laser booster | 101.3 m | 54.8 m |

Table 4.11: Mean detection distances for 50% and 95% detection probabilities (dummy) and 50% and 95% recognition probabilities (square combination) related to the different light distributions (driving speed 60$\frac{km}{h}$) from [26].

As shown in Table 4.11 the highest detection distances of the dummy were determined using the laser booster function (132.3 m), whereas a 95% detection distance could be achieved for passing beam in a distance of 26.4 m, for driving beam in a distance of 70.0 m. The recognition distances were 25.3 m (driving beam) and 54.8 m (laser booster), whereas the participants were not able to recognize the square combination (95% probability) under low beam conditions.

Since it is not possible to perform luminance measurements under dynamic conditions, only static luminance measurements for the evaluation were conducted. Luminance pictures were taken every 10.0 m starting from 30.0 m distance to the detection object (low beam) up to 230.0 m (laser booster combination). For the contrast determination, the object's surface luminance as well as four areas surrounding object's outline were chosen. As it can be seen in Figure 4.23 the luminance pictures were divided into different regions of interest.
Figure 4.23 (left hand side) shows a special case of the dummy contrast determination. If the passing beam was used, only half of the dummy's surface was illuminated. Therefore, Kobbert decided to choose only the illuminated part of detection object as object luminance. The Weber contrast was then calculated as relation between object's surface and minimum of the four luminance values surrounding the object (top, bottom, left, right).

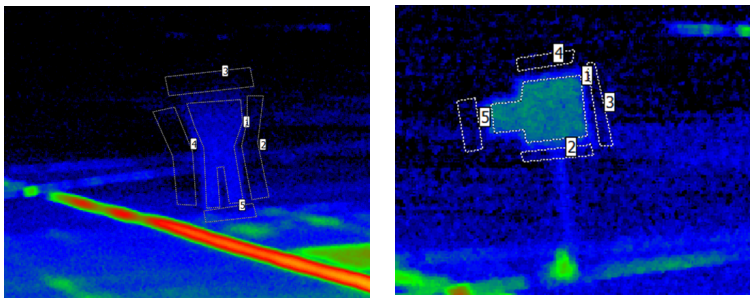

Figure 4.23: Luminance pictures of detection objects that were placed at different position along the test track. Left hand side: human dummy (180.0 cm×35.0 cm, $\rho = 0.05$), right hand side: square combination (Square: 40.0 cm× 40.0 cm, small square: 25.0 cm× 25.0 cm, $\rho = 0.05$) from [26].

Table 4.12 presents the mean detection or recognition distances as well as the detailed object luminance values and lowest background of the dynamic test setup. From Table 4.12 it can be seen that the detection luminance seems to be constant for all headlamp types.

| Headlamp function | Detection distance/ m | $L_O / \frac{cd}{m^2}$ | $L_U / \frac{cd}{m^2}$ | $K$ |
|---|---|---|---|---|
| Dummy | | | | |
| LED, passing beam | 48.2 | 0.103 | 0.034 | 2.03 |
| LED, driving beam | 110.2 | 0.067 | 0.021 | 2.19 |
| LED, laser booster | 168.8 | 0.101 | 0.058 | 0.75 |
| Headlamp function | Recognition probability / m | $L_O / \frac{cd}{m^2}$ | $L_U / \frac{cd}{m^2}$ | $K$ |
| Square combination | | | | |
| LED, passing beam | 14.2 | - | 0.020 | - |
| LED, driving beam | 69.2 | 0.175 | 0.020 | 7.75 |
| LED, laser booster | 101.3 | 0.249 | 0.052 | 3.79 |

Table 4.12: Mean 50% detection and recognition distances of the objects (dummy, square combination) as well as object luminance, lowest background luminance (surrounding the object) and contrast from [26].

In the recognition test, no valid luminance values for passing beam test runs could be determined. The laser booster headlamp system led to essentially higher luminances on the objects surfaces as well as in the environment. It can be noted that the background luminances were significantly different for the light distributions. This study did not take any angular size of detection or identification objects into consideration.

## 4.5 Image Processing

The classical approach to determine the visibility of an object with respect to its environment is to calculate the contrast and assess it in relation to the threshold contrast. This process works well for simple target shapes and uniform backgrounds. For this application only two measurement points would be necessary to derive the

contrast function. As this method is impractical for real applications, an alternative to analyse the object and background luminance is image processing. Implementing this approach for analysing luminance images is complex, mostly because of requirements to arbitrarily defined backgrounds and luminance calculations of non uniform regions.

**Contrast sensitivity functions in digital images according to K. Joulan.** Joulan introduced an image processing method to derive visibility related to headlamp systems [27]. In his investigation he proposed an improvement for the edge visibility computation of Hautière and Dumont [103]. He particularly considered two limitations of their model. Hautière developed a specific threshold $\Delta L$ to indicate the contours as "visible" or "not visible". Hautière and Dumont also defined that the edge visibility is independent of object's size, but according to Joulan a dependency exists. In contrast to Adrian's visibility level definition Joulan did not construct a hypothesis about the object size or background homogeneity. Joulan's visibility level computation is based on a reference model to the human visual system, the contrast sensitivity function. Each receptive field on the retina of the human eye is divided into two regions: The foveal and peripherial area. If a receptive field is stimulated, the neronal response can be expressed by Differential of Gaussian (DoG) filters [104].

As illustrated in Figure 4.24, Joulan introduced an approach for edge detection using a set of spatial filters. Those filters correspond to the visual system. For any contrast sensitivity function of a human a collection of DoG filters can be determined. By using the DoG filters the edges of an object in a luminance picture can be detected in a way which is equivalent to a convolution with the contrast sensitivity function [27].

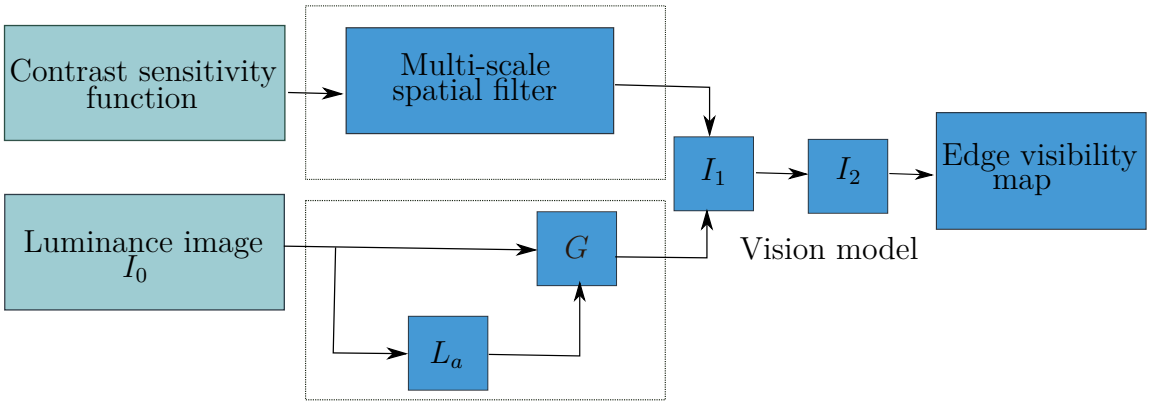


Figure 4.24: Proposed edge computation model of Joulan in luminance images according to [27]. $I_0$: Input luminance image; $L_a$: Adaptation luminance; $G$: Gain factor, is set to the inverse of the adaptation luminance $G = \frac{1}{L_a}$; $I_1$: Image after the convolution (filtering), $I_2$: Image after appliying the vision model.

The model is based on two algorithms. The first algorithm defines the set of the spatial filter (DoG) for the simulation of vision with the corresponding contrast sensitivity function (from literature). Secondly the algorithm is applied to the luminance picture for determining the edges. Hence, the luminance picture is considered

as input for his model, subsequent the object's edges are calculated in the image with a multi-scale spatial filter. The model's output is a visibility map of the edges of possible objects in the scene [27]. An example for a road scene at night-time for three different age groups is shown in Figure 4.25.
Overall it can be stated that Joulan was able to compute the edge visibility with a model that is closer to the human vision. By using the contrast sensitivity functions the output of the model provided absolute visibility values, while Hautière and Bremont were only able to compute relative values (by selecting an arbitrary threshold $\Delta L$). There was a distinct improvement in the algorithm regarding the edge computation and for this purpose also in object detection.

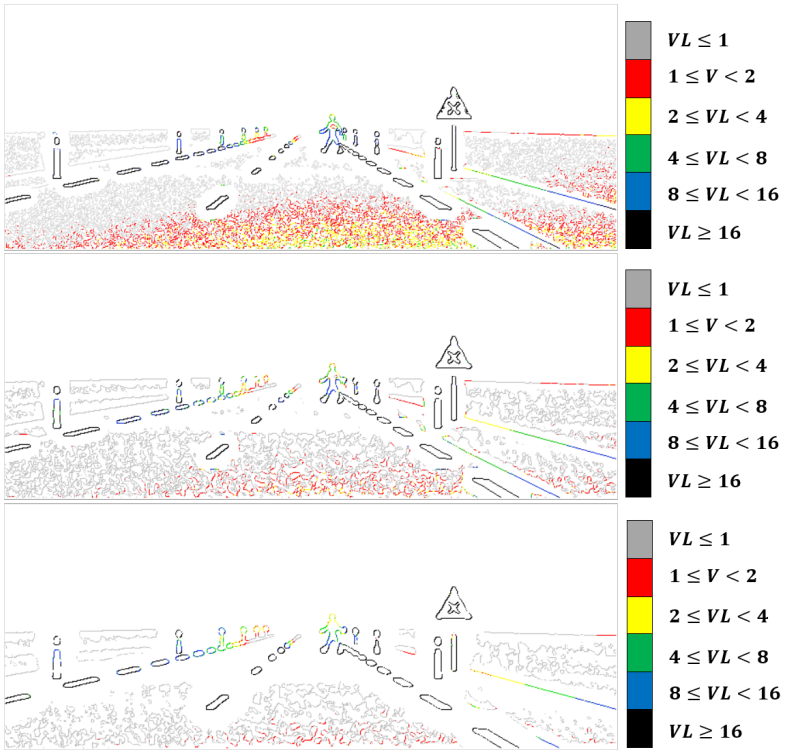


Figure 4.25: Visibility edges in the same road scene at night-time (luminance image) computed for different participant age groups from [27]. Top: 20 years of age; Middle: 60 years of age; Bottom: 80 years of age.

## 4.6 Summary

In Tables 4.13 (laboratory investigations), 4.14 (field investigations) and 4.15 (investigations based on luminance pictures) all methods that have been used for the contrast determination in previous literature research are summarized.
Overall it can be noted that several investigations to calculate the detection distance related to different light distributions have been performed already. However, the developed models show weaknesses, which make reliable detection prediction impossible. In general, the models are preferred over threshold tests.

Adrian's visibility model quantifies available information and evaluates the visual performance of the driver [13]. But it is only meaningful to a limited extent for the determination of the object visibility at night-time. It should be noted that the results for developing Adrian's model arised from psychophysical experiments with uniform targets, which differs from the actual driving situation. In addition, Adrian considered target sizes that were smaller than 1.0° only. Another limiting factor is the assumption of foveal vision at the detection target surface. As real objects do not appear foveally (as on the road) but rather alongside the road, peripheral detection is required at that point. Peripheral vision has a high importance for object detection [48]. Subsequently, the model is based on one specific scenario and considers only one visibility criterion (the luminance contrast).

The visibility level (VL) proposed by Adrian is a relevant visibility index in practice [13]. From experimental data of Blackwell, where visibility thresholds for a circular object with a homogenous background were considered, Adrian proposed visibility thresholds corresponding to a 50 % detection probability of a target. This VL was computed from two luminance measurements, for a reference standard target (uniform circle). He indicated a target as visible if the VL is above a visibility level threshold, which depends on the driving task. Based on the results for participants that were between 20 to 30 years of age, he suggested VL of 10 to 20 [13]. In [88] Adrian found out that a VL of 4 takes into account that the driver is not prepared for the sudden appearance of an object. For older subjects he assumed a higher VL of around 8.

Many of the authors considered a grey card for contrast analysis [18] [20]. In most cases the configuration of object and background luminance showed a high correlation between detection distance and contrast. Moreover, additional influence factors like uniformity or background luminance homogeneity have been analysed. Compared to the influence of the contrast those factors did not affect the detection distance significantly.

The detection distance was also determined based on location-resolved luminance distributions of the headlights [34] [74]. This method uses the models of Adrian and Kokoschka to precalculate the threshold contrast. In principle, it corresponds to the already mentioned model of Kokoschka and Gall, but is new in applications for arbitrary light distributions.
The models of Eckert [5] and Kokoschka [24] provided almost identical detection distances, since they are both based on the data of Blackwell [37]. Detection distances for real objects in road traffic at night were observed as well [39] [98]. Different results were concluded. A correlation between the detection distance and contrast was stable for all object shapes. Therefore, the parameter "contrast" can only be used in a limited way to describe detection distance. From recent literature for real detection objects it can be noted that the object shape seems to have a major influence with regard to the detection distance [102].

Image processing approaches to analyse luminance images were introduced, to

| Year | Author | Detection object | Object size | Position | $\rho$ | Method |
|---|---|---|---|---|---|---|
| 1943 | Berek | Circle | $\leq 1.0°$ | foveal | - | Object and background luminance |
| 1946 | Blackwell | Circle, square | $0.06° - 2.0°$ | foveal extrafoveal | - | Object and background luminance |
| 1987 | Fleck | Letters C and D, rectangle | $0.3°$, $0.45°$, $0.6°$, $0.8°$ | foveal, extrafoveal | - | Object and background luminance |
| 1989 | Adrian | Circle | $\leq 1.0°$ | foveal | <0.05 | Object and background luminance |
| 1991 | Lecocq | Hemispheric targets | - | foveal | 0.02, 0.05 | Luminance distribution on the target's surface |
| 2011 | Brémont | grey square | $1.0°$ | foveal, extrafoveal | <0.04 | Measurement points: square's surface and on each square's edge |
| 2013 | Brémont | grey square, dummy (Human, sign, vehicle) | $1.0°$ | foveal, extrafoveal | <0.04 | Pixels in detection region (excluding target pixels) selected as background pixels. Object luminance: average luminance of object's pixels |
| 2008 | Mayeur | grey square | $1.0°$ | foveal, extrafoveal | <0.04 | Measurement points: square's surface and each square's edge |
| 2009 | Mayeur | grey square | $1.0°$ | foveal, extrafoveal | <0.04 | Measurement points: square's surface and each square's edge |

Table 4.13: Methods of contrast determination in previous laboratory investigations.

| Year | Author | Detection object | Object size | Position | $\rho$ | Method |
|---|---|---|---|---|---|---|
| 1956 | de Boer | grey square | 28.0 cm × 28.0 cm | foveal | 0.08 | Object edges |
| 1995 | Damasky | Square, rod-shaped object | 20.0 cm × 20.0 cm, 140.0 cm × 30.0 cm | foveal, extrafoveal | 0.04 | Object and background luminance |
| 2006 | Akashi | Flip-dot disc, fixation target: deer | 20.0 cm × 20.0 cm, 120.0 cm × 40.0 cm | extrafoveal | 0.4 | - |
| 2006 | Bullough | Flip-dot disc | 10.0 cm × 10.0 cm, 20.0 cm × 20.0 cm | extrafoveal | 0.4 | - |
| 2008 | Ising | grey rectangle | 76.0 cm × 30.0 cm, 183.0 cm × 30.0 cm | extrafoveal | 0.06; 0.12; 0.25 | Average of subdivided target contrast |
| 2009 | Ising | grey rectangle | 76.0 cm × 30.0 cm, 183.0 cm × 30.0 cm | foveal | 0.06; 0.25 | Luminance below and above of targets, as well as at three/ five heights along both sides |
| 2010 | Brémont | grey square | 1.0° | foveal, extrafoveal | <0.04 | Highest contrast among four square edges, adapation luminance fixed to unique value |
| 2010 | Mayeur | grey square | 20.0 cm × 20.0 cm | extrafoveal | <0.04 | Object and background luminance |
| 2015 | Gibbons | grey square | 20.0 cm × 20.0 cm | foveal, extrafoveal | 0.04 | Object and background luminance |
| 2015 | Reagan | grey rectangle | 20.3 cm × 30.5 cm | extrafoveal | 0.1, 0.38 | - |
| 2017 | Reagan | grey rectangle | 20.3 cm × 30.5 cm | extrafoveal | 0.1, 0.38 | - |

Table 4.14: Methods of contrast determination in previous field investigations.

| Year | Author | Detection object | Object size | Position | $\rho$ | Method |
|---|---|---|---|---|---|---|
| 1993 | Eckert | Pedestrian | 180.0 cm × 40.0 cm | foveal, extrafoveal | - | Object edges |
| 2000 | Kokoschka, Gall | grey square | 30.0 cm × 30.0 cm | foveal, extrafoveal | - | Object edges |
| 2002 | Kliebisch, Völker | grey square | 30.0 cm × 30.0 cm | foveal | <0.05 | Object edges |
| 2003 | Locher, Völker | grey square, Dummy (Human, deer, rabbit) | 30.0 cm × 30.0 cm, 180.0 cm × 40.0cm | foveal | <0.05 | Object edges |
| 2004 | Kliebisch | grey square | 30.0 cm × 30.0 cm | foveal | <0.04 | Object edges, measuring points |
| 2006 | Kosmatka | - | - | extrafoveal | 0.04 | Object edges, measuring points |
| 2011 | Joulan | grey square | 1.0° | 30.0 cm × 30.0 cm | <0.04 | Object edges, measuring points |
| 2015 | Kobbert | Dummy (human), square combination | 65.0 cm × 65.0 cm, 180.0 cm × 30.0 cm | extrafoveal | 0.05 | Object and lowest of four background luminances |

Table 4.15: Methods of contrast determination based on luminance pictures.

avoid difficulties with the object's shape or homogeneity or background uniformity [27]. Edge detection algorithms were applied on luminance images (traffic road scene). Based on local luminance contrast the visibility of these edges, that was related to the corresponding objects visibility level, was estimated.

For a driving task in real traffic the whole process of first detecting and second identifying an object need to be considered. Therefore, possible hazards that lead to a reaction of the driver to the current situation, need to be analysed for a sufficient evaluation. The driving task consists of many interconnected processes and is therefore not simply to capture (compare Chapter 2.1). Thus investigations under real conditions are necessary to determine the VL or contrast functions for the detection of objects to obtain suitable data for headlamp applications (e.g. the road surface luminance is always heterogeneous [16] [15]).
Additionally, the effect of vehicle headlamps is completely excluded in the Adrian model. The luminous intensity distribution was only indirectly included by the object and background luminance. The adaptation of the driver that changes continuously during a night-time driving task, is also not included.
According to Völker [34] the models of Eckert [5] and Kokoschka [24] for detection distance calculations are suitable for any vehicle light distribution.

As Adrians investigations were carried out under laboratory conditions the main discussion that has to be conducted is the field factor for real applications. In his experiments Brémont showed that there is a need for including new factors in the road lighting evaluation [16]. The importance of factors like driving speed or other road users still need to be analysed. Results of [22] demonstrated also that the Adrian model did not take all relevant influence parameters related to object detection into account, since factors like headlamp illumination were neglected.
A number of methods have been proposed in the scientific and technical literature including those by the CIE and Illuminating Engineering Society of America (IESNA), but the practical consideration is mostly neglected. The weak points of the proposed models are in terms of the ecological validity [19] in relation to weak relevance to a real driving task.

Still, the contrast criterion is one key factor for the detection of an object and therefore a valuable indicator for road lighting applications [18]. When using visibility as a criterion for the design of new headlamp systems there needs to be an approach to capture the physiology of the visual system. In future investigations the connection to the reality should be more focused to include important parameters with regard to the driving task to improve road lighting specifications.

## 4.7 Hypotheses

As appears from the literature, a number of investigations have been performed considering dependencies of contrast. Using homogeneous background and object luminances, a contrast function for different object sizes can be predicted. It is obvious that a homogenous illumination for real road traffic applications does not

exist. This raises the question in what way the contrast investigations such as contrast determination with squares or Landolt rings under laboratory conditions are relevant and reasonable. It can be stated that 90% of the field studies published in the literature use a grey card as detection object, that is placed on the roadway or at roadside. Since a grey card is excellently suitable for experiments due to its specifications but not for real object detection, the relevance of those results are also disputable.
The aim of the grey card investigations is first to examine the relevance of the detection distances with respect to real detection objects, second to obtain data for a calculation model of the detection distance and third to find a correlation between the theoretically determined threshold contrasts and the real detection distances. In Chapter 4.3, literature concerning detection distances has been analysed.
Based on these results the following hypotheses can be formulated:

- Theoretically determined threshold contrasts apply only to simple and homogeneous (circles or Landolt rings) and standard objects (grey card). This approach is not simply transferable to more complex structures.
- Complex object structures at the same reflection coefficient lead to smaller detection distances.
- The detection distance of a grey card can be determined using the size, background luminance and luminous intensity distribution generated by the headlights. In order to describe a complex object shape, such a method can not be applied, since the boundary conditions are changed.
- Detection distances determined with grey cards can not be used to predict detection distances of real objects.They are merely used to indicate a guideline, since they describe one particular case.
- Inhomogeneous luminance distributions in front of the vehicle have no significant influence on the detection distance.
- The influence of the peripheral object position on the threshold contrast can be described by the empirical equation of Fleck [50]. Since Fleck obtained his findings under photopic conditions, it must be modified for mesopic range.
- For a static test setup, the entire average background luminance should be used as adaptation luminance. The variation of luminances in individual areas of the mean road luminance has no influence on the overall evaluation of the observer (since only the mean luminance is decisive).
- The contrast is a reliable measure for the prediction of detection distances.

# Chapter 5

# Investigations in the laboratory

Investigations on detection or identification of static and moving objects are already present, but most often only the photopic range was considered. In this chapter all results from the laboratory investigations, a mesopic threshold detection experiment by using achromatic (positive contrast) targets, are discussed. Primarily, the selected test parameters and applied methods are introduced. Furthermore, the experiment setup as well as its implementation are illustrated. Subsequently, the results of the laboratory investigations are presented in terms of influencing factors (target shape, target size, age and eccentricity). Finally, the own findings are compared with the visibility model of Adrian (compare Chapter 4.1).

## 5.1 Selection of test parameters

In the following, selected parameters, applied methods and the procedure for performing the experiments as well as the examinated participants are described in more detail.

**Background luminances.** In order to adjust night time scenarios, the target is displayed in a positive contrast, so it appears brighter than the background. Overall two luminances were defined for the tests, which are intended to simulate two situations in road traffic. The first situation simulates a night drive within an urban area (speed of $30.0\frac{km}{h}$). In this case the stopping distance would be 18.0 m. At this distance, the background luminance level corresponds to $1.0\frac{cd}{m^2}$ (area ahead of the vehicle using low beam). The second situation includes a drive along an one-lane country road with no additional light source. The driving speed amount to an average speed of $70.0\frac{km}{h}$. The stopping distance here would be 70.0 m, which corresponds to a background luminance of $0.1\frac{cd}{m^2}$ (area ahead of the vehicle using low beam, near below the H-V-point).

**Eccentricity.** The eccentricity $\theta$ describes the angle between the fixation point in the centre of the field of view (in the experiment the centre of the projection area) and the center of the object to be detected. The eccentricity $\theta$ can be expressed as follows:

$$\theta = \arctan\left(\frac{d_O}{d_{ov_s}}\right) \tag{5.1}$$

with

- $d_O$, distance from the road center axis to the central point of the detection object
- $d_{ov_s}$, overall stopping distance of the vehicle with $d_{ov_s} = \frac{1}{2} \cdot \left(\frac{v}{10} \cdot \frac{v}{10}\right) \frac{h^2}{km^2} \cdot m + \left(\frac{v}{10} \cdot 3\right) \frac{h}{km} \cdot m$ [105]

A total of 5 eccentricites were selected for the examination and are summarized in Table 5.1. These values correspond to positions of pedestrians' appearance in typical road traffic situations.

- 0°: corresponds to foveal vision and is selected as a reference.
- 2.65°: in a typical road traffic situation, a pedestrian is located in a distance of 70.0 m from the vehicle and about 1.25 m (two steps) from right lane. Assuming a road width of 3.0 m and a vehicle width of 1.90 m, starting from the center of the lane, the pedestrian corresponds to an eccentricity of 2.65°.
- 5.0°: in order to be able to compare the results to previous studies as well as for analysing the visual conditions at bends (speed of $70.0\frac{km}{h}$), an eccentricity of 5.0° was chosen.
- 10.0°: a situation in the urban area at a speed of $30.0\frac{km}{h}$ results in a value of 10.0°. This eccentricity has already been used in other investigations and is intended to serve as a comparison [106] [107].
- 20.0°: for comparison to previous studies as well as analysing the visual conditions at intersections (speed of $20.0\frac{km}{h}$), an eccentricity of 20.0° was chosen [106] [6].

| Traffic situation | Speed $v$ | Stopping distance $d_{ov_s}$ | eccentricity $\theta$ |
|---|---|---|---|
| Country road | $70.0\frac{km}{h}$ | 45.5 m | 2.65° |
| Country road | $70.0\frac{km}{h}$ | 45.5 m | 5.0° |
| City | $30.0\frac{km}{h}$ | 13.5 m | 10.0° |
| City | $20.0\frac{km}{h}$ | 8.0 m | 20.0° |

Table 5.1: Investigated eccentricitys $\theta$ for different traffic scenarios.

**Detection objects.** In subsequent investigations, the shape of the detection object was determined to be circular [13] [82]. From these studies it is clear that the geometric size of the environment has little influence on the sensitivity of the subjects [12] [82].
In order to establish a comparison to real objects, a deer was chosen as second object shape, since wild animals occur in everyday traffic situations. Taking the opportunity to compare with other investigations [6] [108], a filled circle of 1.0° and 2.0° diameter was chosen as detection target. The black surface area of the deer was equal to the surface area of the filled circle. The detection targets are illustrated in Figure 5.1. The circle serves as a reference to spectral monochromatic investigations of Schiller [6] and Englisch [106].

(a) (b)

Figure 5.1: Detection objects: (a) circle, (b) deer. The objects have the same surface content.

## 5.2 Experimental setup

The aim of this study is to determine the luminance difference $\Delta L$ at the 99.0% detection threshold and to measure the corresponding contrast. In a large dark environment, achromatic objects (visual targets) with a positive contrast were displayed under a certain eccentricity $\theta$. The investigations were performed in a laboratory setup where the photometric properties were controlled.
The experimental setup is shown in Figure 5.2 and has been used in earlier studies [106] [6]. As illustrated in Figure 5.2 (left hand side), the wall elements are provided with a diffusely reflective black coating, which has a reflectance of less than 5.0%.

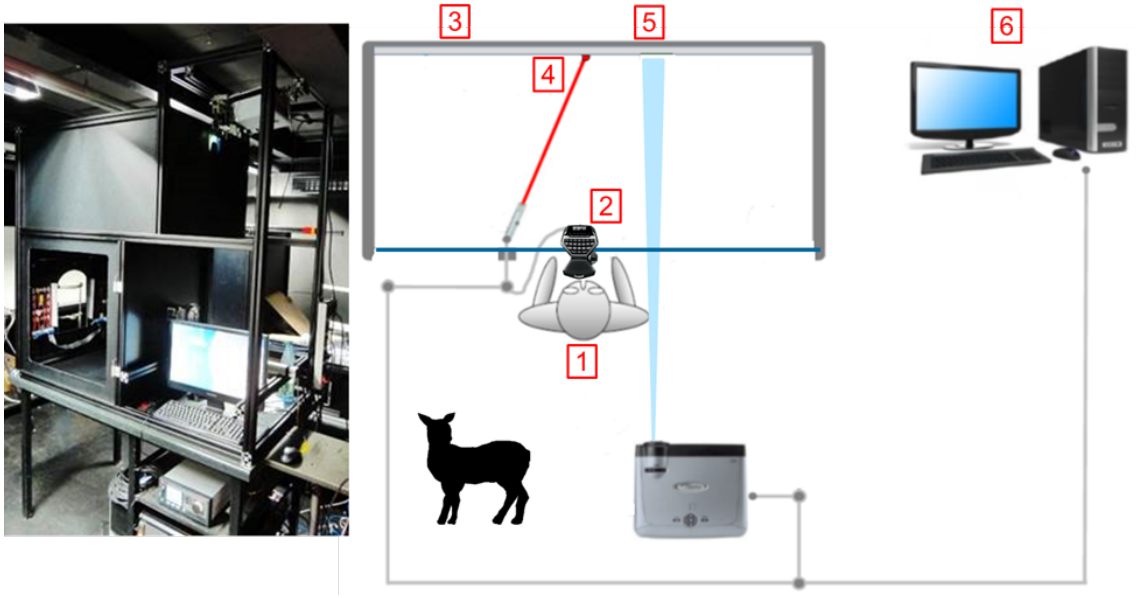


Figure 5.2: Experimental setup. Left hand side: Real photography of the laboratory setup. Right hand side: Outline of the test setup (not to scale) 1: observer, 2: input device, 3: projection surface (inner surface of detection box), 4: fixation point (produced by a red laser diode), 5: detection target (here: "deer" shape), 6: control unit.

A homogeneous background created by a DMD projector was used (Acer, H7532 BD, resolution 1920 × 1080 pixel (full HDTV) [109]. Due to the design, vertically, a smaller number of pixels could be used, since the full height of the projection

surface could not not be exploited. Therefore, approximately 1189 × 1066 pixels of the projector were required to cover the projection surface (74.0 cm × 74.0 cm). A schematic representation of the projection surface is shown in Figure 5.3 [6].

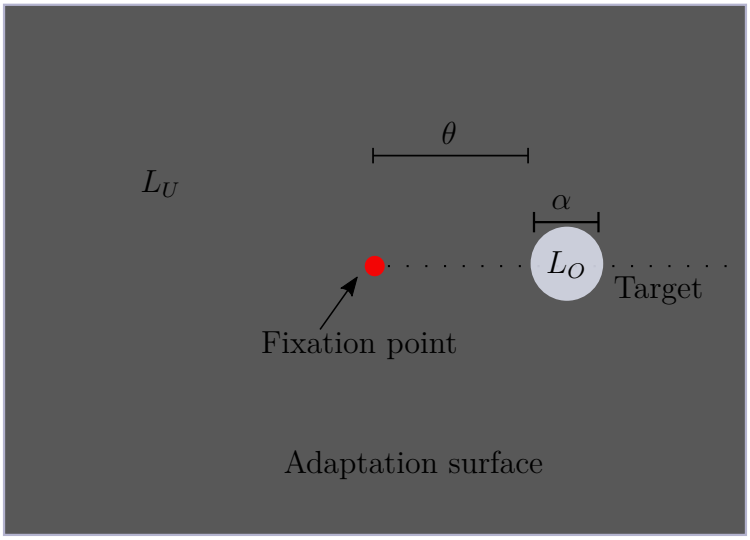


**Figure 5.3: Schematic representation of the projection surface. The fixation point (red laser spot) is located in the centre of the projection surface. $L_U$ : adaptation field luminance, $L_O$ : object luminance, $\alpha$ : target diameter, $\theta$ : eccentricity.**

The digital video projector, used for the detection object presentation, is a central component of the entire structure and decisive for certain characteristics. Hence, the requirements were defined as follows:

1. The resolution had to be high enough to guarantee a detectability of individual pixels of the detection object for the participants.

2. The projection geometry needed to ensure a complete illumination of the projection surface at full image under the given (relatively short) projection distance of approximately 180.0 cm.

3. A low black level of the projector was required to minimize stray light in the experiment.

The projector has a minimum projection distance of 150.0 cm as well as a brightness of 2000 ANSI lumen. The digital light processing (DLP) chip delivers low black levels compared to other projector technologies, whereas the concept is based on a Digital Micromirror Device (DMD). In this principle small tilting mirrors, which are arranged in an array, direct incident light either in objective lens direction or into a light trap. The used P-VIP discharge lamp has a total output of 230.0 W with a maximum lifetime of 4000 hours [109]. Since P-VIP discharge lamps have a significant reduction in the luminous flux over the lifetime, the projector needed to be calibrated at regular intervals. The individual calibration steps are described in detail in [6]. The absolute spectral radiance $L_e(\lambda)$ of the projector is presented in Figure 5.4. The projector was set to maximum brightness.

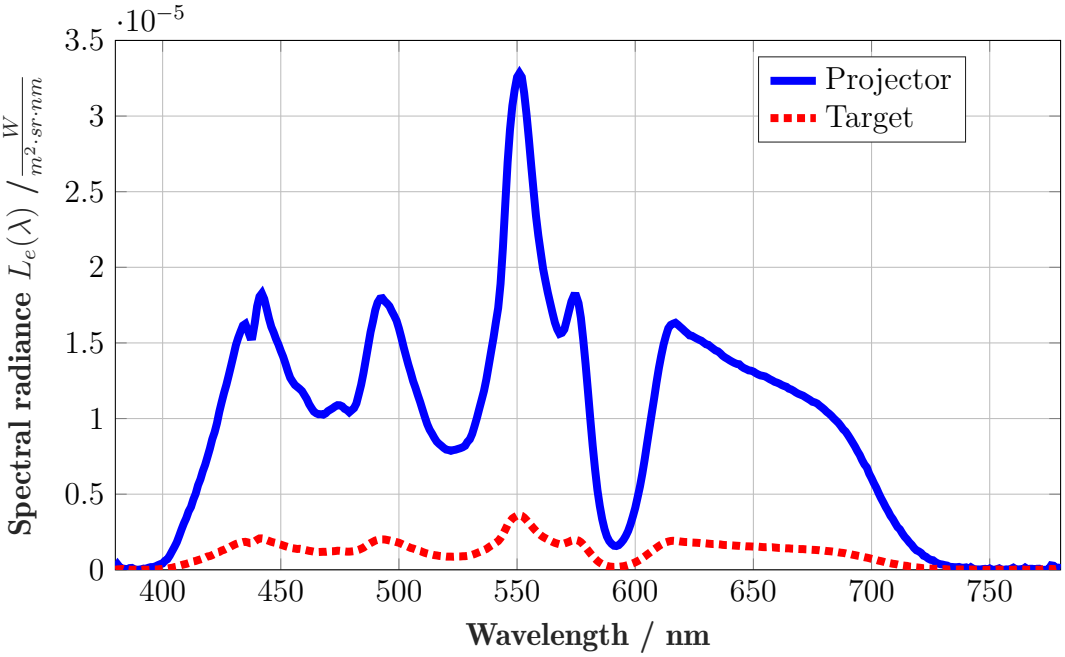


Figure 5.4: Absolute spectral radiance $L_e(\lambda)$ of the projector and the detection target used in the experiments.

The subject's head was fixated in a headrest while holding the input device (gaming controller). The distance between the subject's eyes and the projection surface was 72.0 cm. Based on the headrest the subject had the task to locate a fixation point which was implemented by a red laser spot in the centre of the projection surface. This fixation point is located at an eccentricity of 0.0°, corresponds to the fovea and had to be fixed by the participants during the entire examination. The maximum angle of incidence of a visual sign is horizontally 25.0° to the left and 25.0° to the right. The study was carried out under conditions of binocular vision. The target presentation time of 0.35 s was adopted to obtain the detection probability. According to a study by Narisada [110], a driver can focus on a specific point for a duration of 0.2 s during a day drive, while the fixation time increases to 0.35 s in a night-time driving situation. This can be attributed to the fact that the transmission of information is reduced as the visual system is restricted due to the decreasing background luminance.

## 5.3 Procedure

In total 20 normal-sighted subjects completed the experiment as it can be seen from Figure 5.5. The first age group "young subjects" were between 20 and 45 years old (four of the participants were female). The second age group "old subjects" included a group of people between 46 and 63 years of age (two females). All participants had normal or optically corrected vision and were all licensed drivers.

Before starting the experiment, the subject had to adapt to the current background luminance for 25 minutes. To control the adaptation behaviour of the par-

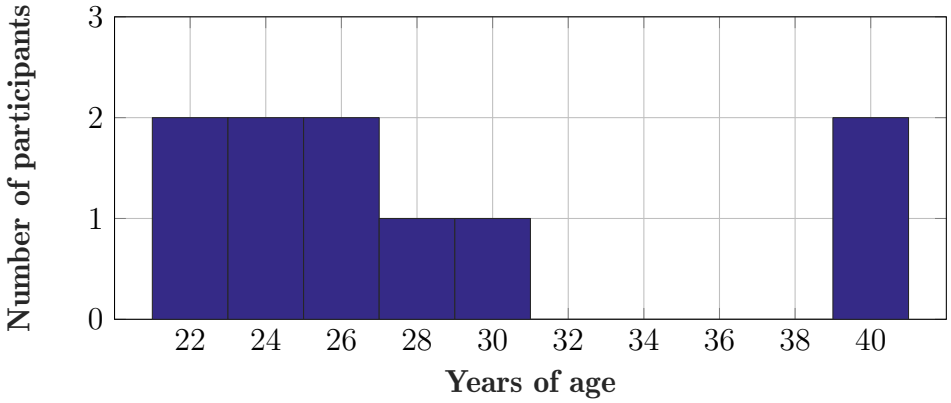


**(a)** Young participants

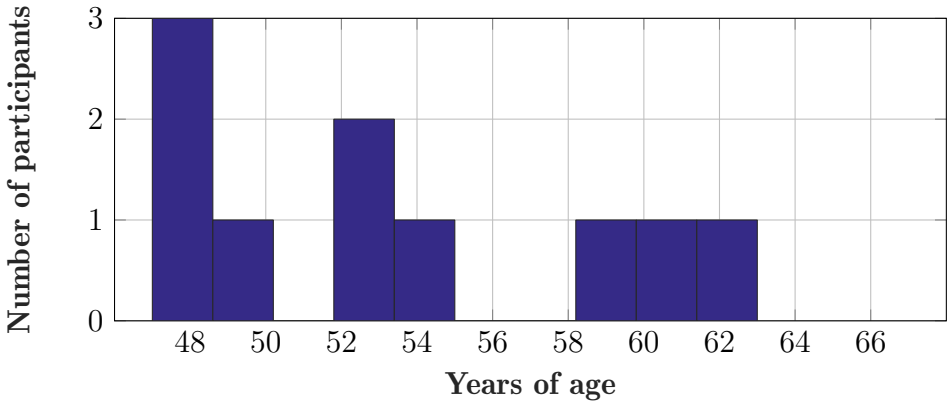


**(b)** Old participants

Figure 5.5: Age distribution of the subjects' groups, "young subjects" (4 females, 6 male) and "old subjects" (2 females, 8 male).

ticipants and also to determine the individual detection thresholds an automatic Staircase method was used (compare Chapter 2.4.3).
Subsequently, the participants had the opportunity to complete a training set in order to become familiar with the input device and the general procedure. The individual detection thresholds of the participants were determined in the foveal and also peripheral vision (at of 20.0°). The aim was to find a description of the link between the stimulus intensity and probability of perceiving the stimulus (described by the psychometric function).
The combination of the two background luminance's with ten individual contrast levels and five eccentricities formed a total of 500 different test conditions. Each test situation occurred randomly, five times during the trial. The two luminance levels were tested separately at two different dates. During a test run that took an hour, a total of 250 stimuli appeared (5 presentations $\times$ 5 eccentricities $\times$ 10 individual contrast levels).
The participants were instructed about the upcoming test sequence by means of a voice information, then the visual signals were displayed in a randomized order in an automated process.
The two target shapes (circle and deer) were presented in sequences independently

of one another, randomly off the visual axis at the right hand side of the fixation point at five eccentricities ($\theta$ = 0.0°, 2.65°, 5.0°, 10.0°, 20.0°). The subjects task was to indicate whether the target can be seen related to his background or not ("present", "not present"). A short sound signal indicated the onset of every single target and the answers were saved by pressing a button on the input device. During the experiment a computer, supervised by the test coordinator, recorded the task performance of the participants. The contrast levels were individually adapted to the particpants' contrast thresholds and were scanned in several computation runs. Every subject completed the experiment three times for both luminance levels. The detection probabilities for the respective eccentricity were then determined for each contrast.

## 5.4 Results

In the following the results of the laboratory experiments are presented. Various influencing parameters are discussed in detail.

### 5.4.1 Influence of target shape

In previous studies, potential targets for the background luminance were determined, which are relevant for night drive situations. For these investigations planar, square objects with an edge length from 20.0 to 50.0 cm were used. However, real objects in road traffic, such as pedestrians or wild animals, are convex and have a prominent contour. Furthermore, an object that occurs in road traffic has never a perfect diffuse homogeneous surface. In a driving situation, the driver must be able to distinguish between different objects on the road axis as well as on the diagonal side at all times. Consequently, both the object size and the distance to the occurring obstacle are considered. A third factor is the luminance distribution around the object to be detected. In road traffic, the background of an object is never homogeneous and changes continuously. Therefore, only relative indications can be made.
While the term "shape sensitivity" is used in light technology, the term "shape perception" is not usual. These definitions should be used to ensure a clear separation of the perception criteria detection and identification. If an object can be perceived not only with its luminance difference to the environment, but also with its shape, this essential visual function is called shape perception [34]. If the visual object is reduced in size so that it is just recognizable, one defines the threshold of the shape perception as shape sensitivity. While detection stands for the contrast sensitivity, shape sensitivity indicates the identification of an object.
In earlier studies, the background luminance ranges, which correspond to scenarios in night traffic, were determined [90] [20]. To describe the detection performance of the visual targets, the quantity luminance contrast was used.

Figure 5.6a shows the detection experiment results of the circle shape. In general, it can be determined that, with a higher background luminance, a low contrast is required for the detection of the object. Considering the behaviour from the foveal to

the peripheral eccentricity (for $L_U = 0.1\frac{cd}{m^2}$), it can be noted that there is a gradually increase in contrast, which remains constant for eccentricities greater than 2.65° at a contrast value of 0.133. However, this course changes for an increased background luminance ($1.0\frac{cd}{m^2}$). For the foveal detection of the circle at $1.0\frac{cd}{m^2}$, a contrast is required, which is lower by a factor of 1.48 compared to the lower luminance level (compare Table 5.2).

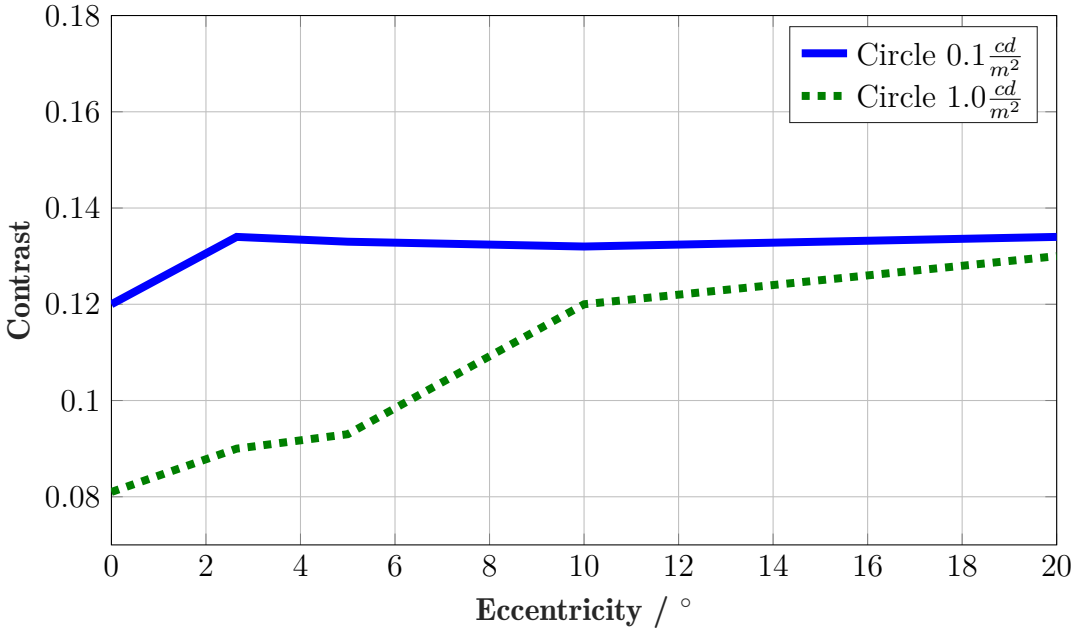


**(a)**

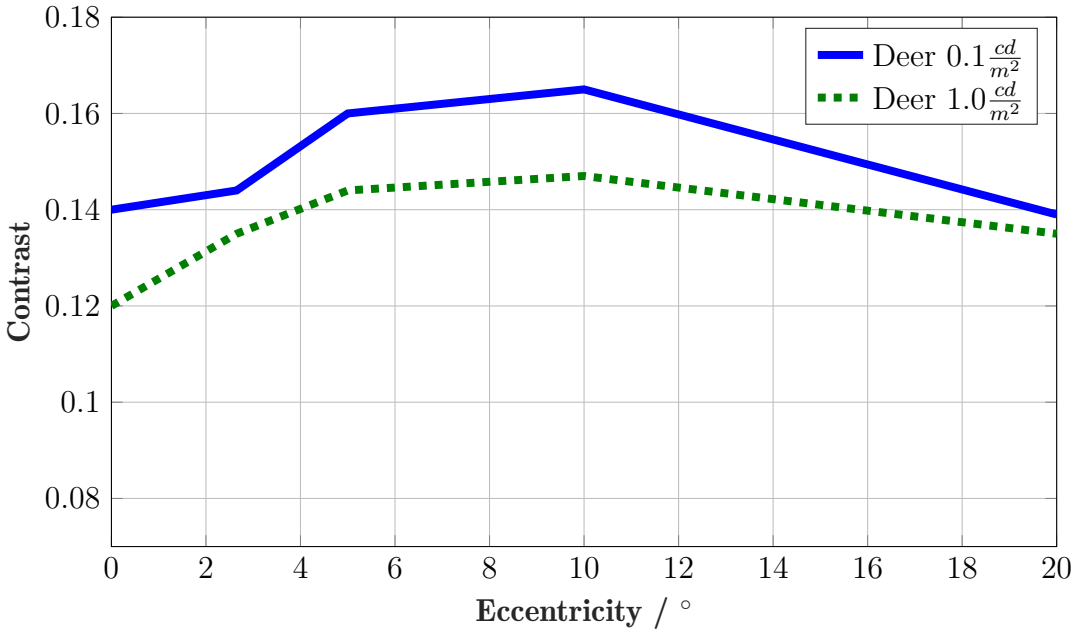


**(b)**

Figure 5.6: Contrast for a 99.0% detection probability at two background luminances; Relation between contrast K and eccentricity $\theta$; Object shapes (a): circle, (b): deer; target size: 1.0°.

| Target shape | $L_U$ | 0.0° | 2.65° | 5.0° | 10.0° | 20.0° |
|---|---|---|---|---|---|---|
| Circle | $0.1\frac{cd}{m^2}$ | 0.120 | 0.134 | 0.133 | 0.123 | 0.134 |
| Deer | | 0.140 | 0.144 | 0.160 | 0.165 | 0.139 |
| Circle | $1.0\frac{cd}{m^2}$ | 0.081 | 0.090 | 0.093 | 0.120 | 0.130 |
| Deer | | 0.112 | 0.112 | 0.127 | 0.119 | 0.130 |

Table 5.2: Contrast for a 99.0% detection probability at two background luminances; Relation between contrast K and eccentricity $\theta$; Object shapes circle and deer, target size: 1.0°.

With an increase in eccentricity, the required contrast increases continuously. For both luminance levels, a maximum contrast value is required for a detection in periphery (20.0°).

In Figure 5.6b the detection results of the deer shape are presented. As already concluded for the circle shape, a lower contrast for a detection is required under higher background luminance conditions. Nevertheless, the development over the individual eccentricities differs significantly from the circle object results. Starting from the foveal (0.0°) to the eccentricity (5.0°), there is a constant increase of the contrast values from 0.14 to a 0.16. There is a maximum at 10.0° (0.165), which then drops again to 0.139 for 20.0°. At the luminance level of $1.0\frac{cd}{m^2}$, the contrast increases gradually from 0.0° to 5.0° by a value of 0.015.
The various areas in which the entire visual field is divided have different characteristics and can receive information accordingly. In the central visual field, objects can be identified, while the peripheral visual field is used to perceive objects and their localization. If the human eye perceives a stimulus in periphery, it is brought to a clear identification with the fovea centralis. The results of this experiment can therefore be traced back to the receptor distribution on the retina. Several receptors are connected neurons and can be seen as a receptive unit. If a visual sign is then imaged within such a receptive group, the visual perception is determined solely by the incident luminous flux [48], that is, the subject is able to detect the object. This is true for the foveal as well as for the extrafoveal region [83].
In summary, it can be retained that with an increase in the background luminance the visual field also increases, which results in better detection performance. In the case of a fixed contrast, the only possibility to extend the visual field is to increase in sensitivity of the eye. This is only possible with an increase of the adaptation level.

### 5.4.2 Influence of age

In Figure 5.7a the detection results of the two age groups, young participants (dotted lines) and old participants (solid lines), for the circle shape as a function of the eccentricity are presented. Comparing the two background luminance levels for small eccentricity angles of up to 5.0°, a contrast difference of 0.02 can be established in the detection performance.
For the peripheral angles 10.0° and 20.0°, the detection performance behaviour is equal for both luminance levels (compare Table 5.3). The participants' results above

45 years of age differ strongly related to the luminance level. Considering the foveal region at the lower background luminance of $0.1\frac{cd}{m^2}$, a higher contrast by factor 1.7 is required for a detection compared to $1.0\frac{cd}{m^2}$. This difference can also be ascertained for the eccentricities 2.65° and 5.0°. Subsequently, the contrast values converge for $0.1\frac{cd}{m^2}$ against 0.187, while at $1.0\frac{cd}{m^2}$, they have a continuous rise to 0.156 with growing periphery.

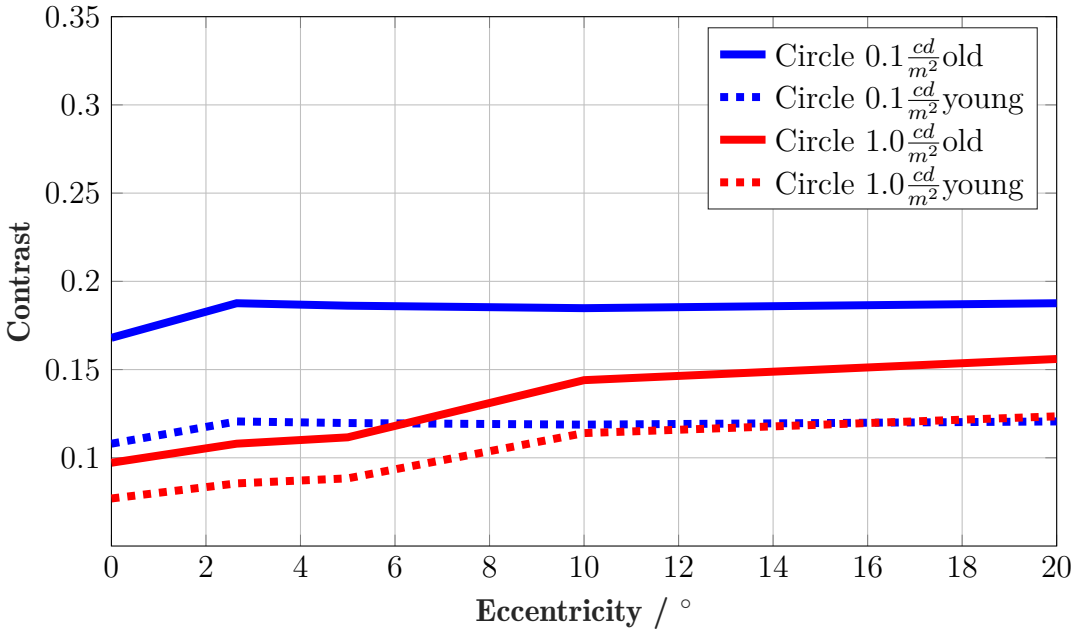


**(a)**

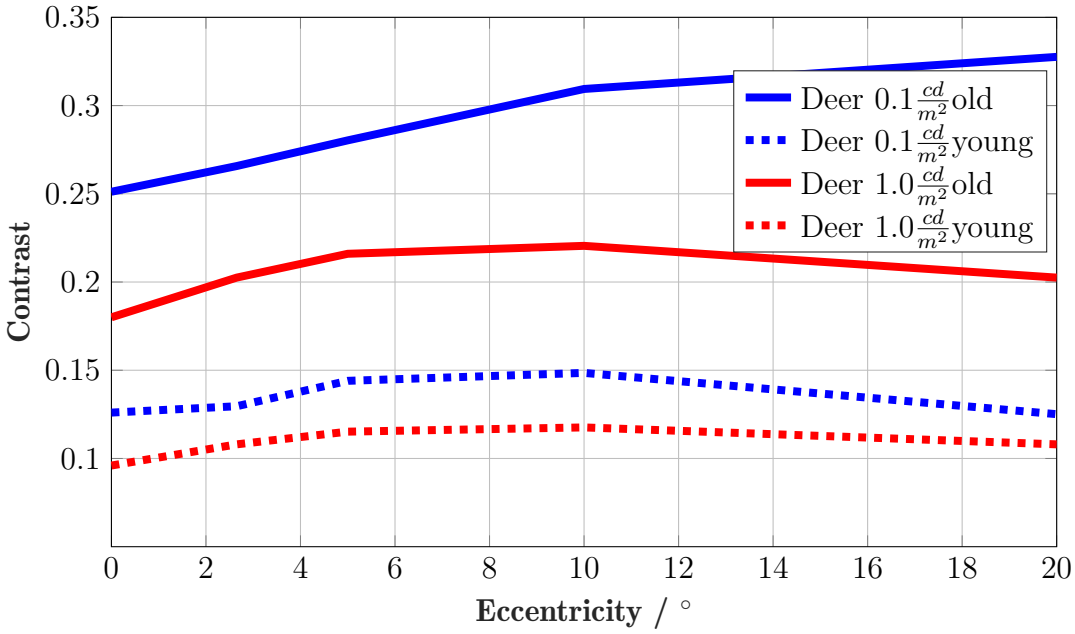


**(b)**

Figure 5.7: Contrast results of two age groups for a 99.0% detection probability at two background luminances; Relation between contrast K and eccentricity $\theta$. (a): circle, (b): deer; target size: 1.0°.

| Age group | Target | $L_U$ | 0.0° | 2.65° | 5.0° | 10.0° | 20.0° |
|---|---|---|---|---|---|---|---|
| Young | Circle | $0.1\frac{cd}{m^2}$ | 0.108 | 0.120 | 0.119 | 0.118 | 0.120 |
| Old | | | 0.168 | 0.187 | 0.085 | 0.184 | 0.187 |
| Young | Circle | $1.0\frac{cd}{m^2}$ | 0.077 | 0.085 | 0.093 | 0.114 | 0.123 |
| Old | | | 0.097 | 0.108 | 0.133 | 0.140 | 0.156 |
| Young | Deer | $0.1\frac{cd}{m^2}$ | 0.126 | 0.129 | 0.144 | 0.148 | 0.125 |
| Old | | | 0.251 | 0.265 | 0.115 | 0.309 | 0.327 |
| Young | Deer | $1.0\frac{cd}{m^2}$ | 0.096 | 0.108 | 0.117 | 0.117 | 0.108 |
| Old | | | 0.180 | 0.202 | 0.108 | 0.220 | 0.202 |

**Table 5.3: Contrast results of two age groups for a 99.0% detection probability at two background luminances; Relation between contrast K and eccentricity $\theta$; Object shapes circle and deer, target size:** 1.0°.

It can be noted that both age groups exhibit a similar behaviour for eccentricities which are larger than 5.0°. For the young participant group, the background luminance does not seem to have a significant influence in the peripheral region.

Compared to the circle shape, the detection results of the deer shape as a function of the two age groups are illustrated in Figure 5.7b. The contrast profiles of the young subjects correlate for all eccentricities. The required contrast of the lower luminance level is on average 1.4 times the contrast value for $1.0\frac{cd}{m^2}$. The results of the second age group differ significantly from the young subjects' results. The contrast values are considerably higher for both luminance levels. If one considers the lower background luminance, it can be stated that a constant increase is evident. While a contrast of 0.25 can be determined for this age group foveally, it reaches a contrast maximum of 0.327 at 20.0°, which means an increase by factor 1.3. At the luminance level of $1.0\frac{cd}{m^2}$ a foveal contrast of 0.18 can be determined. With increasing eccentricity, this contrast rises to 0.22 (10.0°) and then drops off again to 0.202 at 20.0°.

If the two object shapes are compared with each other according to the two age groups, one can recognize substantial differences. The results of the older subjects are to be mentioned. Age phenomena, such as presbyopia or the decrease in responsiveness, play an important role. Therefore, it can be said that a middle-aged person (aged 45 years and above) requires a significantly higher contrast for a lower background luminance in order to be able to detect an object.
Vision is a major factor in cognitive abilities, including memory and reasoning. Earlier studies have approved, that older people have difficulties with rapid processes and also visual search [111] [112]. Furthermore, there are age-related deficits related to attention. To be able to detect an object, the visual system must collect various forms of information. Thereby the key information includes not only the shape, size and contrast of the detection object, but rather the object's position relative the background or to one another. The information about the position is referred to as "spatial phase". This ability to allocate the positional information descends with increasing age [14] [50]. Moreover, the contrast sensitivity declines starting with an age of 30 years [83]. All these factors summarized are an explanation for

the performance of the older participants.

If one also considers the shape sensitivity of the older subject group, it can be concluded that age also has a great influence on the perception. The receptive areas on the retina are locally distributed in different densities on the retina. In part, several receptors are neurons connected to one another and connected to only one ganglion cell. With increasing age more and more nerve fibers are destroyed [112]. For stimulus perception this means that stimuli are not registered at all and thus the information can no longer be transmitted to the brain.

### 5.4.3 Influence of target size

As is known from earlier investigations, the detection target size has a significant influence on the detection performance. Hence the detection experiment was also performed for a target size of 2.0°. Figure 5.8a shows the detection experiment results of the circle shape for two different target sizes (1.0°, 2.0°). The results indicate that the smaller the detection object is, the higher the required contrast values are for a detection.
For the lower luminance level ($L_U = 0.1\frac{cd}{m^2}$), the 2.0° target size contrast varies tremendously for the foveal eccentricity. A contrast of 0.092 is necessary for a target detection, whereas for target size of 1.0° a contrast of 0.12 is required. In general, it can be noted that there is a gradually increase in contrast, which is comparatively low up to 2.65° (compare Table 5.4). For eccentricities greater than 2.65° the contrast rises rapidly to a value of 0.13 and then decreases gently to 0.126 in periphery (20.0°).
For an increased background luminance ($1.0\frac{cd}{m^2}$) the curve progression is different. It should be noted that the required foveal detection contrast for both target sizes is almost identical ($\Delta_K = 0.001$). Starting from the foveal eccentricity to the periphery the contrasts ascend steadily up to 0.11 at 20.0°.

In Figure 5.8b the detection results of the deer shape for two target sizes are presented. For the deer shape, some conspicuities can be noticed. As already found out for the circle shape, a lower contrast is required for the detection of a larger target size. If one considers the individual eccentricities (at $L_U = 0.1\frac{cd}{m^2}$), it can be stated that at 2.65° for the larger target size (2.0°), an even higher contrast is necessary than for the smaller object size. The contrast increases slightly up to 0.155 at 5.0° and drops again to 0.13 at 10.0°. In periphery a contrast value of 0.142 is needed. The development over the individual eccentricities for the luminance level of $1.0\frac{cd}{m^2}$ differs in a clearly noticeable manner from the circle target results. There is a gradually increase from 0.112 to 0.131 at 5.0°, which declines again to 0.119 at 10.0° and remains almost contast in periphery. Overall, the curve progression of both target sizes related to the luminance levels shows a good correlation exluding an eccentricity of 2.65°. As already mentioned the results for both luminance levels suggest that higher luminance values are required for a detection of small targets. Hence, the question is for what reasons this effect occurs. The influence of the target size has already been investigated in various studies [113] [114]. At the same time,

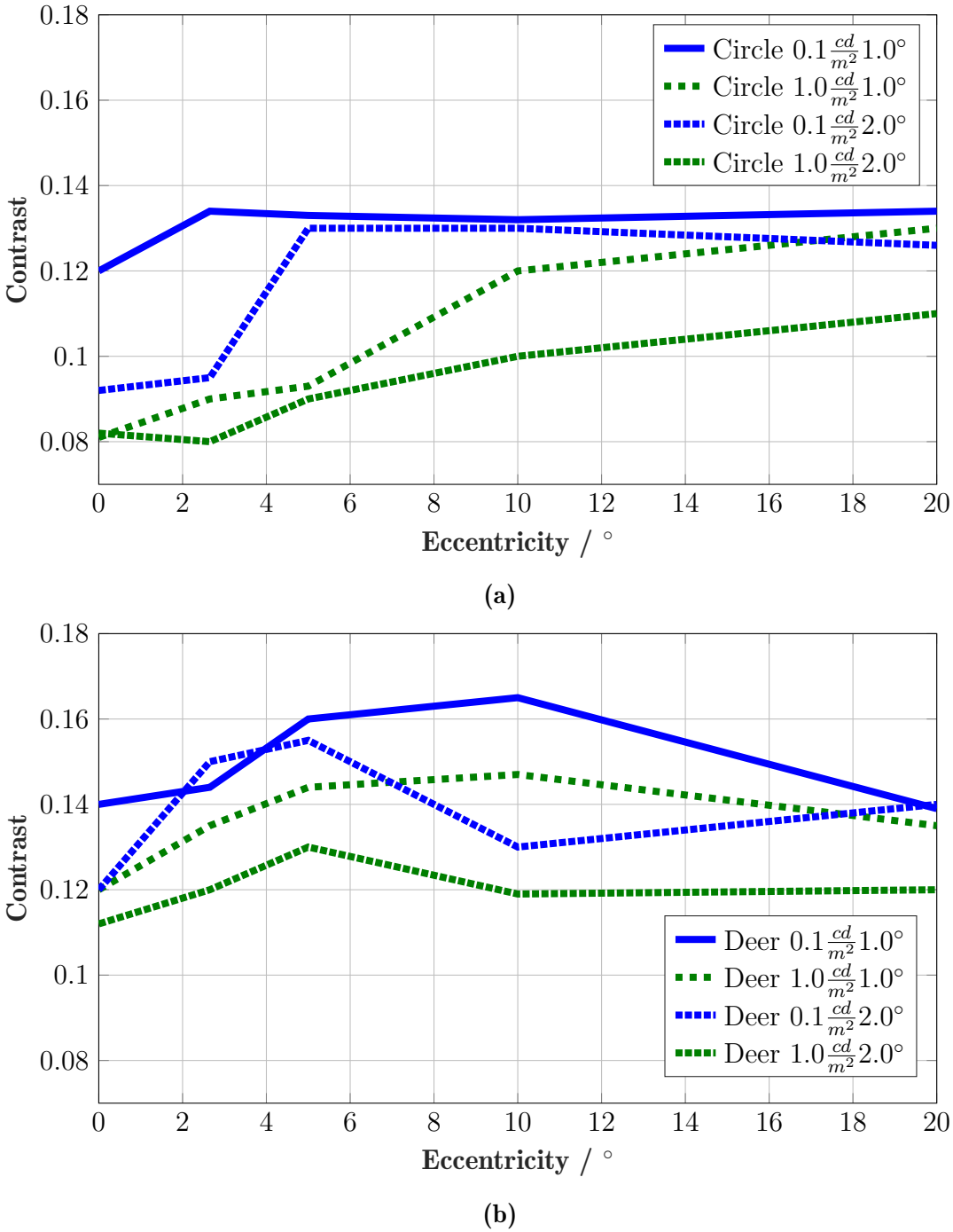


Figure 5.8: Contrast results for a 99.0% detection probability at two background luminances; Relation between contrast K and eccentricity $\theta$. (a): circle, (b): deer; target sizes: 1.0° and 2.0°.

no systematic influence of the size on peripheral perception could be ascertained. Earlier studies have shown that in the case of peripheral performance, the target size significantly contributes to the fact that the eye is able to find modulations that are contained in targets. That is, the probability summation is more pronounced in the peripheral region than foveally [114].

| Target | $L_U$ | 0.0° | 2.65° | 5.0° | 10.0° | 20.0° |
|---|---|---|---|---|---|---|
| Circle | $0.1\frac{cd}{m^2}$ | 0.092 | 0.095 | 0.130 | 0.130 | 0.126 |
| Deer | | 0.121 | 0.151 | 0.155 | 0.130 | 0.142 |
| Circle | $1.0\frac{cd}{m^2}$ | 0.082 | 0.081 | 0.091 | 0.101 | 0.110 |
| Deer | | 0.112 | 0.122 | 0.131 | 0.119 | 0.121 |

Table 5.4: Contrast for two background luminance densities with a detection probability of 99.0%; Relation between contrast K and eccentricity $\theta$; Object shapes circle and deer, target size: 2.0°.

The influence of the target size is also analysed for the two age groups. In Figure 5.9a the detection results of the two age groups, young participants (dotted lines) and old participants (solid lines), for the circle shape (2.0°) as a function of the eccentricity are presented. It can be noted that the overall detection performance behaviour is equal for both luminance levels and both age groups (compare Table 5.5). Considering the young participants' results it can be marked that the curve progression is similar for both luminance levels, whereas an approximately 0.025 higher detection contrast is required for the lower luminance level. In contrast to the 1.0° target size results the contrast values for the peripheral angles 10.0° and 20.0° can be clearly distinguished from each other.
According to the target size, the old participants' results differ strongly, since in total, a considerably lower contrast is required for the detection. Under these conditions the background luminance seems to have a substantially small influence on the detection performance. The two curve progressions are almost identical and differ only slightly in contrast values for lower eccentricities (up to 5.0°).
The detection results of the deer shape (2.0°) as a function of the two age groups are illustrated in Figure 5.9b. Compared to the 1.0° target size results of the young participants, considerable differences can be determined for the 2.0° target size. While for a luminance level of $1.0\frac{cd}{m^2}$, an even larger detection contrast in foveal observation is needed, it descends to 0.072 at 5.0° and then rises slightly to 0.095 in the periphery. As expected, for the lower luminance $0.1\frac{cd}{m^2}$, the contrast increases continuously and reaches its maximum at 0.19 (20.0°).

| Age group | Target | $L_U$ | 0.0° | 2.65° | 5.0° | 10.0° | 20.0° |
|---|---|---|---|---|---|---|---|
| Young | Circle | $0.1\frac{cd}{m^2}$ | 0.089 | 0.091 | 0.110 | 0.120 | 0.122 |
| Old | | | 0.146 | 0.156 | 0.163 | 0.165 | 0.174 |
| Young | Circle | $1.0\frac{cd}{m^2}$ | 0.070 | 0.059 | 0.098 | 0.082 | 0.085 |
| Old | | | 0.109 | 0.117 | 0.130 | 0.156 | 0.161 |
| Young | Deer | $0.1\frac{cd}{m^2}$ | 0.090 | 0.094 | 0.110 | 0.150 | 0.190 |
| Old | | | 0.159 | 0.160 | 0.163 | 0.178 | 0.195 |
| Young | Deer | $1.0\frac{cd}{m^2}$ | 0.098 | 0.087 | 0.072 | 0.093 | 0.095 |
| Old | | | 0.157 | 0.161 | 0.163 | 0.171 | 0.182 |

Table 5.5: Contrast results of two age groups for a 99.0% detection probability at two background luminances; Relation between contrast K and eccentricity $\theta$; Object shapes circle and deer, target size: 2.0° .

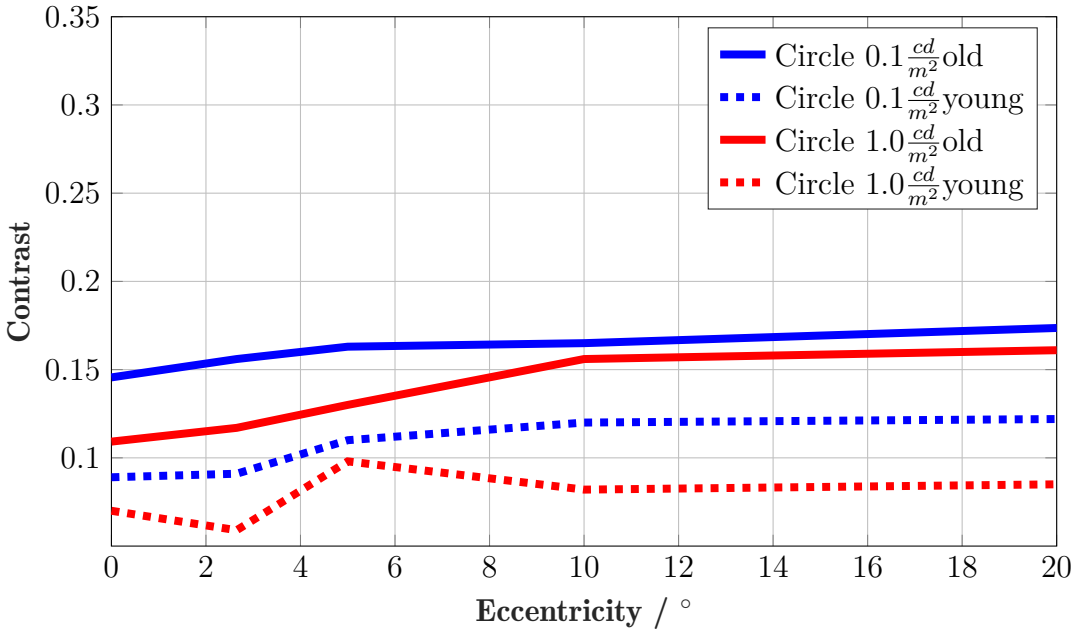


**(a)**

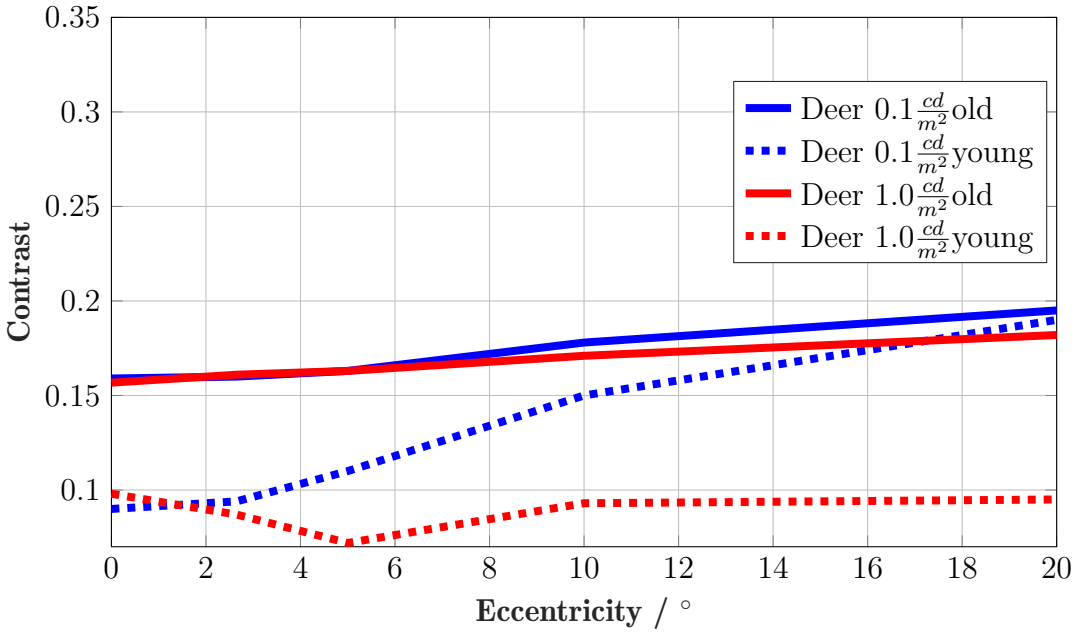


**(b)**

Figure 5.9: Contrast results of two age groups for a 99.0% detection probability at two background luminances; Relation between contrast K and eccentricity $\theta$. (a): circle, (b): deer; target size: 2.0°.

The contrast profiles of the old subjects correlate for all eccentricitys. Nevertheless, it must be noted that the results of the age groups differ in a clearly noticable manner. The old participants' results show that the contrast values are considerably higher for both luminance levels. Additionally, the luminance level does not effect the old participants' detection performance for all eccentricitys.

## 5.5 Statistical analysis

In accordance with requirements for the application of a two-factorial variance analysis (with repeated measurement) the results of the laboratory investigations are presented in the following paragraph.

### 5.5.1 Normal distribution and sphericity

When performing a two-factorial variance analysis with repeated measurements, the variances of all possible differences must be the same (variance homogeneity also known as sphericity) to ensure a normal distribution [68]. In a first step the presence of normally distributed data was proven. On the one hand it was examined whether the values between the tested participants are normally distributed (interindividual test), on the other hand, it was checked whether the two performed repetitions per test condition and participant were normal distributed (intraindividual test).
To prove the sphericity for the combinations of five eccentricities and two background levels the so-called Mauchly test was performed using Matlab (in combination with the two-factorial variance analysis) [115]. The test for sphericity is significant if p $<0.05$, that means the null hypothesis is rejected in favor of an alternative hypothesis.

### 5.5.2 Two-factorial variance analysis

In this section only the most important results and findings that were determined are presented. The complete results of the statistical analysis can be found in Appendix B.
In order to ensure a clearness in illustration of the two-factorial variance analysis, only the most important findings are presented below. Table 5.6 illustrates the structure of the calculation steps that are necessary for a two-factorial variance analysis. Both, the between-groups variation (factor A) and within-groups variation (factor B) are illustrated. SS defines the sum of squares, df indicates the degrees of freedom. MS denotes the mean squared error, which is the quotient $\frac{SS}{df}$ for each source of variation. The F-value represents the ratio of the mean squared errors.

| Source | SS | df | MS | F | p |
|---|---|---|---|---|---|
| Factor A | QSA | I-1 | $MQSA = \frac{QSA}{I-1}$ | $\frac{MQSA}{MQSE}$ | prob > F |
| Factor B | QSB | J-1 | $MQSB = \frac{QSB}{J-1}$ | $\frac{MQSB}{MQSE}$ | prob > F |
| Interaction | QSAB | $(I-1)\cdot(J-1)$ | $MQSAB = \frac{QSAB}{(I-1)\cdot(J-1)}$ | $\frac{MQSAB}{MQSE}$ | prob > F |
| Error | QSE | $I\cdot J\cdot(K-1)$ | $MQSE = \frac{QSE}{I\cdot J\cdot(K-1)}$ | | prob > F |
| Total | QST | $I\cdot J\cdot K-1$ | | | prob > F |

Table 5.6: Application using the two-factorial variance analysis. SS: sum of squares, df: degrees of freedom, MS: mean square error, I: number of factor steps of the first factor A, J: number of factor steps of the second factor B, K: number of observations per factor level (here, equal for all combinations of factor steps) [35].

The p-value is the probability that the test statistic can take a value greater than or equal to the value of the test statistic. F is, according to the underlying model, a random variable with a $F_{k-1,n-k}$ distribution, whereby K defines the number of the investigated groups (factor steps) and N the number of measured values [35]. The indices are called degrees of freedom. The value of the F distribution for given degrees of freedom (F-quantile) can be looked up in [68]. A desired level of significance (the probability of error) must be specified. If the test value F is larger than the quantile, the null hypothesis $H_0$ is rejected, so there is an interaction between the factors A and B.
The influence factors on threshold contrast are analysed by means of a two factorial variance analysis with measurement repeat. The following parameters are analysed:

- Influence of detection object's shape
- Influence of eccentricity
- Influence of background luminance
- Influence of participant's age

Table 5.7 gives an overview of the variance analysis performed. Following this, the individual influencing factors are discussed in more detail.

| Source | $L_U$ | Size | Participants | Factor A | Factor B |
|---|---|---|---|---|---|
| Eccentricity | $0.1\frac{cd}{m^2}$ | 1.0° | Total | Object shape | $L_O$ |
| Eccentricity | | | Young | Object shape | $L_O$ |
| Eccentricity | | | Old | Object shape | $L_O$ |
| Eccentricity | $1.0\frac{cd}{m^2}$ | | Total | Object shape | $L_O$ |
| Eccentricity | | | Young | Object shape | $L_O$ |
| Eccentricity | | | Old | Object shape | $L_O$ |
| Eccentricity | $0.1\frac{cd}{m^2}$ | 2.0° | Total | Object shape | $L_O$ |
| Eccentricity | | | Young | Object shape | $L_O$ |
| Eccentricity | | | Old | Object shape | $L_O$ |
| Eccentricity | $1.0\frac{cd}{m^2}$ | | Total | Object shape | $L_O$ |
| Eccentricity | | | Young | Object shape | $L_O$ |
| Eccentricity | | | Old | Object shape | $L_O$ |
| Eccentricity | $0.1\frac{cd}{m^2}$ | 1.0° vs. 2.0° | Total | Object size | $L_O$ |
| Eccentricity | | | Young | Object size | $L_O$ |
| Eccentricity | | | Old | Object size | $L_O$ |
| Eccentricity | $1.0\frac{cd}{m^2}$ | | Total | Object size | $L_O$ |
| Eccentricity | | | Young | Object size | $L_O$ |
| Eccentricity | | | Old | Object size | $L_O$ |

Table 5.7: Significant influencing factors and interactions in the laboratory investigation (significant if $p < 0.05$). $L_U$: background luminance, $L_O$: object luminance.

Figures 5.10 to 5.11 give an overview of the significance analysis for the different parameter combinations at the two background luminances for the target size of

1.0°. The two age groups are also taken into account.
On the abscissa the five investigated observation angles are shown respectively, on the ordinate both the p- values of the two influencing parameters as well as their interaction are illustrated. Since a F- distribution for $(1 - \alpha) = 0.95$ is assumed the critical value p = 0.05 is illustrated as dashed line. In Table 5.8 the significant results of the two-factorial variance analysis at the two background luminances for the target size of 1.0° are presented. The main effects and also the interactions of all investigated parameter combinations (eccentricity, age group, detection target) were performed.

| $L_U$ / $\frac{cd}{m^2}$ | Size/ ° | Eccentricity /° | Group | Factor | p - value | significant |
|---|---|---|---|---|---|---|
| 0.1 | 1.0 | 2.65 | Total | $L_U$ | 0.0103 | no |
| | | 10.0 | Young | $L_U$ | 0.0013 | no |
| | | 20.0 | Young | $L_U$ | 0.0381 | no |
| 1.0 | 1.0 | 2.65 | Total | Interaction | 0.0285 | yes |
| | | 0.0 | Young | Interaction | 0.0456 | yes |
| | | 2.65 | Young | Interaction | 0.0484 | yes |
| | | 10.0 | Young | Interaction | 0.0394 | yes |
| | | 20.0 | Young | Interaction | 0.0407 | yes |
| | | 0.0 | Old | $L_O$ | 0.0496 | yes |
| | | 5.0 | Old | $L_U$ | 0.0482 | yes |
| | | 10.0 | Old | $L_U$ | 0.0178 | yes |

Table 5.8: Significant results of the two-factorial variance analysis at the two background luminances for the target size of 1.0°, $L_O$: object luminance, $L_U$: background luminance.

As can be seen in Table 5.8 the correlation of the two target shapes was also examined on significance. The following findings were obtained:

- For the background luminance of $0.1\frac{cd}{m^2}$ no significance could be determined.

- Overall, it can be established that for all eccentricities, except the eccentricity of 5.0°, significances can be observed for the young participant group. An interaction between the object shape and the object luminance could be determined.

- Further interaction influences can be ascertained for all participants for the eccentricity of 2.65° (p = 0.0285).

- Considering the old participant group, significances are observed for the eccentricities 0.0° (p = 0.0496), 5.0° (p = 0.0482) and 10.0° (p = 0.0178) in relation to the object luminance $L_O$.

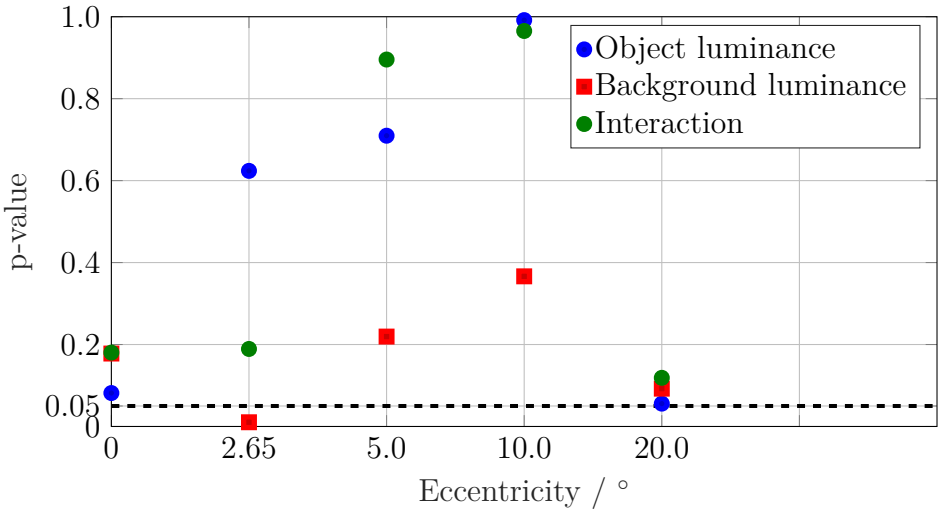


**(a)** All participants

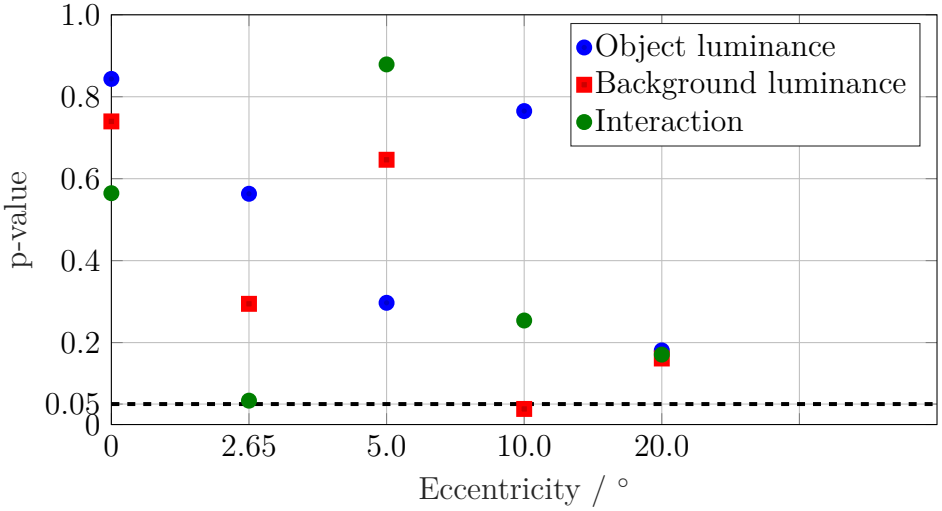


**(b)** Young participants

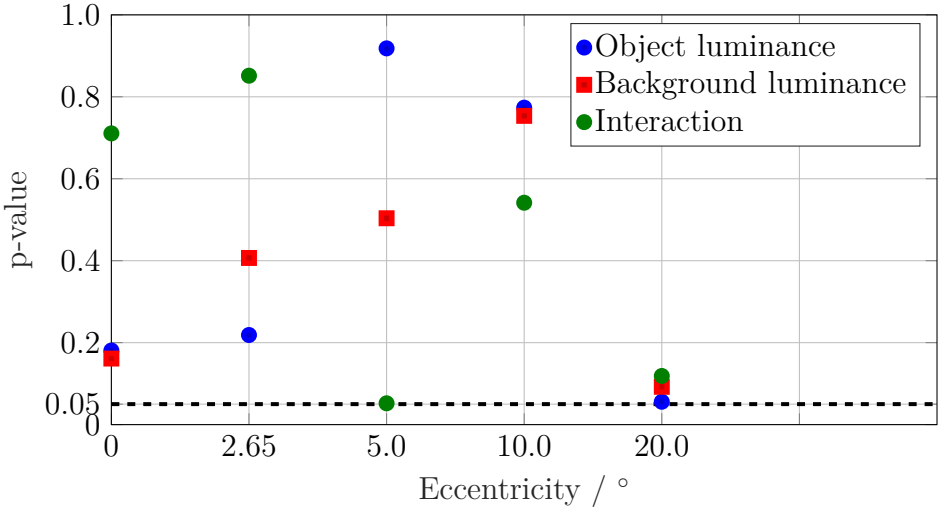


**(c)** Old participants

Figure 5.10: Two-factorial variance analysis considering eccentricities from 0.0° to 20.0°, for $L_U$= 0.1$\frac{cd}{m^2}$, target size of 1.0°, p- values of the two influencing parameters and their interaction. Since a F- distribution for $(1-\alpha) = 0.95$ is assumed the critical value p = 0.05 is illustrated as dashed line.

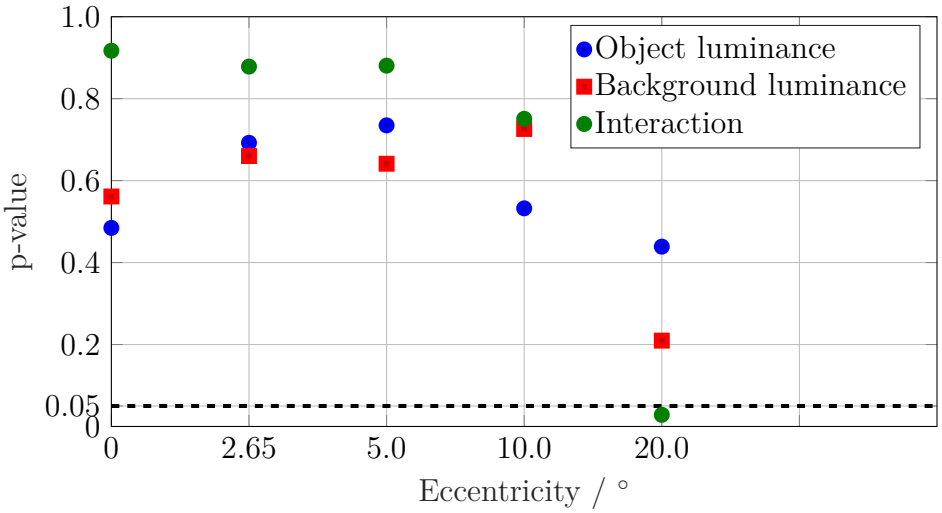


**(a)** All participants

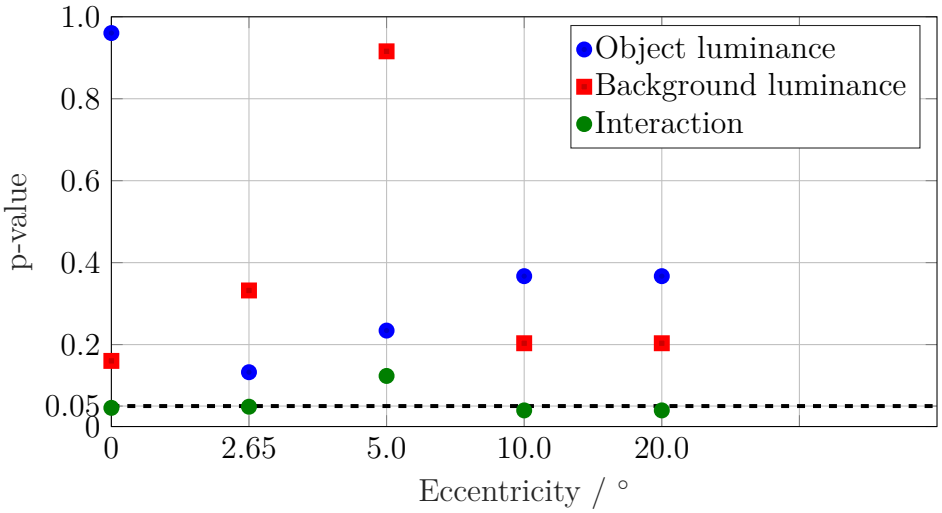


**(b)** Young participants

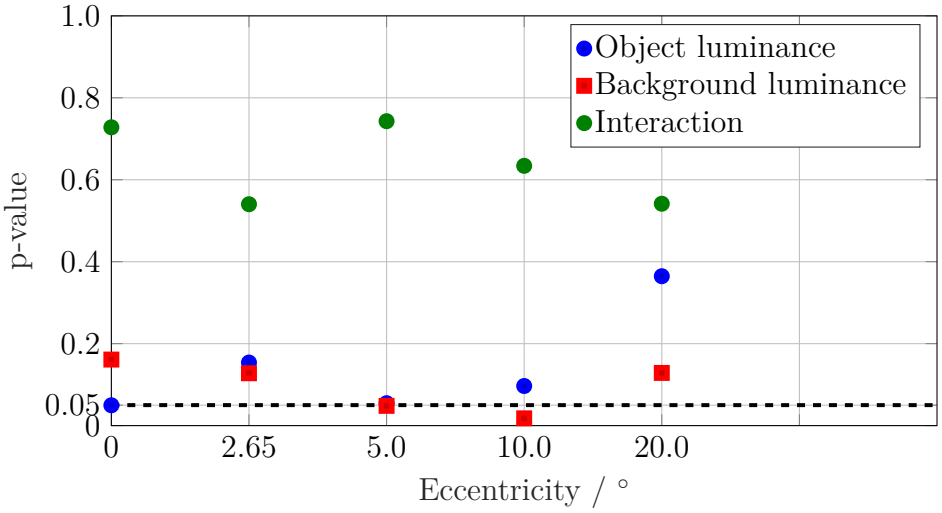


**(c)** Old participants

Figure 5.11: Two-factorial variance analysis considering eccentricities from 0.0° to 20.0°, for $L_U$= 1.0$\frac{cd}{m^2}$, target size of 1.0°, p- values of the two influencing parameters and their interaction. Since a F- distribution for $(1 - \alpha) = 0.95$ is assumed the critical value p = 0.05 is illustrated as dashed line.

## 5.6 Influence of eccentricity

The results of the significance analysis (compare Appendix B) show that the rods with their spectral sensitivity in the investigated conditions are responsible for the influence of the adaptation luminance on the detection threshold.

The rods are activated with decreasing background luminance $L_U$. Considering an eccentrcity of $\theta = 2.65°$ and $L_U = 1.0\frac{cd}{m^2}$, a similar influence of the adaptation spectrum on the perception threshold should be observed under these conditions, as for eccentrcities of $\theta = 5.0°$ and $\theta = 10.0°$, but this is not the case. Since the background luminance is identical for all conditions, only the different eccentricities $\theta$ can be the reason for this.
Investigations of Schiller [6] and Englisch [106] confirm this assumption. The displacement of the sensitivity of the human eye towards shorter wavelengths (blue) is defined as the Purkinje effect, occurs not only by the influence of the adaptation luminance, but also for an increasing eccentricity [63]. An explanation for this, is the irregular distribution of receptors on the retina (compare Chapter 2.1.2). If the eccentricity increases from $\theta = 0.0°$ up to $\theta = 20.0°$, the density of the rods raises by a factor of 2.3. In contrast, the number of cones decreases to about 38% [2]. This means that as the eccentricity increases, the sensitivity especially in the short cones (blue) spectral range increases linearly.

## 5.7 Comparison to Adrian model

In the following the results of the own findings will be compared with the visibility model of Adrian that is presented in Chapter 4.1.3. Factor $k$ describes the probability factor, whereby $k = 2.6$ corresponds to a detection probability of 99% ($k = 1.0$ corresponds to a probability of 50%, compare Table 4.2). From Table 4.1 the respective values of the luminous flux $\sqrt{\phi}$ or luminance function $\sqrt{L}$ can be extracted:

| $0.1\frac{cd}{m^2}$ | | $1.0\frac{cd}{m^2}$ | |
|---|---|---|---|
| $\sqrt{L}$ | $\sqrt{\phi}$ | $\sqrt{L}$ | $\sqrt{\phi}$ |
| 1.575 | 0.323 | 1.256 | 0.072 |

Table 5.9: Luminous flux and luminance functions according to [13].

In his investigations Adrian analysed a presentation time of 2.0 s or an unlimited presentation time [13]. Since the presentation time of the own experiments was 0.35 ms, the target's presentation time term $\frac{a(\alpha \cdot L_u)}{t}$ is calculated and can be taken from Table 5.10:

Using Equation 4.30 the values 1.039 and 1.03 can be calculated for the background luminances $0.1\frac{cd}{m^2}$ and $1.0\frac{cd}{m^2}$. Hence, assuming a target size of $\alpha$=60.0' $\widehat{=}$1.0° and a background luminance $0.1\frac{cd}{m^2}$, Equation 4.15 can be expressed as follows:

| $0.1\frac{cd}{m^2}$ | | $1.0\frac{cd}{m^2}$ | |
|---|---|---|---|
| $a(\alpha)$ | $a(L_u)$ | $a(\alpha)$ | $a(L_u)$ |
| 0.136 | 0.235 | 0.136 | 0.186 |

Table 5.10: $a(\alpha)$ and $a(L_u)$ for a target size of $1.0°$, using background luminances of $0.1\frac{cd}{m^2}$ and $1.0\frac{cd}{m^2}$.

$$\begin{aligned}\Delta L_{thresh_{0.1}} &= k \cdot \left(\frac{\sqrt{\phi}}{\alpha} + \sqrt{L}\right)^2 \cdot \frac{a(\alpha \cdot L_U) + t}{t} \cdot F_{CP} \cdot AF \\ &= 2.6 \cdot \left(\frac{0.323}{60.0} + 1.575\right)^2 \cdot 1.039 \cdot 1.0 \cdot AF = 6.75 \cdot AF\end{aligned} \tag{5.2}$$

For a background luminance of $1.0\frac{cd}{m^2}$ one has

$$\Delta L_{thresh_{0.1}} = 2.6 \cdot \left(\frac{0.072}{60.0} + 1.256\right)^2 \cdot 1.03 \cdot 1.0 \cdot AF = 4.23 \cdot AF \tag{5.3}$$

Since the average age of the young participants was 28.6 years and 53.4 for the old participants, different age factors are derived in Table 5.11 (compare Equations 4.34 and 4.35). To take an example, a person at the age of 55 years would require an average 1.59 times higher threshold luminance level than a young person (23 years of age). This behaviour of the threshold luminance related to participants age is also illustrated in Figure 5.12.

| Years of age | $AF$ |
|---|---|
| 23 | 1.0 |
| 25 | 1.007 |
| 28 | 1.028 |
| 40 | 1.194 |
| 53 | 1.525 |
| 55 | 1.590 |
| 64 | 1.901 |

Table 5.11: Age factors according to Equations 4.34 and 4.35. For calculating the luminance threshold of older participants Equation 4.22 has to be multiplied by $AF$, since it is just valid for young observers with an average age of 23 years ($AF_{23} = 1.0$).

As it can be seen in Figure 5.12 the threshold contrast rises steadily with increasing age starting from age of 46, whereas the gradient of the curve rises even sharper from age of 65. For lower luminances in mesopic region, the gradient is even steeper.

Figure 5.13 presents the luminance difference threshold $\Delta L$ for 99.93% detection probability as a function of the target size $\alpha$ at different background luminances (positive target contrast). To compare his findings with Aulhorn [28], Adrian multiplied his findings by factor 2.4.

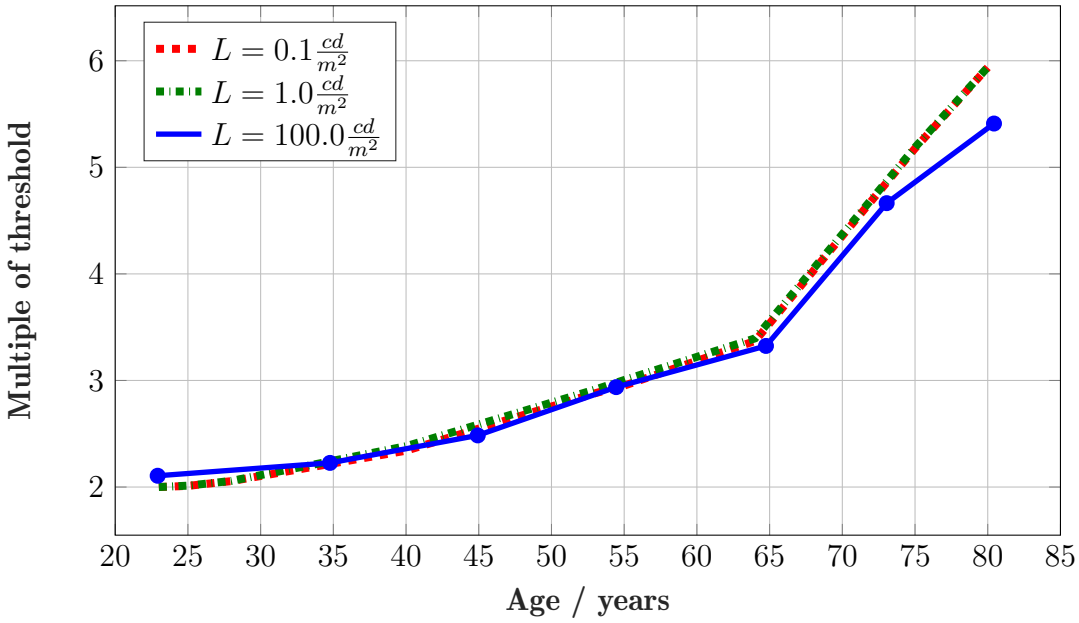


Figure 5.12: Multiple of the contrast threshold for three background luminance levels ($0.1\,\frac{cd}{m^2}$, $1.0\,\frac{cd}{m^2}$, $100.0\,\frac{cd}{m^2}$) that are required for the observer of higher age in relation to a young observer with an average age of 23 years according to [13].

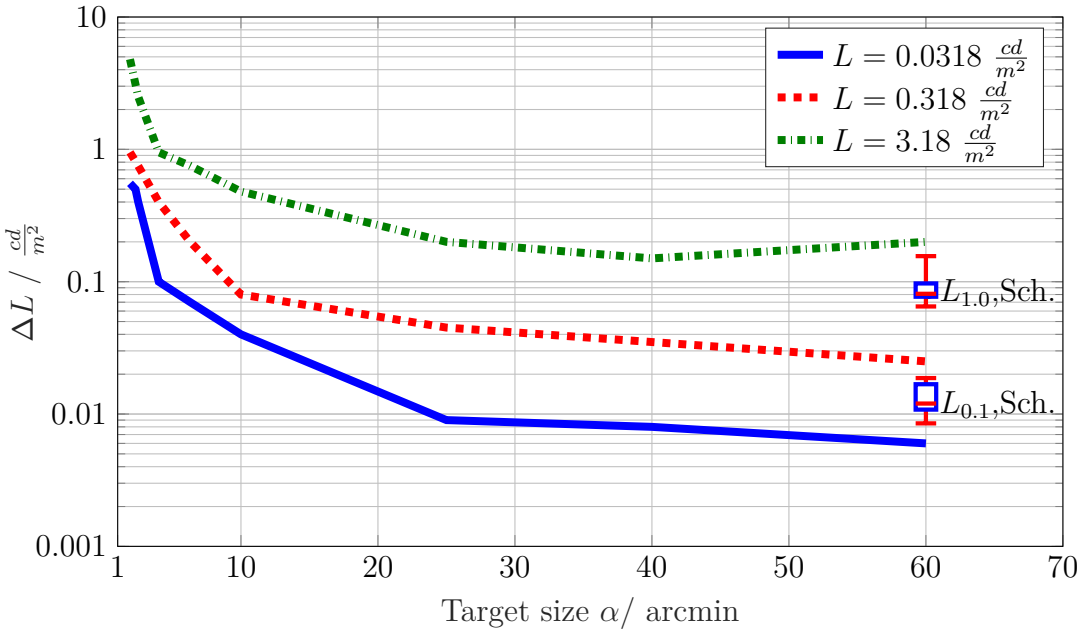


Figure 5.13: Luminance difference threshold $\Delta L$ for 99.93% detection probability as a function of the target size $\alpha$ at different background luminances (positive target contrast). The values are based on Adrian's model and multiplied by factor 2.4 [13], since two "young participants" and one "old participant" with 55 years of age were assumed (AF=1.59, monocular vision (comparison with [28]). In addition, the results for the two background luminances $0.1\,\frac{cd}{m^2}$ and $1.0\,\frac{cd}{m^2}$ of the own findings are illustrated (binocular viewing conditions).

For the determination of this value he assumed three test persons, two "young

participants" and one "old participant" with 55 years of age ($AF_{55} = 1.59$) under monocular vision conditions. Monocular and binocular observation are known to be approximately different by factor 2.0 (Adrian assumed factor 1.64) [13]. Since younger participants require lower detection contrast values compared to older ones, Adrian reduced the factor 2.6 (corresponding a multiplication of $1.64 \cdot 1.59$) to 2.4. In addition, to be able to compare the results directly, the own findings for the background luminance of $0.1\frac{cd}{m^2}$ and $1.0\frac{cd}{m^2}$ are integrated into Figure 5.13. A comparison is only possible to a limited extent, as the boundary conditions of the two investigations were different. Nevertheless, internal similarities within the two studies can be established.

In Table 5.12 the findings of Adrian's experiments as well as the calculated luminance difference thresholds for the two luminance levels are compared to the own findings.

| Author | $L_U$ / $\frac{cd}{m^2}$ | $\Delta L$ / $\frac{cd}{m^2}$ |
|---|---|---|
| Adrian | 0.0318 | 0.006 |
| Adrian calculated | 0.1 | 0.0168 |
| Schneider | 0.1 | 0.012 |
| Adrian | 0.318 | 0.025 |
| Adrian calculated | 1.0 | 0.180 |
| Schneider | 1.0 | 0.081 |
| Adrian | 3.18 | 0.200 |

Table 5.12: Luminance difference threshold $\Delta L$ for or 99.93% detection probability at different background luminances (positive target contrast) for a target size of $\alpha = 1.0°$; foveally.

It can be stated that the results of the own findings show a good compliance with Adrian's results for the background luminance of $0.1\frac{cd}{m^2}$. For higher luminances, it becomes clear that the own investigation exhibit a significant lower luminance difference threshold ($\Delta_{Ad.-Sch.} = 0.099$) compared to the calculated model.
Adrian's model is essentially based on four elements: the probability factor, luminance component, polarity factor and age factor. In the following, further parameters, namely the target size and the target shape, are considered, to validate the obtained results.
In Figure 5.14 results of the individual investigated parameters are compared with Adrian (compare Table 5.13). The dashed lines represent the values calculated with the model of Adrian. As expected, a slightly smaller contrast is required for a larger object size at $0.1\frac{cd}{m^2}$. Compared to both circle sizes a wide dispersion of the data is evident for the deer shape detection.

In total it can be ascertained, that the target shape has the largest influence on the participants' detection performance. Taking these observations into account it can be concluded that a complex target shape leads to an increase in threshold.
Considering the higher luminance level of $1.0\frac{cd}{m^2}$, it is noticeable that the results of the own investigation are significantly lower than the calculated value of Adrian's model (by a factor of 2.6). In principle, the distribution of the results is equivalent to the results at $0.1\frac{cd}{m^2}$. Initially this can be traced back to the already mentioned

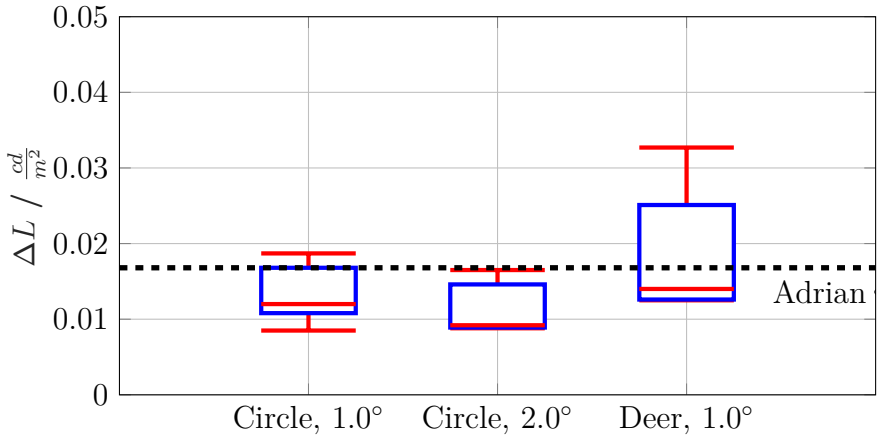


**(a)**

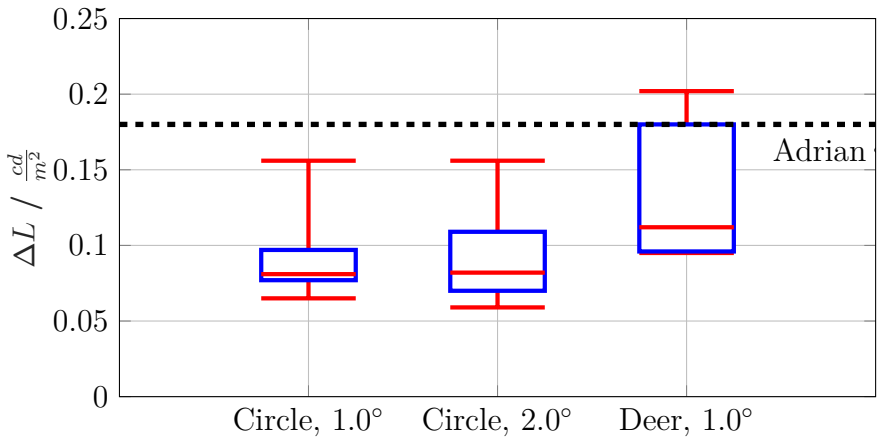


**(b)**

Figure 5.14: Luminance difference threshold $\Delta L$ of the own findings for or 99.93% detection probability in comparison to Adrian's model. The influence of the targets size and shape on the detection performance is presented for the background luminances (a): 0.1$\frac{cd}{m^2}$, (b): 1.0$\frac{cd}{m^2}$ in a positive target contrast, for the target sizes of $\alpha = 1.0°, 2.0°$ and target shapes: circle, deer. Determined values of Adrian's model are represented by dashed lines.

factors. Furthermore, the assumption is that a detection at a higher background luminance leads also to an easier information processing in the eye.

In Adrian's model only a circular shape is accomplished. From the results it can quite clearly be seen, that the complex target structure on the one hand lead to a higher luminance difference threshold and, on the other hand, also to a wide distribution of the measurements.
If the concept of shape sensitivity is used, it is only consistent by analogy with contrast sensitivity, which corresponds to the threshold contrast measurement. Since the shape sensitivity depends on the shape of the target itself, a general measurement parameter for a description of different objects does not exist. Therefore, the visual discrimination of the eye is decisive.

This is further substantiated by Jainski's study on the perception threshold for several targets in the visual field [116]. He also analysed results regarding the influ-

| Author | Target shape | Target size/ ° | $\Delta L$ / $\frac{cd}{m^2}$ |
|---|---|---|---|
| $L_U = 0.1\ \frac{cd}{m^2}$ | | | |
| Adrian calculated | Circle | 1.0 | 0.0168 |
| Schneider | Circle | 1.0 | 0.012 |
| Schneider | Circle | 2.0 | 0.0092 |
| Schneider | Deer | 1.0 | 0.014 |
| $L_U = 1.0\ \frac{cd}{m^2}$ | | | |
| Adrian calculated | Circle | 1.0 | 0.180 |
| Schneider | Circle | 1.0 | 0.081 |
| Schneider | Circle | 2.0 | 0.082 |
| Schneider | Deer | 1.0 | 0.112 |

Table 5.13: Luminance difference threshold $\Delta L$ of the own findings for or 99.93% detection probability in comparison to Adrian's model, for the target sizes of $\alpha = 1.0°, 2.0°$ and target shapes: circle, deer.

ence of the target shape on the threshold contrast. As a result, he concluded that the threshold of a circular object decreases related to the increasing aspect ratio of a rectangular object (assuming the same size). While for a aspect ratio of 1:4 the threshold changed imperceptible, it decreased significantly at an aspect ratio of 1:8 by 25%. Rast also completed investigations on the threshold contrast in relation to the shape sensitivity in structured environments [117]. He also discerned a clear shape dependence of the threshold contrast. He also observed that shape sensitivity is very different for individual persons and differences are most pronounced for complex object shapes (asymmetric, not concise) followed by rectangles with significantly longer height than width.

## 5.8 Summary

From the results of the laboratory investigations the following conclusions can be drawn:

- A clear target shape dependence of the luminance difference threshold can be determined.
- The luminance difference threshold decreases with increasing target size.
- The dependence on the background luminance threshold is similar for different target sizes and shapes.
- The luminance difference threshold decreases with increasing background luminance.
- With increasing eccentricity a higher contrast is required for a detection in periphery.

The results suggest that the participant's collective also has a stronger impact on the results. While Adrian [13] substantiated his findings of three participants (in

addition to the findings of Blackwell [37]), overall twenty young and old subjects were tested in the own investigations. With increasing age, the visual capacity declines due to neuronal changes and optical deteriorations in the eye. Hence, especially older participants demanded significantly higher contrast values for a detection. The shape sensitivity for individual test subject's spreads very strongly. Interindividual differences are most pronounced for the deer shape. Since the participants had all normal sight and the two age groups were uniformly distributed, the impact of the object shape is also age-dependent. Nevertheless, the basic statement of both studies is that a lower contrast is required for a higher luminance, is validated by both studies.

# Chapter 6

# Field study

In the following chapter a field experiment that was conducted in an unlit enclosed area (August Euler Airport in Griesheim, Germany) is described.

The aim of this investigation is to determine the detection distances and therefore the contrast values for two types of objects considering the driving task. The focus of the study is on the driver's peripheral vision under mesopic conditions. Further analysis is enforced to distinguish the differences in performance between old and young subjects. The importance of the findings are highlighted by comparing results against the minimum stopping distance at a particular speed.

## 6.1 Hypothesis

Chapter 2 illustrated the contrast and shape sensitivity of the human eye in mesopic range. From the existing investigations some open questions emerged. What influence does the homogeneity of the light distribution have on the detection distance? Do the higher luminance lead to longer detection distances? What influence does the absolute size of the visual object have? From these questions above, the following hypotheses can be developed:

- The influence of the peripheral position of detection objects on the threshold contrast can be described for the luminance range of the headlamp illumination.
- The threshold value, calculated according to Kokoschka [24], which is based on the Blackwell data [37], can be transferred by means of a practical or field factor.
- According to stray light theory, bright front areas on the road in front of the vehicle lead to an increase in threshold contrast and thus to the reduction of the distance of recognition.

## 6.2 Experimental procedure

The measurements were performed on the August Euler Airport in Griesheim, Germany. Using the 1.3 km long landing strip a detection object was placed at different positions in a distance of 1.0 km to starting point of the landing strip (compare Figure 6.1). Two different scenarios were conducted. The participants started with a dynamic test, where the test vehicle was driven at a speed of $80.0 \frac{km}{h}$. In the second

test setup (static test) the test vehicle remained at the starting point, whereas the detection object headed towards the test vehicle under different observation angles. In a distance of 1.04 km to the test vehicle an additional vehicle was located on the driver's lane to serve as a fixation point. Overall, two different target shapes (human being and deer) that occur in representative traffic situations were presented randomly off the visual axis at the left hand and right hand side of the fixation point for six eccentricities related to a distance of 110.0 m (to the left of the lane: $\theta = 3.0°$, 3.8 m; 2.0°, 5.8 m; to the right of the lane: $\theta = 2.65°$, 5.0 m; 5.0°, 9.6 m; 6.5°, 12.5 m; 8.0°, 15.5 m, compare Figure 6.1).

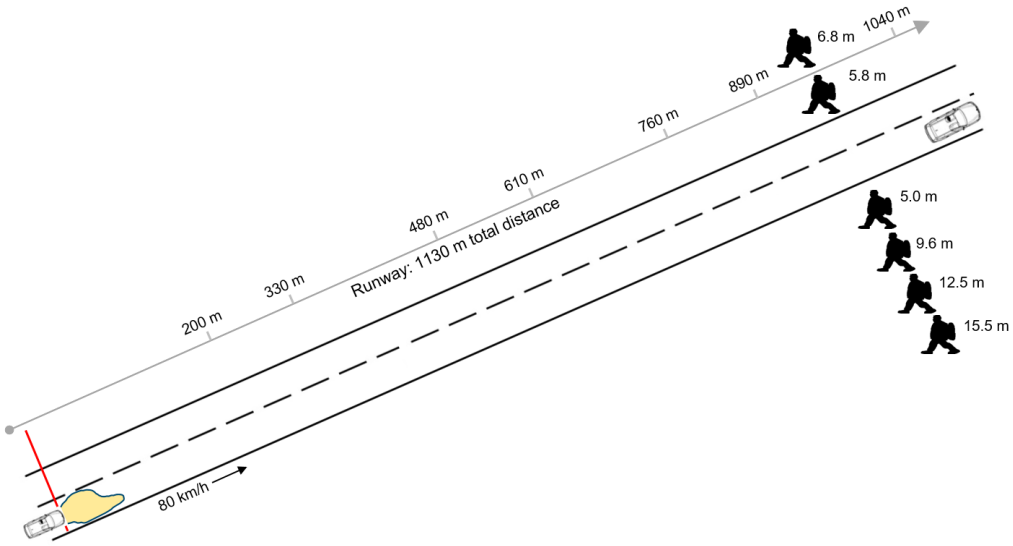


(a)

(b)

(c)

Figure 6.1: (a) Scheme of the landing strip, August Euler Airport, Griesheim, Germany. Dynamic field test: test vehicle is driven at a speed of 80.0$\frac{km}{h}$. Detection object (deer, (b): 5.0m, (c): 12.5m) is placed on the right hand side.

The two positions on the left hand side of the road served only to avoid the learning effect to the participants, so that they were preferably open minded for the next test run. For this reason, these two positions will not be considered in the following course of this work. The objects to be detected were equipped with a GPS sensor for calculating the detection distance. The test vehicle was also provided with a GPS sensor and a notebook to control the measurements at all

times. When performing the field study, the interior lighting of the test vehicle was switched off to enable the adaptation conditions for each participant. Using a previously activated cruise control, the subject was able to perform every test run at a speed of $80.0\frac{km}{h}$, driving along the runway. While driving the subject's task was to indicate the appearance of the object at first time of a detection. As it can be seen in Figure 6.2a the subject's answers were saved by pressing a button on an input device. The subject was instructed to answer as soon as it surely detected the object beside the road.

**(a)** **(b)**

Figure 6.2: Subject inside the test vehicle, (a) indicating the appearance of the object at first time of an detection by pressing a button on the input device; (b) questionaire, completed after test performance.

The first detection object was a real person (female, height 1.76m) completely dressed in black clothes (compare Figure 6.3). The second object was a deer template with a height of 1.40 m, coated with black paint (reflectance coefficient of 5.0%).

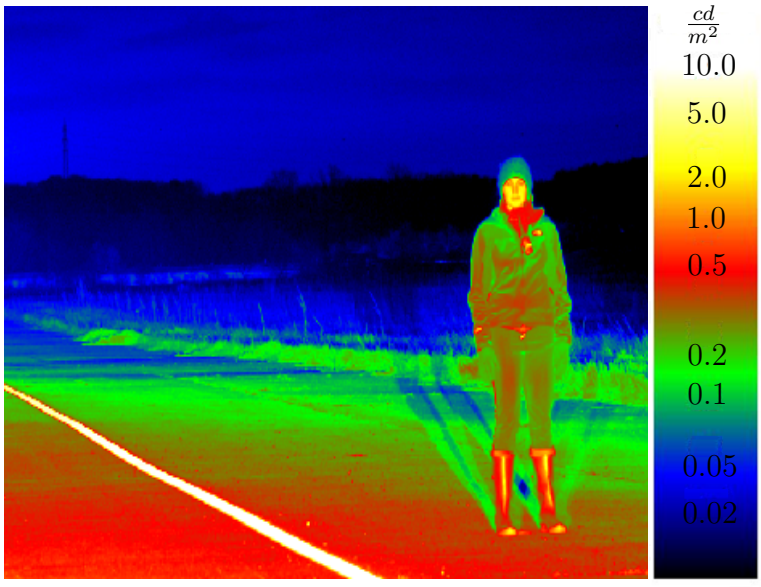


Figure 6.3: Luminance picture, August Euler Airport in Griesheim, detection object: human being, female, height 1.76 m, completely dressed in black clothes, reflection coefficient < 5.0%, equipped with a GPS sensor for calculating the detection distance. The characteristic background luminance values ranged between 0.02 to $0.09\frac{cd}{m^2}$.

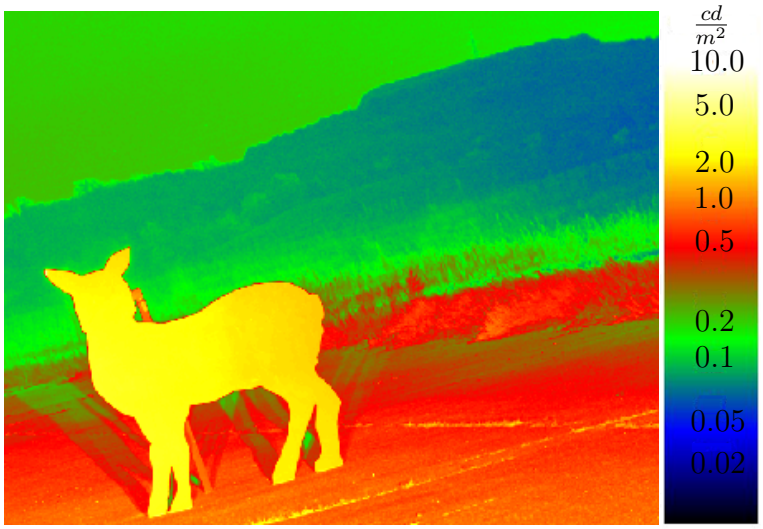


Figure 6.4: Luminance picture, August Euler Airport in Griesheim, detection object: deer, height 1.40 m, reflection coefficient < 5.0%, equipped with a GPS sensor for calculating the detection distance.

Before starting the experiment, the subjects were tested on good eye sight. As presented in Figure 6.5 overall thirty subjects completed the experiment.

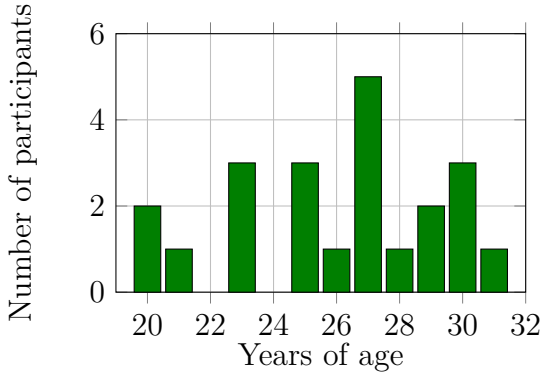


**(a)** Young

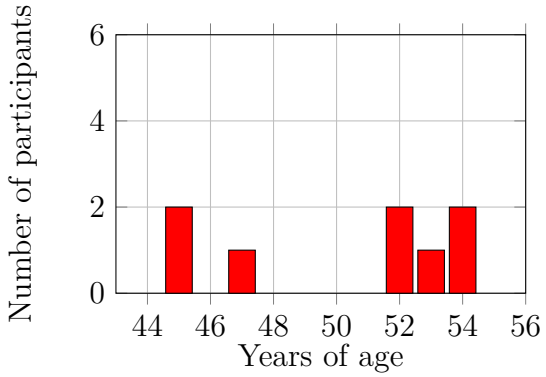


**(b)** Old

Figure 6.5: Age distribution of the subjects' groups " young subjects" (11 females, 11 males) and " old subjects" (1 female, 7 males).

All participants had normal or optically corrected vision and were all licensed drivers (12 women and 18 men between 20 and 54 years old, average age was 29 years). Every subject was asked to complete the dynamic test 32 times whereas the two objects were presented randomly on the different eccentricitys. Within the static field test, only the female person approached the test vehicle 12 times for each participant.

## 6.3 Evaluation

In this section all results of the field study will be discussed. For every single test run the GPS data of the test vehicle as well as the object positions were saved. Hence the exact distance between the test vehicle and the objects position was calculated.

### 6.3.1 Dynamic field setup

In the following paragraph the results of the dynamic field study results related to the object shape and influence of the age are evaluated.

#### 6.3.1.1 Influence of object shape

Figure 6.6 shows the distances that are necessary to detect the objects human (blue) and deer (red). In Table 6.1 the results for the detection distances are listed. The results for the eccentricities from 2.65° to 6.5° (5.0m to 12.5m) are similar for all participants for both target shapes. As it can be seen from Table 6.1 the average detection distance is approximately 90.0 m.

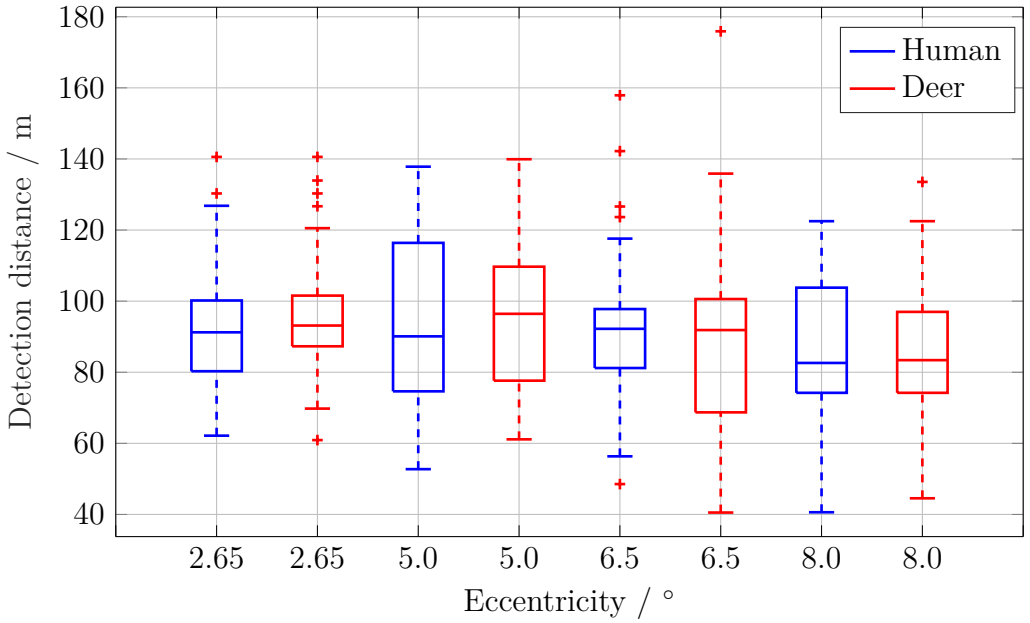


Figure 6.6: Comparison of the target shapes (human being and deer) as a function of the eccentricity (right of the lane: 2.65°, 5.0m; 5.0°, 9.6m; 6.5°, 12.5m; 8.0°, 15.5m).

Whereas the distance range for an eccentricity of $\theta = 2.65°$ varies between 60.9 m and 140.5 m, the corresponding detection distances for $\theta = 5.0°$ extends between 52.7 m to 140.0 m. Within the third position on the right hand side (12.5m, $\theta = 6.5°$)

| Object shape | Detection distance /m | | | |
|---|---|---|---|---|
| Object position | 2.65° | 5.0° | 6.5° | 8.0° |
| Human | 93.18 | 94.52 | 92.88 | 84.07 |
| Deer | 96.85 | 95.51 | 90.36 | 84.17 |
| $\Delta_{\text{human-deer}}$ | -3.67 | -0.99 | 2.52 | -0.10 |

Table 6.1: Mean detection distances of all participants for the two object shapes.

there is a significant difference between the two target shapes. The slightest necessary distance to detect the deer was 40.5 m. In comparison, for the detection of the human 48.5 m were required. For the largest eccentricity ($\theta = 8.0°$) the participants' behaviour shows a good compliance to the $\theta = 6.5°$ eccentricity. With increasing eccentricity the illumination of the driver's visual field decreases. Therefore, high object luminance values are needed for a detection with a probability of 99.0%. If an object is illuminated for reliable visual detection within the limits of the headlamp system's output, the driver is able to detect the object. Because of the high information loss, the driver needs a length of additional 10.0 m to ensure a detection (compare Chapter 6.5).

#### 6.3.1.2 Influence of age

Unfortunately, not many researches have addressed the important influence of the participant's age. Beside from older people's self-reports, very little is known about how object detection and also recognition changes with age in relation to dynamic driving tests.
In Figure 6.7a the detection distance results of the human dependent on the age groups are presented. Since there is an obvious connection between the visual function and aging the participants were divided into two age groups for an improved analysis. The first age group "young participants" was at the age of 20 to 45. The second group "old participants" was at 46 to 54 years of age (compare Figure 6.5). The average detection distance for the young participants is 101.9 m. In a direct comparison of the eccentricities it can be noted that the first and third position were detected previously, as for position two and four detection distances of 96.2 m were ascertained (compare Table 6.2). In total it can be stated that the range of spreading is larger for the young participants (approximately 40.0 m range) than for the second group (32.0 m range). Considering the results of the old participants significant differences in the detection distances can be specified. The distinctions between the individual eccentricities are similar for the old participants and amount to a decrease in detection distance. For example, an older subject needs to be at least 25.0 m closer to the pedestrian to detect him with regard to an eccentricty of $\theta = 2.65°$ ($\Delta_{\text{young-old}}$= 25.56 m). At an eccentricity of $\theta = 8.0°$ at least 12.0 m are necessary for a detection ($\Delta_{\text{young-old}}$= 12.33 m).

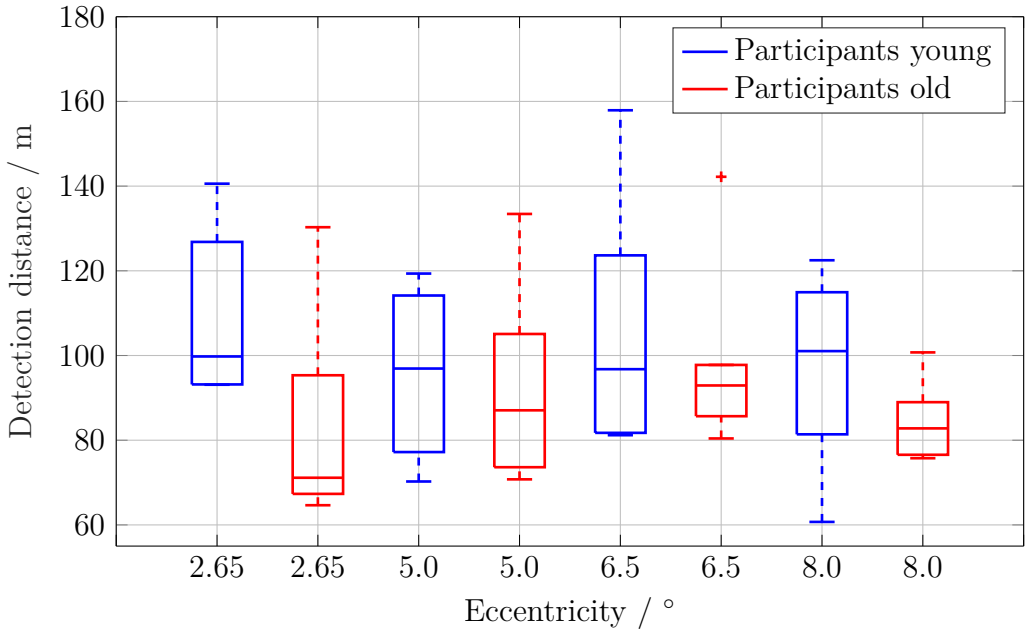


**(a)** Human

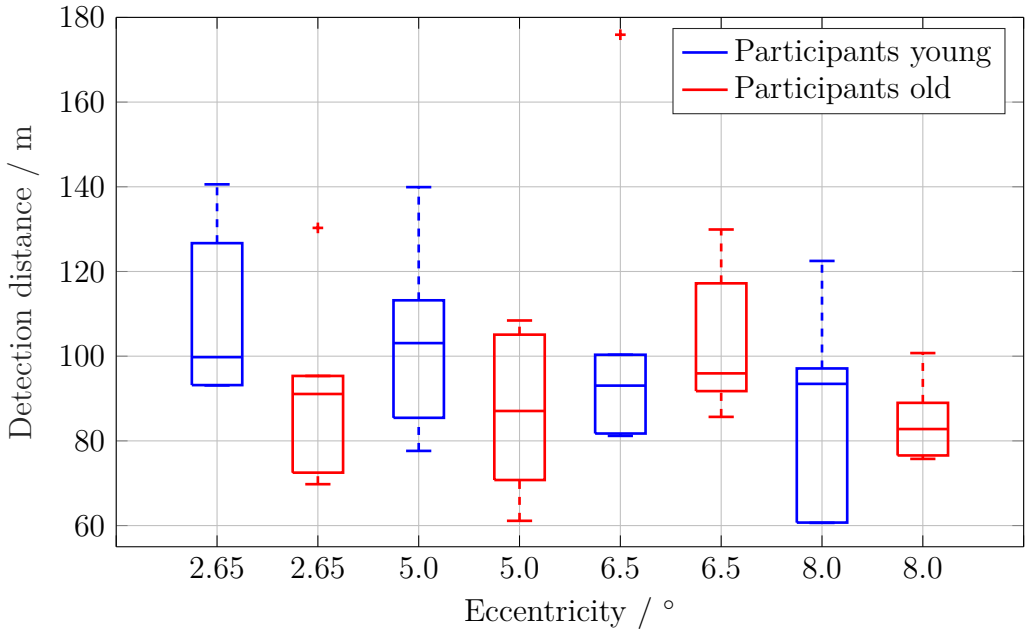


**(b)** Deer

Figure 6.7: Comparison of the age groups as a function of the eccentricity (right of the lane: 2.65°, 5.0m; 5.0°, 9.6m; 6.5°, 12.5m; 8.0°, 15.5m).

In Figure 6.7b the detection distance results for the deer shape of the two age groups (young participants (blue) and old participants (red)) as a function of the eccentricity are presented. The results do not drastically deviate from the results of the human shape. Nevertheless, the target shape has an impact on the detection behaviour of the participants. Except the largest eccentricity ($\theta = 8.0°$) the young participants' behaviour showed a good compliance with the detection distance (approximately 105.0 m). Similar to the results of the human shape a decrease in

| Detection distance/ m | 2.65° | 5.0° | 6.5° | 8.0° |
|---|---|---|---|---|
| Human | | | | |
| Young | 108.87 | 95.80 | 106.33 | 96.93 |
| Old | 83.31 | 92.83 | 98.65 | 84.60 |
| $\Delta_{young-old}$ | 25.56 | 2.97 | 7.68 | 12.33 |
| Deer | | | | |
| Young | 108.84 | 103.72 | 104.21 | 87.97 |
| Old | 91.67 | 86.58 | 102.73 | 84.60 |
| $\Delta_{young-old}$ | 17.17 | 17.14 | 1.48 | 3.37 |

Table 6.2: Mean detection distances of all participants for two age groups. Detection objects: human, deer.

detection distance could be observed for older participants. After the test realisation the participants were asked which of the two objects was easier to detect. Because of its dimensions and prominent shape, eighty percent of the test persons indicated the deer as more conspicuous.
Therefore, as it can be seen in Table 6.2, the decrease in detection distance was not as high as for the human shape. Particular mention should be made of the results for the third eccentricity ($\theta = 6.5°$). As opposed to the other eccentricities it tended to be easier for the old participants to detect the deer at this position. In many scientific studies the stimuli that are used in motion perception are mostly abstract shapes, like circles or rectangles, which appear for a short time period [118]. One of the most important functionalities of the visual system is the ability to detect temporal changes in direction and speed. This efficiency also declines with age.

### 6.3.2 Static test setup

As there are not many data about the participants' answer performances related to moving objects considering the influence of age, a second test setup with a moving detection object and a static observer was provided. For the static test setup the same settings (test vehicle and light distribution) as under dynamic conditions were used. In the static setup the object walked towards the participant sitting in the vehicle. In this case the object was integrated into an environment with constantly changing parameters, means, the subject's task was to connect direction information across time and space to observe the mean direction and speed of the object [118]. The participant's task was to direct the view to the front (as in an ordinary driving task). With appearance of the detection object the participant had to press a button to indicate the detection.
Figure 6.8 represents the comparison between the static and dynamic detection results of the pedestrian. As can be seen in Table 6.3, there are significant deviations between a the static and dynamic test results.

By eliminating the driving task, the driver is able to concentrate on the detection entirely. Overall, a gain of approximately 30.0 m can be obtained for all eccentricities. This clearly shows how much influence the driving task and the associated deflection potential has on the driver. An additional braking distance of almost

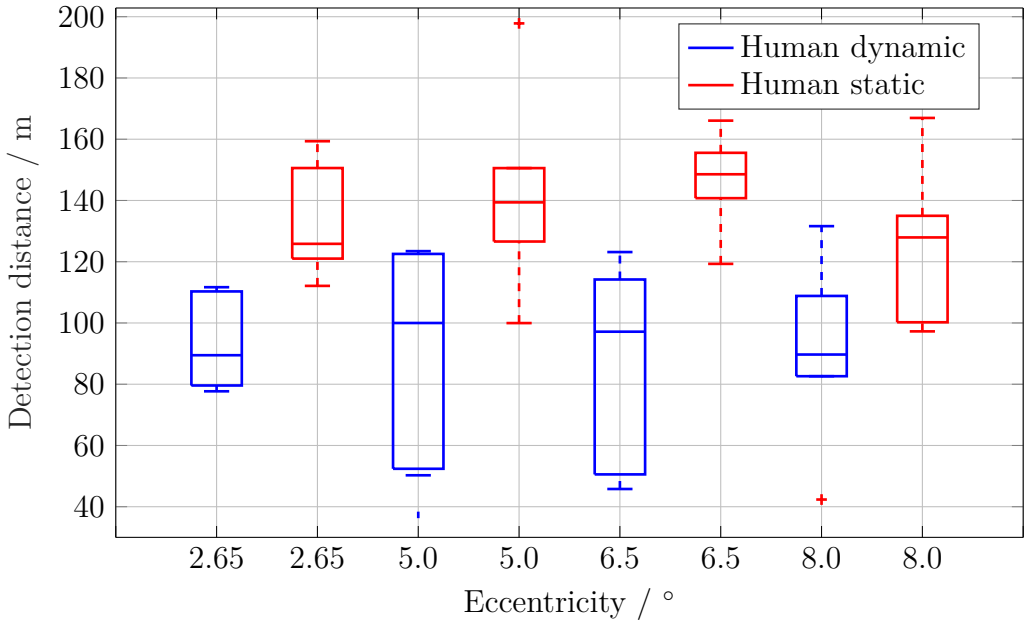


Figure 6.8: Comparison of the dynamic and static field test (target shape: human being) as a function of the eccentricity (right of the lane: 2.65°, 5.0m; 5.0°, 9.6m; 6.5°, 12.5m; 8.0°, 15.5m).

| Setup type | Detection distance /m | | | |
|---|---|---|---|---|
| Object position | 2.65° | 5.0° | 6.5° | 8.0° |
| Dynamic | 93.18 | 94.52 | 92.88 | 84.07 |
| Static | 123.45 | 139.37 | 148.55 | 127.93 |
| $\Delta_{\text{dynamic}-\text{static}}$ | -30.27 | -44.85 | -55.67 | -43.86 |

Table 6.3: Mean detection distances of all participants for dynamic and static test setup, object shape: human.

30.0 m, which means a duration of 1.4 s at a speed of 80.0$\frac{km}{h}$, would make a clear difference in safety and could prevent a possible collision at the analysed speed or even higher speeds. Therefore it can be concluded that a practical factor or field factor is meaningful and should be taken into account.
As illustrated in Table 6.4 the static test results were also considered separately for the two age groups. There is a clear distinction between the age groups, especially the detection behaviour of the old subjects is considerably different compared to the results of the dynamic field test. While the young subjects achieved an average detection distance of 136.2 m, which means a gain in distance of 31.1 m compared to the dynamic test, the old subject's detection distance remained at 89.2 m. Although the driving task was eliminated in this case, a substantial improvement in detection distance could not discerned for the old participant group, which can traced back to the reduction of visual acuity (compare Figure 6.9). Considering the full range of participants' results, it can be concluded that it is much more difficult to the old participants to detect an object, as the detection distance remains at the same level as for the dynamic test. Because of aspects that were presented previously, old

participants need to be closer to the object to be able to detect it. The decrease in contrast sensitivity (visual acuity) has major influence on the participant's performance. With increasing age temporal resolution is reduced which results in deficits in the visual processing, like increased duration of visual afterimages or altered temporal extent of visual masking [51] [64]. Especially in night-time traffic situations the perception of objects, faces or road signs are diminished with increasing age.

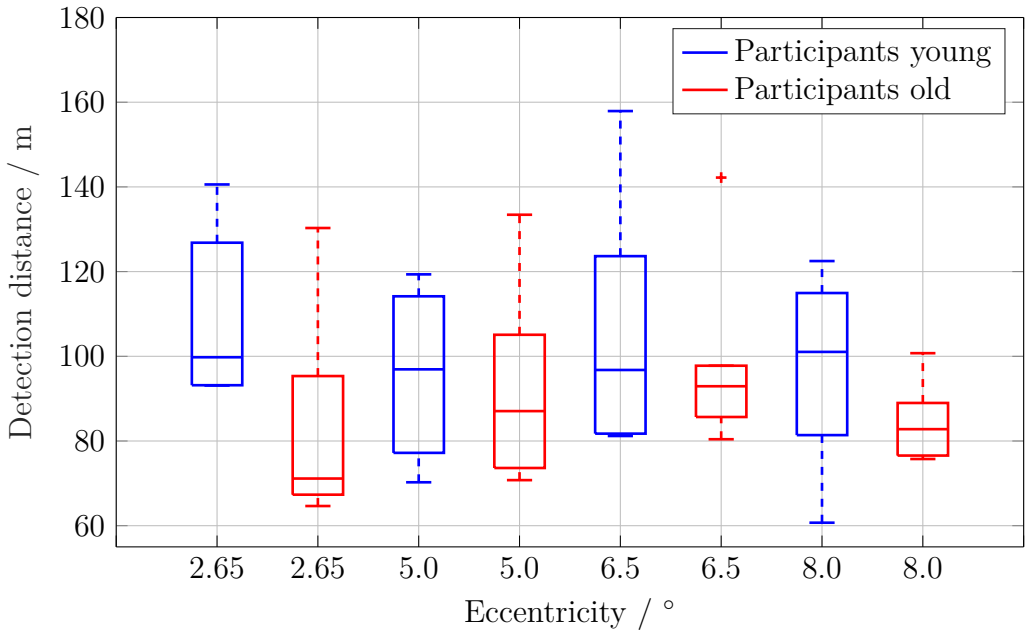


**(a)** Dynamic

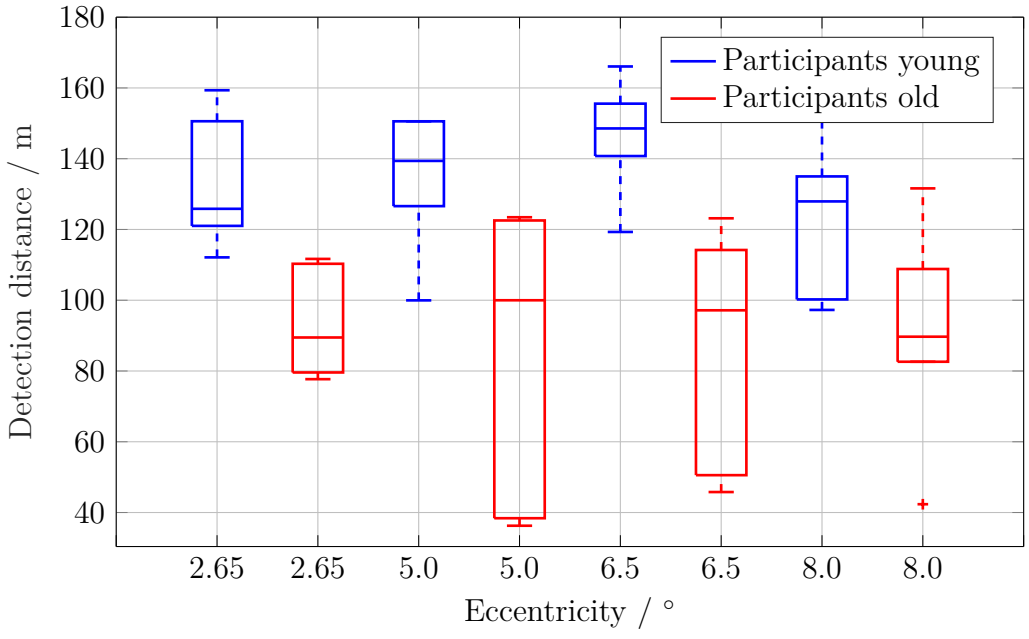


**(b)** Static

Figure 6.9: Comparison of the two age groups for human being (static vs. dynamic) as a function of the eccentricity (right of the lane: 2.65°, 5.0m; 5.0°, 9.6m; 6.5°, 12.5m; 8.0°, 15.5m).

| Detection distance / m | 2.65° | 5.0° | 6.5° | 8.0° |
|---|---|---|---|---|
| Dynamic | | | | |
| Young | 108.87 | 95.80 | 106.33 | 96.93 |
| Old | 83.31 | 92.83 | 98.65 | 84.60 |
| $\Delta_{young-old}$ | 25.56 | 2.97 | 7.68 | 12.33 |
| Static | | | | |
| Young | 132.45 | 142.28 | 146.46 | 125.88 |
| Old | 93.03 | 86.71 | 88.02 | 90.79 |
| $\Delta_{young-old}$ | 39.42 | 55.57 | 58.44 | 35.09 |

Table 6.4: Mean detection distances of all participants for two age groups, dynamic vs. static, detection object: human being.

Table 6.5 illustrates the required distances for a detection probability of 50.0%, 90.0% and 99.0% for the two age groups for both dynamic and static test setup. It can be noted that the necessary distances are significantly higher for old participants compared to young participants. Especially in the static test, clear differences in the two age groups were observed. For the simple driving task, that was constituted on the enclosed area, the threshold values for a detection were already increased. The perception threshold increased for the pedestrian by a factor of 1.7 up to 2.3, while for the deer, this factor was even slightly larger (2.5).

| Detection distance / m | | 50% probability | 90% probability | 99% probability |
|---|---|---|---|---|
| Dynamic | | | | |
| Young | 2.65° | 140.57 | 110.61 | 108.87 |
| Old | | 130.29 | 85.74 | 83.31 |
| Young | 5.0° | 119.35 | 97.12 | 95.80 |
| Old | | 133.42 | 93.32 | 92.83 |
| Young | 6.5° | 157.90 | 108.98 | 106.33 |
| Old | | 142.20 | 101.32 | 98.65 |
| Young | 8.0° | 122.49 | 97.84 | 96.93 |
| Old | | 100.73 | 86.21 | 84.60 |
| Static | | | | |
| Young | 2.65° | 159.34 | 135.74 | 132.45 |
| Old | | 111.67 | 96.45 | 93.03 |
| Young | 5.0° | 197.82 | 144.87 | 142.28 |
| Old | | 123.45 | 90.54 | 86.71 |
| Young | 6.5° | 166.06 | 150.37 | 146.46 |
| Old | | 123.15 | 91.58 | 88.02 |
| Young | 8.0° | 166.94 | 129.89 | 125.88 |
| Old | | 131.61 | 94.63 | 90.79 |

Table 6.5: Required distances for a detection probability of 50%, 90% and 99% for the two age groups, detection object: human being, comparison dynamic vs. static.

Due to the illumination, the object's background has a greater dynamic change for a moving vehicle, so the luminance on the object's surface must be increased more strongly in order to be perceived (compare Chapter 7). While the young participants came naturally to a detection, for detection probabilities of 99%, distances of less than 50.0 m were established for the old participant group, which would mean an increased risk of accident.

## 6.4 Statistical analysis

In the following paragraph the factors that have an influence on the detection distance are analysed by means of a variance analysis.

**Pre-analysis**
In order to obtain an overall view of the independent variables for the two setups, the detection distance is exploratively examined to its influence. The samples are dependent samples that are compared interpersonal. The following parameters are analysed:

- Influence of detection object's shape
- Influence of eccentricity
- Influence of participant's age
- Influence of setup type

An one-factorial variance analysis is performed for each independent variable (eccentricity, age group, detection object shape). The following Table 6.6 summarises the p-values of the analysis performed. If $p < 0.05$, the concerned influence factor needs to be tested on significance [68].

| Group | Setup | Object shape | 2.65° | 5.0° | 6.5° | 8.0° |
|---|---|---|---|---|---|---|
| Total | Dynamic | Human | 0.027 | 0.041 | 0.373 | 0.33 |
| | Static | | 0.141 | 0.149 | 0.185 | 0.125 |
| Young | Dynamic | | 0.317 | 0.155 | 0.012 | 0.459 |
| | Static | | 0.327 | 0.651 | 0.273 | 0.238 |
| Old | Dynamic | | 0.149 | 0.516 | 0.614 | 0.326 |
| | Static | | 0.327 | 0.303 | 0.143 | 0.144 |
| Total | Dynamic | Deer | 0.712 | 0.037 | 0.036 | 0.33 |
| Young | Dynamic | | 0.254 | 0.141 | 0.421 | 0.323 |
| Old | Dynamic | | 0.173 | 0.734 | 0.173 | 0.551 |

Table 6.6: One-factorial variance analysis performed for each independent variable (eccentricity, age group, detection object shape; Dependent variable: detection distance.). The analysis results are represented by p-values (significant: $p < 0.05$).

The pre-analysis of the independent variables shows that the eccentricities are related to the other independent variables object shape and setup type.

Therefore the independent variables that have an influence on the detection distance are analysed by means of a two-factorial variance analysis with measurement repeat.

**Main effects and interaction**
Table 6.7 gives an overview of the variance analysis performed. Following this, the individual influencing factors are discussed in more detail. Since a F- distribution for $(1-\alpha) = 0.95$ is assumed the critical value is $p = 0.05$. If $p < 0.05$, the concerned influence factor needs to be tested on significance [68]. The complete results of the statistical analysis can be found in Appendix C.1.

| Source | Setup | Group | Factor A | Factor B |
|---|---|---|---|---|
| Detection distance | Dynamic | Total | Object shape | Eccentricity |
| Detection distance | | Young | Object shape | Eccentricity |
| Detection distance | | Old | Object shape | Eccentricity |
| Detection distance | Dynamic vs. static | Total | Setup type | Eccentricity |
| Detection distance | | Young | Setup type | Eccentricity |
| Detection distance | | Old | Setup type | Eccentricity |

Table 6.7: Significant influencing factors and interactions in the field study.

In Table 6.8 the significant results of the two-factorial variance analysis for the dynamic test setups are presented. The main effects and also the interactions of all investigated parameter combinations (eccentricity, age group, detection object shape) were performed. Considering the dynamic test setup as result of the two-factorial variance analysis can be stated:
For the young participant group significances are determined considering the object shape for an eccentricity of 6.5°.

| Setup | Eccentricity /° | Group | Factor | p - value | significant |
|---|---|---|---|---|---|
| Dynamic | 2.65 | Total | Eccentricity | 0.0037 | no |
| | 5.0 | Total | Eccentricity | 0.002 | no |
| | 6.5 | Young | Eccentricity | 0.0255 | yes |

Table 6.8: Significant results of the two-factorial variance analysis for dynamic test setup.

As it can be seen in Table 6.9 the ratio of the dynamic to the static test was also examined on significance. The following findings were obtained:

- Overall, it can be established that for all positions, significances can be observed. While for an eccentricity of 2.65° an influence of the setup type ($p = 0.0001$) as well as a connection between the setup type and detection distance ($p = 0.0003$) exists, for the remaining three positions significances are determined with respect to the setup type.
- Considering 6.5°, significances are determined for the young participant group comparing the two detection related to the detection distance.

- In the static test setup an interaction of the age groups and detection distance is found for position 1 (p = 0.0071).
- Further influences can be determined in the two peripheral positions. At 6.5° both influences of the setup type (p = 0.0241) as well as of detection distances (p = 0.0458) are discerned for the young age group.
- Considering the old participants, significance is observed at 8.0° related to the setup type (p = 0.033) and detection distances (p = 0.0099).

| Setup | Eccentricity /° | Group | Factor | p - value | significant |
|---|---|---|---|---|---|
| Dynamic vs. static | 2.65 | Total | Setup type | 0.0001 | yes |
| | 2.65 | Total | Eccentricity | 0.0122 | no |
| | 2.65 | Total | Interaction | 0.0003 | yes |
| | 5.0 | Total | Setup type | 0.0145 | yes |
| | 5.0 | Total | Eccentricity | 0.0255 | no |
| | 5.0 | Total | Interaction | 0.0019 | no |
| | 6.5 | Total | Setup type | 0.0004 | yes |
| | 6.5 | Total | Eccentricity | 0.0067 | no |
| | 6.5 | Total | Interaction | 0.009 | no |
| | 8.0 | Total | Setup type | 0.0327 | yes |
| | 8.0 | Total | Eccentricity | 0.018 | no |
| | 6.5 | Young | Setup type | 0.0241 | yes |
| | 6.5 | Young | Eccentricity | 0.0458 | yes |
| | 8.0 | Old | Setup type | 0.033 | yes |
| | 8.0 | Old | Eccentricity | 0.0099 | yes |

Table 6.9: Significant results of the two-factorial variance analysis for the comparison of dynamic and static test setup.

## 6.5 Consequences

### 6.5.1 Driving task and conspicuity

As already mentioned, the object must be sufficiently conspicuous to provoke a detection. In many traffic situations, critical objects are placed in an environment of more noticeable stimuli, which either impede or prevent the perception. In real driving situations, there are no controllable or standardized conditions as it occurs in laboratory. Here, with conspicuousness is meant, not only the photometrically or physiological parameters, but the relation of the object to its current environment. Only an object, which is above-threshold, conspicuous and visible can be perceived by a vehicle driver. In real traffic, the perception thresholds (triggering thresholds) are determined by the driver's attention load [1]. The driver is forced to concentrate on a specific object in particular or has to balance, which object in the current situation appears to be more dangerous.

### 6.5.2 Stopping distance

The dynamic field test was performed at a speed of $80.0\frac{km}{h}$. To be able to compare the results to ordinary driving situations, the corresponding stopping distance ($d_s$= 64.0 m) and also the reaction distance ($d_r$= 24.0 m) were determined. Since the dynamic field test setup concerns an emergency braking ($d_{s_e}$= 32.0 m) the overall stopping distance $d_{ov_s}$ is calculated as follows [105]:

$$d_{ov_s} = d_{s_e} + d_r \tag{6.1}$$

with

$$d_{ov_s} = \frac{1}{2} \cdot \left(\frac{v}{10} \cdot \frac{v}{10}\right) \frac{h^2}{km^2} \cdot m + \left(\frac{v}{10} \cdot 3\right) \frac{h}{km} \cdot m \tag{6.2}$$

According to Equation 6.2 an overall stopping distance of 56.0 m, assuming a speed of $80.0\frac{km}{h}$, was calculated [6]. According to Table 6.10 it can be specified that by integrating the overall stopping distance, the detection probability descends for both age groups. In a serious situation, this could cause an accident or more serious consequences. At a speed of $80.0\frac{km}{h}$, a driver is still able to stop his vehicle in time if an object suddenly appears next to the road in a distance of 60.0 m.

| Age group | m | $d_{det,99}$ | $d_{det,99} - d_{ov,s}$ | Detection probability | $d_{det,99} - d_{ov,s100}$ |
|---|---|---|---|---|---|
| | | $80.0\frac{km}{h}$ | $80.0\frac{km}{h}$ | | $100.0\frac{km}{h}$ |
| **Young** | 2.65° | 93.10 | 37.10 | 18.12 | 13.10 |
| **Old** | | 64.60 | 8.60 | 2.78 | -15.40 |
| **Young** | 5.0° | 70.25 | 14.25 | 4.58 | -9.75 |
| **Old** | | 70.75 | 14.75 | 4.76 | -9.25 |
| **Young** | 6.5° | 81.18 | 25.18 | 9.69 | 1.18 |
| **Old** | | 80.41 | 24.41 | 9.26 | 0.41 |
| **Young** | 8.0° | 60.76 | 4.76 | 1.85 | -19.24 |
| **Old** | | 75.74 | 19.74 | 6.86 | -4.26 |

Table 6.10: Required distances for a detection probability of 99.0% ($d_{det,99}$) integrating the overall stopping distances at a speed of $80.0\frac{km}{h}$ for the two age groups, detection object: human. In addition, the calculated stopping distances at $100.0\frac{km}{h}$ ($d_{ov,s100}$) are presented as well.

As it can be seen in Figure 6.10 the faster a vehicle is, the longer is the stopping distance. At $100.0\frac{km}{h}$ this is no longer possible ($d_{ov_s}$= 80.0 m), as the driver dashes against the object (in this case the stag) with a terminal velocity of more than $60.0\frac{km}{h}$. According to the detection distances the calculated stopping distances at a speed of $100.0\frac{km}{h}$ are presented in Table 6.10 as well. A comparison is, however, only possible to a limited extent, since the investigation was performed at a speed of $80.0\frac{km}{h}$, which is based on other boundary conditions. Hence, this assumption can not simply be transferred to a higher speed. The calculated distances can therefore only be seen as reference values and serve only for comparison purposes.
The findings clearly reveal that an accident would be unavoidable under most of

the test conditions, as the overall stopping distance exceeds the visibility distance considerably (up to 19.24 m).
It can be concluded that the illumination level of the required roadside areas and in front of the vehicle is still insufficient in terms of the visual field. Even for young participants it would be practically inprobable to detect an object at the right time, as the theoretical ultimate distance to the object would be less than 5.0 m, which is too close, to prevent an accident. In real driving situations at night-time, the attention of the driver, characterictics of the road surface (dry, wet, reflection coefficient) and quality of the vehicle's braking systems are additional factors that need to be considered.

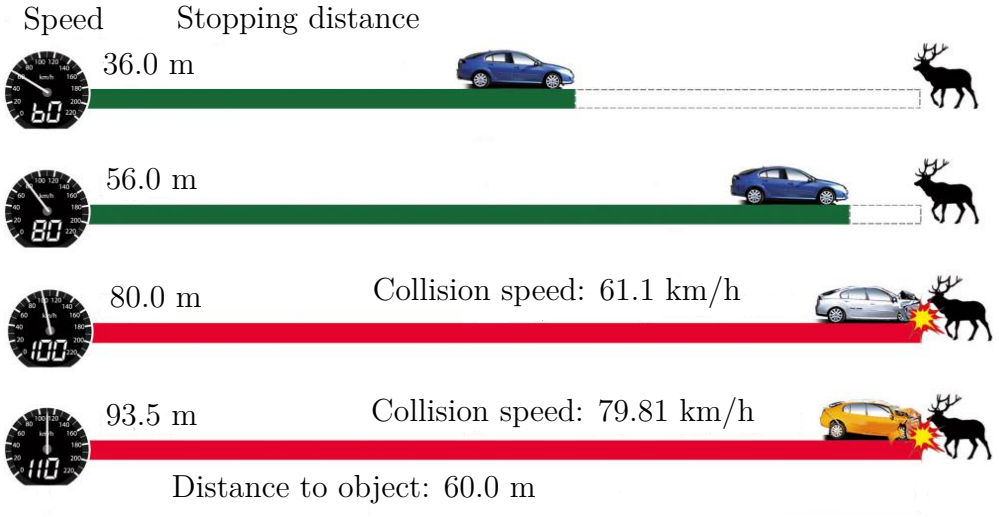


Figure 6.10: Overall stopping distance (emergency braking) for different vehicle velocities ($60.0\frac{km}{h}$, $80.0\frac{km}{h}$, $100.0\frac{km}{h}$, $110.0\frac{km}{h}$) for a distance of 60.0 m to the vehicle according to [29].

Summing up the age-related results for both object shapes it can be concluded that there is a noticeable difference between the two age groups. Overall the young participants were able to detect the objects earlier which is a benefit in emergency situations in relation to accident prevention.

## 6.6 Summary

In this chapter the setup, procedure as well as the results of a field study were presented. Two target shapes that occur in road traffic situations were observed under different eccentricities. Two measurement methods, static and dynamic, were developed for determining the detection distance.
The influence of detection object's shape, eccentricity, participant's age and setup type were discussed. Evaluating the detection distance results regarding the influence of the object shape for all participants, it can be concluded that the results were similar for both target shapes.
Considering the participants in two separate age groups clear distinctions could be established, especially the detection behaviour of the old subjects was considerably

lower compared to young participants.
Significant deviations between the static and dynamic test results could be determined. It can be noted that it was much more difficult to the old participants to detect an object, as the detection distance remained at the same level as for the dynamic test (compare Figure 6.9). Because of age-related aspects that were presented previously (e.g. presbyopia, senile miosis or cataract), old participants need to be closer to the object to be able to detect it.
To compare the results to ordinary driving situations, the corresponding overall stopping distance $d_{ov_s}$ was determined. Assuming a drive with a higher speed like $100.0\frac{km}{h}$, it could be revealed, that an accident would be unavoidable under most of the test conditions, as the overall stopping distance exceeds the visibility distance considerably (up to 19.24 m for $d_{ov_s}$= 80.0 m). Even for young participants it would be practically improbable to detect an object at the right time.

From the findings it can be concluded that the illumination level of the required roadside areas and in front of the vehicle in terms of the visual field is still insufficient. Further influencing factors as the attention of the driver, wheater conditions or road surface characteristics should also be taken into account.
In a next step the results for increment contrast functions based on the determined detection distances are analysed. The purpose here is to find out how much contrast is necessary to detect an object under a certain condition.
Methods to determine and evaluate the contrast of detection objects will be introduced, analysed and finally compared to each other.

# Chapter 7

# Contrast evaluation

In classical physiology it is assumed that seeing mainly consists of the perception of brightness differences or contrasts. Other models interpret the visual system as a contrast filter with special transmittances for the spatial and temporal frequencies of visual objects [48]. However, contrast is defined as the ability of the eye to perceive luminance differences and is therefore used as relevant stimulus size. This chapter is concerned with the contrast perception and measurement in night-time traffic situations. Several methods to determine and evaluate the contrast for a detection object will be analysed. A recommendation for the contrast determination of real detection objects will be given.

## 7.1 Luminance measurements

In the area ahead of the vehicle the luminance range is between 1.0 and $10.0\frac{cd}{m^2}$. Thus, the most common fixation point of the driver is determined by the lower sensitivity limit of the cones. The used luminance measurement device (LMK 5, TechnoTeam [40]) is able to measure low luminances of $0.001\frac{cd}{m^2}$.
As real objects appear alongside or straight on the road, the detection distance is between 40.0 m and 100.0 m. Therefore, the luminance measurement a lens with a high focal length ($f \geq 100.0$ mm) should be used. Only then, a sufficient resolution is ensured with a corresponding high pixel number ($> 1.5$ pixels per mm) [40]. In addition, the lens should be able to image the objects sharply in the range between 20.0 m to 120.0 m. Since driving a vehicle is a dynamic process, another requirement is a dynamically image-resolved luminance measurement, in order to record the perception features as realistic as possible. Nevertheless, the available camera technologies reach their limits, caused by their limited sensitivity and thus connected long exposure times. Therefore, only static luminance measurements are possible so far.

### 7.1.1 Measurement of small luminances

For the assessment of the luminous intensity distribution of headlamps, the evaluation of luminance images is also important. In this case, only very small luminance values between $0.001\frac{cd}{m^2}$ and $10.0\frac{cd}{m^2}$ are considered. Generally, the distances ahead of the vehicle, that are of interest are in distance between 7.0 m to 110.0 m. This means the measurements need to be performed with a integration time as long as possible, to achieve a resolution that is high enough [40]. This corresponds to the maximum

resolution capacity of the human eye (under photopic conditions). Since this capacity is significantly smaller under mesopic conditions, there are still enough pixels for an analysis by means of image arithmetic of average luminances. Measuring the luminance on the surface of an object is comparable to luminance measurements of road surfaces. Nevertheless, the luminance values (from $0.01\frac{cd}{m^2}$ to $0.1\frac{cd}{m^2}$) are even lower compared to those of roads. Because of the low luminance, long integration times are necessary. As the objects to be measured are located in distances between 45.0 and 110.0 m a correspondingly high geometric resolution is required to provide the object's edges with sufficient accuracy. It should be noted that the smallest measurable structure width of an object that is not perpendicular to the optical axis, decreases drastically with the distance into longitudinal direction [5].

### 7.1.2 Luminance pictures

Luminance pictures were taken by a luminance measuring camera type LMK 5 from the company TechnoTeam [40]. With this camera luminous and illuminated scenes by means of the photograph of an image-resolved luminance distribution can be evaluated. The technical data can be found in Table 7.1. With this kind of measurement the analysis of visibility conditions in the road traffic at night, means recording the luminance distribution within the whole visual field or at least many selected parts of it, is possible. The luminance picture is analysed point by point measuring self-luminous and illuminated surfaces in front of the headlamps. The system is also able to capture complex light distributions and can be adapted for the determination of contrasts.

| Parameter | Features |
|---|---|
| Sensor | CCD, imaging matrix system<br>Standard resolution: 1380 x 1030 pixel<br>Higher resolution: 2448 x 2050 pixel,<br>4008 x 2672 pixel, 4008 x 4008 pixel |
| Resolution (dynamic) | Single picture measurement: 1:1100 (61 dB)<br>Multi picture measurement: 1:3600 (71 dB)<br>High dynamic measurement: 1:10000000 (140 dB)<br>A/D conversion: 12 / 14 bit |
| Measurement time | From 1.0 to 15.0 s for different luminances,<br>depending on adjusted exposure time |
| Measurement accuracy | $\Delta$ L < 3% (for standard illuminant A)<br>$\Delta$ x,y < 0.0020 (for standard illuminant A) |
| Spectral matching | With full size filter matched to<br>$V(\lambda)$-function to measure luminances<br>arranged with $\tilde{X}(\lambda)$-, $V(\lambda)$- and $\tilde{Z}(\lambda)$-filter for<br>measuring colour values |

Table 7.1: Technical data of the luminance camera LMKcolor from TechnoTeam [40].

## 7.2 Contrast determination for real objects

A general problem in contrast determination of an object is to define the transition from the object to its background, meaning the edges of the object. Often the object's edges have blurred lines and depending on the dimensions of the object and background the average luminances vary also. If the available models can be applied for the "grey card" (depending on the luminous intensity distribution curve), the question is still, if the results can be transferred to real visual objects. As shown in literature almost exclusively grey cards were used as detection objects. The determination of the size of the detection object is complicated, e.g. a pedestrian is taller and bigger than a rabbit or a dog and has completely different attributes.
One possibility is to calculate the contrast from the object's detection distance. Therefore, the question is, which factors have a bearing on the driver's detection distance according to the headlamp system. The parameters to be examined are:

- Luminance on object's surface (depending on size, shape and position)
- Luminance ahead of the vehicle (depending on position/ sharpness of the cut-off line)

The correlation of the single parameters and their weighting with regard to the detection distance are considered below.

### 7.2.1 Illuminance based model

One of the most common methods is to predict the detection distance from the illumination. Earlier studies have shown that this model is not very suitable for calculating the detection distance [74] [34]. Therefore, this model is not considered further in the following course of this work.

### 7.2.2 Eckert model

Eckert determines the luminance difference $\Delta L$ of a pedestrian using measurement points (compare Figure 4.19). In Figure 7.1 an example is determined using the principle of Eckert's model. In a first step the luminance values from 13 measurement points on the pedestrian's surface and also 13 points on pedestrian's environment are determined.
In Table 7.2 the corresponding luminance values of the object and background luminance are presented.

| Measurement points | $L_{min}/\ \frac{cd}{m^2}$ | $L_{max}/\ \frac{cd}{m^2}$ | $L_{mean}/\ \frac{cd}{m^2}$ |
|---|---|---|---|
| Object | 0.013 | 0.121 | 0.088 |
| Background | 0.048 | 0.060 | 0.032 |

Table 7.2: Luminance analysis of a pedestrian according to [5]. 13 luminance measurement points on pedestrian's surface and also 13 points along pedestrian's outline.

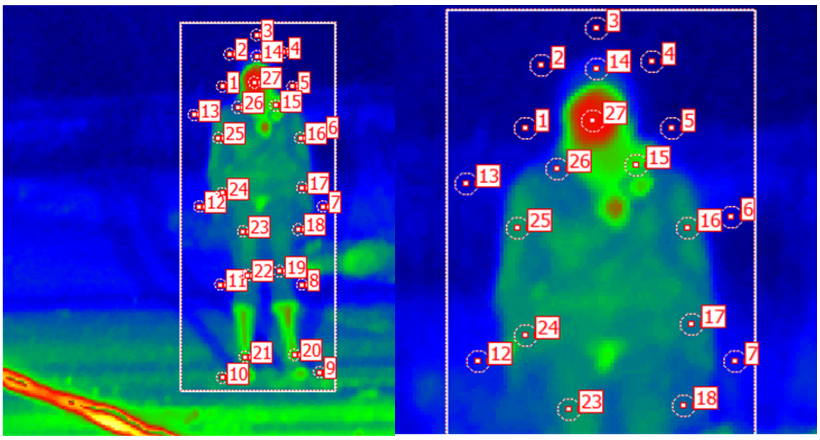


Figure 7.1: Measurement points for luminance analysis of a pedestrian according to [5] (80.0 m distance to the vehicle besides the road). Left hand side: luminance values from 13 measurement points on pedestrian's surface and also 13 points along pedestrian's outline. Right hand side: close-up image.

The values are determined from the mean values of all measurement points. The measurement points are located close to the transition from the silhouette of the object to its background. Subsequent, the average contrast $K$ can be calculated by means of the luminance points as follows:

$$K = \frac{(0.088 - 0.032)\frac{cd}{m^2}}{0.032\frac{cd}{m^2}} = 1.75 \tag{7.1}$$

It can be stated that the model of Eckert is not suitable for a prediction of contrast since it takes only the average contrast into consideration. Hence, the detection distance is calculated if the size of the object is known.
Depending on the course of the luminance on the object's surface, the overall resulting luminance changes (in this case the face and the gumboots of the pedestrian have a significantly higher luminance). Therefore, this method has to be individually adapted to the luminance image and is therefore not suitable for reproducibility.

### 7.2.3 Kokoschka model

For the application of Kokoschka's model, one can start with calculation step number 4 (compare Equation 4.45), since the evaluation is conducted by using the luminance picture.
An edge contrast is calculated for each adjacent edge of the detection object and its background (compare Figure 7.2). In this case the outlines of the human and deer are taken as "edges". In the following, the edge contrast approach of Kokoschka's model is also applied to the own test results.

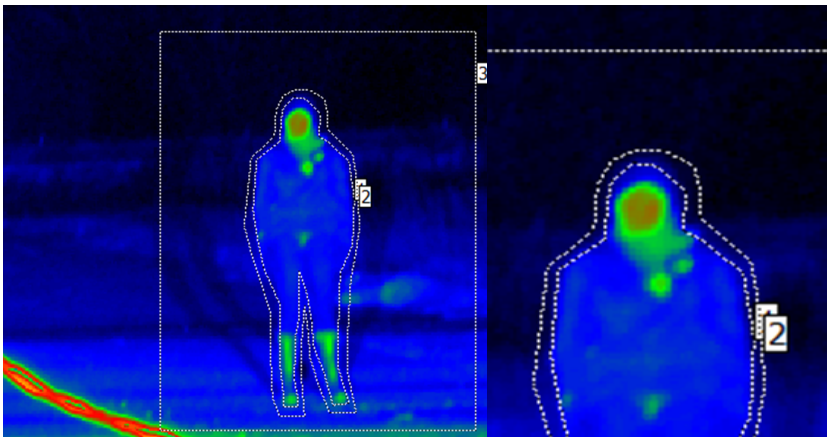


Figure 7.2: Edge contrast determination for a pedestrian (80.0 m distance to the vehicle besides the road). Left hand side: edge contrast for the outline of the detection object and its background. Right hand side: close-up image.

### 7.2.4 Pedestrian contrast determination

Table 7.3 shows the detection distances determined in the field study for the human's positions. Based on the detection distances luminance pictures were taken and evaluated. Figure 7.3 shows an example of the human standing on roadside (5.0 m) for different detection distances from 80.0 m to 110.0 m. From Figure 7.4 it can be seen that the luminance values on both the object's surface and in the background become smaller with increasing distance.

| Age group | Detection distance / m | | | |
|---|---|---|---|---|
| | 5.0 m | 9.6 m | 12.5 m | 15.5 m |
| total | 93.18 | 94.52 | 92.88 | 84.07 |
| young | 108.87 | 95.80 | 106.33 | 96.93 |
| old | 83.31 | 92.83 | 98.65 | 84.60 |

Table 7.3: Mean detection distances of the human being for the two participant groups.

The corresponding luminance values of the environment, the object's surface and the object's outline are listed in Table 7.4. At a distance of 80.0 m, a contrast value of 5.62 can be determined. From this distance, the contrast is continuously reduced and decreases to a contrast of 3.62 at a distance of 110.0 m. If one considers the human's second position (9.6 m beside the road), it can be noted that a contrast of 6.14, which is even higher, can be determined at a distance of 80.0 m (compare Figure 7.5). In this case the contrast also drops with increasing distance. For the remaining two positions, the contrast values are significantly lower, mainly due to the decreasing background luminance towards the roadside. While the contrast is still 6.14 at 9.6 m alongside the road at a distance of 80.0 m, it already drops to 4.78 at a distance of 15.5 m. In Figures 7.5 to 7.7 the results of the remaining object's positions are presented.

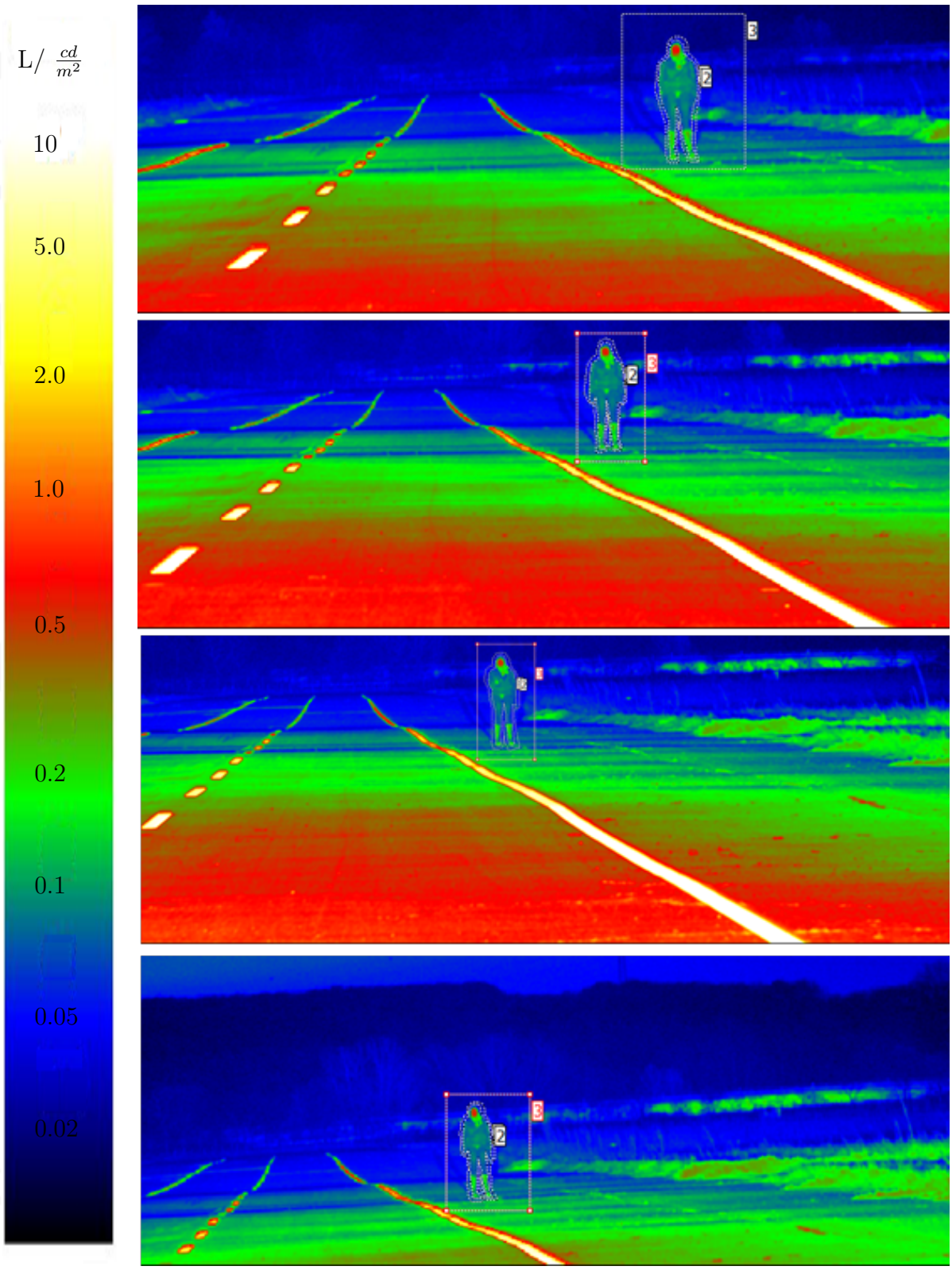


Figure 7.3: Luminance picture: human being placed 5.0 m beside the road in driver's vision field (position 1) at distances of 80.0 m, 90.0 m, 100.0 m and 110.0 m (from top to bottom).

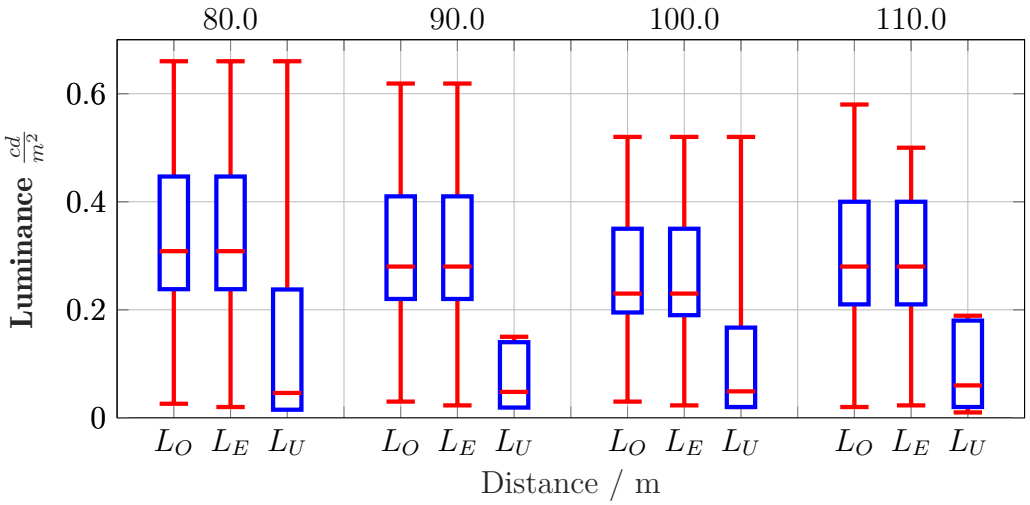


Figure 7.4: Corresponding luminance values of the object ($L_O$), object's edges ($L_E$) and background ($L_U$) to the determined detection distances. Object shape: human, 5.0 m beside the road.

| Distance | Position | $L_O$ / $\frac{cd}{m^2}$ | $L_E$ / $\frac{cd}{m^2}$ | $L_U$ / $\frac{cd}{m^2}$ | Contrast |
|---|---|---|---|---|---|
| 80.0 m | 1 | 0.3085 | 0.3082 | 0.0466 | 5.62 |
| 90.0 m | | 0.2828 | 0.2827 | 0.0493 | 4.73 |
| 100.0 m | | 0.2348 | 0.2346 | 0.0550 | 3.26 |
| 110.0 m | | 0.2814 | 0.2810 | 0.0609 | 3.62 |

Table 7.4: Determined contrast and corresponding luminance values of the object ($L_O$), object's edges ($L_E$) and background ($L_U$) to the determined detection distances. Object shape: human, 5.0 m (position 1) beside the road.

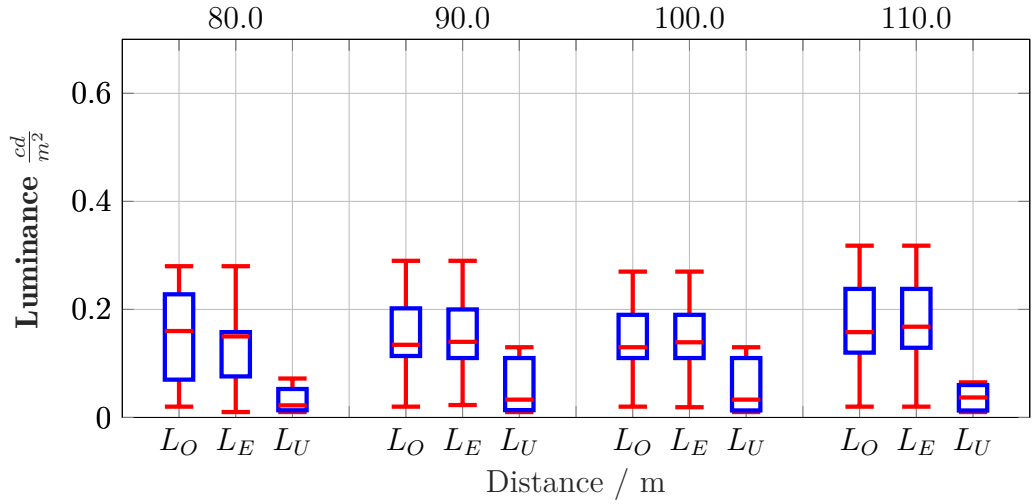


Figure 7.5: Corresponding luminance values of the object ($L_O$), object's edges ($L_E$) and background ($L_U$) to the determined detection distances. Object shape: human, 9.6 m (position 2) beside the road.

| Distance | Position | $L_O$ / $\frac{cd}{m^2}$ | $L_E$ / $\frac{cd}{m^2}$ | $L_U$ / $\frac{cd}{m^2}$ | Contrast |
|---|---|---|---|---|---|
| 80.0 m | 2 | 0.1608 | 0.1553 | 0.0224 | 6.14 |
| 90.0 m | | 0.1341 | 0.1473 | 0.0331 | 3.04 |
| 100.0 m | | 0.1340 | 0.1491 | 0.0330 | 3.06 |
| 110.0 m | | 0.1580 | 0.1686 | 0.0307 | 4.14 |

Table 7.5: Corresponding luminance values of the object ($L_O$), object's edges ($L_E$) and background ($L_U$) to the determined detection distances. Object shape: human, 9.6 m beside the road.

As can be seen from the results in Tables 7.5 to 7.7, the marginal object positions show a similar behaviour as for the pedestrian directly placed next to the road. As expected, the luminance decreases continuously, which leads to a reduction in the contrast values.

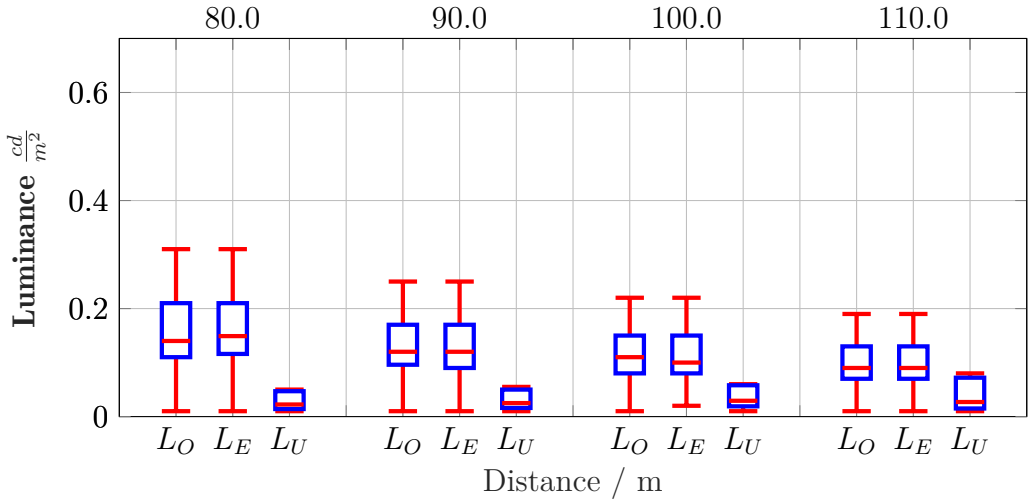


Figure 7.6: Corresponding luminance values of the object ($L_O$), object's edges ($L_E$) and background ($L_U$) to the determined detection distances. Object shape: human, 12.5 m beside the road.

| Distance | Position | $L_O$ / $\frac{cd}{m^2}$ | $L_E$ / $\frac{cd}{m^2}$ | $L_U$ / $\frac{cd}{m^2}$ | Contrast |
|---|---|---|---|---|---|
| 80.0 m | 3 | 0.1471 | 0.1493 | 0.0221 | 5.65 |
| 90.0 m | | 0.1239 | 0.1218 | 0.0255 | 3.85 |
| 100.0 m | | 0.1114 | 0.1046 | 0.0293 | 2.80 |
| 110.0 m | | 0.0923 | 0.0919 | 0.0270 | 2.41 |

Table 7.6: Determined contrast and corresponding luminance values of the object ($L_O$), object's edges ($L_E$) and background ($L_U$) to the determined detection distances. Object shape: human, 12.5 m beside the road.

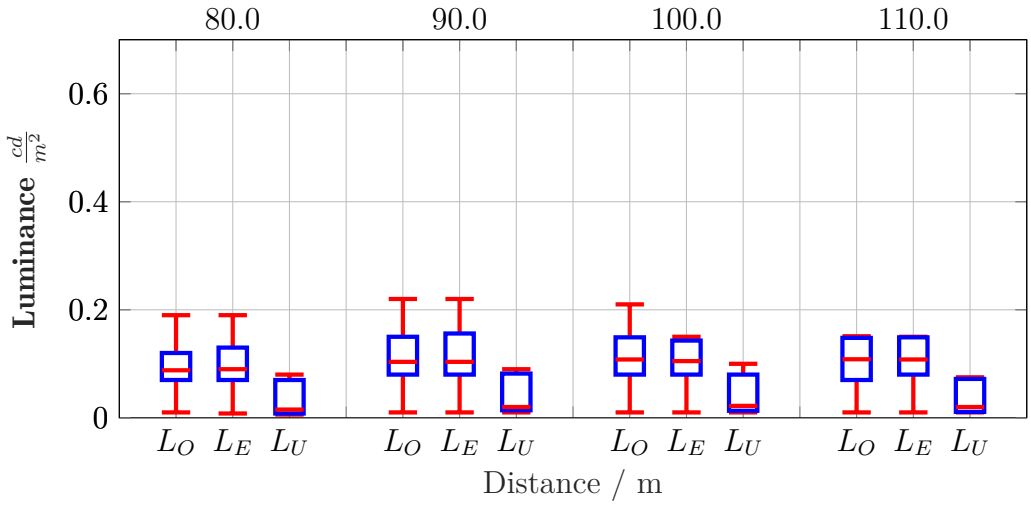


Figure 7.7: Corresponding luminance values of the object ($L_O$), object's edges ($L_E$) and background ($L_U$) to the determined detection distances. Object shape: human, 15.5 m beside the road.

| Distance | Position | $L_O$ / $\frac{cd}{m^2}$ | $L_E$ / $\frac{cd}{m^2}$ | $L_U$ / $\frac{cd}{m^2}$ | Contrast |
|---|---|---|---|---|---|
| 80.0 m | 4 | 0.0885 | 0.0897 | 0.0153 | 4.78 |
| 90.0 m | | 0.1060 | 0.1036 | 0.0216 | 3.91 |
| 100.0 m | | 0.1084 | 0.1035 | 0.0221 | 3.90 |
| 110.0 m | | 0.1083 | 0.1081 | 0.0196 | 4.52 |

Table 7.7: Determined contrast and corresponding luminance values of the object ($L_O$), object's edges ($L_E$) and background ($L_U$) to the determined detection distances. Object shape: human, 15.5 m beside the road.

### 7.2.5 Deer contrast determination

Table 7.8 shows the detection distances determined in the field study for the deer's positions. Considering Figure 7.8 it can be noted that the luminance values on both the object's surface and in the background become smaller with increasing distance. At a distance of 80.0 m, a contrast of 6.26 can be determined. The contrast decreases continuously to 2.27 at a distance of 110.0 m. The corresponding luminance values of the environment, the object's surface and the object's outline are listed in Table 7.9.

| Age groups | Detection distance / m | | | |
|---|---|---|---|---|
| | 5.0 m | 9.6 m | 12.5 m | 15.5 m |
| total | 96.85 | 95.51 | 90.36 | 84.17 |
| young | 108.84 | 103.72 | 104.21 | 87.97 |
| old | 91.67 | 86.58 | 102.73 | 84.60 |

Table 7.8: Mean detection distances of the deer for the two participant groups

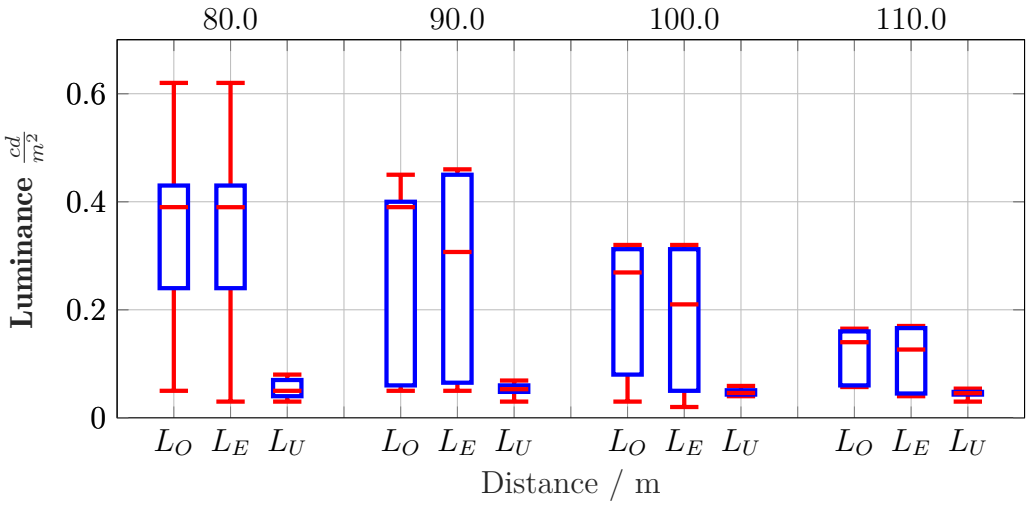


Figure 7.8: Luminance picture: deer placed 5.0 m beside the road in driver's vision field (position 1) at distances of 80.0 m, 90.0 m, 100.0 m and 110.0 m (from top to bottom).

| Distance | Position | $L_O$ / $\frac{cd}{m^2}$ | $L_E$ / $\frac{cd}{m^2}$ | $L_U$ / $\frac{cd}{m^2}$ | Contrast |
|---|---|---|---|---|---|
| 80.0 m | 1 | 0.3925 | 0.3889 | 0.0545 | 6.26 |
| 90.0 m | | 0.3935 | 0.3070 | 0.0530 | 6.42 |
| 100.0 m | | 0.2691 | 0.2193 | 0.0461 | 4.83 |
| 110.0 m | | 0.1495 | 0.1264 | 0.0456 | 2.27 |

Table 7.9: Corresponding luminance values of the object ($L_O$), object's edges ($L_E$) and background ($L_U$) to the determined detection distances. Object shape: deer, 5.0 m beside the road.

As it can be seen in Figure 7.9, at the object's second position the contrast declines to 3.40 at 80.0 m.

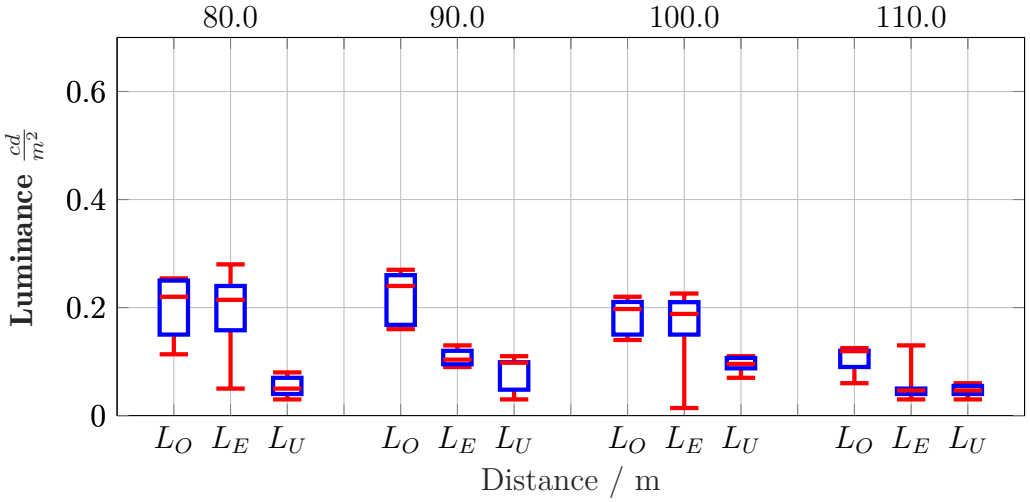


Figure 7.9: Luminance picture: deer placed 9.6 m beside the road in driver's vision field (position 1) at distances of 80.0 m, 90.0 m, 100.0 m and 110.0 m (from top to bottom).

| Distance | Position | $L_O$ / $\frac{cd}{m^2}$ | $L_E$ / $\frac{cd}{m^2}$ | $L_U$ / $\frac{cd}{m^2}$ | Contrast |
|---|---|---|---|---|---|
| 80.0 m | 2 | 0.2224 | 0.2143 | 0.0512 | 3.40 |
| 90.0 m | | 0.2425 | 0.1036 | 0.0098 | 1.44 |
| 100.0 m | | 0.1973 | 0.1882 | 0.0957 | 1.06 |
| 110.0 m | | 0.1193 | 0.0466 | 0.0466 | 1.56 |

Table 7.10: Corresponding luminance values of the object ($L_O$), object's edges ($L_E$) and background ($L_U$) to the determined detection distances. Object shape: deer, 9.6 m beside the road.

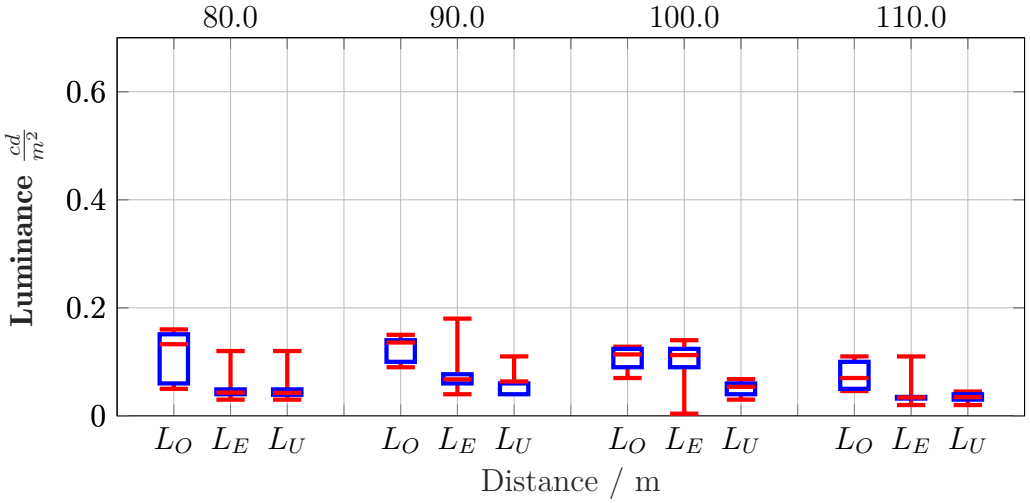


Figure 7.10: Luminance picture: deer placed 12.5 m beside the road in driver's vision field (position 1) at distances of 80.0 m, 90.0 m, 100.0 m and 110.0 m (from top to bottom).

| Distance | Position | $L_O$ / $\frac{cd}{m^2}$ | $L_E$ / $\frac{cd}{m^2}$ | $L_U$ / $\frac{cd}{m^2}$ | Contrast |
|---|---|---|---|---|---|
| 80.0 m | 3 | 0.1326 | 0.0430 | 0.0426 | 2.11 |
| 90.0 m | | 0.1358 | 0.0676 | 0.0638 | 1.12 |
| 100.0 m | | 0.1137 | 0.1125 | 0.0537 | 1.11 |
| 110.0 m | | 0.0761 | 0.0341 | 0.0346 | 1.33 |

Table 7.11: Corresponding luminance values of the object ($L_O$), object's edges ($L_E$) and background ($L_U$) to the determined detection distances. Object shape: deer, 12.5 m beside the road.

Observing the same position in a distance of 90.0 m, the contrast falls off by factor 2.4 to 1.44 (compare Table 7.10). From smaller distances to the road out to the periphery, the values get smaller and decrease at position 3 to 2.11 and at position 4 to 2.07 at 80.0 m distance (compare Figures 7.10 and 7.11).
In the furthest position outwards (15.5 m beside the road) it can be observed that starting from a distance of 90.0 m the contrast falls below 1.0, which means that the detection object is no longer recognizable under real circumstances.

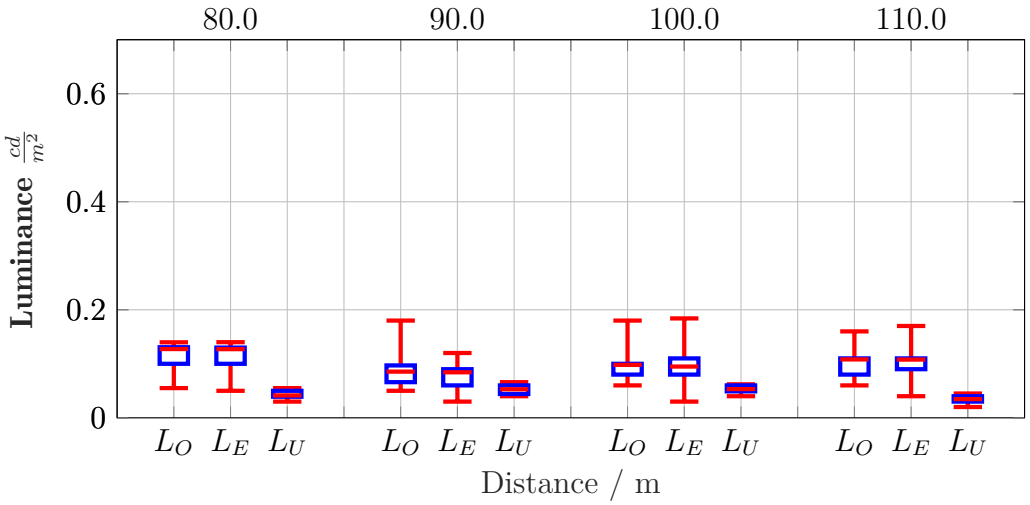


Figure 7.11: Luminance picture: deer placed 5.0 m beside the road in driver's vision field (position 1) at distances of 80.0 m, 90.0 m, 100.0 m and 110.0 m (from top to bottom).

| Distance | Position | $L_O$ / $\frac{cd}{m^2}$ | $L_E$ / $\frac{cd}{m^2}$ | $L_U$ / $\frac{cd}{m^2}$ | Contrast |
|---|---|---|---|---|---|
| 80.0 m | 4 | 0.1273 | 0.1271 | 0.0415 | 2.07 |
| 90.0 m | | 0.0855 | 0.0843 | 0.0528 | 0.61 |
| 100.0 m | | 0.0980 | 0.0949 | 0.0531 | 0.84 |
| 110.0 m | | 0.1081 | 0.1078 | 0.0583 | 0.85 |

Table 7.12: Corresponding luminance values of the object ($L_O$), object's edges ($L_E$) and background ($L_U$) to the determined detection distances. Object shape: deer, 15.5 m beside the road.

### 7.2.6 Comparison of the object shapes

The aim is to attain differences between individual objects. The resulting inclinations between individual objects are indicated. Therefore, the object size is considered first. Here one must distinguish between 175.0 cm × 40.0 cm (human) and 140.0 cm × 140.0 cm (deer). The following tendencies can be observed for a detection probability of 99.0%: for the detection of the deer, the necessary contrast decreases even more sharply since the surface of the deer has a more homogeneous illuminated surface. While the pedestrian has higher contrast values within a range of 4 to 6 due to its bright face, the deer can not be perceived any longer in periphery. Table 7.13 gives an overview of the contrast results of both objects. In summary, the contrast of both detection objects decreases with both increasing peripheral eccentricities and distance to the test vehicle. Considering the detection distances in relation to the age groups, following insights can be noted: for the detection of a pedestrian that appears next to the road, a person of 45 years and above needs a by factor of 1.7 higher contrast than a young person (compare Table 7.13).

In comparison, a larger difference between the two age groups is determined for the deer, when it is located directly on roadside. In this case, older participants

need an almost threefold contrast compared to young participants. However, in the peripheral region, the two age groups present the same behaviour. This can be attributed to the very low background luminances, which makes it nearly impossible to detect the deer due to the low contrast ratio.

| Distance | Position | $L_{O_P}$ / $\frac{cd}{m^2}$ | Contrast human | $L_{O_D}$ / $\frac{cd}{m^2}$ | Contrast deer |
|---|---|---|---|---|---|
| | | | | | |
| 80.0 m | 1 | 0.3085 | 5.62 | 0.3925 | 6.26 |
| 90.0 m | | 0.2828 | 4.73 | 0.3935 | 6.42 |
| 100.0 m | | 0.2348 | 3.26 | 0.2691 | 4.83 |
| 110.0 m | | 0.2814 | 3.62 | 0.1495 | 2.27 |
| | | | | | |
| 80.0 m | 2 | 0.1608 | 6.14 | 0.2224 | 3.46 |
| 90.0 m | | 0.1341 | 3.04 | 0.2425 | 1.44 |
| 100.0 m | | 0.1340 | 3.06 | 0.1973 | 1.06 |
| 110.0 m | | 0.1580 | 4.14 | 0.1193 | 1.56 |
| | | | | | |
| 80.0 m | 3 | 0.1471 | 5.65 | 0.1326 | 2.11 |
| 90.0 m | | 0.1239 | 3.85 | 0.1358 | 1.12 |
| 100.0 m | | 0.1114 | 2.80 | 0.1137 | 1.11 |
| 110.0 m | | 0.0923 | 2.41 | 0.0761 | 1.33 |
| | | | | | |
| 80.0 m | 4 | 0.0885 | 4.78 | 0.1273 | 2.07 |
| 90.0 m | | 0.1060 | 3.91 | 0.0855 | 0.06 |
| 100.0 m | | 0.1084 | 3.90 | 0.0980 | 0.08 |
| 110.0 m | | 0.1083 | 4.52 | 0.1081 | 0.08 |

Table 7.13: Determined contrast values based on the detection distances for a 99.0% detection probability for the two detection objects. $L_{O_P}$: Luminance on pedestrian's surface, $L_{O_D}$: Luminance on deer's surface.

## 7.3 Edge detection

An alternative to analyse the object and background luminance is image processing. For a validation of the determined luminance value, this approach was implemented in Matlab to trace the object's boundaries in the luminance image [119]. As can be seen in Figure 7.12 the luminance picture is converted into a binary picture (including the luminance values) that is dependent on a threshold luminance value.
Here, the term "threshold luminance value" expresses the contrast that was determined from the luminance pictures relating to the computed detection distances. Based on this threshold luminance value the used algorithm traces the exterior boundaries of objects, as well as boundaries of holes inside these objects, in the binary image. It is also able to descend into the outermost objects and trace objects completely enclosed by these objects. In the binary image nonzero pixels belong to an object and zero pixels constitute the background.

Figure 7.12 shows an example for the application of the algorithm for the detection of the pedestrian. For this purpose, a threshold value is initially defined to determine the edges within the image. Figures 7.12a, 7.12c and 7.12e illustrate the results for the luminance thresholds of $0.11\frac{cd}{m^2}$, $0.23\frac{cd}{m^2}$ and $0.33\frac{cd}{m^2}$. In Table 7.14 the determined object luminance values are compared to the corresponding object luminances evaluated from the luminance picture. While for a threshold of $0.11\frac{cd}{m^2}$, the contour of the pedestrian can still clearly be seen (gum foot, head region), the extremities are only slightly recognizable at a threshold of $0.23\frac{cd}{m^2}$.

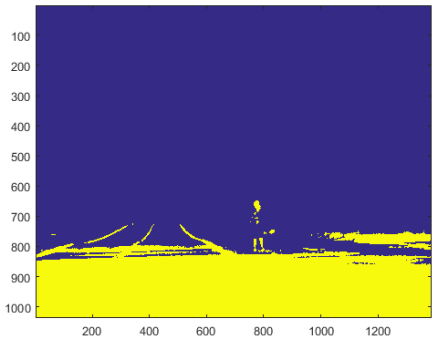


**(a)** Threshold $0.11\frac{cd}{m^2}$

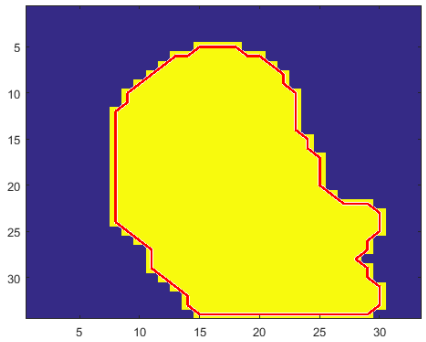


**(b)** Pedestrian's head outline

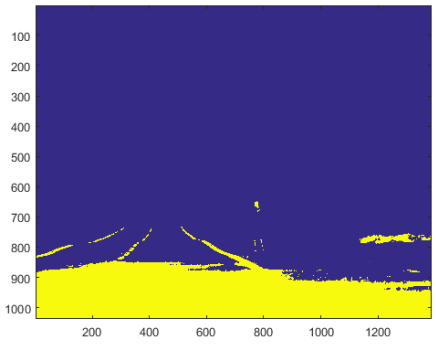


**(c)** Threshold $0.23\frac{cd}{m^2}$

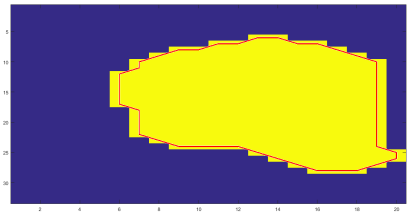

**(d)** Pedestrian's head outline

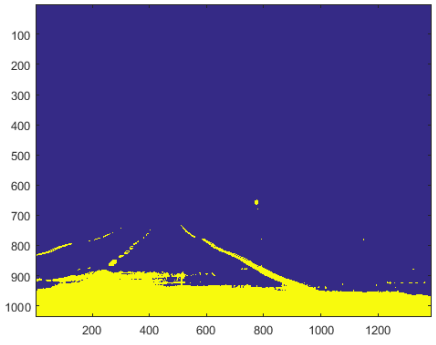


**(e)** Threshold $0.33\frac{cd}{m^2}$

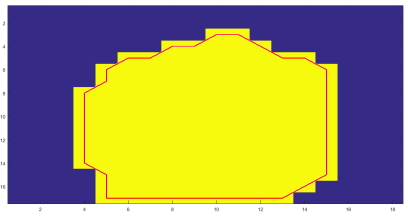

**(f)** Pedestrian's head outline

Figure 7.12: Image processing using Matlab. Pedestrian at position 1 (5.0 m) in a distance of 80.0 m. Left hand side: determined edges based on corresponding threshold values. Right hand side: exterior boundaries of the pedestrian's head.

| Distance | Position | $L_O$ / $\frac{cd}{m^2}$ | $L_{O_{\text{Matlab}}}$ / $\frac{cd}{m^2}$ | $\Delta_{\text{camera}-\text{Matlab}}$ |
|---|---|---|---|---|
| | | | | |
| 80.0 m | 1 | 0.3085 | 0.2685 | 0.04 |
| 90.0 m | | 0.2828 | 0.2462 | 0.04 |
| 100.0 m | | 0.2348 | 0.1997 | 0.12 |
| 110.0 m | | 0.2814 | 0.2952 | -0.01 |
| | | | | |
| 80.0 m | 2 | 0.1608 | 0.1847 | -0.02 |
| 90.0 m | | 0.1341 | 0.1427 | -0.09 |
| 100.0 m | | 0.1340 | 0.1375 | -0.04 |
| 110.0 m | | 0.1580 | 0.1420 | 0.02 |
| | | | | |
| 80.0 m | 3 | 0.1471 | 0.1337 | 0.01 |
| 90.0 m | | 0.1239 | 0.1123 | 0.01 |
| 100.0 m | | 0.1114 | 0.1145 | -0.03 |
| 110.0 m | | 0.0923 | 0.0860 | 0.01 |
| | | | | |
| 80.0 m | 4 | 0.0885 | 0.0739 | 0.01 |
| 90.0 m | | 0.1060 | 0.1039 | 0.01 |
| 100.0 m | | 0.1084 | 0.0948 | 0.01 |
| 110.0 m | | 0.1083 | 0.0918 | 0.02 |

Table 7.14: By image processing determined object luminances compared to the corresponding object luminances evaluated from the luminance picture.

Finally, for a threshold of $0.33\frac{cd}{m^2}$, which is determined by means of the luminance image, only a small circular area can be observed at the corresponding point at which the head of the pedestrian is located. This image therefore corresponds to the image, which the participant perceives at the moment of detection.
It can be concluded, that the pedestrian was detected by his face. Figure 7.13 shows the imaging process based on the deer, which is located at positions 1 to 4 in a distance of 80.0 m. As can be seen from the Figures 7.13a to 7.13g, the background also changes with the position of the object. While at position 1, the contour of the deer can be clearly distinguished from the environment, this changes especially for the two peripheral positions. The deer's outline is integrated into the background and is no longer clearly recognizable (legs disappear in long grass). Therefore it can be seen that the necessary conspicuity and visibility is no longer present, which leads to a considerably more difficult detection.

Since a definition of the distinctive object features is inconclusive to determine, an additional definition of both luminances based on participants' statements were incorporated. The statements of the participants were queried with a questionnaire (after executing the investigation), that is referred in Appendix D. The participants were asked which of the two objects was easier to detect as well as whether they could determine significant distinctive features of the objects. While over 90.0% of the participants stated the face of the human as distinctive

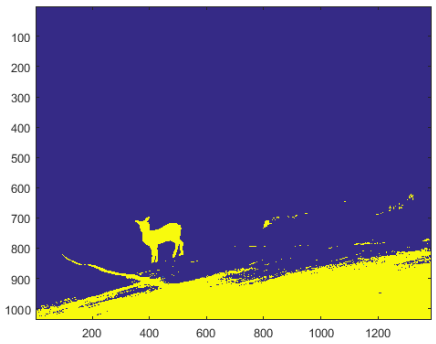


**(a)** Threshold $0.39 \frac{cd}{m^2}$

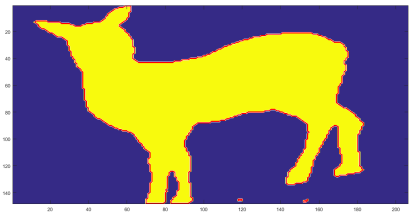

**(b)** Deer's outline

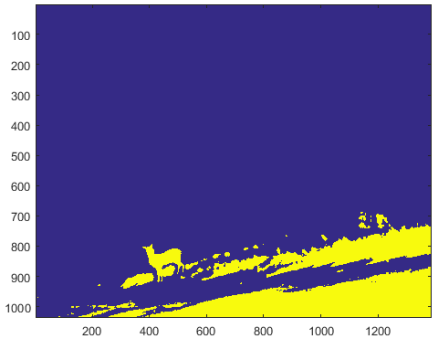


**(c)** Threshold $0.22 \frac{cd}{m^2}$

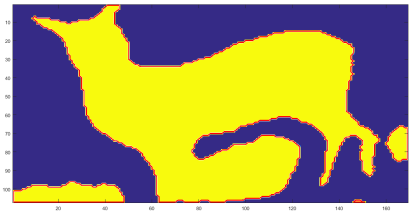

**(d)** Deer's outline

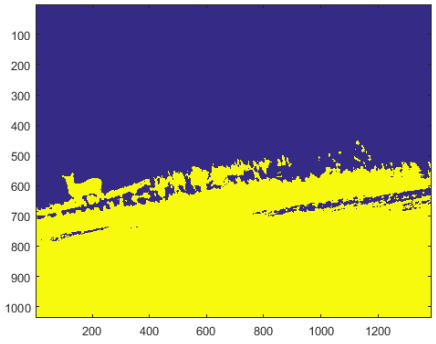


**(e)** Threshold $0.13 \frac{cd}{m^2}$

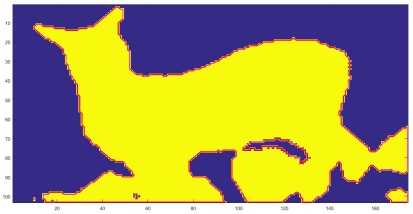

**(f)** Deer's outline

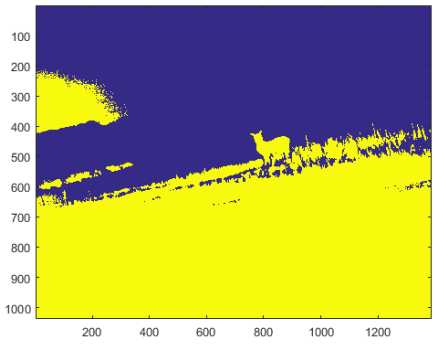


**(g)** Threshold $0.1 \frac{cd}{m^2}$

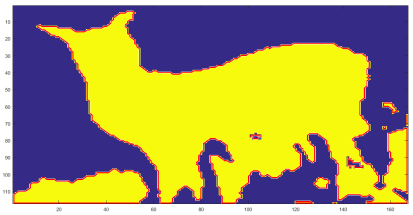

**(h)** Deer's outline

Figure 7.13: Image processing using Matlab. Deer at positions 1 to 4 (5.0 m to 15.5 m) in a distance of 80.0 m. Left hand side: determined edges based on corresponding threshold values. Right hand side: exterior boundaries of the deer.

feature, the answer was inconclusive for the deer. In this case the legs, head (ears) and back of the deer were mentioned as distinctive feature. Within an analysis by usage of luminance pictures and image processing, pronounced areas were determined, which have a high contrast over a certain extent. These areas are used for contrast analysis.
The question of critical visual details is closely linked to the question of perception criterion. The above analyses are based on the criterion "just seen", i.e. an identification of the visual object was not necessary. If an identification of the visual object is taken, other methods, in particular for the selection of regions in the luminance image, must be used (for example, shadows play an essential role).
It can be stated that the determined values show a good correlation to those of luminance pictures. Thus, the luminance values obtained can be validated by means of image processing. The application of image processing can be applied to both object shapes.

## 7.4 Critical object size

Assuming a typical driving situation, objects are projected into the central and paracentral visual field (about 20.0°), that is limited by the stopping distance. In this visual field area critical objects are in a range of a few degrees, so even small deficits in the visual field of the driver can lead to a disappearance of detection objects. If a detection object is closer to the vehicle, it is projected into the left or right horizontal visual field in the periphery [48]. In this case the driver can only react on time if he drives with slow speed.

### 7.4.1 Visual acuity

Visual acuity describes the ability of the eye to resolve small objects with fine detail at high contrast. Since the visual acuity of an emmetropic eye is 1.0, it becomes clear that the critical object sizes are relatively large. A visual acuity of 1.0 is indicated as optimum visual acuity and represents 100% visual faculty [120]. The visual acuity provides information about the individual resolution of the eye. The smaller the details on an object, the larger the value.
Assuming a visual acuity of 1.0, the eye can still see object's details of 1.5 mm size at a distance of five meters. For example, this can be the gap in a ring (Landoltring) as tested by the optometrist. If a person only recognizes at least 3.0 mm object details at this distance, the visual acuity is 0.5. Both values can be declared as "normal" since the visus changes with age. For 20-year-olds the visual acuity is between 1.0 and 2.0 for 80-year-olds values are between 0.6 and 1.0 [121].
The measurement of real road traffic scenarios results in a great variability in objects' contrast values. The question is how a connection between the detail resolution capacity of the eye, means the visual acuity and the critical object size can be established.

In consideration of the object contrast, it is possible to make estimates, which apply only to foveal vision. Taking peripheral vision into account, the threshold must

be significantly higher than in the fovea. There are two possibilities to determine this connection:

- Starting from the background luminance, it is possible, using the results of Adrian [13], to conclude the necessary minimum size of the detection object (compare Chapter 4.1). It should be noted that the data are only valid for circular objects.
  Assuming a critical stopping distance, the object size can also be calculated for real objects. It results in a critical size of less than 25.0 cm (which is considerably below the size of a pedestrian) for a contrast of 0.1 to 1.0 in mesopic range. In mesopic range, the minimum values for the threshold contrast are below 0.05. In the scotopic range, these values increase to 0.1 to 0.4. In Table 7.15 the corresponding critical object sizes are presented.

| Adapatation luminance / $\frac{cd}{m^2}$ | Object contrast | | | |
|---|---|---|---|---|
| | 1.0 | 0.5 | 0.1 | 0.001 |
| $50.0\frac{km}{h}$ | | | | |
| 100 | 0.2 cm | 1.5 cm | 3.0 cm | 4.5 cm |
| 0.1 | 0.7 cm | 4.7 cm | 8.0 cm | 10.7 cm |
| 0.001 | 4.5 cm | 22.9 cm | 32.8 cm | 38.7 cm |
| $100.0\frac{km}{h}$ | | | | |
| 100 | 0.6 cm | 4.7 cm | 9.2 cm | 13.8 cm |
| 0.1 | 2.2 cm | 14.6 cm | 24.7 cm | 33.4 cm |
| 0.001 | 13.9 cm | 70.6 cm | 101.3 cm | 119.3 cm |

Table 7.15: Determined critical object sizes in cm for given adaptation luminances based on the velocities of $50.0\frac{km}{h}$ and $100.0\frac{km}{h}$ according to [1].

- Another opportunity to represent this connection is to convert the critical object size into a spatial frequency of a pattern that is comparable to the eccentricty [41]. From the spatial frequency and by specifying a certain background luminance the modulation sensitivity required for the object perceptibility can be estimated (compare Table 7.16). The object size can also determined according to the required minimum contrast by using results of Adrian [13].
  Assuming a vehicle driving with a speed of 50.0 $\frac{km}{h}$ (allowed speed in urban areas, Germany) and a brake deceleration of $7.00\frac{m}{s^2}$, this results in a stopping distance of 25.0 m, whereas the brake deceleration $a$ is defined as $a = \frac{v^2}{2s}$. A speed of 100.0 $\frac{km}{h}$ would result in a overall stopping distance of 75.0 m.
  For a stopping distance of 25.0 m (at 50.0 $\frac{km}{h}$), the size of a vehicle would correspond to 3.5° in height and 4.1° in width. For a pedestrian this would correspond to 4.4° in height and 1.2° in width. Based on the two calculated traffic scenarios, it can be assumed that contrast values up to 0.4 are required at night-time in order to detect an object outwith the overall stopping distance. Since such high contrasts are not present in real road traffic, critical traffic situations might occur.

| Speed / $\frac{km}{h}$ | Stopping distance / m | Threshold modulation [41] | | Threshold contrast [13] | |
|---|---|---|---|---|---|
| | | Pedestrian | Vehicle | Pedestrian | Vehicle |
| $L_u$ =100.0$\frac{cd}{m^2}$ | | | | | |
| 100.0 | 75.0 | 0.4 | 1.5 | 0.6 | 0.4 |
| $L_u$ =0.1$\frac{cd}{m^2}$ | | | | | |
| | | 1.1 | 1.5 | 4.5 | 2.0 |
| $L_u$ =0.001$\frac{cd}{m^2}$ | | | | | |
| | | 9.5 | 7.0 | 37.5 | 9.9 |
| $L_u$ =100.0$\frac{cd}{m^2}$ | | | | | |
| 50.0 | 25.0 | 1.4 | - | 0.5 | 0.4 |
| $L_u$ =0.1$\frac{cd}{m^2}$ | | | | | |
| | | 1.4 | - | 2.1 | 1.5 |
| $L_u$ =0.001$\frac{cd}{m^2}$ | | | | | |
| | | 7.1 | - | 11.1 | 4.8 |

Table 7.16: Minimum requirements for threshold modulation and object contrasts for different adaptation luminances based on the two vehicle speeds of 50.0$\frac{km}{h}$ and 100.0$\frac{km}{h}$ according to [41].

If one compares the contrast values from Table 7.13 with the statement mentioned above, it can be established that the maximum measured contrast of the own investigations is 6.26 (deer). However, this applies only for the case that the detection object is located directly next to the road. In order to detect a pedestrian, which is positioned at a greater distance from the road (15.5 m), only a relatively low contrast was measured (0.06).

### 7.4.2 Contrast determination according to Damasky

In this section the detection threshold results arising from Damasky's field tests are compared to the own findings [21]. As already mentioned, the task of the observer was to drive along the runway while detected objects. The investigated observation angles are illustrated in Figure 7.14 (compare Table 4.8).
Figure 7.15 shows the luminance values of different detection object sizes used in the field study of Damasky compared to the own findings. Thereby, Damasky analysed the detection task while driving the test vehicle for a probability of 95.0%. The luminance values of overall seven participants were determined for grey objects (distance to the object was 35.0 m).

Considering the findings of Damasky in Figure 7.15, for a detection of the dummy on the left hand side a four times higher luminance is needed compared to the dummy on the right hand side. This can be attributed to the fact that the test vehicle had an asymmetric low beam distribution. Therefore, the background of the "dummy left" appeared darker.
Comparing the two object shapes, the traffic sign required a higher luminance for a detection compared to the dummy shape, projected on the right hand side (factor

3.15 to 12.81). In order to compare the own findings with the investigations of Damasky, the object sizes correspondent to the detection distances were determined.

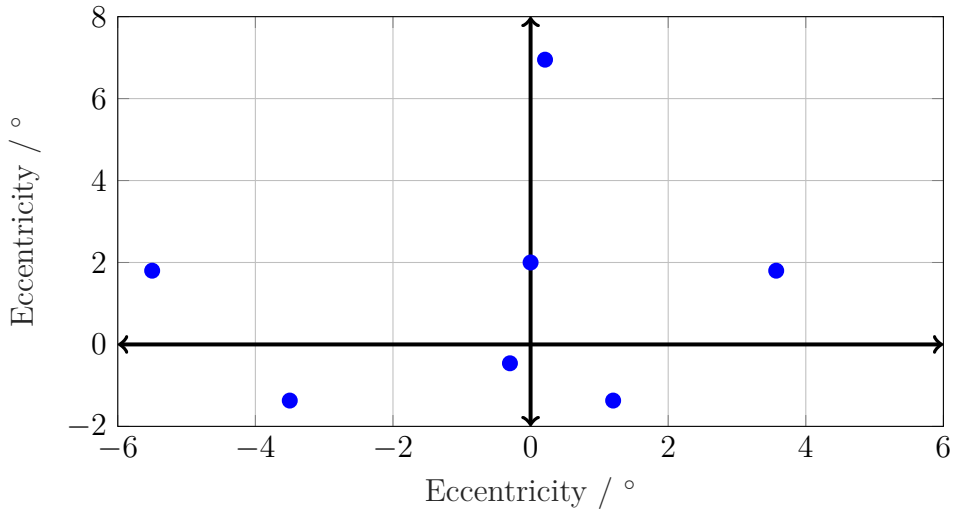


Figure 7.14: Positions of detection objects that were projected into the driver's vision field. The investigated detection objects were: dummy on left hand side /right hand side, traffic signs, squares.

While Damasky positioned the "dummy right" in a distance of 1.0 m next to the road, an average detection distance of 123.45 m could be established for the detection of the pedestrian (5.0 m roadside) in the static test. With an object height of 1.76 m at a distance of 123.45 m, an object size of 0.81° is obtained for the pedestrian, with 1.40 m height a size of 0.64° (deer) is calculated.

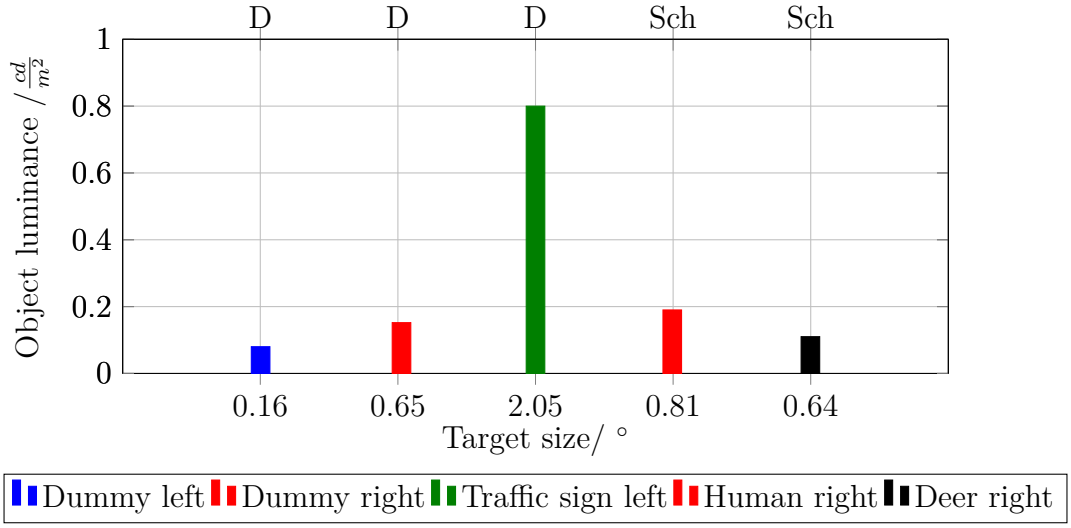


Figure 7.15: Comparison of Damasky's investigations to the own findings of the static test setup. Damasky (D), left hand side: object luminance values for 95.0% detection probability in closed area field study (airport Griesheim, Germany), distance to object: 35.0 m [21]. Own findings (Sch), right hand side: object luminance values for 99.0% detection probability distance to object: 123.45 m.

The corresponding object luminances are $0.19\frac{cd}{m^2}$ and $0.11\frac{cd}{m^2}$. Although the results can not be directly compared with each other, since both the test setup and the test parameters were different, the statement can be made that similar object luminances (range of 0.1 to $0.8\frac{cd}{m^2}$) are exhibited. As a result, the luminance on objects' surfaces must be at least $0.1\frac{cd}{m^2}$ in order to ensure a detection.

In addition to the field study in an enclosed test area, Damasky performed experiments in real traffic space. Supplementary night-time driving experiments were carried out on motorways as well as on urban and country roads.
In Figure 7.16 object luminances for a 95.0% detection probability for a grey dummy on the right hand side and a traffic sign over-head are presented. Especially in urban areas high object luminance values were necessary for a detection (0.6 to $1.1\frac{cd}{m^2}$). This can be traced back due to other road users, traffic lights, street lighting, or advertising surfaces, which are not existent on motorways or country roads. That implies that the detection probabilities determined on the closed area field study were up to 18 times lower than those obtained in real traffic scenarios. Comparatively low background luminances were determined for the remaining road types ($L_U < 0.2\frac{cd}{m^2}$).

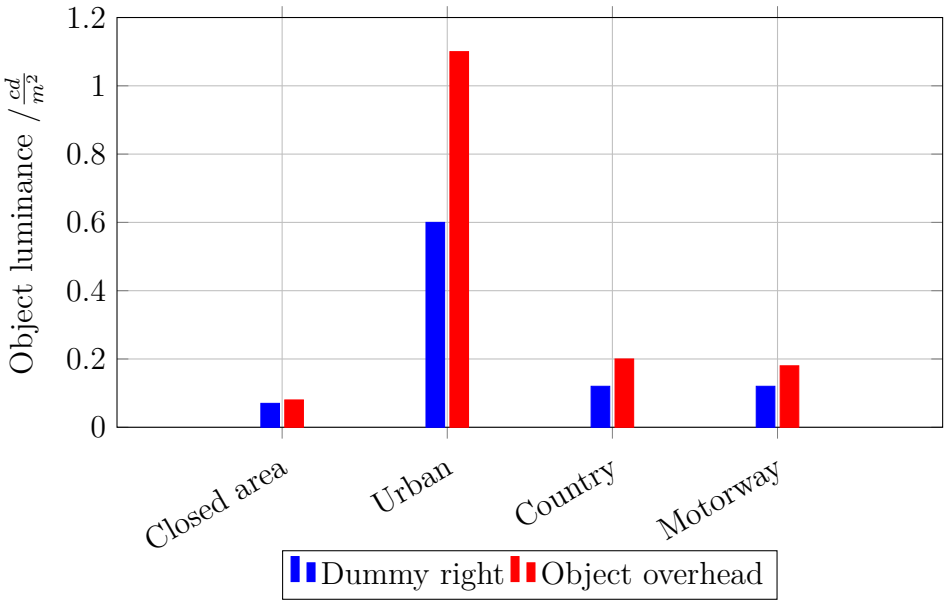


Figure 7.16: Object luminance values for 95.0% detection probability in real traffic space (Germany), for grey dummy ($0.65°$) right hand side and traffic sign ($0.65°$) overhead [21].

## 7.5 Summary

In this chapter factors that influence the calculation of the contrast that is essential for safe object detection (at least 95% probability) were discussed. These factors also include both the luminance on the object's surface, the road surface and in the immediate background. As this chapter showed, the knowledge of a theoretically

calculated threshold contrast for determining the detection distance is useful but not always transferable to reality.
Eckert developed a model for the detection distance calculation of pedestrians for accident reconstruction [5]. Based on Adrian's model [13] he defined 13 pairs of measuring points on the pedestrian's surface and the immediate background, which leads to 13 luminance differences. According to Eckert the object can be detected if the existing values are larger than the threshold values.
In Kokoschka's model, in the first step, the threshold contrast for every possible distance was calculated, in a second step the average edge contrast of the object was calculated. As a measure of the detection distance he used the ratio of the edge contrast and the threshold contrast (VL). He defined the detection distance by a limit value of VL = 1.
Further studies were carried out to determine the contrast. Kliebisch made an approach for a prediction of the detection distance based on headlamps' contrast, by determining the detection distance of a grey card for different luminous distributions [74]. Studies of Locher and Völker illustrated that the luminance in high distances (behind the cut-off line) is the best predictor for detection distance determination compared to factors like the luminous flux or the homogeneity [39].
Overall the problem exists, that a contrast, which is determined experimentally, always refers only to one specific object, whereby it can not be transferred to other object shapes. It can be noted that it does not seem possible to derive the effect of complex object structures from their elementary parameters.
The models of Eckert [5] and Kokoschka [24] use the threshold contrast or the luminance difference threshold. While Kokoschka's model was validated with a luminous intensity distribution, the measurement points in the Eckert model are based on empirical knowledge. Kokoschka proposed the mean edge contrast for the determination of the existing visual object contrast. Since a driver does not wait for an identification with all features, the question is whether this approach is a useful contrast measure. If the pedestrian is detected earlier, however, can not be answered with the known models. Both models include the adaptation luminance and the object size as input data. The influence of the luminance distribution on the object's surface or of the environment were taken into account by means of a practical factor. Using the model of Kokoschka, this practical factor applies only, if the luminous intensity distribution is validated. The extent of the luminous intensity distribution on the practical factor has not been investigated so far.
As result of the own investigations it can be stated that there is a high correlation between contrast and detection distance. The evaluation of Eckert's showed significant deviations between experimental and calculated results. Thus, this model seems to be unsuitable for the detection distance prediction. Kokoschka's model also shows deviations in the results, since the base of the model consists on the contrast of the object and its background, which is more qualified for headlamps. Therefore, it is more suitable for analysing the own investigations.
In summary, it can be noted that a combination of the evaluation with edge contrasts and image processing is most appropriate for a contrast calculation. Nevertheless, the subjective assessment of participants (if possible) should be taken into account, in order to eliminate possible ambiguities.

# Chapter 8

# Comparison of the investigations

In the following chapter, the own results of the laboratory and field investigations are compared to each other. Therefore, the single parameters influencing the detection task are analysed in detail to make a prediction about possible directions. In order to allow a comparison, the data from the field test were first adapted to those from the laboratory tests. Since the average detection distances were determined for a dynamic as well as a static field setup, both scenarios are compared with the laboratory results as it can be seen in Figure 8.1.

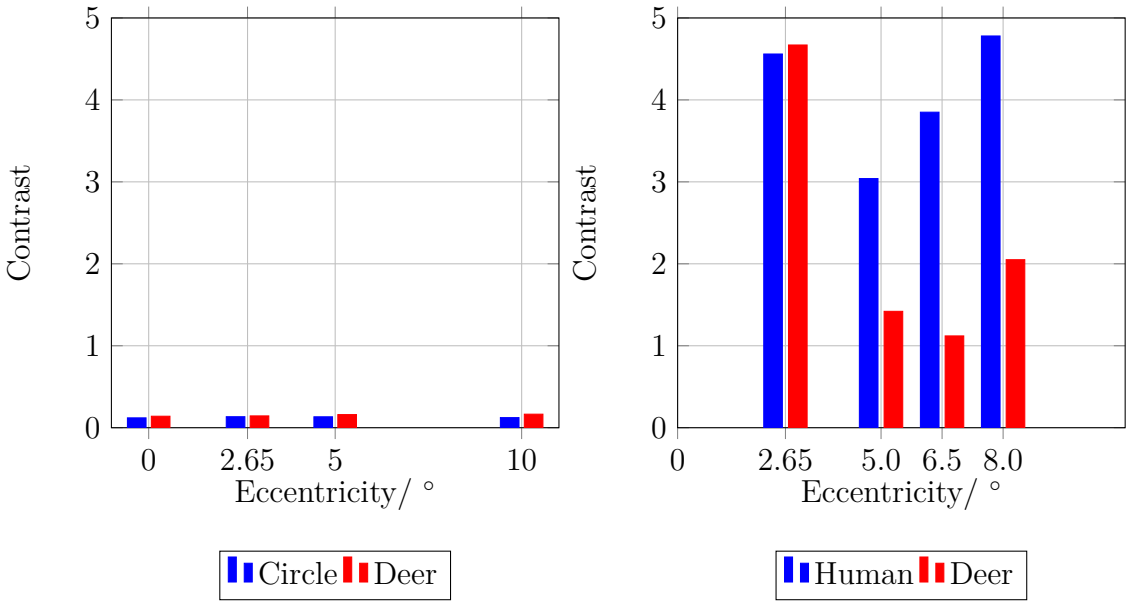


**(a)** Laboratory: all participants **(b)** Field (dynamic test): all participants

Figure 8.1: Determined contrast values for a 99.0% detection probability of all participants. Comparison of the object shapes for background luminances of 0.1 $\frac{cd}{m^2}$ (laboratory) and 0.02 to 0.06 $\frac{cd}{m^2}$ (dynamic field study).

In Table 8.1, the corresponding sizes of the two detection objects are presented in degree measure. In a further step, the eccentricities of the two objects are calculated as a function of the detection distance. Tables 8.2 and 8.3 give an overview of the specific contrast values from the respective examinations. In the field study, background lumiances in a range from 0.02 to 0.06 $\frac{cd}{m^2}$ were determined. The two examinations can only be compared with each other with a limited extent, as within

the field study a maximum peripheral eccentricity of approximately 8.0° was investigated. As presented in Table 8.2, the determined field study contrast values show a good correlation to the findings of the laboratory study. Since the calculated object

| Setup | Object | $\alpha_{5.0}/\,^\circ$ | $\alpha_{9.6}/\,^\circ$ | $\alpha_{12.5}/\,^\circ$ | $\alpha_{15.5}/\,^\circ$ |
|---|---|---|---|---|---|
| Dynamic | Human | 1.08 | 1.06 | 1.09 | 1.2 |
| Static | | 0.81 | 0.72 | 0.67 | 0.78 |
| Dynamic | Deer | 0.83 | 0.83 | 0.89 | 0.95 |

Table 8.1: Determined object sizes from the field study. Size of the human (1.76 m height) assumed for detection distance from 84.07 m (dynamic) to 148.55 m (static). Size of the deer (1.40 m height) assumed for detection distances from 84.13 m to 96.85 m (dynamic).

sizes are in the range of 0.67° to 1.08°, they are compared with the laboratory results of 1.0° target size.

| | $\theta/\,^\circ$ | K | $\theta/\,^\circ$ | K | $\theta/\,^\circ$ | K | $\theta/\,^\circ$ | K | $\theta/\,^\circ$ | K |
|---|---|---|---|---|---|---|---|---|---|---|
| Circle (Laboratory, static) | | | | | | | | | | |
| Total | 0.0 | 0.120 | 2.65 | 0.134 | 5.0 | 0.133 | | | 10.0 | 0.123 |
| Young | 0.0 | 0.108 | 2.65 | 0.120 | 5.0 | 0.119 | | | 10.0 | 0.118 |
| Old | 0.0 | 0.168 | 2.65 | 0.187 | 5.0 | 0.085 | | | 10.0 | 0.184 |
| Human (Field, dynamic) | | | | | | | | | | |
| Total | | | 3.07 | 4.56 | 5.8 | 3.04 | 7.66 | 3.85 | 10.44 | 4.78 |
| Young | | | 2.63 | 3.62 | 5.28 | 3.04 | 6.84 | 2.90 | 9.99 | 4.01 |
| Old | | | 3.12 | 4.55 | 6.32 | 3.03 | 6.95 | 2.81 | 10.38 | 4.78 |

Table 8.2: Determined contrast values for a 99.0% detection probability. Object shapes: circle and human for a background luminance of 0.1 $\frac{cd}{m^2}$ (laboratory) and 0.02 to 0.06 $\frac{cd}{m^2}$ (field study).

| | $\theta/\,^\circ$ | K | $\theta/\,^\circ$ | K | $\theta/\,^\circ$ | K | $\theta/\,^\circ$ | K | $\theta/\,^\circ$ | K |
|---|---|---|---|---|---|---|---|---|---|---|
| Deer (Laboratory, static) | | | | | | | | | | |
| Total | 0.0 | 0.140 | 2.65 | 0.144 | 5.0 | 0.160 | | | 10.0 | 0.165 |
| Young | 0.0 | 0.126 | 2.65 | 0.129 | 5.0 | 0.144 | | | 10.0 | 0.148 |
| Old | 0.0 | 0.251 | 2.65 | 0.265 | 5.0 | 0.115 | | | 10.0 | 0.309 |
| Deer (Field, dynamic) | | | | | | | | | | |
| Total | | | 2.95 | 4.67 | 5.74 | 1.42 | 7.87 | 1.12 | 10.43 | 2.05 |
| Young | | | 2.63 | 4.31 | 5.28 | 1.04 | 6.83 | 1.11 | 9.99 | 0.63 |
| Old | | | 3.12 | 6.41 | 6.34 | 2.75 | 6.93 | 1.10 | 10.38 | 0.68 |

Table 8.3: Determined contrast values for a 99.0% detection probability. Object shapes: deer for a background luminance of 0.1 $\frac{cd}{m^2}$ (laboratory) and 0.02 to 0.06 $\frac{cd}{m^2}$ (field study).

The following results can be obtained: As previously assumed, a significantly higher contrast value is required in a real field test to detect an object (compare Figure 8.2). This deviation (field factor) depends, however, very much on the eccentricity of the object. While for the smallest eccentricity (which corresponds to 2.65°

in laboratory and an object directly next to the road in the field study) massive contrast deviations are determined. The field factor decreases continuously with increasing peripheral eccentricity.

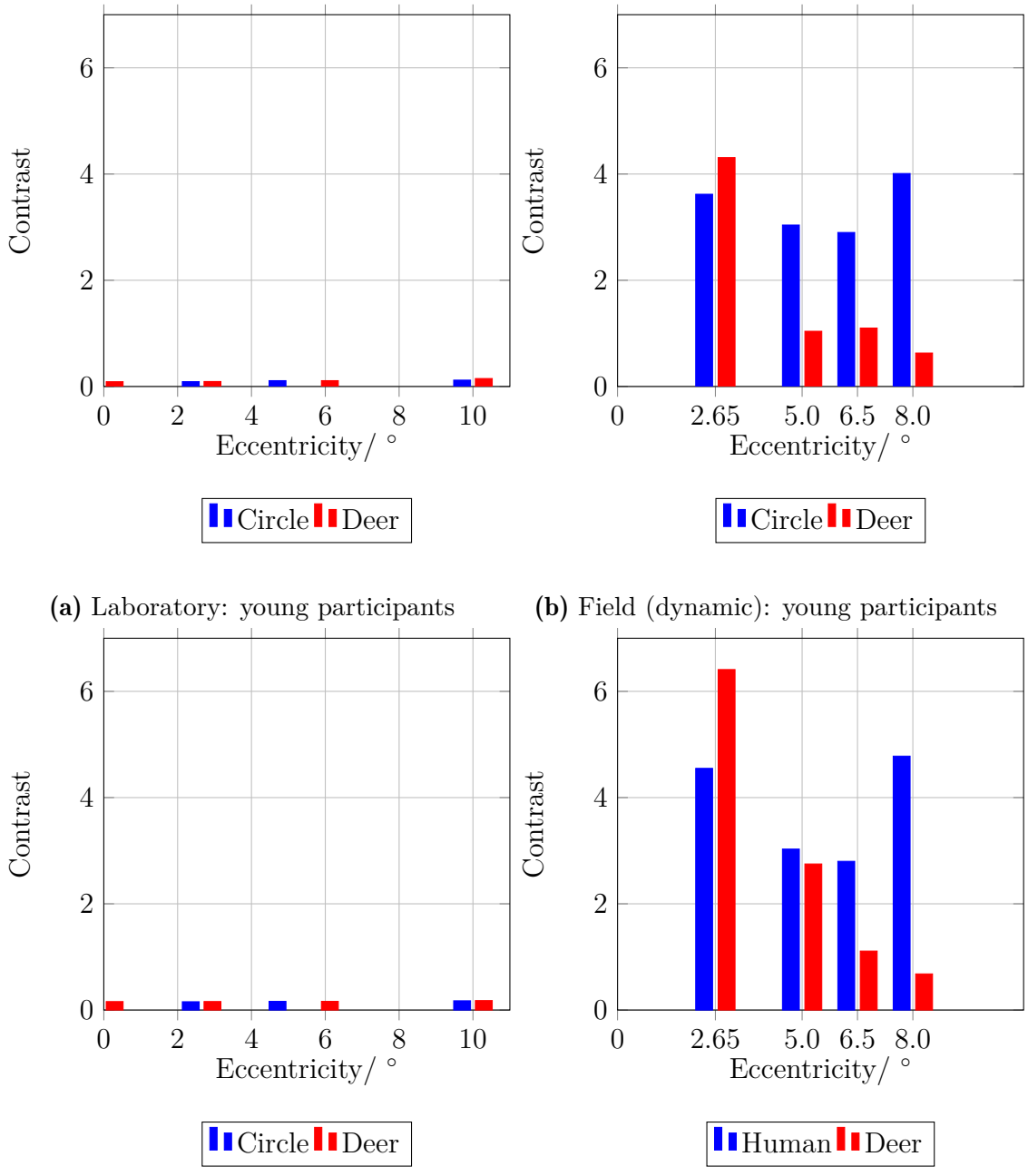


**(a)** Laboratory: young participants

**(b)** Field (dynamic): young participants

**(c)** Laboratory: old participants

**(d)** Field (dynamic): old participants

Figure 8.2: Determined contrast values for a 99% detection probability for two age groups for a background luminance of 0.1 $\frac{cd}{m^2}$ (laboratory) and 0.02 to 0.06 $\frac{cd}{m^2}$ (field study).

Since the circle with its concise shape can only be compared restrictedly with the pedestrian structure, the focus of the comparison lies on the deer shape. A comparison of the deer shape is more meaningful, since both objects have an identical

contour and a homogeneous surface. Considering the three eccentricities, which can be compared directly with one another, it can be stated that the deviation also decreases with increasing peripheral eccentricity. At 2.65° a deviation by factor 32 can be noted, whereas the field factor decreases to 8.75 for an eccentricity of 5.0° and to 8.4 at 10.0°.
In Figure 8.3 the determined field factors for the corresponding eccentricities are presented. It becomes clear that the results of the individual eccentricities are clearly different from each other.

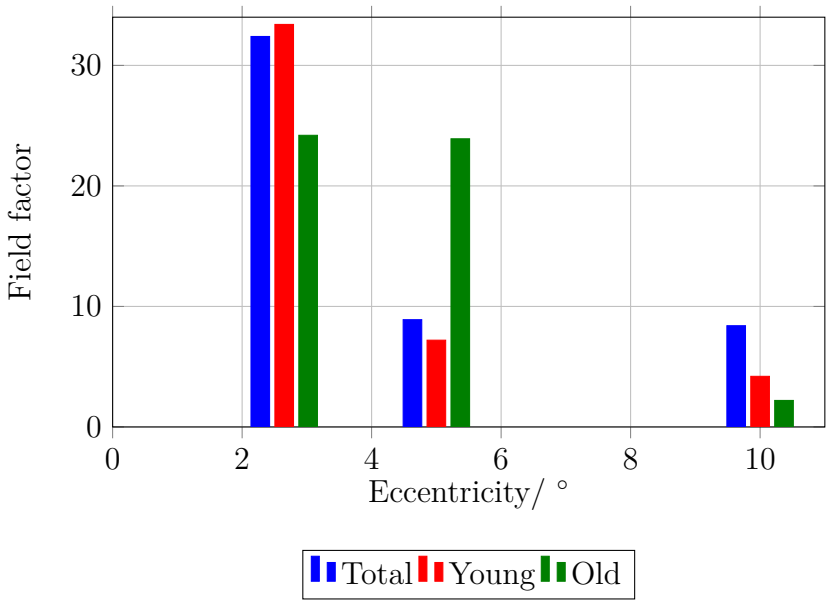


Figure 8.3: Deviations between laboratory experiments and field study (field factor). Determined field factors for the age groups at the corresponding eccentricities 2.65°, 5.0° and 10.0 °. Object shape: deer.

If one regards the old participant group only, it can be determined that the field factor remains almost constant up to 5.0°. At an eccentricity of 10.0° the field factor decreases rapidly from approximately 24.0 to 2.2.
On the contrary, considering the young participants group, the decline in field factor can be seen more clearly with an increasing eccentricity. The highest field factor is measured at an eccentricity of 2.65°. Subsequently, it decreases with increasing periphery from 32 to 4.2. Of particular note is that the field factor of the young participant group is twice as high as for the old age group in periphery, as this was not expected.

## 8.1 Approach for luminance difference description

In the following paragraph, an approach to describe the luminance difference related to object detection is given. The aim is to expand the model of Adrian so that it can also be used as a starting point for real field tests and not only for laboratory investigations. It does not represent a completely new model function, but is a suggestion to express or expand the basic concept meaningful. In the following,

parameters are presented, which have been neglected in the model of Adrian so far or have not been taken into account at all.
Adrian's model is essentially based on four elements: the probability factor, luminance component, contrast factor and age factor (compare Chapter 4.1). From these components the luminous difference $\Delta L$ can be calculated.

### 8.1.1 Influence factors

In order to describe luminance differences not only for a specific application Adrians model should be extended by several parameters.
**Static vs. dynamic procedures.** The most important differences between static and dynamic tests can be divided into attention, physiological differences and the gaze behaviour of the driver. In addition, it is possible that the detection object is moving as well. Therefore the relative velocity of the object needs to be considered also.
**Level of attention.** During a drive several tasks are done at the same time. Listen to the radio, using mobile phones or having conversations always result in distraction. This leads more or less to a divided attention. Hence, the driver's level of attention (depending on scene complexity, glare level, health, fatigue, mood, emotions and driving experience) also need to be taken into account. In contrary, under laboratory conditions, the full attention of a participant can be placed on the detection task. The visual field is also limited on a narrowly defined field in which the appearance of a visual object is expected. Since this kind of detection is simulated situation, it is more probable that objects are detected earlier than in a real situation.
**Adaptation.** The adaptation process takes a specific time and the human eye is not able to change it immediately. Under static conditions temporal changes in luminance can be reduced to a minimum but in real road traffic long adaptation times do not occur. Visual functions are also dependent on the presentation time of an object. In a static setup the presentation time is regularly chosen very low (0.2 s to 0.5 s), whereas visual processes in road traffic repose on very large local and temporal changes.
**Peripheral vision.** Within this work the perception of a peripheral object as a function of the background luminance was also analysed (position in the driver's field of view). As Adrian only performed investigations foveally the pheripheral aspect was not considered.
**Luminances ahead of the vehicle.** Another limitation in the laboratory is the evaluation of the effects of high luminances that are expected in advance (based on the headlamps). According to Damasky and Völker high luminances are fixed more frequently in advance [21] [34]. As the visual field in laboratory is in a range, in which expected effects like bright regions ahead of the vehicle and the related fixation do not appear, those effets can not be simulated under laboratory conditions.
**Vehicle-specific aspects.** The influence of the vehicle-type should also be taken into account. Beginning with the vehicle height, which affects the headlamps' luminous intensity distribution also, the suspension, acceleration or handling of the vehicle have also an influence.

### 8.1.2 Modelling approach

The model should be designed in such a way that it can also be used for practical applications. Therefore the model of Adrian should be extended by the following factors:

$$\Delta L_{appr.} = k \cdot \left( \frac{\nu\phi}{\alpha} + \nu L \right)^2 \cdot \frac{a(\alpha \cdot L_u) + t}{t} \cdot F_{CP} \cdot AF \cdot FF \cdot HL \cdot ad \tag{8.1}$$

- $k$, factor for the detection probability
- $\nu\phi$**,** $\nu L$, luminous flux or luminance function of Ricco's/ Weber's law
- $\alpha$, target size in angular minute
- $a(\alpha \cdot L_u)$, Blondel-Rey constant
- $t$, presentation time in seconds
- $F_{CP}$, factor for positive/ negative contrast calculation
- $AF$, age factor
- $FF$, field factor
- $HL$, headlamp (luminous intensity distribution)
- $ad$, adapdation of the the driver

A proposal for the so called field factor $FF$ is given as follows:

$$FF = set \cdot att \tag{8.2}$$

- $set$, setup type: dynamic or static
- $att$, level of attention of the driver

# Chapter 9

# Luminous intensity distribution implementation

In this chapter, the values determined in the field study are related to practical use. First, the determined contrast values are applied to the luminous intensity distribution, second it is adapted to pixel light headlamps and their resolution limits. Computations of the luminous intensity based on contrast values are performed to derive guidelines for the ADB headlamp light distributions.

## 9.1 Motivation

As described above, the risk of accidents is due to many factors, including those that are not influenced by the driver or his vehicle. In order to reduce the number of accidents through improved illumination using adaptive high beam systems, official analyses need to be studied extensively. In particular, it is important at what time and where accidents occur. An approach would be to determine in which situations an optimized illumination of the road surface reduces the probability of an accident.

The current development status with regard to pixel light headlamps is a continuous increase in the number of pixels. By automatically fading out oncoming or preceding vehicles, the illumination of the road is improved and glare is prevented. The most important questions are: “How many pixels are needed for a high-resolution headlamp system?”, “Does a resolution limit exist?”and “Is there an optimal number of pixels?”.
Current studies specify different values for high-resolution systems. In general, all configurations with more than 1000 pixels or less than 0.2° to 0.4° pixel opening angles are considered as high-resolution [122], the state of the art are 84 pixels, meaning a 1.0° to 2.0° resolution [42] [43].

For discrete LED matrix systems, the maximum number of pixels is currently limited to 150 up to 200 owing to the electronic complexity of the driver circuit and the required accuracy. A subdivision of each LED pixel (typically 1.0° aperture angle) into 4, 9 or 16 smaller pixels can lead to 400, 900 and 1350 pixels (corresponding 0.5°, 0.3° and 0.25°) [43].
Within the framework of the project $\mu$AFS, a solution was presented (which was required by the BMBF project), whereby the LED pixels were not produced as discrete LED chips any more, but with at least 256 pixels in an opto-semiconductor element [123]. Individually controllable pixels with a size of 125 $\mu$m $\times$ 125 $\mu$m and a pixel pitch of 125 $\mu$m in both directions were realized. Each square millimeter of

the LED chips contains 64 LED pixels, which means in total an area of 1024 pixels (16.0 $mm^2$).

The latest development of the project allows completely new light distributions and functions [43] with 3072 pixels per headlamp (3 modules each with 1024 pixels). According to Schmidt [124] the pixel number must be increased by at least one order of magnitude in the next few years.

## 9.2 (UN)ECE regulations

Since more than 95.0% of the required information for road traffic is perceived visually, lighting engineering aspects related to motor vehicles have a high priority. ECE standards define the most important regulations of motor vehicle (light) technology [73] (compare Chapter 3.2.1). The light distribution of a headlamp must then be designed in such a way that the road is illuminated with certain minimum and maximum values (compare Figure 3.3). The luminous intensity distributions of headlights are usually represented in isolux or isocandela diagrams in a plane perpendicular to the headlamp axis (measurement distance is defined as d= 25.0 m).
A typical situation considering oncoming traffic is illustrated in Figure 9.1. While the oncoming vehicle passes the own vehicle, the luminous intensity distribution automatically adapts.

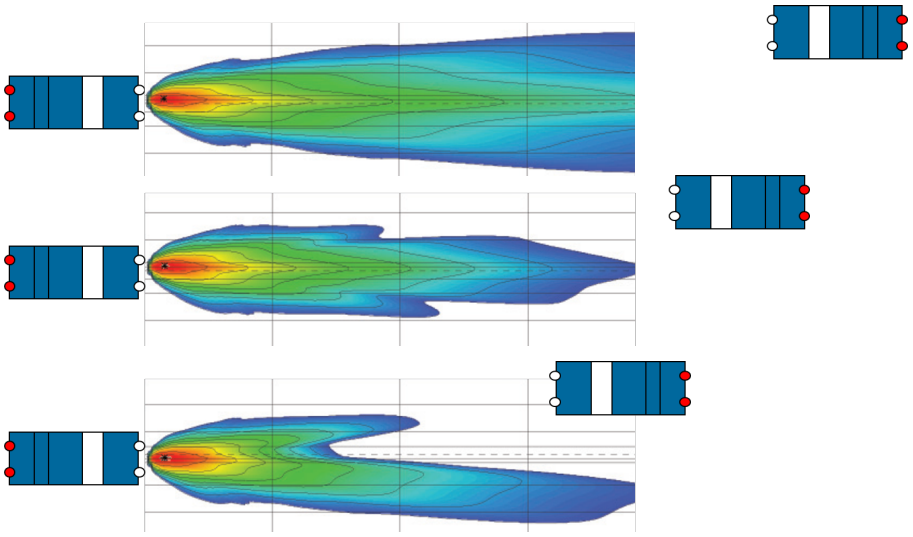

Figure 9.1: Traffic situation: ADB system with oncoming traffic. Isolux diagram in a plane perpendicular to the headlamp axis (measurement distance d =25.0 m). Top: high beam, oncoming vehicle is coming closer; middle: partial high beam, headlamp system adapts to oncoming vehicle; bottom: low beam, glare prevention.

In addition to the approval requirements applicable to the respective light sources, the ECE regulations R 48 [125] and R 123 [31] are relevant for an adaptive driving beam (ADB) system. These are referenced by EU regulations and can therefore be applied to the German legislation. While ECE R 123 specifies the

photometric parameters for an adaptive front lighting system, ECE R 48 regulates how and under which conditions the individual luminous intensity distributions and functions may be activated and contains other mounting regulations.

The photometric requirements of R 123 that are applied to a high beam luminous intensity distribution are summarized in part 6, section 6.3 [31]. The essential text passages are:

- 6.3.2.1. HV shall be located within the isolux 80 per cent of the maximum illumination of the driving beam.

- 6.3.2.1.1. This maximum value (EM) shall not be less than 48 lx. The maximum value shall in no circumstances exceed 240 lx.

- 6.3.2.2. Starting from point HV, horizontally to the right and left, the illumination of the driving beam shall be not less than 24 lx up to 2.6 deg and not less than 6 lx up to 5.2 deg.

- 6.3.3. The illumination or part thereof emitted by the system may be automatically laterally moved (or modified to obtain an equivalent effect), provided that:

  - 6.3.3.1. the system meets the requirements of the paragraphs 6.3.2.1.1. and 6.3.2.2. above with each lighting unit measured according to the relevant procedure indicated in Annex 9.

This section from [31] clearly reveals that there are no complex requirements for a high beam luminous intensity distribution. In fact, only photometric requirements are defined on measurement points, which are all on the H-H line. Thus, as long as a high beam luminous intensity distribution fulfills the requirements for the four mentioned points, an existing light distribution can be changed without objection to the high beam status according to ECE regulations (compare Figure 9.2). It can be concluded that a gradual lowering of the cut-off line in the direction of the H-H line is allowed. Only when this line is reached, one has to switch into low beam mode.
Independent from the modulation of the high beam luminous intensity distribution, it should be ensured that the photometric requirements for low beam are fullfilled at all times (asymmetrical low beam).

In Figure 9.2 a schematic view of a possible high beam pattern are illustrated [30]. The orange (represents the 80.0 % isolux line, $E > 0.8 \cdot E_M$), green (E > 6.0 lx) and yellow (E > 24.0 lx) subregions correspond to different isolux ranges, as required in the ECE R 123.

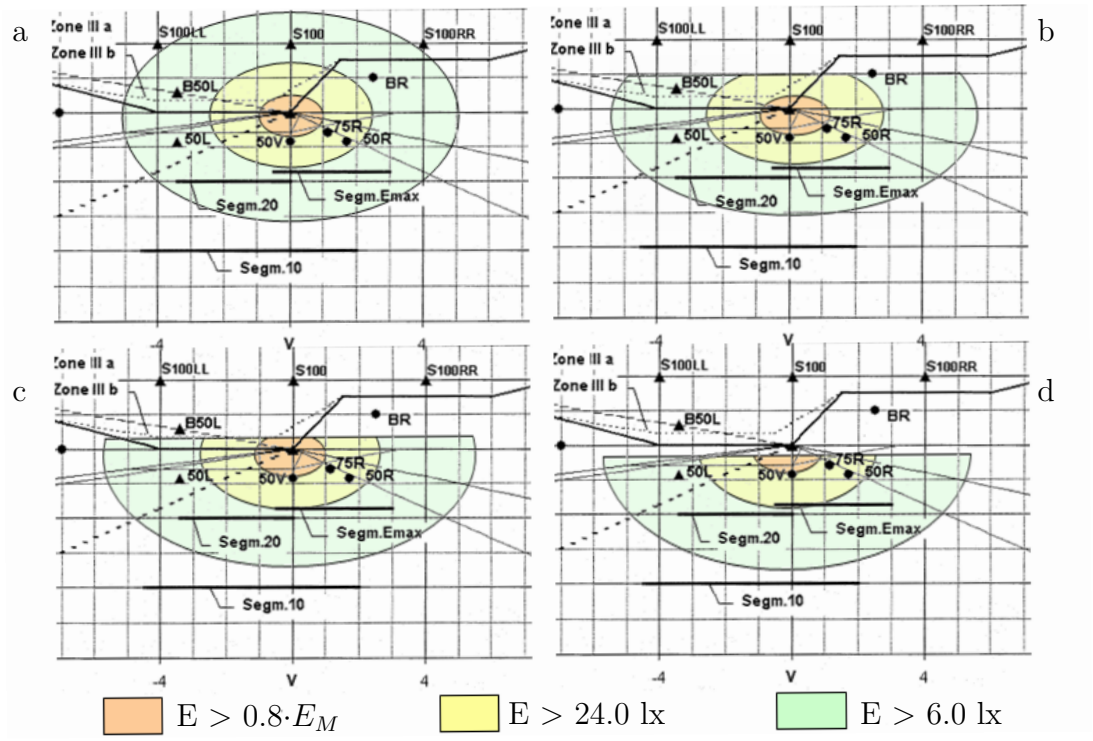


Figure 9.2: Schematic view of a possible high beam pattern according to [30]. The cut-off line is adjusted in high beam mode. Modi a, b and c fulfill the ECE R 123 requirements [31]. State d is not licit as HV is not within 80.0 % isolux-area any more. System switches to low beam pattern.

In Figure 9.3 the positions of detection objects that were analysed in the field study are illustrated (only defined measuring points).

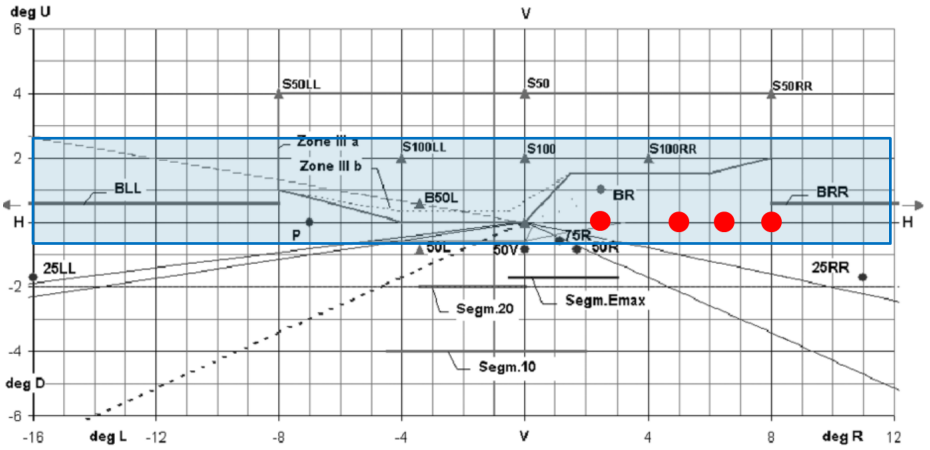


Figure 9.3: Positions of detection objects that were analysed in the field study. The measuring points are marked (red dots) into the perspective image of the roads (for d= 25.0 m) [10]. V-V: vertical line through the vanishing point; H-H: horizontal line through the vanishing point; B50L: observer's point of view of in the opposite vehicle, 50 m away on the left side of the road; 75R: point on the right side of the road, 75 meters away from the spotlight.

## 9.3 Maximum illuminance

As can be seen from the previous sections, a reliable detection of a pedestrian is not always possible at distances of more than 90.0 m. If the surroundings additionally exhibit strong contrast differences, caused, for example, by oncoming traffic or illuminated road signs, lighting situations occur in which the area above the cut-off line can be poorly perceived. In order to direct the driver's attention in such situations, it is essential, not only to regulate light onto the object to be illuminated, but also to take the object's surroundings into account.
Particularly in the dark, the visibility of the driver is limited with low beam and even using high beam. The maximum illuminance needs to be considered from both the legal as well as the physiological perspective. The legal limit values may not be exceeded in order to obtain an authorization of the headlamp system. A balance must be achieved between the maximum permissible glare of a pedestrian and a high visibility range. Since a suitable sensor system has to detect a pedestrian at a distance of more than 100.0 m, so that at this distance a sufficient illuminance for a detection still has to be achieved, the headlamp system should have a distance-dependent luminous intensity.

## 9.4 Luminous intensity distribution determination

The illuminance $E_v$ to be caused by ADB headlamps on the object's surface is determined as follows:

$$E_v = \frac{L_O \cdot \pi}{\rho} \tag{9.1}$$

with $L_O$, luminance on object's surface and $\rho$, reflection coefficient of the object.
The illuminance $E_v$ on the pedestrian's surface with $L_O = 0.3\frac{cd}{m^2}$, using a reflection coefficient of $\rho$=0.05 (placed alongside the road in a distance of 93.18 m, compare Table 9.1), which is necessary to achieve a 99.0% detection probability, can be calculated in the following way:

$$E_v = \frac{L_O \cdot \pi}{\rho} = \frac{0.3\frac{cd}{m^2} \cdot \pi}{0.05} = 18.85\ lx \tag{9.2}$$

The luminous intensity to be sent by the ADB towards the object's direction that is necessary to achieve $E_v$ =18.85 lx equals:

$$I_v = E_v \cdot d^2 = 18.85\ lx \cdot (93.18\ m)^2 = 163.03\ kcd \tag{9.3}$$

Therefore, the adaptive driving beam should provide 163.03 kcd (two headlamps) in the object's direction to illuminate the object at a probability of 99.0%.

In Figure 9.4 the determined luminous intensity values are illustrated for both detection objects. In order to make a comparison with previous studies, the measured luminous intensity values of Kobbert [26] were also integrated.

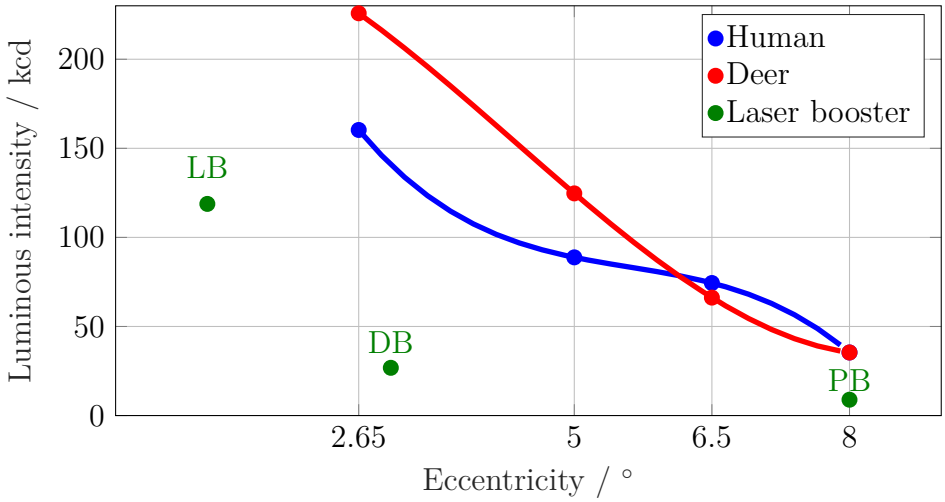


Figure 9.4: Determined luminous intensity values. Positions of detection objects human and deer that were analysed in the field study are illustrated. The measuring points are marked into the perspective image of the roads. For comparison with previous studies, the measured luminous intensity values of Kobbert [26] were also integrated. PB: passing beam, DB: driving beam, LB: Laser booster.

Table 9.1 (human), Table 9.2 (deer) and Table 9.3 (laser booster [26]) illustrate the calculated photometric parameters with regard to the determined detection distances (the luminous intensity values represent the results for two headlamps). Distance here similarly means the mean detection distance of all participants for the respective eccentricities (positions).
It can be seen, that the luminous intensity decreases steadily with increasing periphery. This determination applies for both detection objects. Subsequently, it can be noted that the luminous intensities for a detection of the deer are significantly higher compared to the pedestrian (for an eccentricity of 2.65°). At 8.0° the values are equal for both object shapes. Considering the results of [26] (laser booster function), the determined values of the own investigations were higher for smaller eccentricities for both driving beam and laser booster (compare Table 9.1, Table 9.3).

| Detection distance / m | Position | $L_O$ / $\frac{cd}{m^2}$ | Illuminance / lx | Luminous intensity / cd |
|---|---|---|---|---|
| 93.18 | 1 | 0.30 | 18.85 | 163,033.65 |
| 94.52 | 2 | 0.16 | 10.05 | 88,801.80 |
| 92.88 | 3 | 0.14 | 8.79 | 74,398.56 |
| 84.07 | 4 | 0.08 | 5.02 | 35,421.12 |

Table 9.1: Calculated luminous intensities for the 4 positions of the human in relation to the determined detection distance (the luminous intensity values represent the results for two headlamps). Distance: mean detection distance of all participants.

According to ECE R 98 [75] the maxium permitted illuminance is $E_{max}$= 344.0

| Detection distance / m | Position | $L_O$ / $\frac{cd}{m^2}$ | Illuminance / lx | Luminous intensity / cd |
|---|---|---|---|---|
| 96.85 | 1 | 0.39 | 24.50 | 225,792.00 |
| 95.51 | 2 | 0.22 | 13.82 | 124,725.50 |
| 90.36 | 3 | 0.13 | 8.17 | 66,177.00 |
| 84.13 | 4 | 0.08 | 5.02 | 35,421.12 |

Table 9.2: Calculated luminous intensities for the 4 positions of the deer in relation to the determined detection distance (the luminous intensity values represent the results for two headlamps). Distance: mean detection distance of all participants.

| Detection distance / m | Light distribution | $L_O$ / $\frac{cd}{m^2}$ | Illuminance / lx | Luminous intensity / cd |
|---|---|---|---|---|
| 26.0 | PB (8.0°) | 0.22 | 13.21 | 8,929.96 |
| 63.0 | DB (3.0°) | 0.11 | 6.75 | 26,790.00 |
| 122.0 | LB (1.0°) | 0.13 | 7.98 | 118,774.00 |

Table 9.3: Comparison to field study according to [26]: luminous intensities of a human dummy in relation to the determined detection distance (the luminous intensity values represent the results for two headlamps). Distance: mean detection distance of all participants. Licit for laser headlamps: $E_v$ > 300 lx (200,000.00 cd). PB: passing beam, DB: driving beam, LB: Laser booster.

lx which corresponds to $I_{max}$= 215,000.0 cd (for two headlamps one has $I_{max}$= 430,000.0 cd). Comparing this maximum value with the results of the own investigations it can be stated that the values are rather distant from one another. Nevertheless, considering only two different detection objects, significant differences could be observed ($\Delta_{Pos_1}$= 627.6 kcd). In order to make a reliable statement, further eccentricities would have to be investigated.

### 9.4.1 New legislative proposals for adaptive high beam systems

Adaptive high beam systems such as Matrix Beam or pixel light are not integrated into the existing regulations. For such headlamp systems, which are functional and their usability has been proved, the rules of the European Union provide the possibility of special authorization. This is governed by the provisions of Directive 98/ 14 /EC [126], which provides the possibility of authorizing components that are not capable with existing rules based on technical progresses. The institution Kraftfahrt Bundesamt published an explanatory note to this directive [127]. Systems which need to be approved according to regulations must be investigated whether they fullfill safety and environmental requirements. This is performed by means of technical measures that are captured in relevant ECE regulations.
In order to increase the visibility for the driver and thus the safety during night driving, sensor-controlled headlamps should allow a continuous transition between low beam and high beam.

With the use of luminous intensity distributions between low beam and high beam with regard to the illumination of the road, the driver will not always feel certain which light function is useful at a certain moment. Since such a system is controlled by an unspecified environmental sensor system, it can not be described deterministically. The current legislation restricts the use of such systems, since the current legislation for ADB functions (ECE R123 [31]) only allows the low beam distribution to be swiveled and slightly raised. In contrast to previous ECE regulations, the legislative proposal aims to open up the possibility of changing the luminous intensity distribution through the use of sensors. Sensor systems must be able to adapt the luminous intensity distribution dynamically to the ambient conditions. New regulations will make it possible to create a luminous intensity distribution similar to a high beam in areas where no other road users are located. At the same time, the areas in which other road users are located must have very low illuminances, similar to the low beam.
As already mentioned, ECE regulation R48 [125] provides basic questions concerning the mounting and lighting control. Hence, the headlights must be activated simultaneously or in pairs and the gradual activation is performed automatically. Subsequently, new proposals must specify cases and spatial zones in which certain luminous intensity values are not be exceeded. In addition, in order to ensure the required performance of the environmental sensor system, minimal detection ranges need to be defined. These requirements must be taken into account in new developments.

## 9.5 Summary

Using only very few assumptions and a simple traffic model (country road scenario), key parameters of future ADB modules and their light sources can only be estimated. Since only 4 measuring points were considered, just a tendency can be revealed as pixel count and flux dependent on the required angular range.
The number of headlamp segments defines the resolution and therefore the accuracy of ADB systems. By reducing the amount of segments, large gaps are reduced and the illuminated area increases. Nevertheless, spatial and thermal restrictions lead to a limit for current LED systems [128]. One potential direction could be an increase of the angular range (higher pixel numbers) or a limited angular range. Hence, modulating the light source is independent from the angular range. In the evolution of high beam systems, an adaptive cut-off line is considered. A continuous adjustment of the horizontal cut-off line between low and high beam leads to a glare prevention of oncoming or preceding traffic and an increase of the high beam period. The detection of objects (for example preceding or oncoming vehicles) is based on a camera system (downstream image processing). As a result, the boundary between high and low beam blurs increasingly.
As a step for future development two approaches can be considered for headlamp luminous intensity distributions. The first approach involves an increase in resolution of the headlamp system (as it is currently being investigated). A second approach is to examine and analyse the immediate front area of the vehicle and to implement the approach of the pixel light distribution to the low beam function.

# Chapter 10

# Summary

The visual perception provides the driver of a motor vehicle with nearly all information that are essential for the driving task. The driver adjusts the speed and travel route with regard to a detected obstacle. If an obstacle is perceived by the driver late so that an adequate reaction is not possible any more, a collision occurs. However, the severity of a collision can be reduced by decelerating the vehicle.
Particularly at dawn or darkness, the visibility of the driver is limited by using low beam, and even in areas that are illuminated by high beam, important details can not always reliably be detected. Particularly in case of oncoming traffic, objects with a small reflection coefficient are easily overlooked on the road or roadside. Even with high beam dark objects can be badly perceived. This is due to the fact that the entire illuminated area must be cognitively scanned and the perception is made difficult caused by low contrasts. The high beam only has a sufficiently high intensity in the centre, so that a dark object can stand out from the background at all.

New headlamp concepts with several different luminous intensity distributions, depending on the driving situation, heading for an increase of the driver's visibility. In the field of automotive front lighting, there are two trends of development: on the one hand, light sources (halogen lamps, xenon discharge lamps and LEDs) are available with various luminous intensity distributions. On the other hand, modern assistance-based front lighting systems offer the possibility of optimizing the visual comfort and the detection by means of a spatially more finely resolved light distribution (DMD, LCD, Matrix beam, pixel-light). For this purpose, the light distribution of the headlamps is modelled by using high-resolution LED pixels.
Latest headlight systems consist of discrete constructed LED pixels, that are individually controllable and have an angular resolution of approximately 1.0° [42]. With an increasing number of pixels, the faded out areas can be reduced, which results in a larger illuminated surface. As a consequence, this leads to a considerable gain in safety for the driver caused by an increased use of the high beam function. These developmental tendencies lead to the vision of adapting the light distribution in a spatially resolved manner in order to further optimize the visual comfort and detection.
A safe visibility condition is guaranteed if the luminance of the detection object is high enough to achieve 99% detection probability at a distance longer than the overall stopping distance of the vehicle to avoid a collision. The necessary amount of luminous intensity in object direction can be calculated from the object luminance level or contrast.
For this reason, in a first part, an experimental setup was applied, which offers

the possibility to investigate the influence of the adaptation luminance on the perception threshold. Compared with previous investigations in this thesis perception characteristics in the peripheral vision field were analysed as well (related to a typical night drive situation).
In a second part a field study setup with real detection objects was provided. The object was integrated into an environment with constantly changing parameters. Factors that influence the object luminance values necessary for safe detection were analysed. The most important detection threshold results and consequences were derived to suggest a guideline for future headlamps' light distributions. As mentioned above, these results are suitable to optimize ADB light distributions from the detection performance point of view of.
While in the past exclusively illumination was defined as statistic, the own investigations show that illumination is only suitable to a limited extent for both current and future headlight systems, since it describes the luminous efficacy and contrast sensitivity of the human eye very conditionally. With use of the image-resolved luminance measurement technology correlations between the photometric values such as luminance and the psychometric variables could be determined.
In the third part, the known factors that are essential for a complete calculation of the contrast sensitivity, were summarized. As the results show, at this juncture, it seems to be impossible neither to resume all influence parameters with one particular equation, nor to define a constant field factor (practical factor). On the one hand, the field factor itself depends on the luminance level. On the other hand standard deviations between the participants are comparably high. Therefore, the visual performance needs to be included also.

From the results of the laboratory investigations a clear target shape dependence of the luminance difference threshold could be determined. Subsequently, the luminance threshold decreased with increasing target size and background luminance.
In the field study two measurement methods, static and dynamic, were developed for determining the detection distance. Evaluating the detection distances regarding the object shape's influence for all participants, it was established that the results were similar for both target shapes. Considering the two age groups clear distinctions could be observed, especially the detection behaviour of the old subjects was considerably lower compared to young participants.
Significant deviations between the static and dynamic test results could be determined. It was much more difficult to the old participants to detect an object, as the detection distance remained at the same level as for the dynamic test.
Overall, it could be revealed that laboratory investigations determined by means of circle and deer target shapes, have a similar dependence on the background luminance as the detection distance of a human or deer in the field study. Hence, the theoretically calculated detection threshold contrasts are not only suitable for simple and homogeneously constructed visual objects, but at least for standard detection objects like a grey card.
If the results of the detection contrast investigations (laboratory) are transferred to the detection distance, it can be stated that the contrast (luminance) produced by the headlights is a reliable statistic for the prediction of the detection distance.

To compare the results to ordinary driving situations, the corresponding overall stopping distance was determined. From the findings it was established that the illumination level of the required roadside areas and in front of the vehicle in terms of the visual field is still insufficient. Further influence factors as the attention of the driver, wheater conditions or road surface characteristics should also be taken into account.
In addition, the reflection coefficient of the detection object is of crucial importance. Complex detection object structures (as pedestrians) with the same or even with a higher reflection coefficient lead to longer detection distances.

Furthermore, the factors (as the luminance on the object's surface or immediate background) that influence the contrast were discussed. The problem remains, that a contrast, which is determined experimentally, always refers only to one specific object, whereby it can not be transferred to other object shapes. It can be noted that it does not seem possible to derive the effect of complex object structures from the effect of their elementary parameters.
The findings showed that the knowledge of a theoretically calculated threshold contrast for determining the detection distance is useful but not always transferable to reality. Models for the calculation of the detection distance of Eckert [5] and Kokoschka [101] provided similar results, since they are based on the same model [13]. In contrast to the recommendation of Völker [34], who proposed, that mean edge contrast should not be used for complex visual objects, the Kokoschka model was suitable for the own investigations but must always be adapted to the corresponding scenario. Therefore it can be stated, that for real objects, the determination of the critical distinctive feature should be determined by means of an edge contrast profile respectively. In addition to the visual object size, the contrast can be determined from the luminance difference profile.
In summary, it can be noted that a combination of the evaluation with edge contrasts and image processing is best suited for a contrast calculation. Nevertheless the subjective assessment of participants should be taken in account, in order to eliminate possible ambiguities.

This work presents a comprehensive overview of the influence factors on the important road traffic visual functions, such as luminous efficacy or contrast sensitivity. The work also provides an important connection for fundamental research considering mesopic vision, starting with the luminance difference threshold model of Adrian [13], the investigations of Kokoschka and Gall [24] or Damasky [21].

# Appendix A

# Contrasts for a detection probability of 50.0%

## A.1 Influence of target shape

Figure A.1 and Figure A.2 show the detection experiment results of the circle and deer shape for a detection probability of 50.0%.

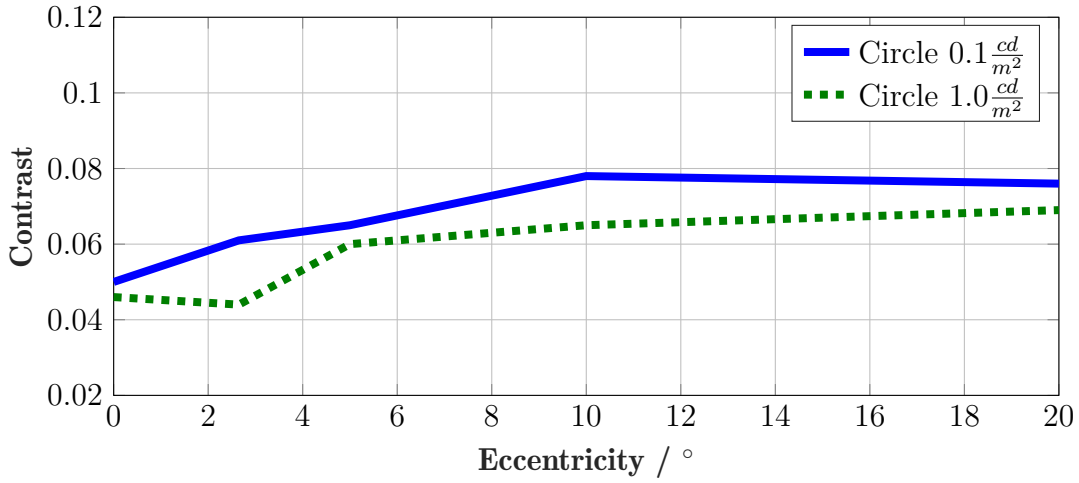


Figure A.1: Contrast for a 50.0% detection probability at two background luminances; Relation between contrast K and eccentricity $\theta$; Object shape: circle; target size: 1.0°.

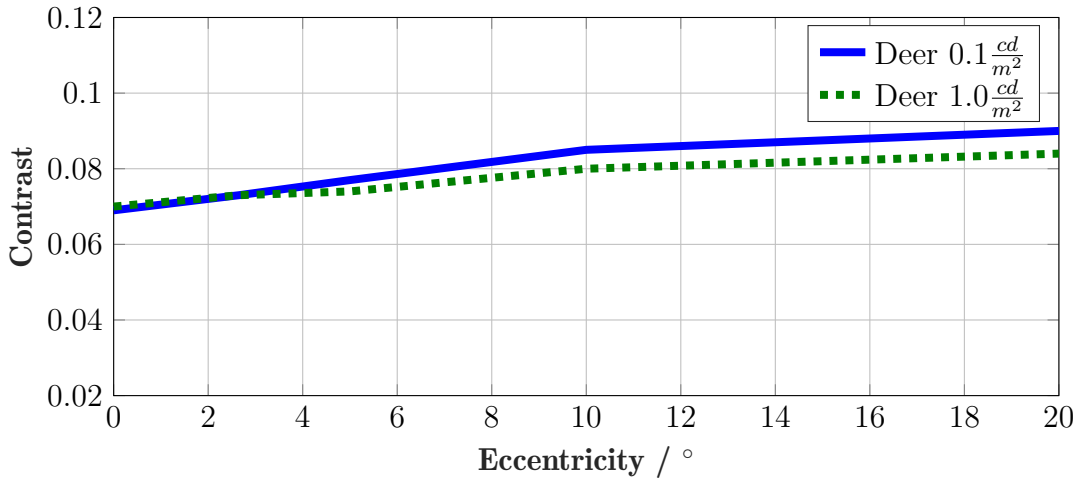


Figure A.2: Contrast for a 50.0% detection probability at two background luminances; Relation between contrast K and eccentricity $\theta$; Object shape: deer; target size: 1.0°.

Table A.1 illustrates the corresponding contrast values for a 50.0% detection probability for both target shapes.

| Target shape | $L_U$ | 0.0° | 2.65° | 5.0° | 10.0° | 20.0° |
|---|---|---|---|---|---|---|
| Circle | $0.1\frac{cd}{m^2}$ | 0.05 | 0.061 | 0.065 | 0.078 | 0.076 |
| Deer | | 0.069 | 0.073 | 0.077 | 0.085 | 0.090 |
| Circle | $1.0\frac{cd}{m^2}$ | 0.046 | 0.044 | 0.060 | 0.065 | 0.069 |
| Deer | | 0.07 | 0.073 | 0.074 | 0.080 | 0.084 |

Table A.1: Contrast for a 50.0% detection probability at two background luminances; Relation between contrast K and eccentricity $\theta$; Object shapes circle and deer, target size: 1.0°.

## A.2 Influence of target size

Figure A.3 and Figure A.4 show the detection experiment results of the circle shape for two different target sizes (1.0°, 2.0°) for a detection probability of 50.0% .

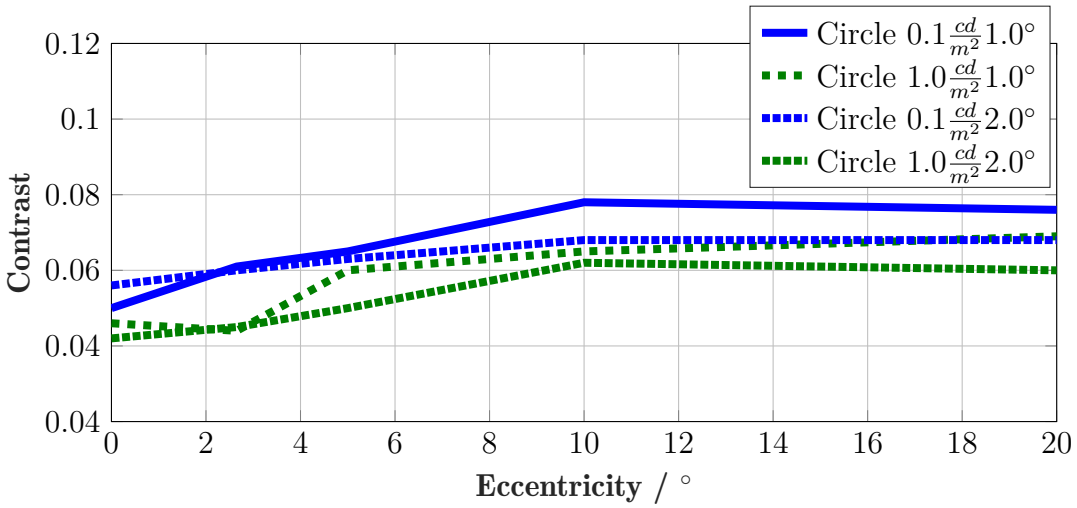


Figure A.3: Contrast results for a 50.0% detection probability at two background luminances; Relation between contrast K and eccentricity $\theta$. Circle; target sizes: 1.0° and 2.0°.

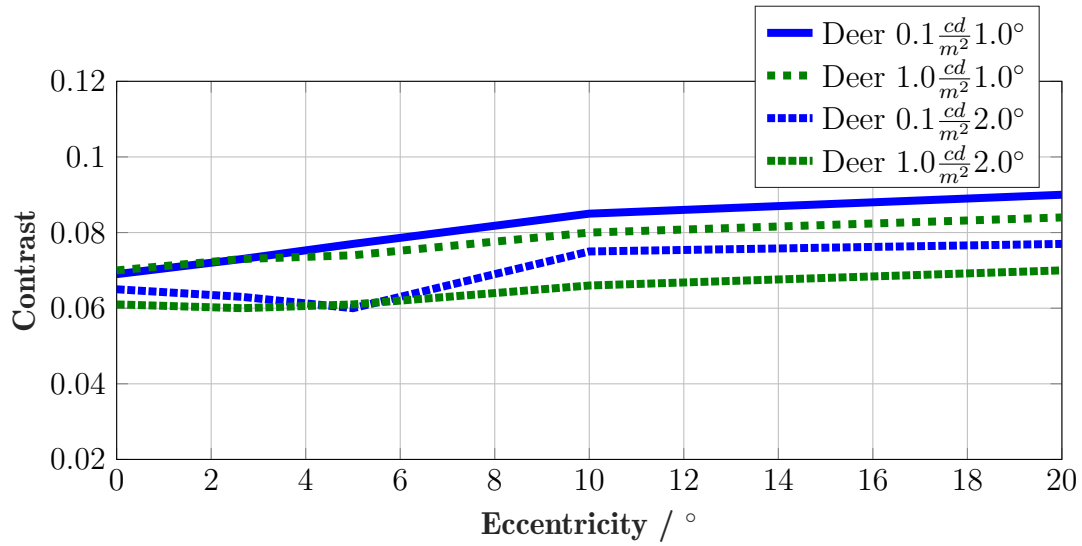


Figure A.4: Contrast results for a 50.0% detection probability at two background luminances; Relation between contrast K and eccentricity $\theta$. Deer; target sizes: 1.0° and 2.0°.

Table A.2 illustrates the corresponding contrast values for a 50.0% detection probability for both target shapes.

| Target | $L_U$ | 0.0° | 2.65° | 5.0° | 10.0° | 20.0° |
|---|---|---|---|---|---|---|
| Circle | $0.1\frac{cd}{m^2}$ | 0.056 | 0.06 | 0.063 | 0.068 | 0.068 |
| Deer | | 0.065 | 0.063 | 0.060 | 0.075 | 0.077 |
| Circle | $1.0\frac{cd}{m^2}$ | 0.042 | 0.045 | 0.050 | 0.062 | 0.06 |
| Deer | | 0.061 | 0.060 | 0.061 | 0.066 | 0.070 |

Table A.2: Contrast for two background luminance densities with a detection probability of 50.0%; Relation between contrast K and eccentricity $\theta$; Object shapes circle and deer, target size: $2.0°$.

## A.3 Influence of age

In Figure A.5 and Figure A.6 the detection results of the two age groups, young participants (dotted lines) and old participants (solid lines), for the circle and deer shape as a function of the eccentricity for a detection probability of 50.0% are presented.

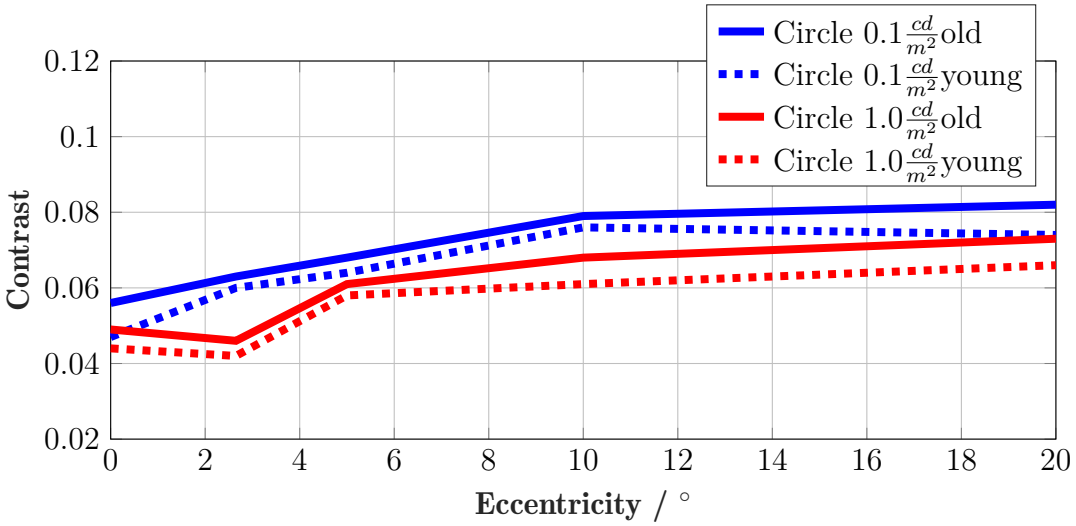


Figure A.5: Contrast results of two age groups for a 50.0% detection probability at two background luminances; Relation between contrast K and eccentricity $\theta$. Circle; target size: 1.0°.

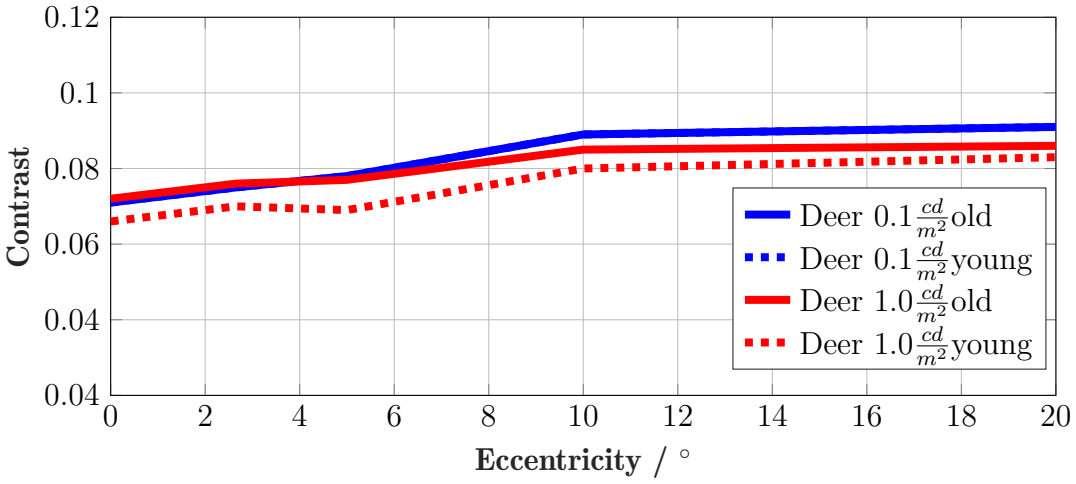


Figure A.6: Contrast results of two age groups for a 50.0% detection probability at two background luminances; Relation between contrast K and eccentricity $\theta$. Deer; target size: 1.0°.

Table A.3 illustrates the corresponding contrast values for a 50.0% detection probability for both target shapes.

| Age group | Target | $L_U$ | 0.0° | 2.65° | 5.0° | 10.0° | 20.0° |
|---|---|---|---|---|---|---|---|
| Young | Circle | $0.1\frac{cd}{m^2}$ | 0.047 | 0.060 | 0.064 | 0.076 | 0.074 |
| Old | | | 0.056 | 0.063 | 0.068 | 0.079 | 0.082 |
| Young | Circle | $1.0\frac{cd}{m^2}$ | 0.044 | 0.042 | 0.058 | 0.061 | 0.066 |
| Old | | | 0.049 | 0.046 | 0.061 | 0.068 | 0.073 |
| Young | Deer | $0.1\frac{cd}{m^2}$ | 0.066 | 0.072 | 0.073 | 0.083 | 0.088 |
| Old | | | 0.071 | 0.075 | 0.078 | 0.089 | 0.091 |
| Young | Deer | $1.0\frac{cd}{m^2}$ | 0.066 | 0.070 | 0.069 | 0.080 | 0.083 |
| Old | | | 0.072 | 0.076 | 0.077 | 0.085 | 0.086 |

Table A.3: Contrast results of two age groups for a 50.0% detection probability at two background luminances; Relation between contrast K and eccentricity $\theta$; Object shapes circle and deer, target size: $1.0°$.

The detection results of the circle and deer shape (2.0°) as a function of the two age groups for a detection probability of 50.0% are illustrated in Figure A.7 and Figure A.8.

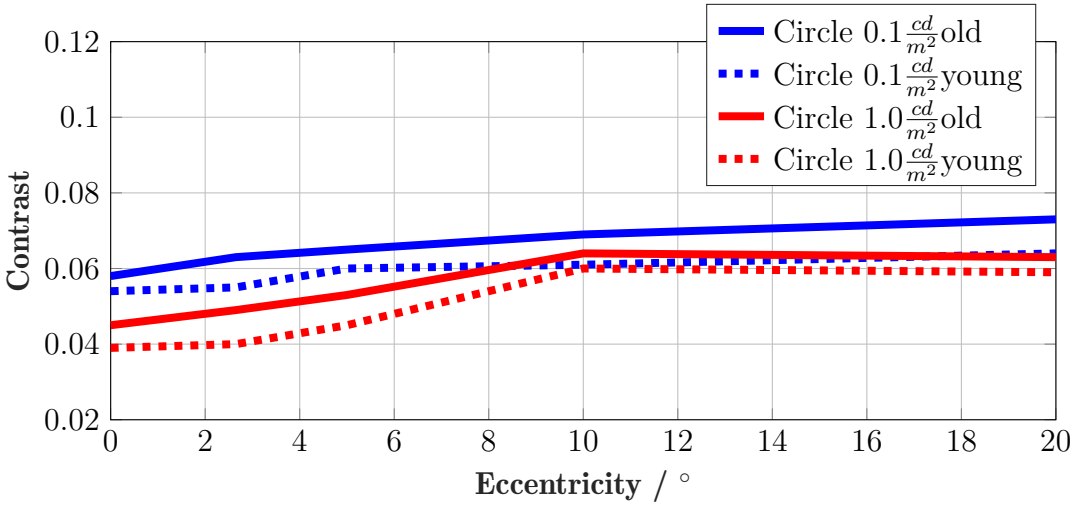


Figure A.7: Contrast results of two age groups for a 50.0% detection probability at two background luminances; Relation between contrast K and eccentricity $\theta$. circle, target size: 2.0°.

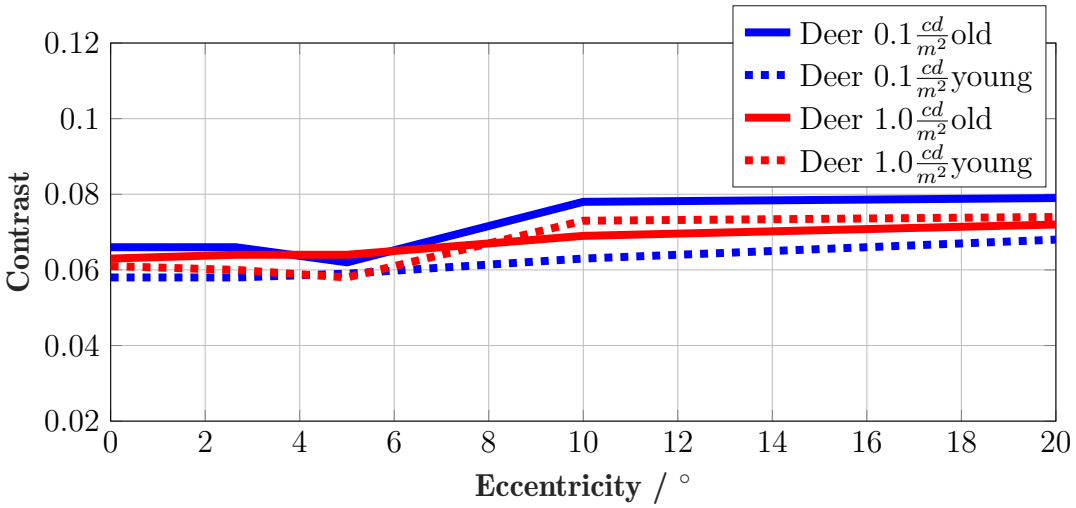


Figure A.8: Contrast results of two age groups for a 50.0% detection probability at two background luminances; Relation between contrast K and eccentricity $\theta$. deer; target size: 2.0°.

Table A.4 illustrates the corresponding contrast values for a 50.0% detection probability for both target shapes.

| Age group | Target | $L_U$ | 0.0° | 2.65° | 5.0° | 10.0° | 20.0° |
|---|---|---|---|---|---|---|---|
| Young | Circle | $0.1\frac{cd}{m^2}$ | 0.054 | 0.055 | 0.060 | 0.061 | 0.064 |
| Old | | | 0.058 | 0.063 | 0.065 | 0.069 | 0.073 |
| Young | Circle | $1.0\frac{cd}{m^2}$ | 0.039 | 0.040 | 0.045 | 0.060 | 0.059 |
| Old | | | 0.045 | 0.049 | 0.053 | 0.064 | 0.063 |
| Young | Deer | $0.1\frac{cd}{m^2}$ | 0.061 | 0.060 | 0.058 | 0.073 | 0.074 |
| Old | | | 0.066 | 0.066 | 0.062 | 0.078 | 0.079 |
| Young | Deer | $1.0\frac{cd}{m^2}$ | 0.058 | 0.058 | 0.059 | 0.063 | 0.068 |
| Old | | | 0.063 | 0.064 | 0.064 | 0.069 | 0.072 |

Table A.4: Contrast results of two age groups for a 50.0% detection probability at two background luminances; Relation between contrast K and eccentricity $\theta$; Object shapes circle and deer, target size: $2.0°$ .

# Appendix B

# Laboratory results

### B.0.1 Main effects and interaction

Tables B.2 to B.6 present the results for the comparison of the two object shapes at the different observation angles. The analysis is explained using an example.
Table B.1 shows results for the comparison of the two target shapes at an eccentricity of 2.65° for a background luminance of $0.1\frac{cd}{m^2}$ and a target size of 1.0°.

| Source | SS | df | MS | F | p |
|---|---|---|---|---|---|
| Object luminance | 81.6 | 1 | 81.649 | 0.24 | 0.6238 |
| Background luminance | 8638.3 | 9 | 959.808 | 2.87 | 0.0103 |
| Interaction | 4448.3 | 9 | 494.251 | 1.48 | 0.1892 |
| Error | 13370.1 | 40 | 334.252 | | |
| Total | 26538.3 | 59 | | | |

Table B.1: Two-factorial variance analysis considering the eccentricity of 2.65°. SS: sum of squares, df: degrees of freedom, MS: mean square error, factor A: object luminance, factor B: background luminance $0.1\frac{cd}{m^2}$, target size: 1.0°.

The column p shows the p-values for the object luminance (0.6238), the background luminance (0.0103), and the interaction between object and background luminance (0.1892). These values indicate that the background luminance has an influence, but there is no evidence of an interaction effect of the two. In the present case, $F_{1,9} = 5.12$. The F-quantile is 5.0% of the probability of error. That means, for all F-values up to the test size of $F = 5.12$ the null hypothesis can not be rejected. As in this case $2.87 < 5.12$ (background luminance) the result is not significant, that is, the null hypothesis can not be rejected.

### B.0.2 Background luminance $0.1\frac{cd}{m^2}$, target size 1.0°

Tables B.2 to B.16 present the results for the comparison of the two target shapes at the different observation angles for a background luminance of $0.1\frac{cd}{m^2}$ and a target size of 1.0°. The two age groups are also taken into account.

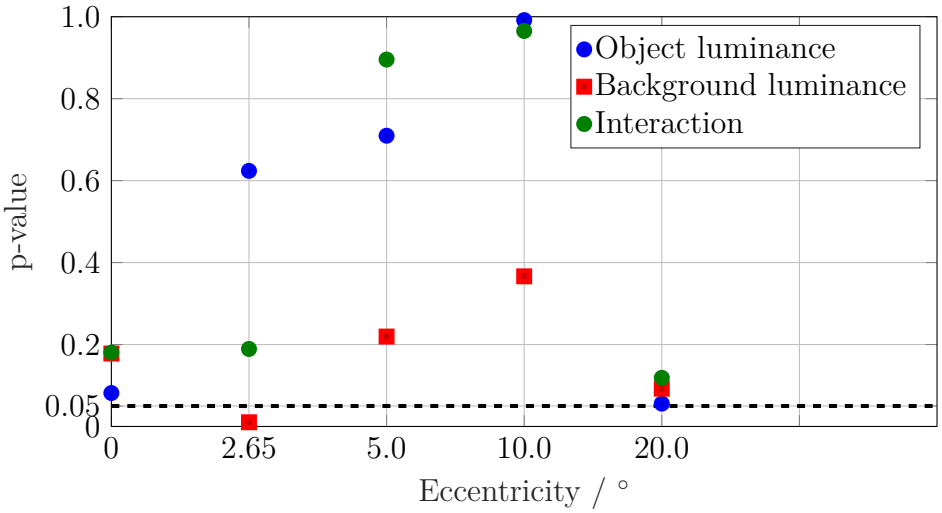


Figure B.1: Two-factorial variance analysis considering eccentricities from 0.0° to 20.0°, p-values of the two influencing parameters and their interaction. Since a F- distribution for $(1-\alpha) = 0.95$ is assumed the critical value p = 0.05 is illustrated as dashed line.

| Source | SS | df | MS | F | p |
|---|---|---|---|---|---|
| Object luminance | 1244.6 | 1 | 1244.55 | 3.19 | 0.0816 |
| Background luminance | 5298 | 9 | 588.67 | 1.51 | 0.178 |
| Interaction | 5275.7 | 9 | 586.19 | 1.5 | 0.1803 |
| Error | 15600.5 | 40 | 390.01 | | |
| Total | 27418.8 | 59 | | | |

Table B.2: Two-factorial variance analysis considering the eccentricity of $0.0°$. SS: sum of squares, df: degrees of freedom, MS: mean square error, factor A: object luminance, factor B: background luminance 0.1 $\frac{cd}{m^2}$, target size: 1.0°.

| Source | SS | df | MS | F | p |
|---|---|---|---|---|---|
| Object luminance | 81.6 | 1 | 81.649 | 0.24 | 0.6238 |
| Background luminance | 8638.3 | 9 | 959.808 | 2.87 | 0.0103 |
| Interaction | 4448.3 | 9 | 494.251 | 1.48 | 0.1892 |
| Error | 13370.1 | 40 | 334.252 | | |
| Total | 26538.3 | 59 | | | |

Table B.3: Two-factorial variance analysis considering the eccentricity of $2.65°$. SS: sum of squares, df: degrees of freedom, MS: mean square error, factor A: object luminance, factor B: background luminance 0.1 $\frac{cd}{m^2}$, target size: 1.0°.

| Source | SS | df | MS | F | p |
|---|---|---|---|---|---|
| Object luminance | 95 | 1 | 95.028 | 0.14 | 0.7096 |
| Background luminance | 8529.2 | 9 | 947.691 | 1.4 | 0.2194 |
| Interaction | 2767 | 9 | 307.444 | 0.46 | 0.8955 |
| Error | 27016.7 | 40 | 675.418 | | |
| Total | 38408 | 59 | | | |

Table B.4: Two-factorial variance analysis considering the eccentricity of $5.0°$. SS: sum of squares, df: degrees of freedom, MS: mean square error, factor A: object luminance, factor B: background luminance 0.1 $\frac{cd}{m^2}$, target size: 1.0°.

| Source | SS | df | MS | F | p |
|---|---|---|---|---|---|
| Object luminance | 0.1 | 1 | 0.052 | 0 | 0.9917 |
| Background luminance | 4847.6 | 9 | 538.626 | 1.13 | 0.3664 |
| Interaction | 1356.7 | 9 | 150.739 | 0.32 | 0.9652 |
| Error | 19102.2 | 40 | 477.555 | | |
| Total | 25306.5 | 59 | | | |

Table B.5: Two-factorial variance analysis considering the eccentricity of $10.0°$. SS: sum of squares, df: degrees of freedom, MS: mean square error, factor A: object luminance, factor B: background luminance 0.1 $\frac{cd}{m^2}$, target size: 1.0°.

| Source | SS | df | MS | F | p |
|---|---|---|---|---|---|
| Object luminance | 1637.8 | 1 | 1637.8 | 3.88 | 0.0558 |
| Background luminance | 46955.5 | 9 | 772.84 | 1.83 | 0.0923 |
| Interaction | 6493.7 | 9 | 721.52 | 1.71 | 0.1187 |
| Error | 16880.6 | 40 | 422.01 | | |
| Total | 31967.6 | 59 | | | |

Table B.6: Two-factorial variance analysis considering the eccentricity of $20.0°$. SS: sum of squares, df: degrees of freedom, MS: mean square error, factor A: object luminance, factor B: background luminance 0.1 $\frac{cd}{m^2}$, target size: 1.0°.

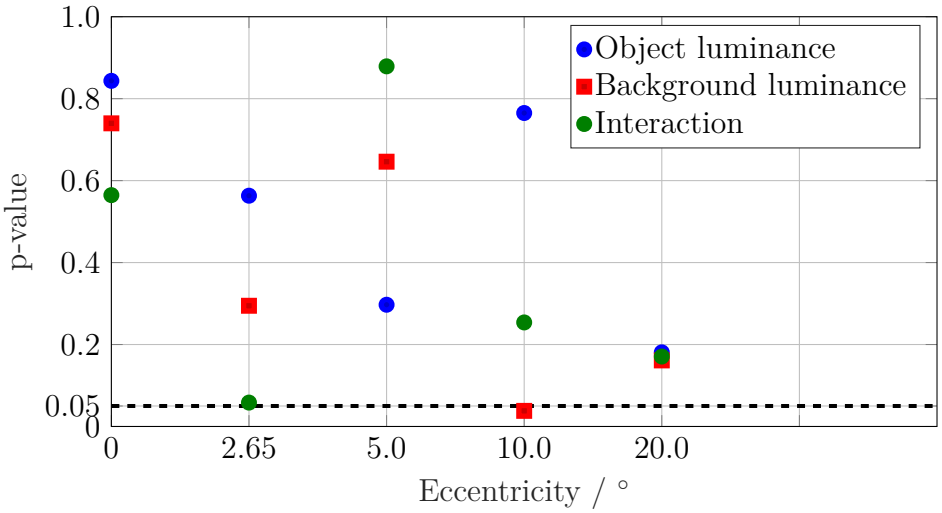


Figure B.2: Two-factorial variance analysis considering eccentricities from 0.0° to 20.0°, p-values of the two influencing parameters and their interaction. Since a F- distribution for $(1 - \alpha) = 0.95$ is assumed the critical value p = 0.05 is illustrated as dashed line.

| Source | SS | df | MS | F | p |
|---|---|---|---|---|---|
| Object luminance | 26.39 | 1 | 26.394 | 0.04 | 0.8435 |
| Background luminance | 75.01 | 1 | 75.013 | 0.12 | 0.7398 |
| Interaction | 228.98 | 1 | 228.979 | 0.36 | 0.5646 |
| Error | 5075.23 | 8 | 634.403 | | |
| Total | 5405.61 | 11 | | | |

Table B.7: Young age group. Two-factorial variance analysis considering the eccentricity of $0.0°$. SS: sum of squares, df: degrees of freedom, MS: mean square error, factor A: object luminance, factor B: background luminance 0.1 $\frac{cd}{m^2}$, target size: 1.0°.

| Source | SS | df | MS | F | p |
|---|---|---|---|---|---|
| Object luminance | 177.11 | 1 | 177.11 | 0.36 | 0.5632 |
| Background luminance | 612.67 | 1 | 612.67 | 1.26 | 0.2946 |
| Interaction | 2374.43 | 1 | 2374.43 | 4.87 | 0.0583 |
| Error | 3897.2 | 8 | 487.15 | | |
| Total | 7061.4 | 11 | | | |

Table B.8: Young age group. Two-factorial variance analysis considering the eccentricity of $2.65°$. SS: sum of squares, df: degrees of freedom, MS: mean square error, factor A: object luminance, factor B: background luminance 0.1 $\frac{cd}{m^2}$, target size: 1.0°.

| Source | SS | df | MS | F | p |
|---|---|---|---|---|---|
| Object shape | 456.28 | 1 | 456.278 | 1.24 | 0.2971 |
| Background luminance | 83.43 | 1 | 83.425 | 0.23 | 0.6462 |
| Interaction | 8.96 | 1 | 8.959 | 0.02 | 0.8797 |
| Error | 2934.68 | 8 | 366.835 | | |
| Total | 3483.34 | 11 | | | |

Table B.9: Young age group. Two-factorial variance analysis considering the eccentricity of $5.0°$. SS: sum of squares, df: degrees of freedom, MS: mean square error, factor A: object luminance, factor B: background luminance 0.1$\frac{cd}{m^2}$, target size: 1.0°.

| Source | SS | df | MS | F | p |
|---|---|---|---|---|---|
| Object shape | 27 | 1 | 26.95 | 0.08 | 0.7737 |
| Background luminance | 11214.6 | 9 | 1246.06 | 3.87 | 0.0013 |
| Interaction | 4045.6 | 9 | 449.51 | 1.4 | 0.2219 |
| Error | 12867.1 | 40 | 321.68 | | |
| Total | 28154.3 | 59 | | | |

Table B.10: Young age group. Two-factorial variance analysis considering the eccentricity of $10.0°$. SS: sum of squares, df: degrees of freedom, MS: mean square error, factor A: object luminance, factor B: background luminance 0.1$\frac{cd}{m^2}$, target size: 1.0°.

| Source | SS | df | MS | F | p |
|---|---|---|---|---|---|
| Object shape | 40.2 | 1 | 40.24 | 0.09 | 0.765 |
| Background luminance | 9007.1 | 9 | 1000.79 | 2.25 | 0.0381 |
| Interaction | 5307.8 | 9 | 589.76 | 1.33 | 0.2539 |
| Error | 17773.6 | 40 | 444.34 | | |
| Total | 32128.7 | 59 | | | |

Table B.11: Young age group. Two-factorial variance analysis considering the eccentricity of $20.0°$. SS: sum of squares, df: degrees of freedom, MS: mean square error, factor A: object luminance, factor B: background luminance 0.1$\frac{cd}{m^2}$, target size: 1.0°.

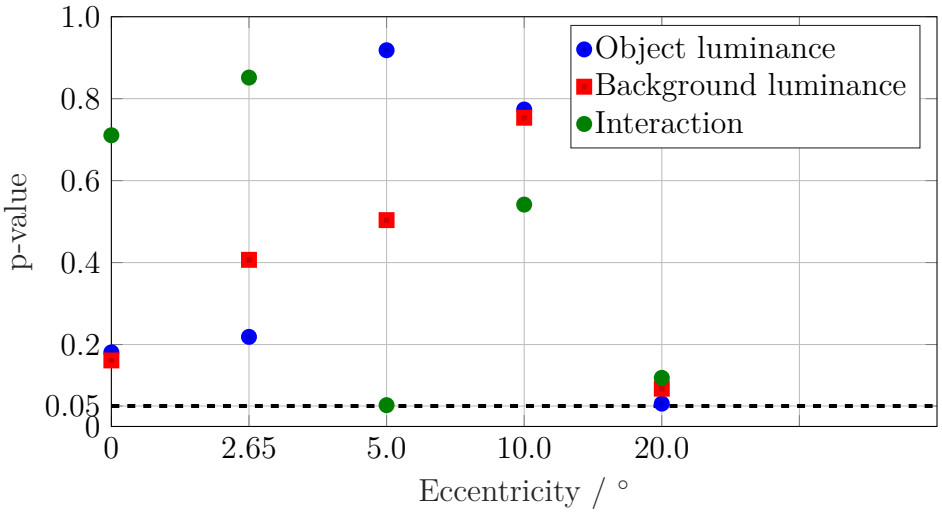


Figure B.3: Two-factorial variance analysis considering eccentricities from 0.0° to 20.0°, p-values of the two influencing parameters and their interaction. Since a F- distribution for $(1-\alpha) = 0.95$ is assumed the critical value p = 0.05 is illustrated as dashed line.

| Source | SS | df | MS | F | p |
|---|---|---|---|---|---|
| Object shape | 884.81 | 1 | 884.811 | 2.15 | 0.1809 |
| Background luminance | 981.8 | 1 | 981.796 | 2.38 | 0.1612 |
| Interaction | 60.88 | 1 | 60.88 | 0.15 | 0.7107 |
| Error | 3295.84 | 8 | 411.98 | | |
| Total | 5223.32 | 11 | | | |

Table B.12: Old age group. Two-factorial variance analysis considering the eccentricity of $0.0°$. SS: sum of squares, df: degrees of freedom, MS: mean square error, factor A: object luminance, factor B: background luminance 0.1 $\frac{cd}{m^2}$, target size: 1.0°.

| Source | SS | df | MS | F | p |
|---|---|---|---|---|---|
| Object shape | 881.53 | 1 | 881.526 | 1.78 | 0.2187 |
| Background luminance | 379.46 | 1 | 379.462 | 0.77 | 0.4067 |
| Interaction | 18.49 | 1 | 18.492 | 0.04 | 0.8515 |
| Error | 3958 | 8 | 494.75 | | |
| Total | 5237.48 | 11 | | | |

Table B.13: Old age group. Two-factorial variance analysis considering the eccentricity of $2.65°$. SS: sum of squares, df: degrees of freedom, MS: mean square error, factor A: object luminance, factor B: background luminance 0.1 $\frac{cd}{m^2}$, target size: 1.0°.

| Source | SS | df | MS | F | p |
|---|---|---|---|---|---|
| Object shape | 6.53 | 1 | 6.53 | 0.01 | 0.9182 |
| Background luminance | 285.13 | 1 | 285.13 | 0.49 | 0.5036 |
| Interaction | 3025.75 | 1 | 3025.75 | 5.2 | 0.052 |
| Error | 4650.57 | 8 | 581.32 | | |
| Total | 7967.97 | 11 | | | |

Table B.14: Old age group. Two-factorial variance analysis considering the eccentricity of $5.0°$. SS: sum of squares, df: degrees of freedom, MS: mean square error, factor A: object luminance, factor B: background luminance $0.1\frac{cd}{m^2}$, target size: 1.0°.

| Source | SS | df | MS | F | p |
|---|---|---|---|---|---|
| Object shape | 34.18 | 1 | 34.182 | 0.09 | 0.7735 |
| Background luminance | 40.71 | 1 | 40.71 | 0.11 | 0.7535 |
| Interaction | 156.77 | 1 | 156.774 | 0.41 | 0.5415 |
| Error | 3083.85 | 8 | 385.481 | | |
| Total | 3315.51 | 11 | | | |

Table B.15: Old age group. Two-factorial variance analysis considering the eccentricity of $10.0°$. SS: sum of squares, df: degrees of freedom, MS: mean square error, factor A: object luminance, factor B: background luminance $0.1\frac{cd}{m^2}$, target size: 1.0°.

| Source | SS | df | MS | F | p |
|---|---|---|---|---|---|
| Object luminance | 1637.8 | 1 | 1637.8 | 3.88 | 0.0558 |
| Background luminance | 46955.5 | 9 | 772.84 | 1.83 | 0.0923 |
| Interaction | 6493.7 | 9 | 721.52 | 1.71 | 0.1187 |
| Error | 16880.6 | 40 | 422.01 | | |
| Total | 31967.6 | 59 | | | |

Table B.16: Old age group. Two-factorial variance analysis considering the eccentricity of $20.0°$. SS: sum of squares, df: degrees of freedom, MS: mean square error, factor A: object luminance, factor B: background luminance $0.1\frac{cd}{m^2}$, target size: 1.0°.

### B.0.3 Background luminance $1.0\frac{cd}{m^2}$, target size 1.0°

Table B.17 to B.31 present the results for the comparison of the two target shapes at the different observation angles for a background luminance of $1.0\frac{cd}{m^2}$ and a target size of 1.0°. The two age groups are also taken into account.

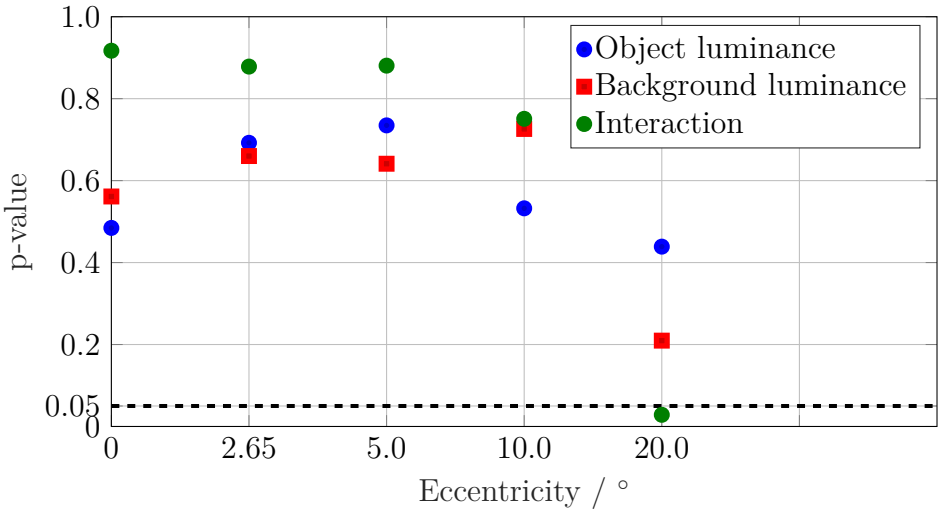


Figure B.4: Two-factorial variance analysis considering eccentricities from 0.0° to 20.0°, p-values of the two influencing parameters and their interaction. Since a F- distribution for $(1 - \alpha) = 0.95$ is assumed the critical value p = 0.05 is illustrated as dashed line.

| Source | SS | df | MS | F | p |
|---|---|---|---|---|---|
| Object luminance | 1622.2 | 1 | 1622.24 | 0.54 | 0.4846 |
| Background luminance | 1109.1 | 1 | 1109.14 | 0.37 | 0.5613 |
| Interaction | 34.9 | 1 | 34.94 | 0.01 | 0.917 |
| Error | 24164.1 | 8 | 3020.51 | | |
| Total | 26930.4 | 11 | | | |

Table B.17: Two-factorial variance analysis considering the eccentricity of $0.0°$. SS: sum of squares, df: degrees of freedom, MS: mean square error, factor A: object luminance, factor B: background luminance 1.0$\frac{cd}{m^2}$, target size: 1.0°.

| Source | SS | df | MS | F | p |
|---|---|---|---|---|---|
| Object luminance | 684.8 | 1 | 684.78 | 0.17 | 0.6923 |
| Background luminance | 1848.7 | 1 | 848.7 | 0.21 | 0.66 |
| Interaction | 101.6 | 1 | 101.65 | 0.02 | 0.8783 |
| Error | 32540 | 8 | 4067.51 | | |
| Total | 34175.2 | 11 | | | |

Table B.18: Two-factorial variance analysis considering the eccentricity of $2.65°$. SS: sum of squares, df: degrees of freedom, MS: mean square error, factor A: object luminance, factor B: background luminance 1.0$\frac{cd}{m^2}$, target size: 1.0°.

| Source | SS | df | MS | F | p |
|---|---|---|---|---|---|
| Object luminance | 463.1 | 1 | 463.15 | 0.12 | 0.7348 |
| Background luminance | 882 | 1 | 882.02 | 0.23 | 0.6412 |
| Interaction | 90.5 | 1 | 90.55 | 0.02 | 0.8806 |
| Error | 30100.5 | 8 | 3762.56 | | |
| Total | 131536.2 | 11 | | | |

Table B.19: Two-factorial variance analysis considering the eccentricity of $5.0°$. SS: sum of squares, df: degrees of freedom, MS: mean square error, factor A: object luminance, factor B: background luminance 1.0$\frac{cd}{m^2}$, target size: 1.0°.

| Source | SS | df | MS | F | p |
|---|---|---|---|---|---|
| Object luminance | 1368.8 | 1 | 1368.82 | 0.43 | 0.5324 |
| Background luminance | 423.3 | 1 | 423.28 | 0.13 | 0.7261 |
| Interaction | 347.5 | 1 | 347.48 | 0.11 | 0.7508 |
| Error | 25719.2 | 8 | 3214.9 | | |
| Total | 27858.8 | 11 | | | |

Table B.20: Two-factorial variance analysis considering the eccentricity of $10.0°$. SS: sum of squares, df: degrees of freedom, MS: mean square error, factor A: object luminance, factor B: background luminance 1.0$\frac{cd}{m^2}$, target size: 1.0°.

| Source | SS | df | MS | F | p |
|---|---|---|---|---|---|
| Object luminance | 602.1 | 1 | 602.11 | 0.66 | 0.4389 |
| Background luminance | 1690.2 | 1 | 1690.24 | 1.86 | 0.2095 |
| Interaction | 6452.4 | 1 | 6452.44 | 7.11 | 0.0285 |
| Error | 7259 | 8 | 907.38 | | |
| Total | 16003.8 | 11 | | | |

Table B.21: Two-factorial variance analysis considering the eccentricity of $20.0°$. SS: sum of squares, df: degrees of freedom, MS: mean square error, factor A: object luminance, factor B: background luminance 1.0$\frac{cd}{m^2}$,

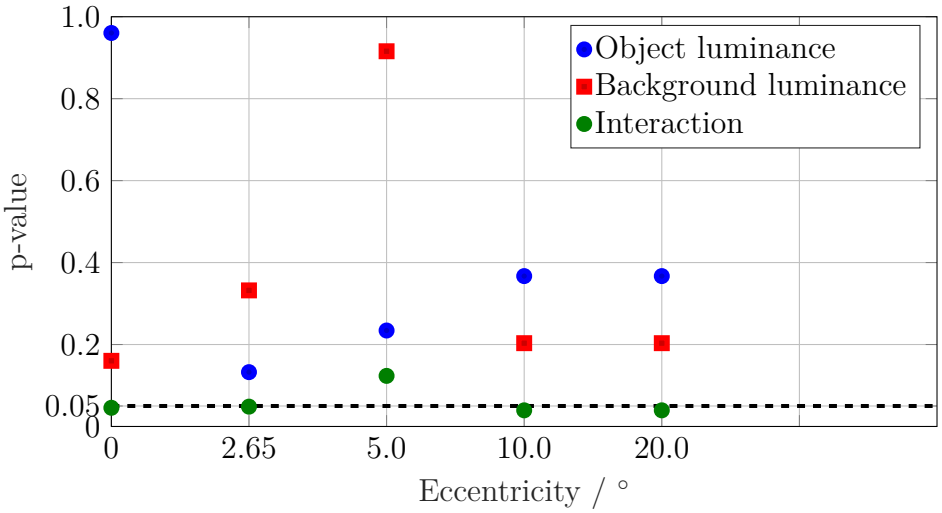


Figure B.5: Two-factorial variance analysis considering eccentricities from 0.0° to 20.0°, p-values of the two influencing parameters and their interaction. Since a F- distribution for $(1 - \alpha) = 0.95$ is assumed the critical value p = 0.05 is illustrated as dashed line.

| Source | SS | df | MS | F | p |
|---|---|---|---|---|---|
| Object luminance | 6.1 | 1 | 6.1 | 0 | 0.9603 |
| Background luminance | 5531.4 | 1 | 5531.4 | 2.4 | 0.1602 |
| Interaction | 12902.3 | 1 | 12902.3 | 5.59 | 0.0456 |
| Error | 18461.4 | 8 | 2307.7 | | |
| Total | 36901.3 | 11 | | | |

Table B.22: Young age group. Two-factorial variance analysis considering the eccentricity of $0.0°$. SS: sum of squares, df: degrees of freedom, MS: mean square error, factor A: object luminance, factor B: background luminance 1.0$\frac{cd}{m^2}$, target size: 1.0°.

| Source | SS | df | MS | F | p |
|---|---|---|---|---|---|
| Object luminance | 2574.7 | 1 | 2574.68 | 2.8 | 0.1326 |
| Background luminance | 978.5 | 1 | 978.53 | 1.07 | 0.3321 |
| Interaction | 4969.7 | 1 | 4969.68 | 5.41 | 0.0484 |
| Error | 7346.7 | 8 | 918.34 | | |
| Total | 15869.6 | 11 | | | |

Table B.23: Young age group. Two-factorial variance analysis considering the eccentricity of $2.65°$. SS: sum of squares, df: degrees of freedom, MS: mean square error, factor A: object luminance, factor B: background luminance 1.0$\frac{cd}{m^2}$, target size: 1.0°.

| Source | SS | df | MS | F | p |
|---|---|---|---|---|---|
| Object luminance | 979.81 | 1 | 979.81 | 1.66 | 0.2342 |
| Background luminance | 7.06 | 1 | 7.06 | 0.01 | 0.9157 |
| Interaction | 1753.3 | 1 | 1753.3 | 2.96 | 0.1235 |
| Error | 4734.88 | 8 | 591.86 | | |
| Total | 7475.05 | 11 | | | |

Table B.24: Young age group. Two-factorial variance analysis considering the eccentricity of $5.0°$. SS: sum of squares, df: degrees of freedom, MS: mean square error, factor A: object luminance, factor B: background luminance $1.0\frac{cd}{m^2}$, target size: 1.0°.

| Source | SS | df | MS | F | p |
|---|---|---|---|---|---|
| Object luminance | 2184.5 | 1 | 2184.5 | 0.91 | 0.367 |
| Background luminance | 4587.6 | 1 | 4587.6 | 1.92 | 0.2033 |
| Interaction | 14455.3 | 1 | 14455.3 | 6.05 | 0.0394 |
| Error | 19119.6 | 8 | 2390 | | |
| Total | 40347 | 11 | | | |

Table B.25: Young age group. Two-factorial variance analysis considering the eccentricity of $10.0°$. SS: sum of squares, df: degrees of freedom, MS: mean square error, factor A: object luminance, factor B: background luminance $1.0\frac{cd}{m^2}$, target size: 1.0°.

| Source | SS | df | MS | F | p |
|---|---|---|---|---|---|
| Object luminance | 41.9 | 1 | 41.9 | 0.04 | 0.843 |
| Background luminance | 607.1 | 1 | 607.1 | 0.61 | 0.4584 |
| Interaction | 5950.3 | 1 | 5950.25 | 5.95 | 0.0407 |
| Error | 8004.9 | 8 | 1000.62 | | |
| Total | 14604.2 | 11 | | | |

Table B.26: Young age group. Two-factorial variance analysis considering the eccentricity of $20.0°$. SS: sum of squares, df: degrees of freedom, MS: mean square error, factor A: object luminance, factor B: background luminance $1.0\frac{cd}{m^2}$.

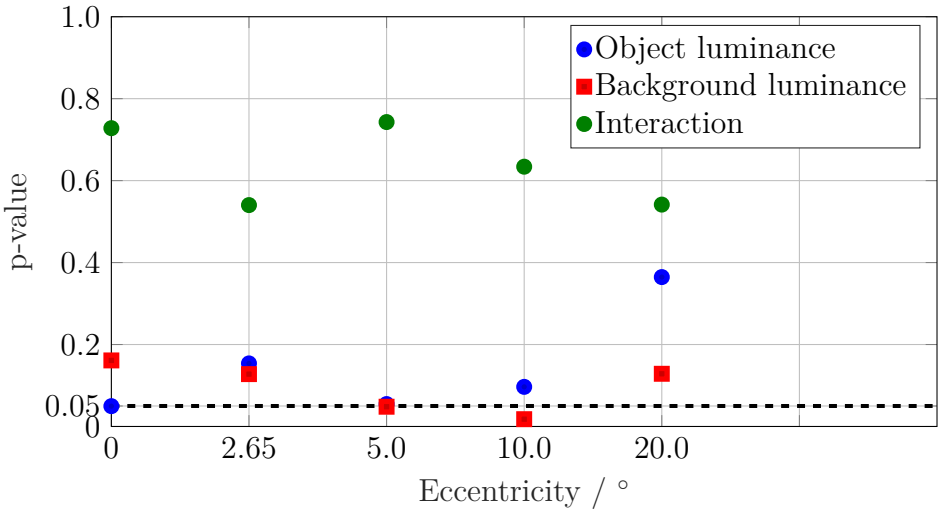


Figure B.6: Two-factorial variance analysis considering eccentricities from 0.0° to 20.0°, p-values of the two influencing parameters and their interaction. Since a F- distribution for $(1-\alpha) = 0.95$ is assumed the critical value p = 0.05 is illustrated as dashed line.

| Source | SS | df | MS | F | p |
|---|---|---|---|---|---|
| Object luminance | 3868.3 | 1 | 3868.27 | 5.34 | 0.0496 |
| Background luminance | 981.8 | 1 | 981.796 | 2.38 | 0.1612 |
| Interaction | 94 | 1 | 94.03 | 0.13 | 0.728 |
| Error | 5796 | 8 | 724.5 | | |
| Total | 11068.7 | 11 | | | |

Table B.27: Old age group. Two-factorial variance analysis considering the eccentricity of 0.0°. SS: sum of squares, df: degrees of freedom, MS: mean square error, factor A: object luminance, factor B: background luminance 1.0$\frac{cd}{m^2}$, target size: 1.0°.

| Source | SS | df | MS | F | p |
|---|---|---|---|---|---|
| Object luminance | 1250.39 | 1 | 1250.39 | 2.48 | 0.1539 |
| Background luminance | 1454.6 | 1 | 1454.6 | 2.89 | 0.1278 |
| Interaction | 206.19 | 1 | 206.19 | 0.41 | 0.5403 |
| Error | 4032.49 | 8 | 504.06 | | |
| Total | 6943.67 | 11 | | | |

Table B.28: Old age group. Two-factorial variance analysis considering the eccentricity of 2.65°. SS: sum of squares, df: degrees of freedom, MS: mean square error, factor A: object luminance, factor B: background luminance 1.0$\frac{cd}{m^2}$, target size: 1.0°.

| Source | SS | df | MS | F | p |
|---|---|---|---|---|---|
| Object luminance | 1956.24 | 1 | 1956.24 | 5.06 | 0.0547 |
| Background luminance | 2099.23 | 1 | 2099.23 | 5.42 | 0.0482 |
| Interaction | 44.64 | 1 | 44.64 | 0.12 | 0.7429 |
| Error | 3095.72 | 8 | 386.97 | | |
| Total | 7195.83 | 11 | | | |

Table B.29: Old age group. Two-factorial variance analysis considering the eccentricity of $5.0°$. SS: sum of squares, df: degrees of freedom, MS: mean square error, factor A: object luminance, factor B: background luminance 1.0$\frac{cd}{m^2}$, target size: 1.0°.

| Source | SS | df | MS | F | p |
|---|---|---|---|---|---|
| Object luminance | 1590.37 | 1 | 1590.37 | 3.54 | 0.0967 |
| Background luminance | 3967.65 | 1 | 3967.65 | 8.83 | 0.0178 |
| Interaction | 110.06 | 1 | 110.06 | 0.24 | 0.634 |
| Error | 3595.47 | 8 | 449.43 | | |
| Total | 9263.55 | 11 | | | |

Table B.30: Old age group. Two-factorial variance analysis considering the eccentricity of $10.0°$. SS: sum of squares, df: degrees of freedom, MS: mean square error, factor A: object luminance, factor B: background luminance 1.0$\frac{cd}{m^2}$, target size: 1.0°.

| Source | SS | df | MS | F | p |
|---|---|---|---|---|---|
| Object luminance | 468 | 1 | 468 | 0.92 | 0.3646 |
| Background luminance | 1455.1 | 1 | 1455.1 | 2.87 | 0.1286 |
| Interaction | 206 | 1 | 206 | 0.41 | 0.5415 |
| Error | 4053.01 | 8 | 506.63 | | |
| Total | 6182.1 | 11 | | | |

Table B.31: Old age group. Two-factorial variance analysis considering the eccentricity of $20.0°$. SS: sum of squares, df: degrees of freedom, MS: mean square error, factor A: object luminance, factor B: background luminance 1.0$\frac{cd}{m^2}$, target size: 1.0°.

# Appendix C

# Field study results

## C.1 Main effects and interaction

The following Tables C.1 to C.4 show results of the main effects and interactions in the dynamic test setup assuming a F- distribution for $(1 - \alpha) = 0.95$.
Tables C.1 to C.4 present the results for the comparison of the two object shapes at the different observation angles.

| Source | SS | df | MS | F | p |
|---|---|---|---|---|---|
| Object shape | 202.4 | 1 | 202.42 | 0.67 | 0.418 |
| Eccentricity | 9174.1 | 9 | 1019.34 | 3.37 | 0.0037 |
| Interaction | 1037 | 9 | 115.22 | 0.38 | 0.9373 |
| Error | 12090 | 40 | 302.25 | | |
| Total | 22503.5 | 59 | | | |

Table C.1: Two-factorial variance analysis considering position 1 (2.65°). SS: sum of squares, df: degrees of freedom, MS: mean square error, factor A: object shape, factor B: eccentricity.

| Source | SS | df | MS | F | p |
|---|---|---|---|---|---|
| Object shape | 14.8 | 1 | 14.8 | 0.04 | 0.8344 |
| Eccentricity | 11037.5 | 9 | 1226.38 | 3.67 | 0.002 |
| Interaction | 1369.6 | 9 | 152.18 | 0.46 | 0.8954 |
| Error | 13367.7 | 40 | 334.19 | | |
| Total | 25789.6 | 59 | | | |

Table C.2: Two-factorial variance analysis considering position 2 (5.0°). SS: sum of squares, df: degrees of freedom, MS: mean square error, factor A: object shape, factor B: eccentricity.

| Source | SS | df | MS | F | p |
|---|---|---|---|---|---|
| Object shape | 95 | 1 | 95.028 | 0.14 | 0.7096 |
| Eccentricity | 8529.2 | 9 | 947.691 | 1.4 | 0.2194 |
| Interaction | 2767 | 9 | 307.444 | 0.46 | 0.8955 |
| Error | 27016.7 | 40 | 675.418 | | |
| Total | 38408 | 59 | | | |

Table C.3: Two-factorial variance analysis considering position 3 (6.5°). SS: sum of squares, df: degrees of freedom, MS: mean square error, factor A: object shape, factor B: eccentricity.

| Source | SS | df | MS | F | p |
|---|---|---|---|---|---|
| Object shape | 0.1 | 1 | 0.052 | 0 | 0.9917 |
| Eccentricity | 4847.6 | 9 | 538.626 | 1.13 | 0.3664 |
| Interaction | 1356.7 | 9 | 150.739 | 0.32 | 0.9652 |
| Error | 19102.2 | 40 | 477.555 | | |
| Total | 25306.5 | 59 | | | |

Table C.4: Two-factorial variance analysis considering position 4 (8.0°). SS: sum of squares, df: degrees of freedom, MS: mean square error, factor A: object shape, factor B: eccentricity.

### C.1.1 Dynamic setup - age groups

Tables C.5 to C.12 present the results for the comparison of the two object shapes at the different observation angles considering the two age groups (young and old).

| Source | SS | df | MS | F | p |
|---|---|---|---|---|---|
| Object shape | 0 | 1 | 0 | 0 | 0.9983 |
| Eccentricity | 1534.71 | 1 | 1534.71 | 5.04 | 0.0551 |
| Interaction | 0 | 1 | 0 | 0 | 0.9983 |
| Error | 2437.55 | 8 | 304.69 | | |
| Total | 3972.26 | 11 | | | |

Table C.5: Young age group. Two-factorial variance analysis considering position 1 (2.65°). SS: sum of squares, df: degrees of freedom, MS: mean square error, factor A: object shape, factor B: eccentricity.

| Source | SS | df | MS | F | p |
|---|---|---|---|---|---|
| Object shape | 188.45 | 1 | 188.449 | 0.35 | 0.5714 |
| Eccentricity | 565.8 | 1 | 565.8 | 1.05 | 0.3365 |
| Interaction | 0 | 1 | 0 | 0 | 0.9998 |
| Error | 4329.81 | 8 | 541.227 | | |
| Total | 5084.06 | 11 | | | |

Table C.6: Young age group. Two-factorial variance analysis considering position 2 (5.0°). SS: sum of squares, df: degrees of freedom, MS: mean square error, factor A: object shape, factor B: eccentricity.

| Source | SS | df | MS | F | p |
|---|---|---|---|---|---|
| Object shape | 13.5 | 1 | 13.55 | 0.02 | 0.8931 |
| Eccentricity | 5283.3 | 1 | 5283.3 | 7.5 | 0.0255 |
| Interaction | 0.6 | 1 | 0.63 | 0 | 0.9769 |
| Error | 5635.8 | 8 | 704.47 | | |
| Total | 10933.3 | 11 | | | |

Table C.7: Young age group. Two-factorial variance analysis considering position 3 (6.5°). SS: sum of squares, df: degrees of freedom, MS: mean square error, factor A: object shape, factor B: eccentricity.

| Source | SS | df | MS | F | p |
|---|---|---|---|---|---|
| Object shape | 240.69 | 1 | 240.689 | 0.37 | 0.5595 |
| Eccentricity | 11.47 | 1 | 11.473 | 0.02 | 0.8975 |
| Interaction | 240.69 | 1 | 240.689 | 0.37 | 0.5595 |
| Error | 5194.31 | 8 | 649.289 | | |
| Total | 3483.34 | 11 | | | |

Table C.8: Young age group. Two-factorial variance analysis considering position 4 (8.0°). SS: sum of squares, df: degrees of freedom, MS: mean square error, factor A: object shape, factor B: eccentricity.

| Source | SS | df | MS | F | p |
|---|---|---|---|---|---|
| Object shape | 209.78 | 1 | 209.78 | 0.42 | 0.5331 |
| Eccentricity | 1445.12 | 1 | 1445.12 | 2.92 | 0.1257 |
| Interaction | 209.78 | 1 | 209.78 | 0.42 | 0.5331 |
| Error | 3955.8 | 8 | 494.47 | | |
| Total | 5820.47 | 11 | | | |

Table C.9: Old age group. Two-factorial variance analysis considering position 1 (2.65°). SS: sum of squares, df: degrees of freedom, MS: mean square error, factor A: object shape, factor B: eccentricity.

| Source | SS | df | MS | F | p |
|---|---|---|---|---|---|
| Object shape | 117.19 | 1 | 117.188 | 0.2 | 0.6671 |
| Eccentricity | 18.96 | 1 | 18.959 | 0.03 | 0.8619 |
| Interaction | 117.19 | 1 | 117.188 | 0.2 | 0.6671 |
| Error | 4703.41 | 8 | 587.927 | | |
| Total | 4956.75 | 11 | | | |

Table C.10: Old age group. Two-factorial variance analysis considering position 2 (5.0°). SS: sum of squares, df: degrees of freedom, MS: mean square error, factor A: object shape, factor B: eccentricity.

| Source | SS | df | MS | F | p |
|---|---|---|---|---|---|
| Object shape | 50.02 | 1 | 50.021 | 0.14 | 0.7205 |
| Eccentricity | 964.01 | 1 | 964.014 | 2.65 | 0.1423 |
| Interaction | 50.02 | 1 | 50.021 | 0.14 | 0.7205 |
| Error | 2911.98 | 8 | 363.998 | | |
| Total | 3976.04 | 11 | | | |

Table C.11: Old age group. Two-factorial variance analysis considering position 3 (6.5°). SS: sum of squares, df: degrees of freedom, MS: mean square error, factor A: object shape, factor B: eccentricity.

| Source | SS | df | MS | F | p |
|---|---|---|---|---|---|
| Object shape | 4.99 | 1 | 4.993 | 0.02 | 0.8982 |
| Eccentricity | 859.63 | 1 | 859.631 | 3 | 0.1213 |
| Interaction | 537.26 | 1 | 537.264 | 1.88 | 0.2079 |
| Error | 2289.95 | 8 | 286.243 | | |
| Total | 3691.83 | 11 | | | |

Table C.12: Old age group. Two-factorial variance analysis considering position 4 (8.0°). SS: sum of squares, df: degrees of freedom, MS: mean square error, factor A: object shape, factor B: eccentricity.

### C.1.2 Dynamic vs. static test setup

Tables C.13 to C.16 present the results for the comparison of the dynamic and static test setup for the two object shapes at the different observation angles.

| Source | SS | df | MS | F | p |
|---|---|---|---|---|---|
| Setup type | 10907.6 | 1 | 10907.6 | 18.51 | 0.0001 |
| Eccentricity | 14811.7 | 9 | 1645.7 | 2.79 6 | 0.0122 |
| Interaction | 25028.7 | 9 | 2781 | 4.72 | 0.0003 |
| Error | 23568.8 | 40 | 589.2 | | |
| Total | 74316.8 | 59 | | | |

Table C.13: Comparison of the dynamic and static test setup. Two-factorial variance analysis considering position 1 (2.65°). SS: sum of squares, df: degrees of freedom, MS: mean square error, factor A: setup type, factor B: eccentricity.

| Source | SS | df | MS | F | p |
|---|---|---|---|---|---|
| Setup type | 6160.7 | 1 | 6160.7 | 6.53 | 0.0145 |
| Eccentricity | 20740.9 | 9 | 2304.54 | 2.44 | 0.0255 |
| Interaction | 31437.2 | 9 | 3493.03 | 3.7 | 0.0019 |
| Error | 37750.1 | 40 | 943.75 | | |
| Total | 96088.9 | 59 | | | |

Table C.14: Comparison of the dynamic and static test setup. Two-factorial variance analysis considering position 2 (5.0°). SS: sum of squares, df: degrees of freedom, MS: mean square error, factor A: setup type, factor B: eccentricity.

| Source | SS | df | MS | F | p |
|---|---|---|---|---|---|
| Setup type | 11475.2 | 1 | 11475.2 | 14.82 | 0.0004 |
| Eccentricity | 21484.5 | 9 | 2387.2 | 3.08 | 0.0067 |
| Interaction | 20488.9 | 9 | 2276.5 | 2.94 | 0.009 |
| Error | 30972.1 | 40 | 774.3 | | |
| Total | 84420.6 | 59 | | | |

Table C.15: Comparison of the dynamic and static test setup. Two-factorial variance analysis considering position 3 (6.5°). SS: sum of squares, df: degrees of freedom, MS: mean square error, factor A: setup type, factor B: eccentricity.

| Source | SS | df | MS | F | p |
|---|---|---|---|---|---|
| Setup type | 4647.3 | 1 | 4647.31 | 4.89 | 0.0327 |
| Detection distance | 22279.1 | 9 | 2475.46 | 2.61 | 0.018 |
| Interaction | 13777.4 | 9 | 1530.82 | 1.61 | 0.1448 |
| Error | 37979.1 | 40 | 949.48 | | |
| Total | 78682.9 | 59 | | | |

Table C.16: Comparison of the dynamic and static test setup. Two-factorial variance analysis considering position 4 (8.0°). SS: sum of squares, df: degrees of freedom, MS: mean square error, factor A: setup type, factor B: eccentricity.

### C.1.3 Dynamic vs. static test setup - age groups

Tables C.17 to C.24 present the results for the comparison of the dynamic and static test setup at the different observation angles considering the two age groups (young and old).

| Source | SS | df | MS | F | p |
|---|---|---|---|---|---|
| Setup type | 743.81 | 1 | 743.81 | 2.72 | 0.138 |
| Eccentricity | 1394.67 | 1 | 1394.67 | 5.09 | 0.054 |
| Interaction | 3.49 | 1 | 3.49 | 0.01 | 0.9129 |
| Error | 2191.3 | 8 | 273.91 | | |
| Total | 4333.28 | 11 | | | |

Table C.17: Young age group. Comparison of the dynamic and static test setup. Two-factorial variance analysis considering position 1 (2.65°). SS: sum of squares, df: degrees of freedom, MS: mean square error, factor A: setup type, factor B: eccentricity.

| Source | SS | df | MS | F | p |
|---|---|---|---|---|---|
| Setup type | 3626.9 | 1 | 3626.85 | 3.51 | 0.0977 |
| Eccentricity | 757.6 | 1 | 757.62 | 0.73 | 0.4164 |
| Interaction | 13.9 | 1 | 13.93 | 0.01 | 0.9104 |
| Error | 8255.0 | 8 | 1031.87 | | |
| Total | 12653.4 | 11 | | | |

Table C.18: Young age group. Comparison of the dynamic and static test setup. Two-factorial variance analysis considering position 2 (5.0°). SS: sum of squares, df: degrees of freedom, MS: mean square error, factor A: setup type, factor B: deccentricity.

| Source | SS | df | MS | F | p |
|---|---|---|---|---|---|
| Setup type | 3056.47 | 1 | 3056.47 | 7.7 | 0.0241 |
| Eccentricity | 2216.53 | 1 | 2216.53 | 5.58 | 0.0458 |
| Interaction | 696.97 | 1 | 696.97 | 1.76 | 0.2218 |
| Error | 3176.8 | 8 | 397.1 | | |
| Total | 9146.76 | 11 | | | |

Table C.19: Young age group. Comparison of the dynamic and static test setup. Two-factorial variance analysis considering position 3 (6.5°). SS: sum of squares, df: degrees of freedom, MS: mean square error, factor A: setup type, factor B: eccentricity.

| Source | SS | df | MS | F | p |
|---|---|---|---|---|---|
| Setup type | 2694.97 | 1 | 2694.97 | 4.16 | 0.0756 |
| Eccentricity | 67.61 | 1 | 67.61 | 0.1 | 0.7548 |
| Interaction | 15.25 | 1 | 15.25 | 0.02 | 0.8818 |
| Error | 5176.97 | 8 | 647.12 | | |
| Total | 7954.79 | 11 | | | |

Table C.20: Young age group. Comparison of the dynamic and static test setup. Two-factorial variance analysis considering position 4 (8.0°). SS: sum of squares, df: degrees of freedom, MS: mean square error, factor A: setup type, factor B: eccentricity.

| Source | SS | df | MS | F | p |
|---|---|---|---|---|---|
| Setup type | 2138.65 | 1 | 2138.65 | 6.62 | 0.033 |
| Eccentricity | 63.3 | 1 | 63.3 | 0.2 | 0.6697 |
| Interaction | 3654.71 | 1 | 3654.71 | 11.31 | 0.0099 |
| Error | 2584.26 | 8 | 323.03 | | |
| Total | 8440.92 | 11 | | | |

Table C.21: Old age group. Comparison of the dynamic and static test setup. Two-factorial variance analysis considering position 1 (2.65°). SS: sum of squares, df: degrees of freedom, MS: mean square error, factor A: setup type, factor B: eccentricity.

| Source | SS | df | MS | F | p |
|---|---|---|---|---|---|
| Setup type | 914.6 | 1 | 914.62 | 0.36 | 0.5634 |
| Eccentricity | 9451 | 1 | 9451.04 | 3.75 | 0.0887 |
| Interaction | 8234.7 | 1 | 8234.73 | 3.27 | 0.1081 |
| Error | 20141.8 | 8 | 2517.73 | | |
| Total | 38742.2 | 11 | | | |

Table C.22: Old age group. Comparison of the dynamic and static test setup. Two-factorial variance analysis considering position 2 (5.0°). SS: sum of squares, df: degrees of freedom, MS: mean square error, factor A: setup type, factor B: eccentricity.

| Source | SS | df | MS | F | p |
|---|---|---|---|---|---|
| Setup type | 95.68 | 1 | 95.68 | 0.17 | 0.6923 |
| Eccentricity | 1569.31 | 1 | 1569.31 | 2.76 | 0.1351 |
| Interaction | 244.56 | 1 | 244.56 | 0.43 | 0.5302 |
| Error | 4546.04 | 8 | 568.26 | | |
| Total | 6455.6 | 11 | | | |

Table C.23: Old age group. Comparison of the dynamic and static test setup. Two-factorial variance analysis considering position 3 (6.5°). SS: sum of squares, df: degrees of freedom, MS: mean square error, factor A: setup type, factor B: eccentricity.

| Source | SS | df | MS | F | p |
|---|---|---|---|---|---|
| Setup type | 115.18 | 1 | 115.18 | 0.23 | 0.6411 |
| Eccentricity | 368.44 | 1 | 368.443 | 0.75 | 0.4115 |
| Interaction | 641.88 | 1 | 641.882 | 1.31 | 0.2859 |
| Error | 3927.32 | 8 | 490.915 | | |
| Total | 5052.83 | 11 | | | |

Table C.24: Old age group. Comparison of the dynamic and static test setup. Two-factorial variance analysis considering position 4 (8.0°). SS: sum of squares, df: degrees of freedom, MS: mean square error, factor A: setup type, factor B: eccentricity.

# Appendix D

# Questionnaire

The statements of the participants were queried with a questionnaire after executing the fieldy study (see below).
The participants were asked which of the two objects was easier to detect as well as whether they could determine significant distinctive features of the objects.
Answering question 17,"Which of the two object shape was easier to detect?", 92.0% of the participants indicated the deer as easier to detect, while the remaining 8.0% named the pedestrian.
Table D.1 summarizes the participants' answers with regard to questions 18 to 21. For a better overview only the most common answers are listed and specified in percent.
The questionnaire (in German) is presented below.

| Identification pedestrian | Distinctive feature pedestrian | Identification deer | Distinctive feature deer |
|---|---|---|---|
| Face (75.0%) | Face (90.0%) | Shape (93.0%) | Legs (35.0%) |
| Shape (15.0%) | Blonde hair (6.0%) | Four legs (4.0%) | Ears (30.0%) |
| Two legs (6.0%) | Gum boots (2.0%) | Ears (3.0%) | Back (24.0%) |
| Eyes (3.0%) | Shape (2.0%) | | No feature (11.0%) |
| Hair (2.0%) | | | |

Table D.1: Participants' answers with regard to questions 18 to 21 of the questionnaire. The participants were asked which of the two objects was easier to detect as well as whether they could determine significant distinctive features of the object shapes.

It can be stated that face of the human was the most named as distinctive feature, while the answers were inconclusive for the deer shape. In this case the legs, the head (ears) and also the back of the deer were mentioned as a distinctive feature.

FACHGEBIET LICHTTECHNIK

TECHNISCHE UNIVERSITÄT DARMSTADT

# Detektionsuntersuchung

Geschlecht:
Alter:
Sehhilfe (Brille/ Kontaktlinsen/Dioptrie ±):
Bekannte Sehschwäche (z.B. Farbfehlsichtigkeit):

1. Seit wann besitzen Sie Ihren Führerschein?

---

2. Wie viele Kilometer fahren Sie circa pro Jahr?

---

3. In welchem Land fahren Sie hauptsächlich?

---

4. Welches Fahrzeug fahren Sie?

---

5. Welchen Lampentyp besitzt ihr Fahrzeug?

   - ☐ Halogen
   - ☐ Xenon
   - ☐ LED
   - ☐ Nicht sicher

6. Inwieweit sind sie zufrieden mit Ihrem Lampentyp?

□ gar nicht □ wenig □ mittelmäßig □ überwiegend □ sehr

7. Wie oft lassen Sie Ihre Scheinwerfer einstellen?

□ Einmal im Jahr

□ Alle zwei Jahre

□ Weniger als alle zwei Jahre

□ Noch nie

□ Nicht sicher

8. Empfinden Sie das Fahren bei Dunkelheit anstrengender als bei Tag?

□ gar nicht □ wenig □ mittelmäßig □ überwiegend □ sehr

9. Wo fahren Sie am häufigsten bei Dunkelheit?

Landstraße

□ gar nicht □ wenig □ mittelmäßig □ überwiegend □ am häufigsten

Stadtstraße

□ gar nicht □ wenig □ mittelmäßig □ überwiegend □ am häufigsten

Autobahn

□ gar nicht □ wenig □ mittelmäßig □ überwiegend □ am häufigsten

10. Wünschen Sie sich bessere Sicht bei Dunkelheit?

□ gar nicht □ wenig □ mittelmäßig □ oft □ sehr häufig

11. Besitzt ihr Fahrzeug ein Lichtassistenzsystem und wenn ja welches? Mehrere Antworten sind möglich.

    - □ Abbiegelicht: Realisiert durch eine Zusatzleuchte oder ein Nebellicht, welches beim Abbiegevorgang in die Zielstraße leuchtet
    - □ AFS: Verschiedene Abblendlichtverteilungen, wie z.B. Schlechtwetterlicht, Autobahnlicht, Landstraßenlicht
    - □ Kurvenlicht: Licht schwenkt während der Fahrt in den Kurvenradius
    - □ Fernlichtassistent: System schaltet automatisch zwischen Fernlicht und Abblendlicht
    - □ Gleitende Leuchtweite: Die Leuchtweite des Abblendlichtes wird dem vorausfahrenden oder entgegenkommenden Verkehr angepasst
    - □ Blendfreies Fernlicht: System fährt mit Fernlicht und blendet den Gegenverkehr automatisch aus
    - □ Kein Lichtassistenzsystem
    - □ Nicht sicher

12. In welcher Umgebung empfinden Sie die Anstrengung beim Autofahren in der Nacht am größten?

    Landstraße

    □ gar nicht □ wenig □ mittelmäßig □ überwiegend □ am häufigsten

    Stadtstraße

    □ gar nicht □ wenig □ mittelmäßig □ überwiegend □ am häufigsten

    Autobahn

    □ gar nicht □ wenig □ mittelmäßig □ überwiegend □ am häufigsten

13. Gibt es Dinge oder Geschehnisse, die Sie beim Autofahren im Dunkeln stören? Beim nächtlichen Fahren stört mich:

14. Hatten Sie jemals einen Unfall während des Fahrens bei Dunkelheit? (ja / nein) Wenn ja, wodurch wurde er verursacht?

---

15. Falls Sie in eine gefährliche Situation geraten sind: Um welche Situation handelte es sich? Mehrere Antworten sind möglich!

    - ☐ Person übersehen/ zu spät gesehen
    - ☐ Fahrzeug übersehen/ zu spät gesehen
    - ☐ Wild übersehen/ zu spät gesehen
    - ☐ Sonstiges Objekt übersehen/ zu spät gesehen
    - ☐ Nicht identifizierbares Objekt übersehen/ zu spät gesehen

16. Falls es zu einem Unfall gekommen ist: Welche Art von Unfall war es? Mehrere Antworten sind möglich

    - ☐ Mit Sachschaden
    - ☐ Mit Personenschaden
    - ☐ Mit Sach- und Personenschaden
    - ☐ Mit Wildschaden
    - ☐ Sonstiges

17. Welches der beiden gezeigten Objekte (Person, Reh) konnten Sie leichter detektieren?

---

18. Woran haben Sie erkannt, dass es sich bei dem Objekt um eine Person handelt?

---

19. Hatte die Person ein signifikantes Erkennungsmerkmal?

---

20. Woran haben Sie erkannt, dass es sich bei dem Objekt um ein Reh handelt?

---

21. Hatte das Reh ein signifikantes Erkennungsmerkmal?

---

# Appendix E

# Reflection coefficients

In [32] a series of reflection coefficient measurements of objects that are important for the surroundings of the vehicle were performed. The measurements are illustrated in Figure E.1.
For calculating the contrast between an object and its background both the object's reflection coefficient and distance between vehicle and object or object and background is important. Since the illuminance decreases quadratically with increasing distance, the background that is located 10.0 m behind the object, depending on the distance to the light source, is illuminated with a 25.0% to 85.0% illuminance of the object only.
On a relatively straight line it can be assumed that an object located at the edge of the road is about half as far from the road's center point compared to the vegetation near the road. Therefore, the distance of the object's background to the vehicle is about twice as far than the distance to the object itself. Therefore, irrespective of the current distance between vehicle and object, only 25.0% illuminance on the object's surface also reaches the background (inverse square law). Thus a clear contrast between background and object arises.

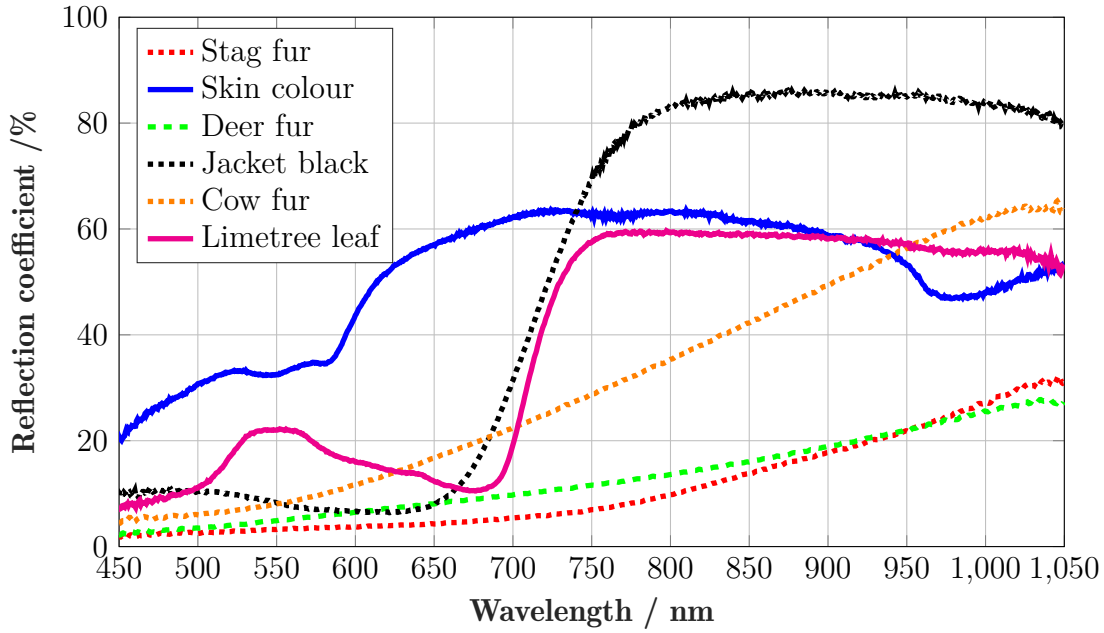


Figure E.1: Reflection coefficients of objects that are relevant for the surroundings of the vehicle according to [32].

# Bibliography


[1] B. Lachenmayr. *Gesehen und Gesehen werden: Sicher unterwegs im Straßenverkehr.* Verlag Shaker 1995 (1995)

[2] E. Goldstein. *Wahrnehmungspsychologie.* Verlag Technik GmbH Berlin, München, 1 Aufl. (1993)

[3] G. Osterberg. *Topography of the Layer of Rods and Cones in the Human Retina.* Acta Opthalmologica **6** (1935) 1–103

[4] *Contrast, visual performance at night-time.* `http://slideplayer.org/slide/2318473/8/images/5/Sehaufgabe+in+der+Dunkelheit.jpg`. Viewed on 30.06.2017

[5] M. Eckert. *Lichttechnik und optische Wahrnehmungssicherheit im Straßenverkehr.* Springer Verlag Heidelberg, Heidelberg, 9 Aufl. (1993)

[6] C. Schiller. *Spektrale Detektions- und Kontrastempfindlichkeit im mesopischen Bereich* (2015). PhD thesis, Technische Universität Darmstadt

[7] M. Taylor, C. D. Creelman. *Pest: Efficient estimates on probability functions.* The Journal of the Acoustical Society of America **41** (1967)(4A) 782–787

[8] *Verkehrsunfälle (November 2016).* Statistisches Bundesamt (Destatis) (2016) 21-41

[9] *Unfälle von Senioren im Straßenverkehr.* Statistisches Bundesamt (Destatis) (2016) 6-14

[10] *Regulation No.20 -Uniform provisions concerning the approval of motor vehicle headlamps emitting an asymmetrical passing beam or a driving beam or a driving bean or both and equipped with halogen filament lamps (H4 lamps).* Wirtschaftskommission für Europa der Vereinten Nationen (Economic Commission for Europe(ECE)) (1995) 551-566

[11] M. Berek. *Zum physiologischen Grundgesetz der Wahrnehmung.* Zeitschrift für Instrumentenkunde **9** (1943) 298–309

[12] W. Adrian. *Die Unterschiedsempfindlichkeit des Auges und die Möglichkeit ihrer Berechnung.* Lichttechnik **21** (1969) 2A–7A

[13] W. Adrian. *Visibility of Targets: Model for Calculation.* Lighting Research and Technology **21** (1989) 181–188

[14] H.-J. Fleck. *Periphere Wahrnehmung und Gesichtspunkte für die Darbietung visueller Information.* Licht **5** (1988) 380–384

[15] R. Brémont, A. Nouailles-Mayeur. *Some drawbacks of the visilbility level as an index of visual performance while driving.* CIE 27th Session proceedings **1** (2011) 1140–1143

[16] R. Brémont, V. Bodard, E. Dumont, A. Nouailles-Mayeur. *Target visibility level and detection distance on a driving simulator.* Lighting Research and Technology **45** (2013) 76–89

[17] P. Moon, D. Spencer. *The visual effect of non-uniform sorrounds.* Journal of the Optical Society of America **35** (1945) 233–247

[18] A. Mayeur, R. Brémont, J. Bastien. *The effect of Task and Eccentricity of the Target on Detection Thresholds in Mesopic Vision: Implications for Road Lighting.* Human Factors **50** (2008) 712–721

[19] A. Mayeur, R. Brémont, J. Bastien. *Effects of the viewing context on peripheral target detection. implications for road lighting design.* Elsevier, Applied Ergonomics **41** (2010) 461–468

[20] J. de Boer, W. Morass. *Berechnung der Sehweite aus der Lichtverteilung von Automobilscheinwerfern.* Lichttechnik **10** (1956) 433–437

[21] J. Damasky. *Lichttechnische Entwicklung von Anforderungen an Kraftfahrzeugscheinwerfer* (1995). Phd thesis, Technische Hochschule Darmstadt

[22] K. Ising. *Threshold Visibility Levels Required for Night time Pedestrian Detection in a Modified Adrian/CIE Visibility Model.* Journal of the Illuminating Engineering Society of North America **5** (2008) 63–75

[23] A. Mayeur, R. Brémont, J. Bastien. *The effect of the driving activity on target detection as a function of the visibility level: Implications for road lighting.* Elsevier, Transportation Research **13** (2010) 115–128

[24] S. Kokoschka, D. Gall. *Fasival - Entwicklung und Validierung eines Sichtweitenmodells zur Bestimmung der Fahrersichtweite.* Universität Karlsruhe, Technische Universität Ilmenau (2000)

[25] D. Kliebisch, S. Völker. *Examinations of the Recognition Distance of Headlamps.* Proceedings of the 6th International Symposium on Automotive Lighting **1** (2005) 1113–11243

[26] J. Kobbert, K. Schneider, K. Kosmas, D. Polin, T. Q. Khanh. *Field Test of Visibility distances and recognition rates - comparison of led and laser systems.* Proceedings of the 11th International Symposium on Automotive Lighting **1** (2015) 365–374

[27] K. Joulan, N. Hautière, R. Brémont. *Contrast sensitivity functions for road visibility estimation in digital images.* CIE 27th Session proceedings **1** (2011) 1144–1149

[28] E. Aulhorn. *Studien über den Grenzkontrast.* Graefe's Archive for Clinical and Experimental Ophthalmology **167** (1964)(1) 3–23

[29] *Jagdverband, animal-vehicle crash statistics.* `https://www.jagdverband.de/content/wildunfC3A4lle-verhindern`. Viewed on 07.05.2017

[30] J. H. Sprute, T. Q. Khanh. *Approval Requirements for a Front-Lighting System with Variable Cut-Off Line in Europe.* Proceedings of the 7th International Symposium on Automotive Lighting **1** (2007) 31–37

[31] *Regulation No.123- Uniform provisions concerning the approval of adaptive front lighting systems (AFS) for motor vehicles.* Wirtschaftskommission für Europa der Vereinten Nationen (Economic Commission for Europe(ECE)) (2010), 1-32

[32] D. Schneider. *Markierungslicht - eine Scheinwerferlichtverteilung zur Aufmerksamkeitssteurung und Wahrnehmungssteurung von Fahrzeugführern* (2010). PhD thesis, Technische Universität Darmstadt

[33] M. Burckhardt. *Reaktionszeit bei Notbremsvorgängen. Fahrzeugtechnische Schriftenreihe.* Verlag TÜV Rheinland (1985)

[34] S. Völker. *Hell- und Kontrastempfindung - ein Beitrag zur Entwicklung von Zielfunktionen für die Auslegung von Kraftfahrzeug-Scheinwerfern* (2006). Postdoctoral thesis

[35] P. Zöfel. *Statistik für Psychologen im Klartext.* Pearson, München, 11 Aufl. (2003)

[36] T. Khanh. *Lichttechnik I: Grundlagenvorlesungen der Lichttechnik.* Technische Universität Darmstadt, Fachgebiet Lichttechnik (2017)

[37] H. R. Blackwell. *Contrast thresholds of the human eye.* Journal Of The Optical Society Of America **36** (1946) 624–643

[38] D. Kliebisch, S.Völker. *Die Erkennbarkeitsentfernung - Neue Methoden der Scheinwerferbewertung.* Universität Parderborn (2007)

[39] J. Locher, S. Völker. *Der Einfluss der Kfz-Lichtverteilung auf Sicherheit und Akzeptanz.* OWL 2002 **1** (2002) 4–14

[40] *Techno Team, LMK 5, operations manual.* `http://www.technoteam.de/produktuebersicht/lmk/downloads/index_ger.html`. Viewed on 08.05.2017

[41] F. van Nes, M. Bouman. *Spatial modulation transfer in the human eye.* Journal of the Optical Society of America **57** (1967) 401–406

[42] I. Möllers, J. Moisel. *Ein effizienter hochauflösender ADB-Scheinwerfer auf Basis von mikrointegrierten LED- Arrays.* VDI Berichte **2278** (2016) 37–50

[43] I. Möllers, J. Moisel. *Requirements for future high resolution ADB modules.* Proceedings of the 11th International Symposium on Automotive Lighting **1** (2015) 161–170

[44] L.-H. Haase, B. Pfeffer, M. Maier. *Heller, weiter, schneller.* Automobiltechnische Zeitschrift (ATZ) **5** (2016) 44–48

[45] *The MathWorks, Matlab.* `https://de.mathworks.com/products/matlab.html`. Inc.,P.O. Box 845428, Boston, MA 02284-5428, USA: Matlab Simulink, viewed on 29.06.2017

[46] H.-J. Schmidt-Clausen. *Grundlagen der Lichttechnik, Skriptum zur Vorlesung.* Technische Hochschule Darmstadt, Darmstadt, 1 Aufl. (1993)

[47] M. Hamm. *Untersuchung der spektralen Schwellenempfindlichkeit und der Reizverarbeitungszeiten im menschlichen Auge* (1997). PhD thesis, Technische Hochschule Darmstadt

[48] O.-J. Grüßer, U. Grüßer-Cornehls. *Physiologie des Sehens, Grundriss der Sinnesphysiologie.* Springer Verlag, Berlin, 5 Aufl. (1985)

[49] E. Horn. *Vergleichende Sinnesphysiologie.* Gustav Fischer Verlag, Stuttgart, 1 Aufl. (1982)

[50] H.-J. Fleck. *Zur peripheren Wahrnehmung von Sehzeichen.* VDI Verlag, Düsseldorf, 34. Aufl. (1987)

[51] A. E. Kadzin. *Encyclopedia of Psychology.* American Psychological Association, Oxford University Press, Oxford, 8 Aufl. (2000)

[52] J. de Boer, W. van Bommel. *Road Lighting.* Kluwer (1980)

[53] H.-J. Fleck. *Measurement and Modeling of Peripheral Detection and Discrimination Thresholds.* Biological Cybernetic **61** (1989) 437–446

[54] B. Inditsky, H.-W. Bodmann, H.-J. Fleck. *Elements of visual performance: contrast metric - visibility lobes - eye movements.* Lighting Research and Technology **14** (1982) 218–231

[55] B. Inditsky. *Analysis of visual performance: theoretical and experimental investigation of visual search* (1978). PhD thesis, Technische Hochschule Karlsruhe

[56] A. Cohen. *Einflussgrößen auf das nutzbare Sichtfeld.* Bericht zum Forschungsprojekt 8005 der Bundesanstalt für Straßenwesen (1984)

[57] B. Lachenmayr, O. Lund. *Sehvermögen und Straßenverkehr: die speziellen Probleme des älteren kraftfahrers. Sicher unterwegs im Straßenverkehr.* Münchener Medizinische Wochenzeitschrift **131** (1989) 648–651

[58] R. Mourant, T. Rockwell, J. Rackoff. *Driver's eye movements and visual workload.* Highway Research Record **292** (1969) 1–10

[59] *An analytical model for describing the influence of lighting parameters upon visual performance.* Commission Internationale De L'Eclairage (CIE) 19.2 (1981)

[60] J.Lecocq. *Visibility and lighting of wet road surfaces.* Lighting Research and Technology **26** (1994) 75–87

[61] *American national standard practice for roadway lighting.* Illuminating Engineering Society of North America (IESNA) (2000)

[62] *Road lighting* (2005). European Committee for Standardization (CEN)

[63] S. Silbernagl, A. Despopoulos. *Taschenatlas Physiologie.* Thieme (2007)

[64] A. Sekuler, P. Benett, F. Piacenza. *Spatial phase discrimination in older observers.* Investigative Ophtalmology and Visual Science Supplement **36** (1995) 36

[65] F. Wichmann, N. Hill. *The psychometric function: I. Fitting, sampling, and goodness of fit.* Attention, Perception, & Psychophysics **63** (2001)(8) 1293–1313

[66] S. Klein. *Measuring, estimating, and understanding the psychometric function: A commentary.* Attention, Perception, & Psychophysics **63** (2001)(8) 1421–1455

[67] M. Linschoten, L. Harvey, P. Eller, B. Jafek. *Fast and accurate measurement of taste and smell thresholds using a maximum-likelihood adaptive staircase procedure.* Perception and Psychophysics **63** (2001) 1330–1347

[68] J. Bortz, N. Döring. *Forschungsmethoden und Evaluation für Human-und Sozialwissenschaftler.* Springer-Verlag (2007)

[69] *Recommended System for Mesopic Photometry Based on Visual Performance* (2010). Commission Internationale De L'Eclairage (CIE)

[70] *Verkehrs- und Unfalldaten - Kurzzusammenstellung der Entwicklung in Deutschland.* Bericht der Bundesanstalt für Straßenwesen (BAsT) (2016) 1-2

[71] *Straßenverkehrsunfälle mit Personenschaden: Bundesländer, Jahre, Straßenklasse, Ortslage* (2016). Statistisches Bundesamt (Destatis) (2016) 19-41

[72] H. Winner, G. W. S. Hakuli. *Handbuch Fahrerassistenzsysteme: Grundlagen, Komponenten und Systeme für aktive Sicherheit und Komfort.* ATZ/MTZ-Fachbuch. Vieweg+Teubner Verlag (2011)

[73] *Wirtschaftskommission für Europa der Vereinten Nationen (economic commission for europe(ece).* `https://www.unece.org/oes/nutshell/governing_bodies.html`. Viewed on 07.07.2017

[74] D. Kliebisch. *Entwicklung eines Modells zur Berechnung der Erkennbarkeitsentfernung aus Leuchtdichtebildern* (2004). Diploma thesis, Technische Universität Ilmenau

[75] *Regulation No.98- Uniform provisions concerning the approval of motor vehicle headlamps equipped with gas-discharge light sources.* Wirtschaftskommission für Europa der Vereinten Nationen (Economic Commission for Europe(ECE)) (1995) 551-556

[76] R. Weigel, O. Knoll. Das Licht **10** (1940) 197

[77] H. Siedentopf. *Neue Messungen der visuellen Kontrastschwelle.* Astronomische Nachrichten **271** (1941) 193

[78] B. Schönwald. *Das Riccosche Gesetz und die Sehschärfe.* Das Licht **11** (1941) 15

[79] W. Arndt. *Über die Unterschiedsempfindlichkeit des Auges.* Licht **7** (1937) 101–104

[80] R. Schumacher. *Die Unterschiedsempfindlichkeit des helladaptierten Auges.* Das Licht **11** (1941) 134

[81] W. Adrian. *Visibility of Targets.* Transportation Research Record **1247** (1989) 39–45

[82] W. Adrian, K. Eberbach. *Über den Zusammenhang zwischen Sehschwelle und Umfeldgröße.* Optik 28 **2** (1968) 132–142

[83] F. Löhle. *Über die Abhängigkeit des Reizschwellenwertes vom Sehwinkel.* Zeitschrift für Physik **54** (1929) 137

[84] D. Meschede. *Gerthsen Physik.* Springer, 23 Aufl. (2006)

[85] W. Adrian. *Change of Visual Acuity with Age.* Lichttechnik **21** (2012) 2A–7A

[86] O. Mortensen-Blackwell, H. Blackwell. *Visual Performance Data for 156 Normal Observers of Various Ages.* Illuminating Engineering Institute, New York Project **30** (1980) B

[87] W. Adrian. *Visibility Levels under night-time driving conditions.* Journal of the illuminating engineering society **16** (1987) 3–12

[88] W. Adrian, R. Stemprok. *Required Visibility Levels in Road Scenes at Night Time Driving.* International Symposium on Automotive Lighting **1** (2005) 559–571

[89] H. Lossagk. *Deutsche Kraftfahrtforschung BVM (Ministry of Transport)* **90** (1955)

[90] C. Dunbar. *Necessary values of brightness in artificially lighted streets.* Illuminating Engineering Society in England **3** (1938) 187–196

[91] J. Boer. *Fundamental experiments of visibility and admissible glare in road lighting.* Proceedings of the CIE-Conference **1** (1951)

[92] Y. Akashi, M. Rea, J. D. Bullough. *Driver decision making in response to peripheral moving targets under mesopic light levels.* Lighting Research and Technology **39** (2007) 53–67

[93] J. D. Bullough, J. V. Derlofske, Y. Akashi. *Strategies for Optimizing Headlamp Illumination and Visibility Along Curves.* SAE International **1** (2006) 489

[94] K. Ising. *The Distribution of Visibility Levels at Target Detection in a modified Adrian/ CIE Visibility model.* Human Factors and Ergonomics Society Annual Meeting Proceedings **53** (2009) 1796–1800

[95] *CIE collection on glare.* Commission Internationale De L'Eclairage (CIE 146) (2002) 19

[96] R. Brémont, E. Dumont, V. Ledoux, A.Mayeur. *Photometric measurements for Visibility Level computation.* Lighting Research and Technology (2010) 1–10

[97] R. B. Gibbons, T. Terry, R. Bhagavathula, J. Meyer, A. Lewis. *Applicability of mesopic factors to the driving task.* Lighting Research and Technology (2015) 1–13

[98] I. Reagan, M. Brumnelow, T. Frischmann. *On-road experiment to assess drivers' detection of roadside target as function of headlight refelectance.* Accident Analysis and Prevention **76** (2015) 74–82

[99] I. Reagan, M. Brumnelow. *Drivers' detection of roadside targets when driving vehicles with three headlight system during high beam activation.* Accident Analysis and Prevention **99** (2017) 44–50

[100] L. L. Holladay. *The fundamentals of glare and visibility.* Journal of the Optical Society of America **12** (1926)(4) 271–319

[101] S. Kokoschka. *Zur Berechnung von Schwellenkontrasten für die Detektion einfacher Sehobjekte.* Das Licht **4** (1988) 1

[102] W. Kosmatka. *Udc - Uniform Detection Characteristic for Detecting Roadway Obstacles.* SAE Technical Paper **1** (2006)(948)

[103] N. Hautiere, E. Dumont. *Assessment of visibility in complex road scenes using digital imaging.* CIE 26th Session proceedings **1** (2007) D4 96–99

[104] F. Campbell, J. Robson. *Application of Fourier analysis to the visibility of gratings.* Journal of Physiology **197** (1968) 551–566

[105] S. Burgmann, U. Hildach, F. Lenz, W. Schlohbohm, M. Streh. *Der Berufskraftfahrer LKW, Omnibus - Prüfungsleitfaden und Nachschlagewerk.* Vogel (2005)

[106] D. Englisch, C. Schiller, P. Bodrogi, T. Khanh. *Mesopic increment detection sensitivity, Part I Phenomenological analysis.* Lighting Research and Technology (2016) 1–16

[107] *Performance based model for mesopic photometry.* Project MOVE- Mesopic Optimisation of Visual Efficiency (2004)

[108] P. Bodrogi, C. Schiller, T. Khanh. *Testing the CIE systems for mesopic photometry in a threshold detection experiment.* Lighting Research and Technology **1** (2015) 1–13

[109] *Acer h7532bd projector, datasheet.* `https://www.acer.com/datasheets/2014/4829/H7/MR.JG411.001.html`. Viewed on 30.04.2017

[110] K. Narisada, K. Yoshikawa. *Tunnel entrance lighting- effect of fixation point and other factors on the determination of requirements.* Lighting Research and Technology **6** (1974) 9–18

[111] G. M. F. Speranza, B. Schneider. *Age related changes in binocular vision: Detection of noise masked targets in young and old observers.* Journal of Gerontology B, Psychological Science and Social Science **50** (1995) 114–123

[112] G. G. R. Spinks, C. Thomas. *Age simulation of a sensory deficit does impair cognitive test performance.* Cognition and Aging Conference Atlanta **1** (1996) 1

[113] L. Marks. *Brightness and Retinal Locus: Effects of Target Size and Spectral Composition.* Perception and Psychophysics **41** (1971) 26–30

[114] N. Osaka. *Target Size and Luminance in Apparent Brightness of the Peripheral Visual Field.* Perception Motion Skills **41** (1975) 49–50

[115] J. W. Mauchly. *Significance test for sphericity of a normal n-variate distribution.* The Annals of Mathematical Statistics **11** (1940)(2) 204–209

[116] P. Jainski. *Die Wahrnehmungsschwelle des Auges für mehrere Sehdinge im Gesichtsfeld.* Lichttechnik **7** (1955) 382–387

[117] M. Rast. *Kontrastuntersuchungen bei strukturierten Gesichtsfeldern* (1980). Diploma thesis, Technische Hochschule Ilmenau

[118] A. Walkling. *Untersuchungen zur physiologischen Blendung bei Beleuchtung von nassen und trockenen Straßen* (2015). PhD thesis, Technische Universität Ilmenau

[119] R. Gonzalez, R. Woods, S. Eddins. *Digital Image Processing using MATLAB.* McGraw Hill Education (2013)

[120] *Visual acuity, Berufsverband der Augenärzte Deutschlands e.V.* `http://cms.augeninfo.de/hauptmenu/presse/aktuelle-presseinfo/pressemitteilung/article/mehr-als-100-prozent-sind-moeglich.html`. Viewed on 07.07.2017

[121] *Ophthalmological examination, Berufsverband der Augenärzte Deutschlands e.V.* `http://cms.augeninfo.de/hauptmenu/presse/statistiken.html`. Viewed on 07.07.2017

[122] B. Reisinger, N. Winterer, M. Reinprecht. *Auf der Suche nach der Auflösung: Überlegungen zu hochauflösenden Scheinwerfersystemen: Optische Technologien in der Fahrzeugtechnik.* VDI-Tagung, Karlsruhe **7** (2016)

[123] S. Grötsch, A. Pfeuffer, T. Liebetrau, H. Oppermann, M. Brink, R. Fiederling, I. Möllers, J. Moisel. *Integrated High Resolution LED Light Sources in an AFS/ADB Headlamp.* Proceedings of the 11th International Symposium on Automotive Lighting **1** (2015) 241–250

[124] C. Schmidt, B. Willeke, B. Fischer. *Laser versus Hochleistungs-LED: Vergleich der Einsatzmöglichkeiten bei hochauflösenden Matrix-Scheinwerfer Systemen: Optische Technologien in der Fahrzeugtechnik.* VDI-Tagung, Karlsruhe **7** (2016)

[125] *Regulation No.48 - Uniform provisions concerning the approval of vehicles with regard to the installation of lighting and light-signalling devices.* Wirtschaftskommission für Europa der Vereinten Nationen (Economic Commission for Europe(ECE)) (2011) 46-152

[126] *Richtlinie 98/14/EG der Kommission vom 6. Februar 1998 zur Anpassung der Richtlinie 70/156/EWG des Rates zur Angleichung der Rechtsvorschriften der Mitgliedstaaten über die Betriebserlaubnis für Kraftfahrzeuge und Kraftfahrzeuganhänger an den technischen Fortschritt.* Europäische Kommission (1998)

[127] *Merkblatt zur Richtlinie 98/14/EG: "Neue Technologien oder Merkmale" (mtm), gem. Art. 8, Abs. 2, Buchstabe c".* Kraftfahrt Bundesamt (1998)

[128] C. Funk, J. Reim, S. Omerbegovic. *New world of lighting based driver assistance systems - Good bye low beam.* Proceedings of the 11th International Symposium on Automotive Lighting **1** (2015) 131–140